Local Energy Markets

Simulative Evaluation and Field Test Application of Energy Markets on Distribution Grid Level

Zur Erlangung des akademischen Grades Doktor-Ingenieur (Dr.-Ing.) genehmigte Dissertation von Sebastian Hieronymus Schreck, geboren in Pforzheim, Deutschland
Tag der Einreichung: 20.09.2022, Tag der Prüfung: 24.02.2023

1. Gutachten: Prof. Dr.-Ing. Stefan Niessen, MBA
2. Gutachten: Prof. Dr. rer. nat. Florian Steinke
Darmstadt – D17, Technische Universität Darmstadt

TECHNISCHE UNIVERSITÄT DARMSTADT

Elektrotechnik und Informationstechnik Department

Technik und Ökonomie Multimodaler Energiesysteme

Local Energy Markets
Simulative Evaluation and Field Test Application of Energy Markets on Distribution Grid Level

Accepted doctoral thesis by Sebastian Hieronymus Schreck

Date of submission: 20.09.2022
Date of thesis defense: 24.02.2023

Darmstadt – D17, Technische Universität Darmstadt

Bitte zitieren Sie dieses Dokument als:
URN: urn:nbn:de:tuda-tuprints-236747
URL: https://tuprints.ulb.tu-darmstadt.de/id/eprint/23674
Jahr der Veröffentlichung auf TUprints: 2023

Dieses Dokument wird bereitgestellt von tuprints,
E-Publishing-Service der TU Darmstadt
http://tuprints.ulb.tu-darmstadt.de
tuprints@ulb.tu-darmstadt.de

Erklärungen laut Promotionsordnung

§ 8 Abs. 1 lit. c PromO

Ich versichere hiermit, dass die elektronische Version meiner Dissertation mit der schriftlichen Version übereinstimmt.

§ 8 Abs. 1 lit. d PromO

Ich versichere hiermit, dass zu einem vorherigen Zeitpunkt noch keine Promotion versucht wurde. In diesem Fall sind nähere Angaben über Zeitpunkt, Hochschule, Dissertationsthema und Ergebnis dieses Versuchs mitzuteilen.

§ 9 Abs. 1 PromO

Ich versichere hiermit, dass die vorliegende Dissertation selbstständig und nur unter Verwendung der angegebenen Quellen verfasst wurde.

§ 9 Abs. 2 PromO

Die Arbeit hat bisher noch nicht zu Prüfungszwecken gedient.

Nürnberg, 20.09.2022

S. Schreck

Für meinen Vater Edgar

Acknowledgments

I foremost want to thank my supervisor Prof. Stefan Niessen for his constant support and great interest in the topic. Without our detailed discussions, especially on energy markets and market modeling, the quality of this Thesis would certainly have suffered. I want to thank Prof. Florian Steinke for taking over the co-supervision after guiding me during the first months of my Thesis. His remarks and feedback on methodological and modeling aspects notably sharpened the Thesis.

This Thesis was accomplished during my work in the research group of infrastructure operation at Siemens Technology in Erlangen. Many thanks to the whole research group and particularly to Dr. Sebastian Thiem for supporting me in all matters as a supervisor and manager. Special thanks to the colleagues involved in the research project pebbles Lisa, Arvid and Nejc for jointly bringing this ambitious Local Energy Market project to life. I also want to thank all other project partners for the great collaboration and the BMWI for funding the project.

During my time at Siemens I had the pleasure to work together with an amazing group of PhD students. I'm extremely grateful for the intense discussions and support from Oliver D., Oliver W., Lukas, Thanh and Robin not only in front of whiteboards but also outside the office. Additionally, I want to mention and thank all PhD students involved in PhD seminars of the labs *Technology and Economics of Multimodal Energy Systems* and *Energy Information Networks and Systems* at TU Darmstadt.
I had the honor to supervise outstanding Master's Thesis and internship students. Without your support this endeavor would not have been possible: Inès, Léna, Albertine, Clotilde, Houssame, Konstantin, Barthélemy, Ileskhan, Weibo and Clementine (in order of appearance).

Writing a doctoral Thesis is no picnic - Speaking in the words of the poet Christopher Wallace: "...everything you get ya gotta work hard for it". I could not have undertaken this journey without my family and friends who helped me persevere through the lows and granted me countless highs during this part of my life. Special shout-out to Wesley Moore for proofreading the script.

Words cannot express my gratitude to my parents who raised me to be a curious thinker and to my brother Leo for his great interest in my work and countless discussions. Myra, I'm extremely grateful to have such a loving significant-other who accompanied and sometimes endured me through the last four years.

Abstract

Widespread introduction of Distributed Energy Resources (DERs) such as volatile renewable generation, electric vehicles, heat-pumps and battery storages causes a paradigm shift of the power system. Traditional power systems with few large-scale power plants are expanded or replaced by millions of small- to medium-size DERs. Local Energy Markets (LEMs) are a promising approach to facilitate the optimal operation and dispatch of DERs and enhance grid-integration on regional grid levels.

In this Thesis, a novel linear-optimization-based market model for LEMs is developed. The market matching problem aims to maximize the social welfare of participants while considering technical and financial aspects of participants' assets and the distribution grid.

A simulative framework is set-up to evaluate the model with regards to its capabilities to foster the optimal use of flexibilities, to provide sufficient financial incentives for participants and to improve grid-integration. Yearly simulations of LEMs and a benchmark case are carried out for three different grid types (rural, semiurban, urban) and scenario years ranging from 2020 until 2035 in 5 year steps. The simulation results reveal that self-consumption and self-sufficiency of the local energy system can be increased by 4 ... 23 and 1 ... 9 percentage points depending on the grid type when compared to a business as usual benchmark case. An analysis of possible designs for regulated electricity price components in LEMs shows that a reduction of feed-in and load peaks of 30 ... 64 % can be achieved when considering power fees in the market matching problem.
The simulative evaluation also shows that the market model is able to generate temporal, spatial, and asset-specific prices signals. Depending on the grid type and its load-generation ratio, participants with generation assets have higher benefits in urban, load-dominated grids whereas consumers have higher benefits in generation-dominated rural and semiurban grids.
Load forecast uncertainty is identified as one of the major challenges in LEMs. Compared to simulations with perfect foresight, benefits of market participants are substantially decreased taking into account typical electric load forecast errors on the level of individual households.

The application of the market model in a six months field-test in Southern Germany demonstrates the real world applicability of the developed approach. The field-test confirms findings from the simulative evaluation regarding the implication of forecast errors and generated price signals. It additionally shows that market interfaces to the Distribution System Operator (DSO) might further increase grid-integration capabilities of LEMs. By taking into account active power constraints of the DSO, 1499 events of critical grid load could be avoided.

Zusammenfassung

Die fortschreitende Dezentralisierung des Energiesystems, getrieben durch den Ausbau erneuerbarer Energien, Elektromobilität, Wärmepumpen und Batteriespeicher, bewirkt einen Paradigmenwechsel im Stromversorgungssystem. Traditionelle Stromversorgungssysteme mit wenigen Großkraftwerken werden durch Millionen kleiner bis mittelgroßer verteilter Erzeuger erweitert bzw. ersetzt. Lokale Energiemärkte (LEMs) sind ein vielversprechender Ansatz für die optimale Betriebsführung verteilter Erzeuger, Verbraucher und Speicher sowie die Netzintegration auf regionaler Ebene.

Diese Arbeit behandelt die Entwicklung eines neuartigen Marktmodells für LEMs basierend auf linearer Optimierung. Das Modell zielt darauf ab, den Gesamtnutzen der Marktteilnehmer unter Berücksichtigung finanzieller und technischer Randbedingungen der Anlagen, der Teilnehmer und des Verteilnetzes zu maximieren. Das Marktmodell wird durch ein Simulationsverfahren im Hinblick auf die optimale Nutzung von Flexibilitäten, die Schaffung finanzieller Anreize für die Teilnehmer sowie bezüglich Aspekten der Netzintegration untersucht. Jahressimulationen drei verschiedener Verteilnetztypen (ländlich, halbstädtisch, städtisch) werden für die Szenariojahre 2020, 2025, 2030 und 2035 durchgeführt. Dabei wird insbesondere der Betrieb des Energiesystems durch einen LEM mit einem Benchmark-Fall ohne eine Einführung eines LEMs verglichen.

Die Simulationsergebnisse zeigen, dass der Eigenverbrauch und der Autarkiegrad des lokalen Energiesystems abhängig vom Verteilnetztyp durch die Einführung eines LEMs um 4,3 ... 22,5 bzw. 1,1 ... 9,4 Prozentpunkte gesteigert werden können. Eine Analyse möglicher Ausgestaltungen von regulierten Strompreiskomponenten in LEMs zeigt weiterhin, dass eine potenzielle Reduktion von Einspeise- und Lastspitzen von 30 ... 64 % erreicht werden kann, wenn Leistungspreise im Marktmodell berücksichtigt werden.
Die simulative Auswertung zeigt außerdem, dass das Marktmodell in der Lage ist, zeitliche, räumliche und anlagenspezifische Preissignale zu erzeugen. Abhängig vom Verteilnetztyp und dessen Last-/Erzeugungsverhältnis weisen Teilnehmer mit Erzeugungsanlagen in städtischen Netzen höhere wirtschaftliche Vorteile auf, wohingegen Verbraucher einen höheren Nutzen in erzeugungsdominierten, ländlichen und halbstädtischen Netzen erreichen.
Unsicherheiten von Lastprognosen stellen sich als eine der größten Herausforderungen von LEMs heraus. Verglichen mit Simulationen mit perfekter Vorraussicht werden die Vorteile der Marktteilnehmer erheblich verringert, wenn typische Lastprognosefehler auf der Ebene der einzelnen Haushalte berücksichtigt werden.

Die Anwendung des Marktmodells in einem sechsmonatigen Feldversuch in Süddeutschland demonstriert die Praxistauglichkeit des entwickelten Ansatzes. Der Feldversuch bestätigt die Erkenntnisse aus der simulativen Untersuchung bezüglich des Einflusses von Lastprognosefehlern und Preisanreizen. Darüber hinaus zeigt der Feldtest, dass Marktschnittstellen zum Verteilnetzbetreiber die Netzintegrationsfähigkeit von LEMs weiter erhöhen können. Durch die Berücksichtigung von Wirkleistungsbeschränkungen konnten 1499 Fälle kritische Netzüberlastungen verhindert werden.

Contents

Acknowledgments vii

List of Figures xv

List of Tables xx

1 Introduction 1
- 1.1 Motivation . . . 1
- 1.2 Objective, structure and contributions . . . 3

2 Background and Analysis 7
- 2.1 Problem formulation . . . 7
  - 2.1.1 Grid integration . . . 7
  - 2.1.2 Current market design . . . 9
  - 2.1.3 Measures for grid integration of DER . . . 12
- 2.2 Local Energy Markets . . . 17
  - 2.2.1 Roles and actors . . . 17
  - 2.2.2 Market features . . . 20
  - 2.2.3 State of the art . . . 21
  - 2.2.4 Research gap analysis . . . 24
  - 2.2.5 Research questions . . . 28
- 2.3 Modeling requirements and scoping . . . 30
  - 2.3.1 Model type . . . 30
  - 2.3.2 Spatial model scope and distribution grid assumptions . . . 32
  - 2.3.3 Temporal model scope . . . 33

3 Modeling 35
- 3.1 Market model . . . 35
  - 3.1.1 Order definition . . . 36
  - 3.1.2 Market matching problem . . . 38
  - 3.1.3 Grid topology and fees . . . 41
  - 3.1.4 Backup energy supply . . . 44
- 3.2 Participant model . . . 46
- 3.3 Asset models . . . 48
  - 3.3.1 Electric vehicles . . . 48
  - 3.3.2 Heat pumps . . . 51

4 Method 55
- 4.1 Overview . . . 55

4.2 Scenario generation . . . 57
4.2.1 Benchmark grids . . . 57
4.2.2 Order prices . . . 59
4.3 Simulation . . . 63
4.3.1 Business as usual scenario . . . 63
4.3.2 Local energy market . . . 65
4.3.3 Generation of synthetic forecast errors . . . 68
4.3.4 Scalability analysis . . . 71
4.3.5 Simulation framework . . . 72
4.4 Evaluation metrics . . . 73
4.4.1 Market . . . 73
4.4.2 Participants . . . 74
4.4.3 Grid . . . 76

5 Simulative evaluation **77**
5.1 Effects of grid type and scenario year: Comparison to BAU . . . 77
5.1.1 Overview of main scenario KPIs . . . 77
5.1.2 Economic evaluation . . . 79
5.1.3 Exchange with upstream grid . . . 82
5.2 Effects of regulated electricity price components . . . 85
5.2.1 Operational differences . . . 85
5.2.2 Impact on the distribution grid . . . 89
5.2.3 Analysis of economic impacts . . . 91
5.3 Impacts of load forecast uncertainty . . . 93
5.4 Scalability analysis . . . 96
5.5 Discussion . . . 99

6 Field test **101**
6.1 Field test description . . . 101
6.2 Setup and scenarios . . . 104
6.3 Results . . . 105
6.3.1 Overview . . . 105
6.3.2 Flexibility . . . 107
6.3.3 Market prices . . . 109
6.3.4 Grid utilization . . . 110
6.3.5 Forecast uncertainty . . . 113
6.4 Discussion . . . 118

7 Conclusion and outlook **121**
7.1 Conclusions . . . 121
7.2 Outlook . . . 122

Bibliography **125**

A Appendix **141**
A.1 Appendix to background and analysis chapter . . . 141
A.2 Appendix to modeling chapter . . . 141
A.3 Appendix to method chapter . . . 143

A.4 Appendix to results chapter 146

List of Figures

1.1 Development of photovoltaic capacities per German postal code and inhabitants which do not receive feed-in subsidies after 20 years operation time. Data is based on the energy market data register [10]. Neglecting degradation and assuming an average technical lifetime of 30 years. Plotting functionality provided by [11]. 2
1.2 Overview of the current status quo and challenges of the European energy system and the aspects LEMs can address in the future. 3
1.3 Structure of the Thesis. 4

2.1 Simplified representation of the traditional compared to the current/future power system structure. 8
2.2 Measurements at low-voltage feeder with high PV penetration on three summer days in southern Germany (Wildpoldsried). 9
2.3 Simplified representation of zonal market bidding zones in central Europe. Dotted lines represent intra-country zones. Status of September 2020. . . 10
2.4 Caption for LOF 10
2.5 Composition of retail energy prices in Germany (2020) data from [9] and [43]. 11
2.6 Overview of measures to improve grid integration ranging from demand and generation side measures to market and grid adaption 12
2.7 Overview of roles within the context of local energy markets. Roles can be fulfilled by various actors in the energy system. Table 2.1 provides details on the roles and possible actors. 18
2.8 Number of scientific publications queried from *google scholar* [85] advanced search using the terms: "Local energy market" OR "Peer to Peer energy" OR "Transactive energy" in the title. Date of queries: 15.08.2022 21
2.9 Simplified overview of possible market architectures for local energy markets. Own illustration based on [78], [86]. 22
2.10 Radar chart of evaluated market designs and scope of this Thesis based on qualitative assessment (Table 2.3) 25
2.11 Categorization of reviewed literature in the field of LEMs and the focus of this Thesis with regards to addressed market features and technical maturity. . 26
2.12 Caption for LOF 29
2.13 Overview of possible modeling formulations for LEMs. Own illustration based on [115]. 30

3.1 Overview of the modeling chapter. 35
3.2 Representation of orders and participant energy system in the market matching 38

3.3 Representation of a typical radial distribution grid topology (a) and the respective simplified model of the LEM (b). Colors of arrows indicate a possible splitting of REPCs along the grid topology [21]. 42
3.4 Overview of a generic participant energy system model with all considered energy assets. 46
3.5 Model of EV within the participant energy system 48
3.6 Overview of modeling approach to generate synthetic EV charging curves as an input for the LEM model. 49
3.7 Probability of departure times for trips on weekdays and weekends. Based on empirical data in [138] with selected trip reasons work ("Arbeit, dienstlich / geschäftlich") and education ("Ausbildung") for weekdays - shopping ("Besorgung") and leisure ("Freizeit") for weekends. 50
3.8 Generated plugin state and SOC for plugin and plugout events for home charging in an example week. Assumptions: Battery capacity = 30 kWh, one way distance to work = 25 km, average speed = 50 km/h, working hours = 8 h. 51
3.9 Model of HP, electric boiler and thermal system within the participant energy system. 52

4.1 Overview of the methodological framework and steps for the simulative evaluation. 56
4.2 Scenario assumptions for the development of electric vehicles per household based on [142], [143] and [144]. 57
4.3 Historic and projected guaranteed feed-in tariffs for PV power plants with a rated capacity between 0 and 100 kWp in Germany based on [152], [153]. 59
4.4 Development of weighted average feed-in tariffs and the share of PV plants without feed-in tariff for in Germany. Based on [151]–[153]. 60
4.5 Histograms of feed-in tariffs or minimum sell price assumptions for 2010, 2015 and the modeled scenarios (2020, 2025, 2030, 2035). Bin size: 1 ct/kWh. 61
4.6 Exemplaric day ahead spot market price and arbitrage opportunities for a week in January 2018. Data source: [156]. 62
4.7 Simulated daily operation of residential system with PV and storage for the BAU case. PV rated power = 6 kW_p, storage capacity = 5 kWh. 63
4.8 Overview of the simulation scenarios varying the grid tariff design. 65
4.9 Simplified overview of the simulation method for one LEM simulation case. 67
4.10 Schematic overview of the method to generate realistic electric load forecast profiles with a previously defined error set point from [22]. 68
4.11 Schematic illustration of weights for the vertical shifting of the demand. Figure from [22]. 70
4.12 Exemplaric results for the application of the method for an example day of a household load profile for (a) 30 % MAPE and (b) 50 % MAPE. Figure from [22]. 71

5.1 Development of self-consumption in the BAU and LEM scenarios over the scenario years and a variation of grid types. LEM REPCs scenario: *Flat*. . . 77
5.2 Development of self-sufficiency in the BAU and LEM scenarios over the scenario years and a variation of grid types. LEM REPCs scenario: *Flat*. 78

5.3 Share of generation sold via the LEM over the scenario years for a variation of grid types. LEM REPCs scenario: *Flat*. 79
5.4 Weighted average sell price over the scenario years for a variation of grid types. LEM REPCs scenario: *Flat*. 80
5.5 Heatmaps of the weighted average buy price at the LEM (*Flat* scenario) over one simulation year (2035) for the grid scenarios Rural (a), Semiurban (b) and Urban (c). 81
5.6 Average benefit of various asset types for the simulation year 2035. The benefit represents an increased revenue for Storage and PV systems and a cost reduction for demand assets compared to the BAU scenario. 82
5.7 Heatmaps of the exchanged power with the backup (load of the LV/MV transformer) for one simulation year (2035) for the Rural grid and for the Business As Usual (BAU) (a) and Local Energy Market (LEM) (b) scenario. Positive values indicate import from backup supplier, negative values indicate export. 83
5.8 Relative change of absolute daily load- (a) and feed-in- (b) peaks between the scenarios Business As Usual (BAU) and Local Energy Market (LEM) for a variation of scenario years and grid types. The relative change is calculated as the average of the 5 % highest daily peaks. 84
5.9 Exemplary market matching results for a variation of REPC scenarios. Grid: rural, scenario year: 2035. 86
5.10 Exemplary asset specific market results results for a variation of REPC scenarios. Grid: rural, scenario year: 2035. 88
5.11 Load duration curves of the REPC scenario variation. Positive residues represent import from the MV grid. Negative values represent feed-in. Figure (a) shows the full load duration curve of all 30,540 15-min timesteps of the simulation. Figure (b) shows the 100 timesteps with the highest feed-in and Figure (c) the 100 timesteps with the highest import. Grid type: Rural, Scenario year: 2035. 89
5.12 Relative change of daily load- (left) and feed-in- (right) peaks between the scenarios Business As Usual (BAU) and Local Energy Market (LEM) for a variation of scenario years (x-axis) and REPC scenarios. Different grid types are represented by Subplots. The relative change is calculated as the average of the 5 % highest daily peaks. 91
5.13 Relative contributions to the highest 5 % demand peaks per asset type. Scenario year: 2035, Grid type: Rural 92
5.14 Average asset benefit of assets types for a variation of fee scearios. Scenario year: 2035, Grid type: Semiurban. 92
5.15 Collected Regulated Electricity Price Components (REPC) for the different grid types and scenarios. Scenario year: 2035 93
5.16 Average yearly consumption profile and the 10-90 % percentile of generated forecast errors of an exemplary household and a MAPE of 30 %. 94
5.17 Application case of the forecast uncertainty evaluation. 94
5.18 Participant benefit of two households for a variation of forecast error and penalty prices. 95
5.19 Participant benefit of 20 household participants (consumers) over increasing forecast errors. Penalty price: 2 ct/kWh. 95

5.20 Elapsed solver time over an increasing number of market participants and a variation of the share of participants with a battery storage systems. Constant parameter settings: Number of timesteps: 96, number of nodes: 1, problem formulation: LP. 96
5.21 Elapsed solver time over an increasing number of market participants and a variation of the number of timesteps. Constant parameter settings: Share of participants with battery storage: 50 %, number of nodes: 1, problem formulation: LP. 97
5.22 Elapsed solver time over an increasing number of market participants and a variation of the number of nodes. Constant parameter settings: Number of timesteps: 24, share of participants with battery storage: 0, problem formulation: LP. 98

6.1 Sequence diagram of one market cycle within the field test. 103
6.2 Representation of a typical radial distribution grid topology (a) and the applied fee structure and grid limitations in the field test (b). 105
6.3 Calculated relative daily generation share of local and nonlocal generation during the field test. Data gap in August due to planned downtime of the system. 106
6.4 Calculated relative daily generation share of generation different generation types during the field test. Data gap in August due to planned downtime of the system. 107
6.5 Three example days (12.04.2021 - 15.04.2021) of the generation share within 15 min trading periods in the scenario 2020 *reduced fees*. 108
6.6 Three example days (03.05.2021 - 06.05.2021) of the generation share within 15 min trading periods in the scenario 2020 *regular fees*. 108
6.7 Calculated heatmap of the storage usage throughout the field test. 109
6.8 Calculated heatmap of weighted average buy prices at the LEM within the demonstrator period. 110
6.9 Calculated weighted average buy prices at 8 substations in the field test over the share of generation at the same substation (self-sufficiency). Each scatter represents one substation. 111
6.10 Example of low voltage feeder limits and residual load of feeder #N4 between 05.04.2021 and 10.04.2021. The residual load represents the result of all buy, sell and storage orders traded locally at the feeder. Feeder limits are inputs from the DSO. 111
6.11 Boxplots of the calculated utilization factor at low voltage feeders for all 15 minute intervals during the field test. 112
6.12 Sum of all 15 minute time intervals where a voltage violation is avoided (feeder is fully utilized) during the field test period. 112
6.13 Day-ahead load forecast error of different real participants during the first 4 scenarios of the demonstrator (01.04.2021-30.07.2021) 113
6.14 Example days of the measured and forecasted demand of participant B20 (participant with EV). 114
6.15 Measured heatmap of the electric demand of participant B20 during the first 4 scenarios. 115

6.16 Measured heatmap of the electric demand of participant H26 during the first 4 scenarios. 115
6.17 Example days of the measured and forecasted demand of participant H26. 116
6.18 Example days of the measured and forecasted demand of participant L29 (commercial). 116
6.19 Measured heatmap of the electric demand of participant L29 during the first 4 scenarios. 117

A.1 Temporal sequence of energy and ancillary service markets in Germany. Own illustration based on [185]. 141
A.2 Piecewise linear interpolation of EV consumption dependency of ambient temperature (θ_a) and driving speed for an average vehicle based on [139]. 142
A.3 Probability of arriving at work based on empirical data in [138]. 142
A.4 Overview of tradable electricity product categories on the LEM 143
A.5 Day ahead spot market price and arbitrage opportunities for the time frame 2016-2018 143
A.6 Boxplots of the daily maximum and minimum exchange with the backup utility for a variation of scenario years and REPC scenarios. 147
A.7 Heatmaps for a variation of REPC scenarios. Grid type: Rural, Scenario year: 2035. 148
A.8 Day ahead spot market prices for the zone Germany/Luxembourg at EPEX Spot during the field test. Source: [156]. 149

List of Tables

2.1 Role descriptions and definitions of actors in Local Energy Markets. 19
2.2 Evaluation categories for market design to market feature coverage 24
2.3 Qualitative evaluation of the capability of described market designs to provide market features introduced in section 2.2.2. 25

3.1 Overview of the definition of a generic sell order. 37
3.2 Overview of the definition of a generic buy order. 37
3.3 Overview of the definition of a generic storage order. 38
3.4 Overview of the grid topology input parameters. 41

4.1 Simulation scenario parameters and assumptions for the scenario year 2035. 58
4.2 Overview of parameters and parameter variations of the scalability analysis 72

6.1 Set up of market participants of the field test for the baseline (2020) and expansion (2030) scenarios. 104
6.2 Distribution of Regulated Electricity Price Components (REPC)s for the two fee structure scenarios 105
6.3 Overview of time periods of the field test scenarios years and fee structures 106
6.4 Scenario assumptions for base case, medium and high expansion cases . . 107

A.1 Simulation scenario parameters and assumptions for the scenario year 2020. 144
A.2 Simulation scenario parameters and assumptions for the scenario year 2025. 145
A.3 Simulation scenario parameters and assumptions for the scenario year 2030. 146

Acronyms

ADMM Alternating Direction Method of Multipliers

ANN Artificial Neural Network

AR Autoregressive

BAU Business As Usual

C&I Commercial and Industrial

CB Cost Benefit

CCGT Combined Cycle Gas Turbine

CHP Combined Heat and Power

COP Coefficient Of Performance

DER Distributed Energy Resources

DSO Distribution System Operator

ECW Energy Campus Wildpoldsried

EMS Energy Management System

ES Exponential Smoothing

EV Electric Vehicle

FiT Feed-in Tariff

HH Household

HP Heat Pump

HV High Voltage

HWS Hot Water Storage

ICT Information and Communications Technology

ISO Independent System Operator

KPI Key Performance Indicator

LCOE Levelized Cost of Electricity

LEM Local Energy Market

LHS Left Hand Side

LMP Locational Marginal Pricing

LP Linear Program

LV Low Voltage

MAPE Mean Absolute Percentage Error

MBED Multi-Bilateral Economic Dispatch

MILP Mixed Integer Linear Program

MPC Model Predictive Control

MV Medium Voltage

NRMSE Normalized Root Mean Square Error

P2P Peer-to-Peer

PB Participant Benefit

PCC Point of Common Coupling

PF Persistence Forecast

PTDF Power Transfer Distribution Factor

PV Photovoltaic

RB Revenue Benefit

RE Renewable Energy

REPC Regulated Electricity Price Components

SC Self-Consumption

SGAM Smart Grid Architecture Model

SL Share LEM

SOC State Of Charge

SSR Self-Sufficiency Ratio

SW Social Welfare

TE Transactive Energy

TSO Transmission System Operator

UF Utilization Factor

VPP Virtual Power Plant

VRE Variable Renewable Energy

VSC Voltage Sensitivity Coefficients

Notation

Remarks on nomenclature and notation

Definition of sets, variables and parameters for the main model in this Thesis are listed below. All symbols are additionally defined in the text when introduced or used. In general, variables are defined with upper case letters. Parameters are defined with lower case letters. Superscripts of parameters and variables are descriptive and non-cursive. Subscripts of parameters and variables define variable indices and are cursive. P_t^{in} for example would define the variable P for the index t (e.g., from a set $\mathcal{T}$ of timesteps) specified for inwards direction. Deviations might apply in some contexts. In this case the symbols are specifically defined in the text. Subsets are notated with a subscript. For example, $\mathcal{S}_p$ is the subset of all sell orders $\mathcal{S}$ belonging to a participant p, i.e., $\mathcal{S}_p \subseteq \mathcal{S}$.

Sets

Set	Description
$\mathcal{T}$	Set of T timesteps (indexed with t).
$\mathcal{P}$	Set of P market participants (indexed with p).
$\mathcal{N}$	Set of N nodes (indexed with n).
$\mathcal{L}$	Set of L lines (indexed with l).
$\mathcal{B}$	Set of B buy orders (indexed with b).
$\mathcal{S}$	Set of S sell orders (indexed with s).
$\mathcal{ST}$	Set of ST storage orders (indexed with st).

Variables

Variable	Unit	Description
$P_{b,t}$	[kW]	Active power of buy order b at timestep t
$P_{s,t}$	[kW]	Active power of sell order b at timestep t
$P^{\mathrm{ch}}_{st,t}$	[kW]	Active charging power of storage order st at timestep t
$P^{\mathrm{dch}}_{st,t}$	[kW]	Active discharging power of storage order st at timestep t
$E_{st,t}$	[kWh]	State of charge/filling level of storage order st at timestep t
$P_{(j,k),t}$	[kW]	Active power at line l from node j to node k at timestep t
$P^{\mathrm{in}}_{p,t}$	[kW]	Active power inflow of participant p at timestep t
$P^{\mathrm{out}}_{p,t}$	[kW]	Active power outflow of participant p at timestep t
$P^{\mathrm{in}}_{n,t}$	[kW]	Active power inflow of node n at timestep t
$P^{\mathrm{out}}_{n,t}$	[kW]	Active power outflow of node n at timestep t
$P^{\mathrm{bu}}_{s,t}$	[kW]	Active power of sell order s from the backup utility bu at timestep t
$P^{\mathrm{bu}}_{b,t}$	[kW]	Active power of buy order b from the backup utility bu at timestep t

Parameters

Scope	Parameter	Unit	Description
Sell order	$c_{s,t}^{\min}$	[ct/kWh]	Minimum sell price for each timestep
	$p_{s,t}^{\max}$	[kW]	Maximum power output for each timestep
	$e_{s}^{\max}$	[kWh]	Maximum amount of sold energy
	ε_s	[0/1]	Defines the exclusiveness of the order
Buy order	$c_{b,t}^{\max}$	[ct/kWh]	Maximum buy price for each timestep
	$p_{b,t}^{\max}$	[kW]	Maximum power input for each timestep
	$e_{b}^{\max}$	[kWh]	Maximum amount of requested energy
	ε_b	[0/1]	Defines the exclusiveness of the order
Storage order	$e_{st,t}^{\max}$	[kWh]	Maximum storage capacity
	e_{st}^{ini}	[kWh]	Initial storage capacity
	e_{st}^{end}	[kWh]	Final storage capacity
	$c_{st}^{\text{dch,min}}$	[ct/kWh]	Minimum discharge price
	$p_{st,t}^{\text{max,ch}}$	[kW]	Maximum charging power
	$p_{st,t}^{\text{max,dch}}$	[kW]	Maximum discharging power
	$\eta_{st}^{\text{ch}}, \eta_{st}^{\text{dch}}$	[-]	Charge and discharge efficiency
	$n_{st}^{\max}$	[-]	Maximum number of cycles
Line	j, k	[-]	Start and end node of line
	$p_{(j,k),t}^{\max}$	[kW]	Maximum real power capacity for a specific timestep
	$c_{(j,k),t}^{\text{e}}$	[ct/kWh]	Line energy fee
	$c_{(j,k)}^{\text{p}}$	[ct/kW]	Line power fee
	$p_{l}^{\text{min,p}}$	[kW]	Contracted power above which power fees apply
Node	$p_{n,t}^{\text{max,in}}$	[kW]	Maximum real power capacity for an import to the node
	$p_{n,t}^{\text{max,out}}$	[kW]	Maximum real power capacity for an export from the node
	$c_{n,t}^{\text{e,in}}$	[ct/kWh]	Node energy fee
Participant	$p_{p,t}^{\text{max,in}}$	[kW]	Maximum real power for an import to the participant
	$p_{p,t}^{\text{max,out}}$	[kW]	Maximum real power for an export from the participant
	$c_{p,t}^{\text{e,in}}$	[ct/kWh]	Participant energy fee in

1. Introduction

1.1. Motivation

The ongoing, widespread expansion of Variable Renewable Energy (VRE) technologies is introducing a significant transformation process to power systems world-wide. Traditional power systems with few large-scale power plants are expanded by small- to medium-size Distributed Energy Resources (DER). Renewable generation capacity accounted for 82 % of the global generation capacity additions in 2020 [1]. Alongside with continuously decreasing costs [2] and ambitious emission reduction targets this trend seems likely to continue and accelerate in the coming decades. In countries with already well advanced VRE installations like Germany[1] grid expansion and advanced grid integration measures will be required to achieve the target of 65 % renewable energy in the electricity sector by 2030 [4], [5].

Parallel to this development, the electrification of the sectors heat and transport is envisaged to further decarbonize other major emitting sectors [6]. This electrification process manifests in an increase of electricity demand mainly through Heat Pump (HP)s and Electric Vehicle (EV)s. Like distributed generation assets, these demand assets are dominantly connected to the distribution grid leading to an increase in demand peaks due to high simultaneity factors of, e.g., EV charging processes [7]. Both described trends can lead to critical states in the distribution grid at times of peak feed-in or peak demand.

Besides the described technical developments, the current energy market design in Europe (zonal energy markets) does not consider intra-zonal grid infrastructure constraints and is hence not able to reflect regional scarcity or excess. This leads to increasing costs for system security measures such as redispatch and feed-in management measures, e.g., 1.3 bn. € in Germany 2019[2] [8]. Additionally the uniform, zonal pricing scheme in most European countries does not provide locational price signals which would be needed to steer future generation and flexibility investments to the best suitable regions. At retail level, the consumption tariffs for end-customers are dominated by taxes, levies, and fees. Only a small portion reflects the actual marginal costs of generation, e.g., 12 % in Germany in 2020 [9]. Hence, there is little financial incentive for residential and other small end-customers to flexibly respond to price signals and shift their consumption to times of lower electricity prices (demand response). The same observation holds true for subsidized distributed generation which is remunerated with feed-in tariffs fixed for a certain timeframe. In this case there is no incentive to, e.g., shift the feed-in to times of high consumption with high prices. Asset owners additionally face the upcoming challenge of marketing their generation after the guaranteed feed-in tariffs expire. In the upcoming decade numerous DERs, especially photovoltaic

[1] >1.9 mio installed VRE assets (May 2020) [3] and a share of 42 % of the supplied demand in 2019.

[2] The year 2019 is chosen as a reference here as energy demand decreased in 2020 and 2021 due to the COVID pandemic.

and wind power plants, will leave the 20 years guaranteed feed-in time, but still be technically operable. Fig 1.1 shows this development for solar Photovoltaic (PV) systems in Germany. It is clear to see that especially in regions of early adaption, e.g., in Southern Germany, new ways of marketing this renewable capacity will be required.

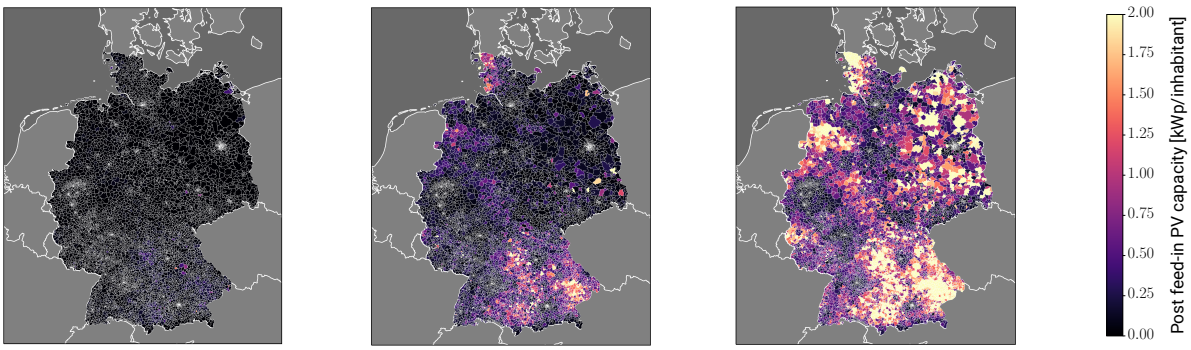

2025 2030 2035

Figure 1.1.: Development of photovoltaic capacities per German postal code and inhabitants which do not receive feed-in subsidies after 20 years operation time. Data is based on the energy market data register [10]. Neglecting degradation and assuming an average technical lifetime of 30 years. Plotting functionality provided by [11].

The concept of automated integration of residential and other smaller consumers into the energy market is nothing new and was already proposed in the 1980s, e.g., by Schweppe et al.:

> "*This sophisticated residential customer under the 24-hour update spot price has a small, special-purpose computer which automatically dials the utility once each day to get the 24 prices for the next day. The computer then controls the space conditioning and water heating to meet this customer's desires (as told to or learned by the computer) with minimum cost.*" [12]

However, until now only few opportunities of small-scale end-customer engagement with energy markets are realized ,e.g., time of use pricing schemes. Increasing demand at end-customer level through EVs, HPs, an increasing amount of prosumer owned VRE and the availability of cheap "special-purpose computers" might be the relevant developments to make the vision from Schweppe et al. [12], [13] now a reality.

Local Energy Markets (LEMs) have recently been proposed as a measure to address the described challenges at the distribution grid level [14]–[17]. A LEM provides a virtual trading layer on top of the existing distribution grid infrastructure enabling formerly passive consumers, producers, and prosumers to actively engage in the energy market. This adds an additional business and information layer on top of the physical layer. Enabling technologies such as smart meters and edge devices are being rolled out and provide the necessary connectivity (information layer) to link the physical asset layer with the virtual trading layer [18]. In contrast to the current market design in Europe, LEMs would allow to address local grid congestions directly in the distribution grids.

Although the regulatory basis for such a concept does not exist yet in most countries, new legislation is on the way to support and enable decentralized energy trading or sharing within energy communities, e.g., in Europe [19].

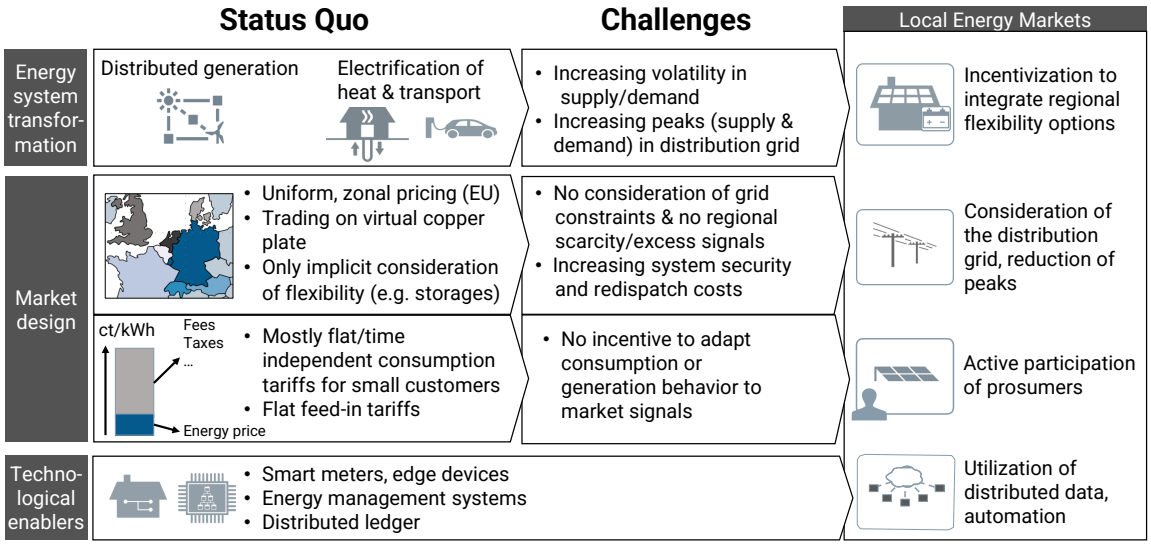

Figure 1.2.: Overview of the current status quo and challenges of the European energy system and the aspects LEMs can address in the future.

1.2. Objective, structure and contributions

The introduction of LEMs to the power system could both facilitate the integration of flexibility inherent in prosumer energy systems and reduce the shortcomings of current electricity market designs by considering regional grid limitations (Figure 1.2). As concepts for LEMs are continuously evolving many questions on the design and operation of LEMs are still uncovered. This Thesis deals with the following main research question:

How can a Local Energy Market be designed to incentivize regional flexibility options and contribute to the grid integration of VREs, EVs, HPs?

In order to answer this question the Thesis is structured as follows (Figure 1.3):
Chapter 2 formulates the problems of the current market designs, evolving grid integration challenges and possible measures to address these challenges. Local Energy Markets are identified and classified as one possible measure to integrate prosumer flexibility and DER. The current state of the art is then examined to determine research gaps and derive more precise research questions. The chapter concludes by defining relevant modeling requirements and the necessary spatial and temporal scope to address the defined research questions.

In Chapter 3 a novel market model and market mechanisms is developed. This market framework, introduced in [20], aims at providing an optimal dispatch of DER within the limits of the distribution grid. A linear-optimization based market matching formulation is proposed to achieve this. Constraints and parameters for the optimization problem are implicitly provided by the participants through market orders. These market orders reflect technical and economic properties of demand, generation, and flexibility of the respective assets. The market model is then further extended to incorporate a simplified grid topology. This allows to not only consider grid constraints during

matching, but also to introduce topology specific grid fees and taxes as demonstrated in [21]. Besides the market model, considered participant models and asset models are formulated in this Chapter.

The methodological and simulative framework to evaluate the proposed market model is described in Chapter 4. A variation of different scenarios for generic distribution grids (rural, semiurban, urban) and the respective residential and commercial market participants are introduced. The generation of simulation scenarios and the input data and expansion scenarios for various penetration levels of DER are described. Different approaches to design the tariff structure in a LEM are specified as well as a benchmark (business as usual) operation scenario assuming no regulatory change. To study the impact of load forecast uncertainty on the LEM a method to generate synthetic forecast errors is developed [22]. Consequently, the evaluation criteria for the following quantitative analysis are introduced.

Chapter 5 is dedicated to the quantitative evaluation of the developed LEM design. In a first analysis, simulation results with a focus on the comparison to the benchmark case are evaluated with regards to the distribution grid type and scenario years. A second, more detailed analysis, focuses on the effect of various grid tariff designs in LEMs introduced in [23]. The impacts of load forecast uncertainty on the profitability of participating in a LEM are subsequently evaluated followed by a scalability analysis of the developed LEM matching algorithm.

Additionally to the simulative evaluation, Chapter 6 provides first results of a real world field test in the pebbles project [24] where the developed market model is implemented at a rural test site in southern Germany. Insights from the field test results are subsequently discussed regarding further design considerations for LEMs.

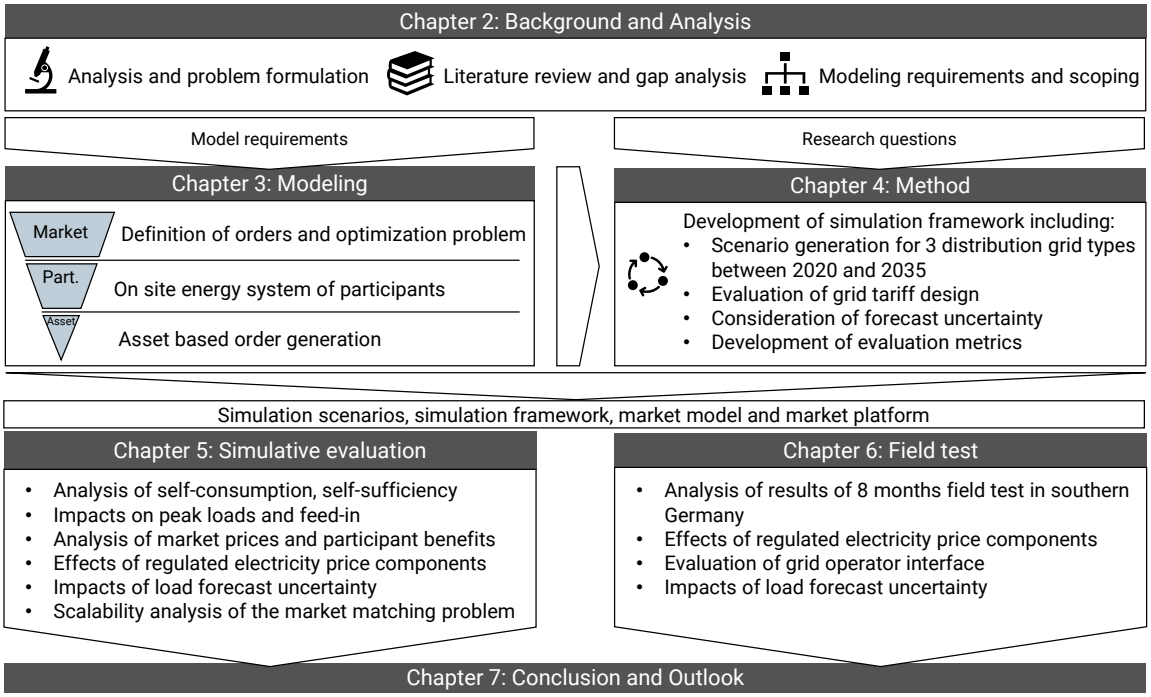

Figure 1.3.: Structure of the Thesis.

Parts of the results of this dissertation have been published in:

[20] S. Schreck, S. Thiem, A. Amthor, M. Metzger, and S. Niessen, “Activating current and future flexibility potential in the distribution grid through local energy markets”, in *CIRED 2020 Berlin Workshop (CIRED 2020)*, 2020, pp. 606–609. DOI: 10.1049/oap-cired.2021.0133.
Author contributions: Conceptualization, Methodology, Software, Analysis, Writing

[21] S. Schreck, S. Thiem, A. Amthor, M. Metzger, and S. Niessen, “Analyzing potential schemes for regulated electricity price components in local energy markets”, in *2020 17th International Conference on the European Energy Market (EEM)*, IEEE, 2020, pp. 1–6, ISBN: 9781728169194. DOI: 10.1109/EEM49802.2020.9221959
Author contributions: Conceptualization, Methodology, Software, Analysis, Writing

[22] S. Schreck, I. Prieur De La Comble, S. Thiem, and S. Niessen, “A Methodological Framework to support Load Forecast Error Assessment in Local Energy Markets”, *IEEE Transactions on Smart Grid*, vol. 11, no. 4, pp. 3212–3220, 2020, ISSN: 19493061. DOI: 10.1109/TSG.2020.2971339
Author contributions: Conceptualization, Methodology, Software, Analysis, Writing

[23] S. Schreck, R. Sudhoff, S. Thiem, and S. Niessen, “On the Importance of Grid Tariff Designs in Local Energy Markets”, *Energies*, vol. 15, no. 17, 2022, ISSN: 1996-1073. DOI: 10.3390/en15176209. [Online]. Available: https://www.mdpi.com/1996-1073/15/17/6209
Author contributions: Conceptualization, Methodology, Software, Analysis, Writing

2. Background and Analysis

2.1. Problem formulation

This section gives an overview over the main technical and economical challenges arising with the large-scale deployment of DER, EVs and HPs. The current energy market design at wholesale and retail level is analyzed in this context. Various measures to cope with the technical and economical challenges are evaluated and LEMs are classified within these measures. The following analysis is focusing on Germany but is also applicable for other countries with deregulated energy markets and an increasing share of DER.

2.1.1. Grid integration

Traditional power systems are designed to supply customers with a few central large-scale power plants from the highest voltage level to the lowest voltage level (top-down). With an increasing number of DER this paradigm currently shifts as decentralized, small-scale power plants are now feeding in mainly at distribution grid level (>90 % [25]) regionally and temporalily reversing the load flow lower to higher voltage levels.

Figure 2.1 describes this transition for the different voltage levels in Germany. In the traditional system design, large coal, nuclear or gas-fired power plants are feeding in at the transmission (220/380 kV) and high voltage level (110 kV). The power is transmitted cross regionally throughout the European transmission grids (horizontal power flow) and then distributed through high- (110 kV), medium- (5-30 kV) and low voltage grids (0.4 kV) to the consumers (unidirectional vertical power flow).

With the uptake of VRE, a bidirectional vertical power flow is introduced as small scale residential PV, utility scale PV and small windfarms are mainly connected to the distribution grid.

Among others, two major technical challenges arise:

1. Balancing of an increasing volatile supply through VRE and mostly inflexible demand on a temporal and spatial dimension to maintain security of supply and frequency stability (global parameters).

2. Regionally concentrated feed-in of DER can compromise the secure grid operation through violations of thermal or voltage limits of lines and other grid infrastructure (local parameters).

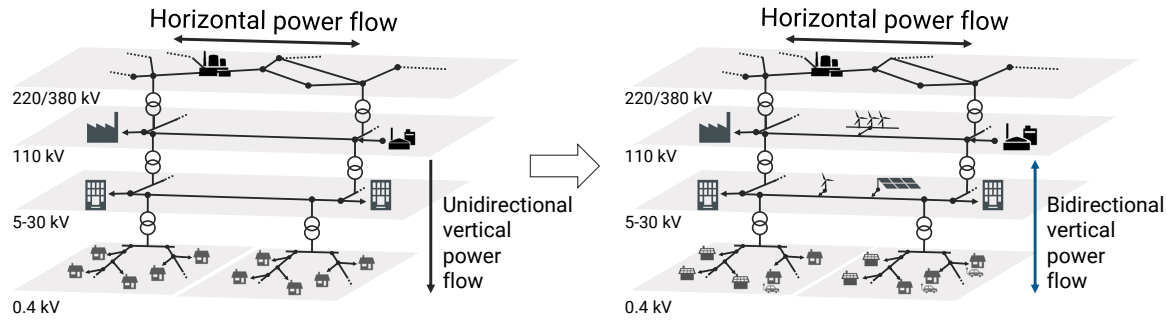

a) Traditional energy system structure

b) Energy system with distributed generation

Figure 2.1.: Simplified representation of the traditional compared to the current/future power system structure.

In the current German power system the main grid integration challenges affect the transmission grid where concentrated, high feed-in of wind power predominantly in the north can cause congestion during the transportation to load centers in the south [26], [27]. Costly congestion management measures like curtailment of VRE or redispatch[1] are applied to guarantee the secure operation of the overall system.

At distribution grid level, the main grid integration challenge lies in the secure operation of the grid in the range of the tolerable power quality limits defined in grid codes, e.g., for voltage in [28]. Especially in rural radial distribution grids, the feed-in of active power from DERs can increase the voltage in the grid above the tolerable limits [29]. Additional demand, e.g., through uncontrolled charging of EVs, substantially decreases the voltage during times of low regional generation [30], [31].

Where high installation density of VRE meets low demand, a reversed vertical load flow is induced in times of high feed-in. Figure 2.2 shows this effect for a low-voltage feeder line with high PV penetration in the village of Wildpoldsried[2] in Germany . The Figure also illustrates the high variability of this reverse load flow due to the cloud-induced volatility of PV feed in, e.g., at midday of June 21, 2018.

Generation capacities in Germany are expected to further increase from 50.5 GW to 75.5 ... 85.5 GW for wind and 42.4 GW to 72.9 ... 104.5 GW for PV for different scenarios of the energy regulator *Bundesnetzagentur* for the year 2030 [33]. Additionally, large amounts of distributed demand through heat-pumps (1.1 ... 4.1 mio.) and electric vehicles (1 ... 10 mio.) are envisaged to foster the usage of renewable power in other sectors. Against this background the described technical challenges will exacerbate, thus requiring advanced measures for grid integration (described in Section 2.1.3).

[1] Imposed interference of the Transmission System Operator (TSO) to the market-determined schedule of power plants to avoid or cure congestion in the transmission grid.

[2] With a feed-in of renewable energy covering 8 times the annual demand [32], Wildpoldsried is a frontrunner of the energy transition.

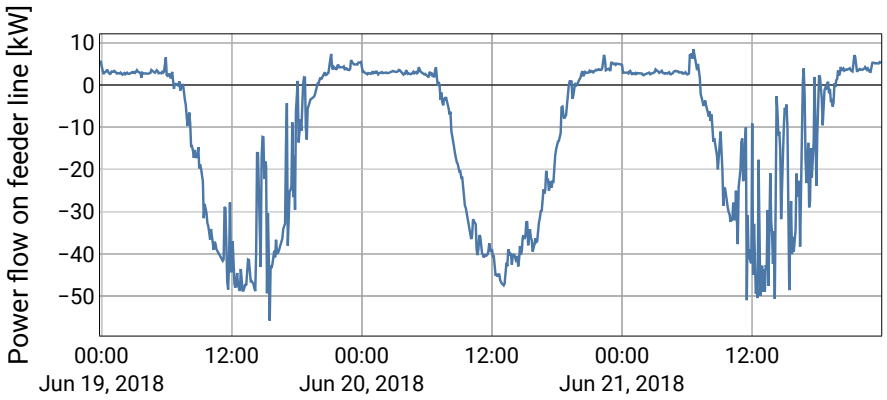

Figure 2.2.: Measurements at low-voltage feeder with high PV penetration on three summer days in southern Germany (Wildpoldsried).

2.1.2. Current market design

Wholesale market

Energy markets can provide a cost efficient short-term coordination of demand and supply as well as long-term investment signals. In liberalized energy markets energy is traded either bilaterally, e.g., through brokers, in so called Over The Counter (OTC) trades or via power exchanges such as EPEX SPOT [34]. Energy can be traded either in advance for long term contracts (futures/forward market) or on spot markets (day-ahead and intraday) for the next day (Figure A.1). In Europe, energy market participants submit bid and ask orders to the power exchanges for a specific bidding zone mostly defined by the country border (Figure 2.3). Trading across zones/countries is possible but limited by interconnection capacities.

Such a zonal market allows a large number of market participants and high liquidity, however, does not account for potential transmission grid constraints within the zones. Therefore, the Transmission System Operator (TSO) needs to account for planned schedules determined by the energy market and react with redispatch or curtailment if they jeopardize secure system operation. In addition to the energy market, the reserve market enables the TSOs to acquire up- downward flexibility, ensuring the balance of supply and demand at all times (see Figure A.1 for details). This is necessary to stabilize the grid frequency due to deviations of the planned generation and demand (compare section 2.1.1).

The day-ahead market at *EPEX SPOT* is organized as an auction with a closed-order book[3]. The orders are formulated as tuples of price and quantity for a specific or multiple hours of the day. Uniform pricing is applied as a pricing scheme setting the price for all market participants to the price the last generation unit needed to serve the demand has bid (Figure 2.4). In a market with perfect competition[4] power producers have an incentive to bid with or close to their marginal costs, i.e., the cost to supply an additional quantity including fuel, CO_2 certificates, etc. [35]. The

[3]Bid and ask orders are submitted until the market closing time (12:00) without disclosure to the market participants.
[4]No market participant is able to affect the market price by bidding prices other than the marginal costs.

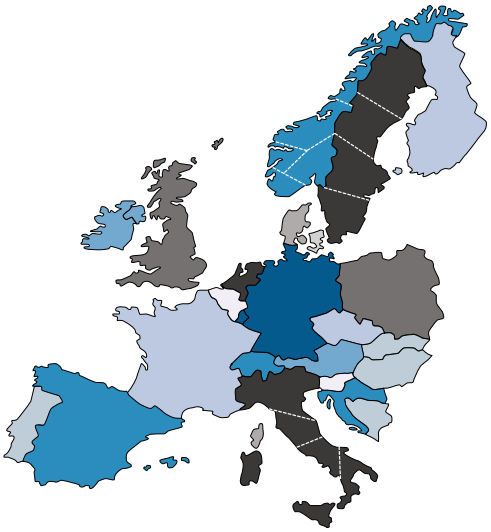

Figure 2.3.: Simplified representation of zonal market bidding zones in central Europe. Dotted lines represent intra-country zones. Status of September 2020.

market price is then determined by the intersection of the mostly inflexible demand curve and the generators marginal costs in ascending order.

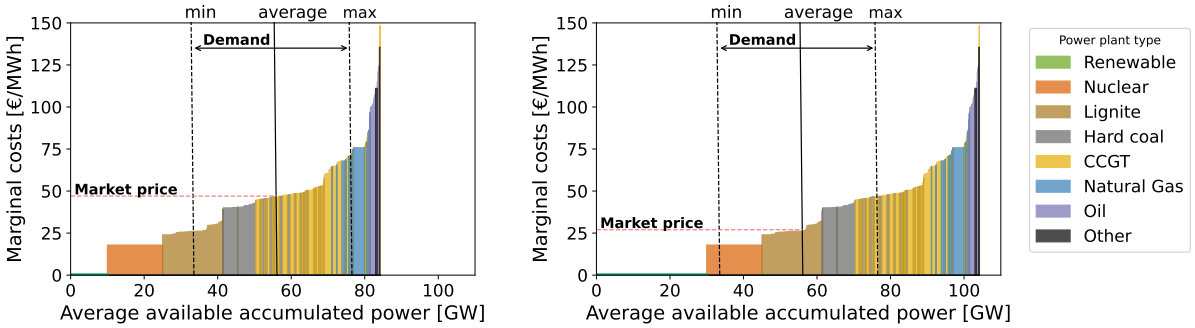

(a) Renewable energy feed-in = 10 GW

(b) Renewable energy feed-in = 30 GW

Figure 2.4.: Merit order curves of power plants for Germany (data for 2019 from [36]) for different renewable energy feed-in scenarios. Total demand ranges and price elasticity derived from [37] and [38].

In this case, generation units bidding below the market price can recover parts of their fixed costs while generation units with operational costs above the market price do not win the bid (so called merit order curve). As shown in Figure 2.4, the market price is mainly determined by two factors. The overall demand influences the price to the extent of the possible ranges between low demand at night and high morning or evening demand. A growing influence on the price is determined by the feed-in of VRE. As they are fueled by solar radiation, wind or water, they bid with zero marginal costs and shift the merit order curve to the right lowering the market price (Figure 2.4 (b)). This so called merit order effect increased the price fluctuation on the energy markets significantly during the last two decades [39], [40].

Strong temporal variability in energy prices could theoretically incentivize the usage of highly needed flexibility [41], i.e., by shifting demand to times of low prices or charging storages at low prices and discharging at high prices. The first concepts of electricity spot markets developed in the 1980s ([12], [13], [42]) already envisaged that the volatile price signals could propagate to end customers and incentivize demand side flexibility. However, these price signals are still not well propagating to consumers and producers at the retail level as outlined in the following section.

Retail market

End-users of electricity such as Household (HH) or Commercial and Industrial (C&I) customers are typically supplied by energy retailers with contracts lasting months to years. Before the liberalization of the electricity markets, few vertically integrated utilities[5] supplied all end-users.

Despite increasing competition on the wholesale market, average retail prices for households increased significantly in Germany over the past decade [9]. While purchasing prices from the wholesale market declined, Regulated Electricity Price Components (REPC)s such as grid fees, taxes and other levies increased. Figure 2.5 shows the decomposed cost structure of one kWh for a residential customer with a yearly demand of 3500 kWh.

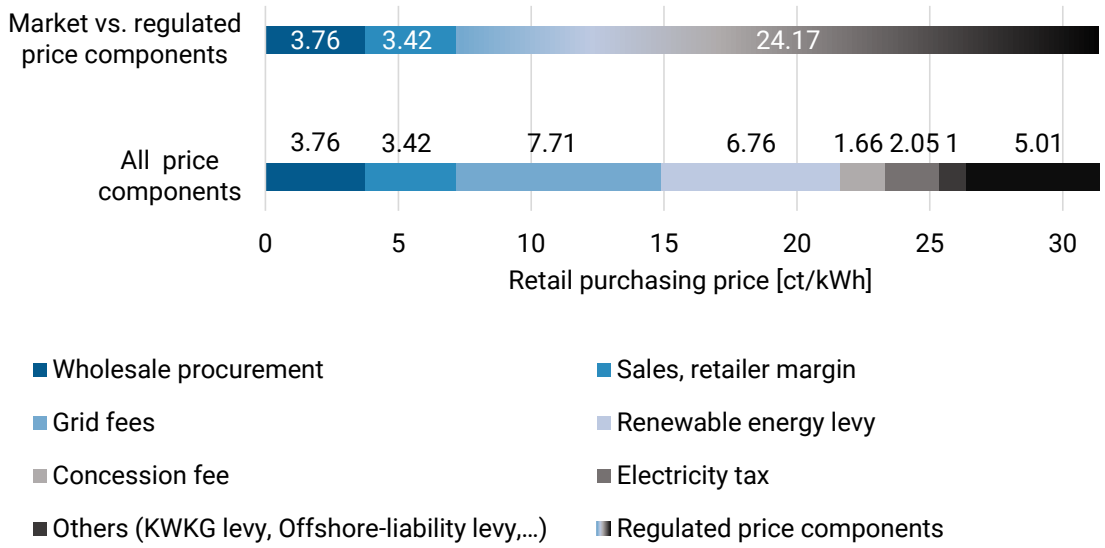

Figure 2.5.: Composition of retail energy prices in Germany (2020) data from [9] and [43].

The actual power procurement costs from the wholesale market only account for about 12 % (3.76 $\frac{ct}{kWh}$) of the overall costs structure. Including sales costs, the margin of the retailer and grid fees needed for the financing and operation of the grid infrastructure, still around 52 % of the costs remain for taxes renewable energy levy and other fees.

For large-scale customers, e.g. industrial customers, reduced REPCs apply increasing the incentive to shift energy consumption to times of low prices. Volatile price signal from the wholesale market do, however, not propagate to small-scale end consumers as the market price only accounts for

[4]Combined Cycle Gas Turbine (CCGT)
[5]An entity operating at all levels of the electricity supply chain through generation, transmission to distribution

a small portion of the overall price which is dominated by constant REPCs. This strongly limits incentives for end-customers to shift their demand to times of low energy market prices. In [44], the authors show that the current regime of REPC highly distorts the operation decision of actors in the power system leading to suboptimal dispatching decisions and efficiency losses. Although there are several tariff structures which offer variable end-customer tariffs, e.g., lower prices during the night for night storage heating, widespread application in Germany is limited [45]. Other approaches to reinforce the propagation of the wholesale market price signal to end customers are discussed in Section 2.1.3.

2.1.3. Measures for grid integration of DER

Various technical and regulatory measures to cope with the described grid integration challenges are discussed in the literature. They can be classified along the dimensions of demand, generation, market and grid (Figure 2.6). Additionally, these measures can be categorized with regards to their application at different states of the grid. The traffic light concepts defined in [46] describes these states as:

- Green: Uncritical grid state, unrestricted trading on markets.
- Yellow: Partial critical grid state, responsible grid operators interact with market participants to establish grid stability.
- Red: Critical grid state, grid operators directly intervene in operation.

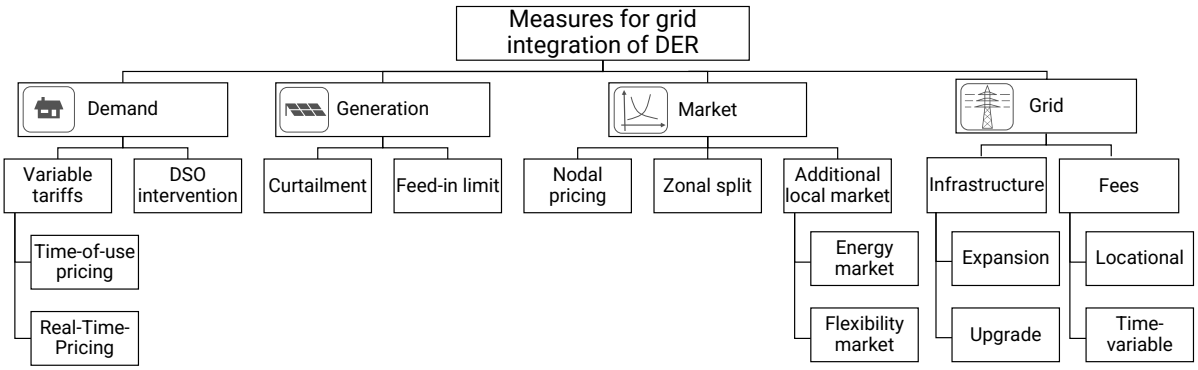

Figure 2.6.: Overview of measures to improve grid integration ranging from demand and generation side measures to market and grid adaption

In this section, measures for grid integration shown in Figure 2.6 are analyzed and classified in the context of the traffic light concept for distribution grids. LEMs are then identified as one solution combining several aspects within the range of measures.

Demand

Variable tariffs

In order to activate demand side flexibility through price signals, various schemes for variable tariffs are possible [47]. Variable tariffs can take effect in the green grid phase, when applied to

a significant share of end consumers, they could shift demand away from peak consumption to peak feed-in of VRE. Static time-of-use pricing defines fixed time blocks throughout the day with varying prices, e.g., day-night tariffs, to roughly reflect the peak demand in the grid. These tariffs are rather easy to implement, however, only approximate the actual grid situation based on typical demand patterns. The actual situation of demand and supply is not reflected which can differ substantially due to VRE feed-in.

Dynamic real-time pricing tries to overcome this issue by propagating the time varying supply and demand situation, i.e., the wholesale market prices, to the end customers. This can be achieved by dynamization of REPCs such as grid fees or other levies such as the renewable energy levy as proposed in [45], [48]. However, an implementation of such a concept is complex and implies high transaction costs [44].

For both approaches to variable tariffs it should be mentioned that the potential of this measure is highly limited due to the low and time-variable short-term price elasticity of residential customers [49]. To harvest the full potential, the operation of the residential energy system has to be automated and optimized on the basis of the price signal [50]. In this case, further flexibility potential , e.g., of home battery storage systems, can be tapped into.

DSO intervention

Grip operators are empowered to switch off so called interruptible loads in critical grid situations (red grid phase) [51]. This affects energy intensive industry process (TSO level), but also devices with a relatively high peak demand such as HPs, electric heating and possibly EVs in the future. Direct DSO interventions can be seen as a curative measure and are only allowed for critical grid situations as they interfere with the operation of the on-site devices of the customer.

Generation

VRE can be marketed via constant feed-in tariffs or through direct marketing, i.e., directly selling to the wholesale market. Direct marketing of VRE, e.g., aggregated in a Virtual Power Plant (VPP) combining multiple DERs, allows to optimize generation based on wholesale market prices. The main instruments to reduce feed-in peaks of VRE are active curtailment and feed-in limits.

Curtailment

Like the direct intervention of grid operators to reduce loads, generation from VRE can also be reduced or curtailed. Plant operators have to provide the grid operator with an interface to reduce the feed-in power [52]. This affects mostly larger installations, e.g., installations larger than 30 kWp for PV. Although curtailment is only used to prevent or relieve congestions in the red phase, in Germany around 5.4 TWh were curtailed in 2018 [26].

Feed-in limit

Besides the curtailment of VRE, feed-in limits are implemented which constrain the maximum power output to a certain share of the nominal peak power. Feed-in of PV power plants is, e.g., limited to 70 % of the nominal capacity of the plant for certain ranges of the rated power [53]. Government subsidized coupled PV and battery systems are even limited to 50 % of the nominal

PV capacity [54]. Weniger et al. [55] show that this limitation only causes a minor reduction of energy yield through curtailment and a slight self-consumption decline, however, only if a Model Predictive Control (MPC) is implemented. If the on-site energy system is operated using typical rule based management, i.e., charging the battery if the feed-in is greater than the demand, average curtailment losses of 8 % are to be expected [55].

Market

As described in Section 2.2.3, energy markets in most European countries are structured as a zonal market with uniform pricing. While providing high liquidity and low opportunities to exercise market power, these zonal markets do not provide locational price signals which might lead to inefficient operation and investment decisions on the generation and flexibility side [56], [57]. Additionally, extensive grid expansion is necessary to ensure the matching of demand and supply in the long run, e.g., if generation capacity is locally concentrated and far from load centers. Several approaches to adapt or extend the current market design, based on the findings in [56], [58], [59], are described and discussed in the following subsection.

Nodal pricing

Nodal pricing, also called Locational Marginal Pricing (LMP), considers the grid limitations during price determination. To achieve this, an Independent System Operator (ISO) calculates the economic dispatch of the market including the grid topology and its limitations. If there is no anticipated congestion in the grid, i.e., the grid does not operate at its limit to serve the load, a uniform market price is determined for the overall market. However, if certain lines are congested the prices at the nodes affected by the congestion diverge. This scarcity signal reflects the need for expansion measures and can lead to a more efficient grid expansion and allocation of generation and flexibility. As a nodal pricing scheme only allows a power plant dispatch compliant with grid limitations it can be seen as a preventive measure for grid congestion opposed to the curative measure of redispatch after the market matching in a zonal market (compare Section 2.2.3).

The operation of a nodal market, as, e.g., applied in multiple US states/systems, requires the ISO as an entity operating both the spot market as well as the transmission grid or at least needs sufficient information on the grid topology and its limitations. Additionally, the generated locational price signals do not necessarily justify long-term investment as they are subject to short-term change due to grid or generation expansion [60].

Zonal split

If intra-zonal congestion is structural or increases over time, a splitting of the market zone along the major grid bottlenecks can induce regional price incentives for generation and flexibility as well as for expanding the grid capacity between zones. Compared to the introduction of nodal pricing, this approach is less complex and does not imply structural changes such as the introduction of the role of an ISO. Trepper et al. [61] show that such a zonal split in Germany into a Northern and a Southern zone could reduce upcoming increasing congestion events.

On the other hand, this zonal split comes with the effect of undesirable distributional effects as prices for consumers in the South would increase. Another shortcoming of this approach compared

to a nodal pricing scheme is that grid congestions are dynamic and change over time, hence the zonal borders would ideally need to be adapted permanently. Additionally, intra-zonal congestions are also not accounted for during the day-ahead market matching which again requires redispatch measures.

Additional local markets

In addition to the zonal energy and reserve market, additional local markets are recently discussed to address and integrate the increasing flexibility of DER into the energy market. Two types of markets need to be differentiated. Local flexibility markets aim to empower DSOs to procure up- and downward flexibility in their distribution grid area for the yellow grid phase [62]. Additional local energy markets or regional order books as, e.g., described in [63], aim at increasing the scope of the energy market to small prosumers and generate locally highly resolved price signals. The introduction of additional local markets, however, needs to be accompanied with an appropriate regulatory framework to account for the increasing market power or possible market-distorting gaming on multiple markets as described in [56].

Grid

Infrastructure expansion

Clearly, the most straight-forward approach to solve grid congestions in the long run is to expand the grid infrastructure accordingly. This however requires long planning and implementation effort and high costs [5], [33]. Grid expansion, however, might not be the most cost effective measure to cope with rarely occuring congestions. The process of grid expansion can additionally be prolonged when the regionally affected population is not satisfied with the process and the planning is challenged through protests [64], [65].

Infrastructure upgrade

The necessary expansion of the grid can be limited by the implementation of feed-in limits as described above, but also through the upgrade of existing grid infrastructure. The application of innovative electrical equipment such as smart transformers[6] might lead to a reduction of the necessary grid expansion costs of more than 20 % [5], [25].

Locational grid fees and tax exemptions

To foster the regional installation of generation assets and hence reduce necessary transmission capacities, locational grid tariffs can be applied. This could, e.g., be a reduction of certain REPCs for consumption of electricity generated within a certain regional scope. In Germany, e.g., there is an exemption from the electricity tax for small power plants (< 2MWp) if the distance between seller and buyer is less or equal to 4.5 km [66]. In Austria, a similar approach is planned, i.e., a reduction of REPC for exchanges within renewable energy communities [67].

Storage flexibility

Flexibility, e.g., provided by battery storages, is not explicitly shown in Figure 2.6, because it can be applied as a grid integration measure at multiple dimensions. An increasing number of residential storage systems are recently deployed in the German energy system [68]. Currently,

[6]Local substations or transformers capable of automatically steering the voltage between the tolerable limits through tap changes.

the main use case for these storages at the residential domain is to increase the self-consumption of generated electricity behind the meter [69]. This use case is profitable, as, for most parts of the country, the Levelized Cost of Electricity (LCOE) for a PV-Battery system has fallen below the price of utility electricity. In this case they can be used to shift peak generation to times of peak demand by storing generation which would be otherwise curtailed, e.g., solar PV at midday, and supplying peak demand (e.g., EV charging at the evening). Klein et al. [70] show that the most economical operation of residential storage, a maximization of self-consumption, prevents the usage of this flexibility in a "system-friendly" way[7]. Other operation strategies of PV-battery systems, e.g., based on wholesale market price signals, are uneconomical due to high REPC and constant feed-in tariffs (as described in section 2.2.3). In [71], the authors show that a flexible operation of PV-inverters and battery storages can significantly increase the hosting capacity of PV in distribution grids up to 45 % without the need for costly grid expansion.

2.2. Local Energy Markets

The previous section introduced present and upcoming challenges arising with the grid integration of DER and possible measures to cope with these challenges. In this section Local Energy Markets are introduced as one of these measures. First, a taxonomy of roles and actors in Local Energy Markets is developed. Relevant market features and requirements are then derived from the grid integration challenges. Common market designs found in the literature are evaluated with regards to market features and technical maturity. From this research gap analysis, relevant research questions, covered in this Thesis, are then derived.

2.2.1. Roles and actors

This subsection provides an overview of roles and actors within the context of LEMs. This taxonomy is required to later classify existing market design concepts of LEMs and put the market framework, developed in this thesis, into context.

Figure 2.7 shows the main roles required for the operation of a LEM. Most of the roles already occur in the current energy system landscape, however, the entities or actors which fulfill these roles are not yet defined and might be different for each regulatory framework. The following role and responsibility descriptions are focused on the German energy market, however have similarities to other liberalized energy markets.

Table 2.1 describes the roles and possible actors to fulfill these roles. This description has no claim to completeness, but shall provide the reader with some definitions for further analysis.

As described in [72], the different roles and especially the role of the LEM operator are not yet well defined. Depending on the market design (compare Section 2.2.3) this role can be seen as an auctioneer, aggregator or middleman for trading with the wholesale market. Also it should be mentioned that one actor might fulfill multiple roles. An energy retailer could for example act as both, the platform operator, and the balance responsible party.

[7] For example reducing consumption or feed-in peaks.

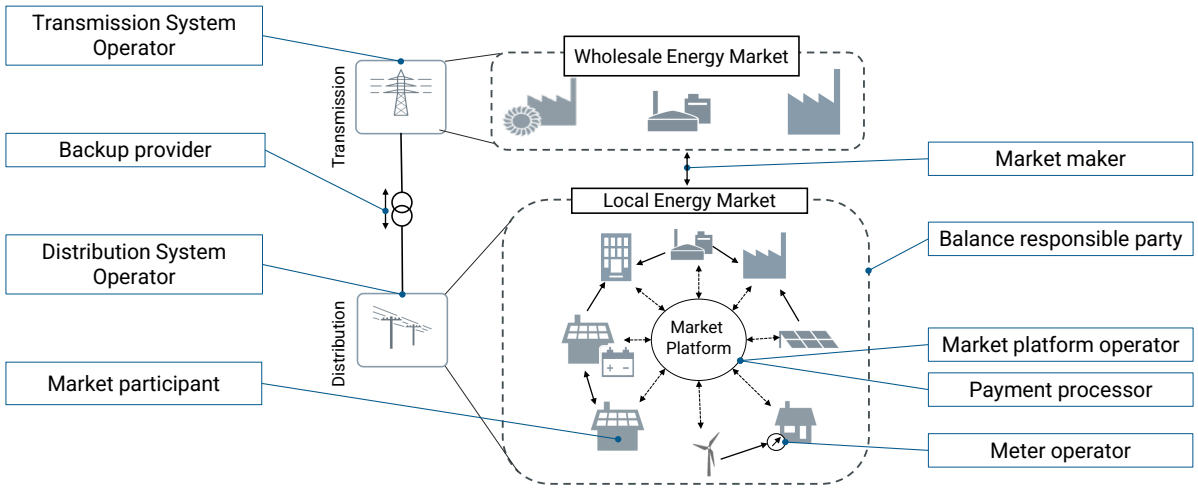

Figure 2.7.: Overview of roles within the context of local energy markets. Roles can be fulfilled by various actors in the energy system. Table 2.1 provides details on the roles and possible actors.

Table 2.1.: Role descriptions and definitions of actors in Local Energy Markets.

Role	**Role description in the context of LEMs**	**Possible actors**
Backup provider	Supplies locally unmatched demand or buys unmatched generation.	Energy retailer, aggregator
Balance responsible party	Procures imbalance energy for mismatch between forecasts and measurements at the LEM.	Energy retailer, DSO, aggregator
Distribution System Operator (DSO)	Responsible for the reliable operation of the distribution grid. Communication of grid limitations to market operator to ensure trading within grid constraints.	Distribution System Operator (DSO)
Market maker	Provides liquidity on the local market, e.g. through bidding and offering at a proxy of the wholesale market prices.	Energy retailer, energy trader, energy utility
Market participant	Owns or manages generation, consumption or flexibility assets in the spatial proximitiy of the LEM. Sends orders to market operator. Operates assets based on market results.	Consumers, producers, prosumers, flexibility providers, aggregators
Market platform operator	Receives orders of participants. Calculates market matching. Sends results to participant.	Energy retailer, DSO, technology provider, possibility for new actors
Payment processor	Handles clearing, billing, financial settlement and credit risk.	Banks, Fintechs
Meter operator	Operates measurement devices at participant site. Communicates measurements to 3rd parties (e.g. DSO, retailer).	DSO, meter operator, possibility of new actors

2.2.2. Market features

In order to address the challenges of grid-, market- and prosumer- integration described in Section 2.1 a LEM has to provide several features. These market features are derived as requirements for a market design based on the previous analysis and serve to classify the state of the art in the following section.

1. **Optimal dispatch of distributed generation and demand**
   To tackle the challenges of grid integration, one of the key features of a LEM is the cost optimal coordination of increasing DER deployment.

2. **Consideration of flexibility**
   Peak loads and peak feed-in will be the main challenges regarding the integration of HPs, EVs and VRE. A LEM has to consider and incentivize demand- and generation-side flexibility as well as storage flexibility to reduce peak loads and feed-in in the grid.

3. **Consideration of grid infrastructure**
   To account for the limitations of local grid infrastructure, the LEM should incorporate information on the grid infrastructure (e.g., the grid topology or maximum power limits) during the market matching. With this information, consumption and feed-in can be limited (compare Section 2.1.3). Additionally, demand-, generation and storage-flexibility can be utilized to reduce peak demand and feed-in at specific nodes in the grid.

4. **Participation incentive**
   In addition to the technical market features, a LEM also has to incentivize participation.

   - Financial incentives: For a purely rational market participant, participation at the LEM has to be financially beneficial compared to other opportunities like direct delivery from retailer (demand) or a constant feed-in tariff (generation). This can for example be achieved through the adaption of reduced REPCs for local energy trading as described previously in Section 2.1.3. An additional feature of the market design is to derive price signals for investments in specific asset types, i.e., for a region with a low share of renewable generation the market prices should indicate a high benefit for additional generation whereas a region with a large share of renewables should rather indicate high benefits for additional load.

   - Participant preferences: Despite purely financial incentives, market participation can also be driven by "soft" incentives such as buying electricity directly from the neighbor or buying based on personal preferences such as a preference for green and local electricity [73]–[76].

5. **Autonomy and privacy of participants**
   Compared to a direct intervention on the market participants energy system (e.g., intervention of a DSO), the operator of a LEM should not directly interfere with appliances "behind the meter" of the market participant to avoid a deprivation of the participants autonomy.

The listed features focus on the use case of a LEM to harvest the technical potential of assets of market participants for grid integration. Additional desirable economic properties of energy markets, e.g., market efficiency, incentive compatibility, cost recovery or revenue adequacy [12], [77] should be considered in detailed economic evaluations. Additionally, careful consideration should be given to the possibility of strategic behavior of market participants.

2.2.3. State of the art

While first approaches of local coordination of DER through markets were already proposed in 2009 [14], increasing challenges of system integration, prosumer-engagement and large scale deployment of Information and Communications Technology (ICT), the research field is growing rapidly in the last decade (Figure 2.8).

Zhou et al. [78] reviewed 30 journal papers on P2P energy trading. They identified the main research foci as market design and trading platform followed by social science perspectives, physical and ICT infrastructure, and policy. Besides academic research, various pilot and commercial projects are deployed world-wide (e.g., [24], [79]–[84]). In [78] the authors also reviewed 20 pilot projects of which almost all projects used distributed ledger technologies such as blockchain to facilitate local energy trading.

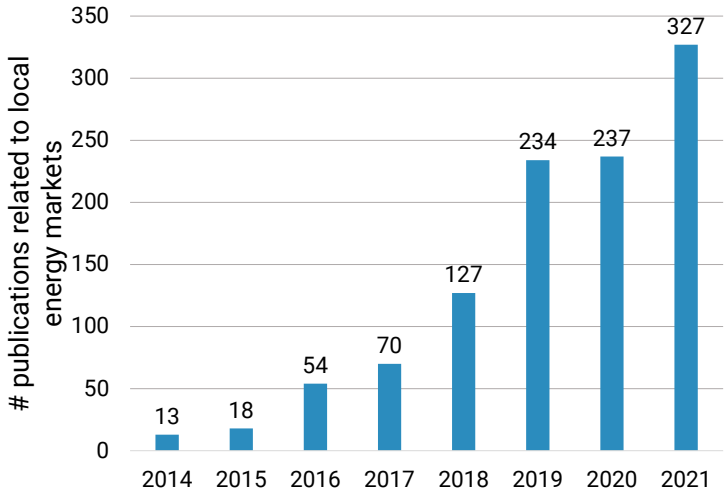

Figure 2.8.: Number of scientific publications queried from *google scholar* [85] advanced search using the terms: "Local energy market" OR "Peer to Peer energy" OR "Transactive energy" in the title. Date of queries: 15.08.2022

The following sections provide a characterization and analysis of typical market designs, market matching algorithms and market features. On this basis, the research gap and a distinction of this thesis from previous research is formulated.

Market design

Market designs for LEMs are typically divided into three categories: 1) Decentralized or Peer-to-Peer (P2P), 2) Distributed or community and 3) Centralized or coordinated (Figure 2.9). The following subsection provides an overview of these concepts and works out advantages and disadvantages.

1. Decentralized/P2P

In a P2P market, both the information exchange on either volume and/or price and the resulting energy contracts are organized in a decentralized fashion without a central coordinator. Instead,

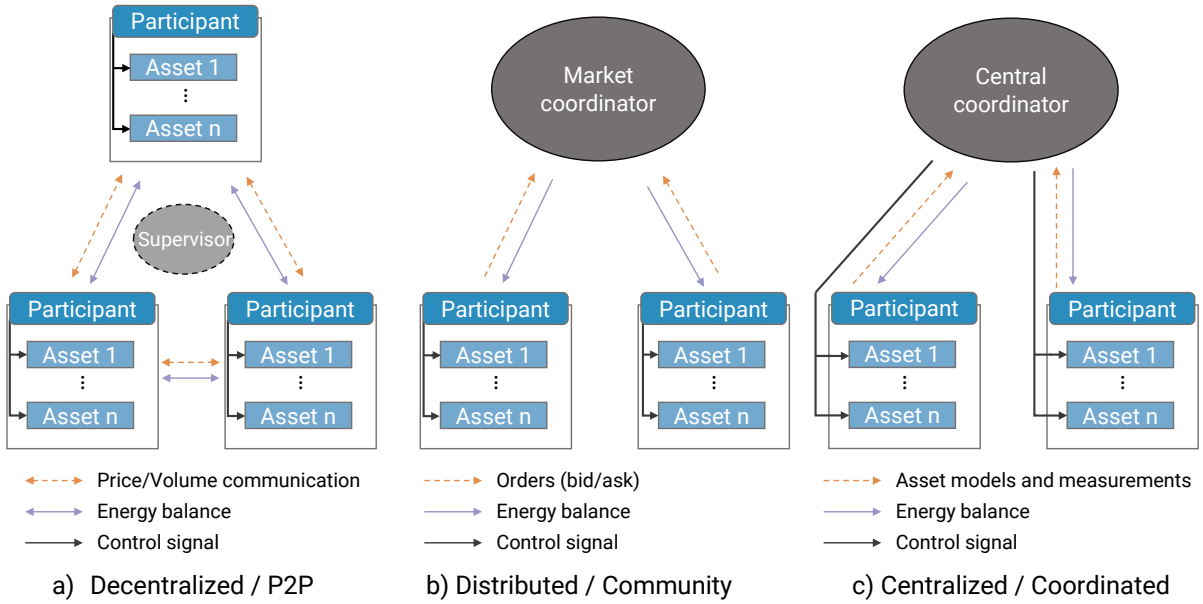

Figure 2.9.: Simplified overview of possible market architectures for local energy markets. Own illustration based on [78], [86].

the role of the market operator can be defined as a supervisor which is responsible to control and enforce market rules. The advantage of this approach is that participants keep full autonomy and privacy on the information and control of their assets behind the meter [87]. Additionally, the social factor of participant engagement, i.e., the gained ability of a participant to virtually exchange energy directly with a peer, is fostered in such a system.

However, in a purely decentralized negotiation set up, necessary information exchange between a number of participants n scales non-linearly with an increasing number of participants. In a fully connected graph $(n-1) \cdot n$ information exchanges would be necessary for one negotiation step. First research shows that this scalability issue can be tackled by applying relaxation techniques to decrease the amount of necessary communication.

A Multi-Bilateral Economic Dispatch (MBED) formulation is proposed by Sorin et al. in [88]. They propose a novel algorithm for decentralized optimization (Relaxed Consensus + Innovation). Their approach shows results close to the global optimum (deviation of a few percentage) after an average of 298 iterations. As their simulation use case covers 12 participating agents and a simplified economic dispatch problem, scalability of this approach is not covered in detail.
Another way to reduce the communication overhead is to form coalitions within the P2P market. This approach is, e.g., described in [89], where the authors introduce a blockchain based Multi-Agent coalition network leading to increased scalability.
In other approaches in the literature, distributed optimization methods are applied. Mostyrn et al. [90], for example make use of the Alternating Direction Method of Multipliers (ADMM) to find a solution to the nested optimization problem. They can show that their optimization approach works for several participants, but scaling up the number of participants is not covered.

The rather complex formulation of these, until now theoretical, approaches requires fast response

and information transportation times between participants or intermediaries. In a real system, this could lead to problems due to package losses, asynchronous responses or the lack of a sufficiently fast transfer rate [91].

Besides this issue, the lack of a central coordinator also limits the ability of the system to incorporate information of third parties like the DSO to account for grid constraints within the distribution grid [87], [92]. The lack of full information on all system parameters also complicates the calculation of an optimal dispatch of all generation demand and storage assets throughout multiple time steps and might lead to suboptimal results.

2. Distributed/Community

Distributed market designs, also referred to as community market, share properties of decentralized and centralized solutions. The market operator acts as a coordinator or auctioneer receiving information on price and energy through market orders from the participants. After performing the market matching (compare Section 3.1.2), the resulting energy balance and price is sent back to the participants. The market participant in turn need to control their respective assets to obey the contracted energy at the Point of Common Coupling (PCC)[8]. With this setup, the necessary information flow and revealed parameters of each participant can be limited to one set of parameters defined in an order, e.g., energy and price limit. The central formulation of the market matching allows to obtain optimality in the overall objective function (e.g., Social Welfare (SW) maximization, cost minimization, CO_2 minimization). However, the optimality of the market matching with regards to the overall system operation is limited to the set of parameters submitted by the participants and defined in the market design.

El-baz et al. [93] propose a double-sided auction[9] for energy trading in microgrids. A home energy management system is operating the participants assets and communicates the asset specific demand and generation via buy and sell orders to a market platform operator. By shifting demand to times of high feed-in from renewables, an increase of self-consumption and self-sufficiency can be observed.
In [94], the authors propose an iterative mechanism for energy trading with a central market operator as an Energy Sharing Provider (ESP). They also report an increase of locally consumed PV energy and cost savings for the prosumers compared to constant feed-in tariffs.

In principle, the distributed energy market design allows the market operator to incorporate information from third parties, e.g., grid operator or energy retailer (wholesale market coupling), however, this has not yet been studied in detail. Distributed energy market designs lack the feature of providing "real" or direct P2P interaction between participants which would reduce responsibilities of a market operator.

3. Centralized/Coordinated

In a centralized local energy market design, the market operator acts as a central controller of the assets of the participants. To achieve an optimal operation of the energy system, full asset models and parameters and measurement information is provided to the market operator. This

[8] Interconnection point of the participants energy system with the public grid.
[9] Buyers and sellers can submit tuples of energy and price limits.

leverages the advantage that a centralized control can provide an optimal solution with regards to the optimization target. Also, third party parameters such as grid constraints can be directly incorporated in this optimization. Additionally, the central coordinator can directly steer assets based on a request from a grid operator to ensure the save operation of the grid in the yellow or red phase. Centrally coordinated markets can be compared to economic dispatch problems using model predictive control. These are intensively studied in the literature (e.g., [95], [96]).

On the other hand, a centralized approach interferes with the data privacy and autonomy of the market participants in operating their energy system. Regarding the increasing number of distributed assets (as shown in Section 2.1.1), solving such a complex problem in a central way is computationally challenging. Yet, there are theoretical approaches and studies to overcome this issue, e.g., through graph theory based algorithms [97].

The exploitation of market power can be an issue in energy markets with imperfect competition [98]. Both decentralized and distributed market set ups can be affected by market power. Due to their small scope in terms of installed capacities, dominant players, e.g., with large generation units, can influence market prices.

2.2.4. Research gap analysis

Market design

Table 2.3 provides a qualitative assessment of the described market design categories with respect to the desired market features. Based on the analysis of the three market design categories in Section 2.2.3, the implementation feasibility of the market features are evaluated with following categories:

Table 2.2.: Evaluation categories for market design to market feature coverage

Quality	Description
++	Market feature can be fully covered by the market design
+	Market feature can be partially covered the market design
0	Market feature could be covered by the market design, but is currently not found in the literature
-	Market feature can be covered by the market design with high implementation effort
- -	Market feature can not be covered by the market design or only with very high implementation effort

In summary, market designs with a centralized coordinator are best suited to tackle the technical challenges described in Section 2.1. However, they lack the capability of enabling and incentivizing prosumers to become autonomous participants in the energy market of the future. On the other hand, purely decentralized P2P designs operate without an intermediary guaranteeing full autonomy and privacy of participants. Yet, an optimal dispatch of the energy system with consideration of 3rd party information like grid constraints is highly limited and only approachable with complex interaction schemes.

Distributed market designs provide an interim solution between the P2P and centralized approach. However, the consideration of flexibility, optimal dispatch and grid limited trading have not yet been addressed in detail in the literature. In [93], e.g., storage flexibility and grid constraints are

Table 2.3.: Qualitative evaluation of the capability of described market designs to provide market features introduced in section 2.2.2.

Market feature	Market design		
	P2P	Distributed	Centralized
1. Optimal dispatch	-	0	++
2. Consideration of flexibility	-	0	++
3. Consideration of grid infrastructure	- -	0	++
4. Participation incentive	++	+	-
5. Autonomy and privacy of participants	++	+	- -

not explicitly considered in the optimization problem of the market operator. In The developed market design in this Thesis (section 3.1) tries to fill this gap by extending the functionality of distributed energy market designs to account for the consideration of grid constraints, flexibility incentivization and optimal dispatch (Figure 2.10).

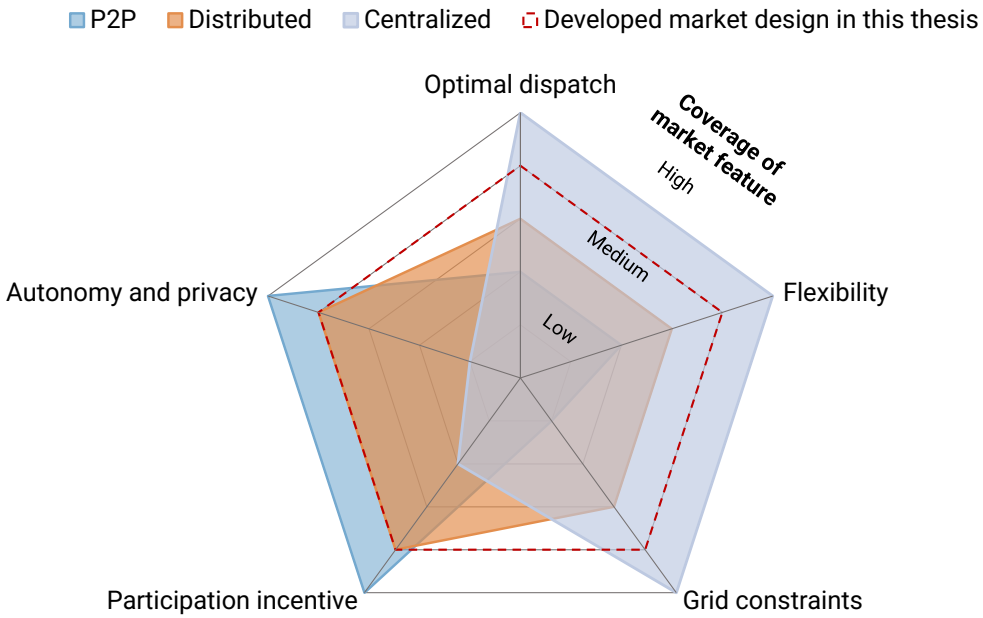

Figure 2.10.: Radar chart of evaluated market designs and scope of this Thesis based on qualitative assessment (Table 2.3)

Aspects of real-world application

Besides the described research gap regarding the theoretical market designs, there is also a broad range of in research concerning the technical maturity or real-world applicability of LEM designs. State of the art research can be subdivided into three categories ranging from rather methodology-focused theoretical research over comprehensive simulations to first pilot projects. Along this range, the addressed market features differ significantly. Figure 2.11 shows a categorization of market

designs in the literature with regards to the technical maturity and addressed market features, which are described in the following sections.

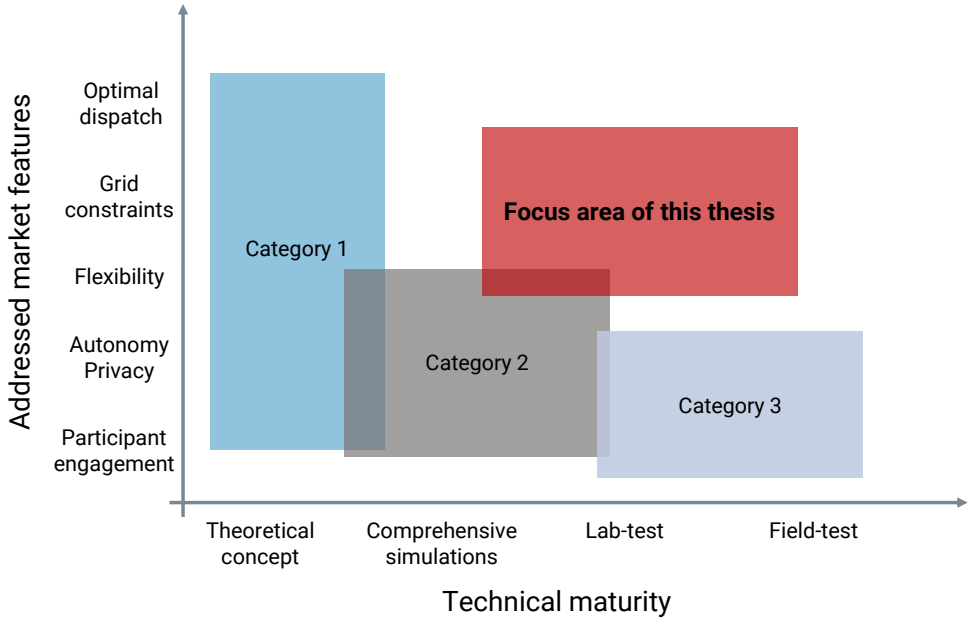

Figure 2.11.: Categorization of reviewed literature in the field of LEMs and the focus of this Thesis with regards to addressed market features and technical maturity.

Category 1

The reviewed literature in Section 2.2.3 mainly focuses on theoretical market designs and concepts. Research in this category covers detailed work on a wide range of certain aspects like game-theoretic modeling of participants, negotiation mechanisms for P2P trading, consideration of grid constraints or computational properties of local energy trading.
Chakraborty et al. [99], for example propose a scalable P2P negotiation scheme with full autonomy and privacy of participants aiming at an increase of system efficiency through optimized flexibility dispatch. In a first use case with simulations of example days, they show that their approach increases social welfare and system efficiency through decentralized coordination. The effects of local energy trading on the distribution grid are not covered in their research.
This aspect is covered, e.g., in [100] where the authors propose a P2P framework which only allows trading within the grid constraints of the low voltage network. They use an iterative scheme estimating the impact of trades on the grid via Voltage Sensitivity Coefficients (VSC)s and Power Transfer Distribution Factor (PTDF)s. In a test scenario, they show that the proposed method is able to operate the distribution grid within its limit while increasing the exported energy of prosumers compared to other approaches like constant upper limits for generation. While this approach is well suited to tackle grid-integration challenges, the approach requires access to the detailed grid topology data of the DSO and the involvement of the DSO in the iterative P2P trading process. This requires a complex interaction between the market platform operator and third parties such as the DSO and might be a blocker for realization.
Ghorani et al. [101] investigate various bidding strategies of market agents in local energy markets. They show that profit/losses of every participant is highly depending on the agent's bidding strategy.

In [90], the authors provide a comprehensive P2P market framework ("Multi-Class energy management") enabling trading of specific energy products (e.g., green energy, subsidized energy, grid energy) instead electricity as a commodity. They propose an Alternating Direction Method of Multipliers (ADMM) based market matching mechanism considering the constraints of the distribution grid, however, requiring a complex iterative communication between prosumers and platform agent.
The mentioned papers serve as examples of research in Category 1. All market features described in Section 2.2.2 are addressed in this category through detailed mathematical analysis and methodological work. However, most of the studies are limited with regards to comprehensive stimulative assessment of the approaches, i.e., most studies are only evaluated through stimulative studies using dummy data or sample days. More importantly, real-world application of the approaches might be limited due to complex negotiation schemes [91], [102], or the neglection of imperfect information amongst the actors in a LEM environment (e.g., between the DSO and the market operator).

Category 2

Category 2 covers simulative studies on LEMs as well as hardware and software architecture designs and first lab-test. The focus of addressed market features is reduced compared to Category 1 to rather simple market designs with regards to communication effort, i.e., auction based markets instead of multi-bilateral negotiation schemes. Still, market features like flexibility, autonomy, privacy and participant engagement are addressed.
In [93], the authors introduce a market design based on the physical properties of the assets of the participants, e.g., PV, EV, HP, CHP. They propose a model architecture where each prosumer is equipped with an energy management system and a market agent controlling the specific assets via a device controller. Comprehensive simulation based on weather data, detailed building models and physical device models show that the proposed double-sided auction can significantly increase the self-sufficiency and self-consumption of the overall system while reducing CO_2-emissions through harvesting the flexibility of distributed assets. Measures to directly reduce grid-constraint violations or other interfaces to the DSO are not covered in this research.
Bullich-Massagué et al. [103] describe a hardware and software architecture for local energy markets based on the Smart Grid Architecture Model (SGAM). The proposed communication architecture based on several cloud services (market service, metering service, control services) allows a a direct communication of set points to DER unit controllers via a communication platform. They test this system in a laboratory environment emulating loads, batteries and PV. In [104], they build on this architecture to introduce a model for a local flexibility market allowing the DSO to optimally schedule and activate flexibility from DER. They cover the use case of flexibility procurement for a DSO, however, do not address the optimal dispatching of DER and flexibility.
Summing up, research in Category 2 includes comprehensive simulations, first prototypes and lab-tests of LEMs mainly addressing specific market features while neglecting others.

Category 3

Recently, several field tests have been launched demonstrating the implementation of LEM technologies. A prominent case study, the Brooklyn microgrid, is introduced in [79], [105]. The project

enables local electricity trading of PV within a neighborhood. The market design allows for simple trading between the participants and the respective billing. However, a clear explanation how this ex post approach can incentivize flexibility over multiple timesteps is not provided.
A similar project is introduced in Wallenstadt, Switzerland [106]. The trading among 37 participants is facilitated via blockchain and a simple market design. Prosumers can set their preference prices for selling and buying locally. As the market design in this project also only accounts for ex post determination of prices for P2P trades, no direct incentivization of flexibility usage at prosumer level is induced[10]. In the Landau Microgrid Project (LAMP) [80], an energy market with generation from PV and CHP is demonstrated. Price preferences of prosumers are taken into account in an ex post market matching using the Borda count voting mechanism proposed in [107]. Grid constraints or the incentivation of demand or generation side flexibility are not accounted for in the project.

To conclude, there is a large gap between theoretical work covering the whole range of market features with a focus on grid-integration challenges (optimal dispatch, grid constraints, flexibility) and first field tests which cover only simple use cases focusing on participant engagement and autonomy and privacy aspects. Theoretical work often assumes complex communication schemes between actors in the market. This assumption however might block real-world application of these systems due to package losses, asynchronous responses or the lack of a sufficiently fast transfer rate [91], [92] as well as general scalability issues [102]. Within this Thesis, this gap is addressed by proposing a market design which tackles grid-integration challenges with limited communication effort between participants and market operator (3.1.2) as well as market operator and DSO (Section 3.1.3).
On the other side of the spectrum, first commercial and non commercial field tests only implement ex post market mechanisms which do not tackle the challenges of grid-integration described in Section 2.1.1. Several adaptions to the market design need to be made to integrate the necessary market features like optimal dispatching of flexible demand, generation and storage in real-world LEM applications.

Most importantly, optimum scheduling of DER requires forecasting of the relevant variables like inflexible load and generation. Therefore, the market needs to be designed as a forward/ex ante market. Due to the stochastic nature of single household consumption profiles an accurate prediction is very challenging. The reported errors in state-of-the art load forecasting depend on the forecast horizon, the forecast granularity and the forecasting method (Figure 2.12). These forecast errors might lead to high penalty payments and consequently a high burden to participate in a LEM, when balancing penalty mechanisms are used [108]. This effect of forecasting uncertainty in LEMs has not yet been studied systematically in detail [22], [92] or is often neglected in studies (e.g., [109]). Hence, a novel methodological framework for the systematic assessment and sensitivity analysis is proposed (Section 4.3.3) and applied (Section 6.3.5) in this Thesis.

2.2.5. Research questions

After the introduction of the challenges of grid integration and market design and the analysis on the state of the art and the research gaps, the initial research question proposed in the introduction

[10] Except a community battery which is directly controlled to charge or discharge if the community exports or imports electricity.

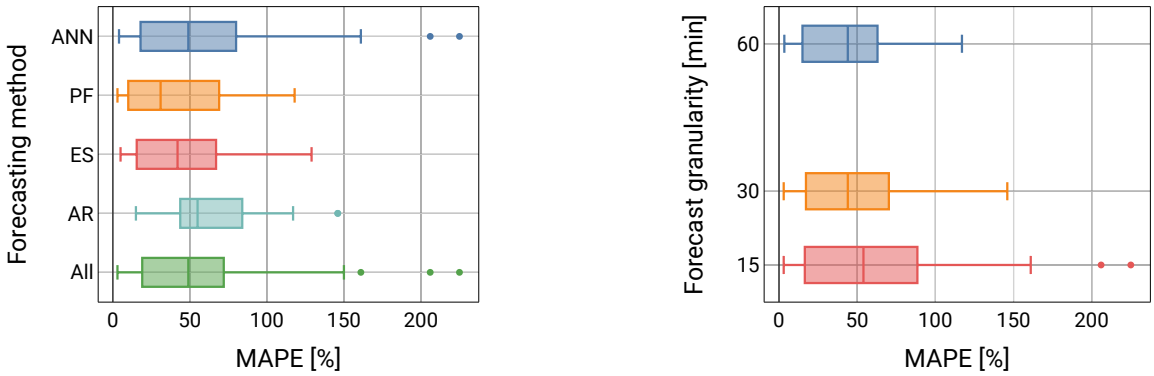

(a) Forecast errors (MAPE) for a variation of forecasting methods including forecasting granularities of 15, 30 and 60 minutes

(b) Forecast errors (MAPE) of day-ahead forecasts for ANN, PF, ES and AR models and a variation of timestep granularity

Figure 2.12.: Forecast errors for day-ahead load forecast for individual households. Figure from own publication [22] based on data in [110]–[114]. Analyzed methods: Artificial Neural Network (ANN), Persistence Forecast (PF), Exponential Smoothing (ES), Autoregressive (AR).

can be refined with additional sub-questions.

Main research question

How can a Local Energy Market be designed to incentivize regional flexibility options and contribute to the grid integration of VREs, EVs, HPs?

Sub-questions

1. How can an optimized scheduling of DER be achieved through a LEM without a central coordinator while providing real world applicability?

2. What effect does a dynamization of Regulated Electricity Price Components (REPCs) have on local energy trading? How can REPCs be utilized to steer local energy trading in a grid-friendly manner?

3. Does the LEM produce price signals which financially incentivize the participation of prosumers? How does forecast uncertainty affect the benefit of participation of prosumers?

Research question 1 tackles the research gap on LEM market designs derived in Section 2.2.3, 2.2.4 as well as aspects of real world application. Research question 2 aims at the aspect of incentivization of regional flexibility options through a systematic adaption of REPC. In research question 3 a key challenge of real-world implementation of LEMs - load forecast uncertainty - is addressed.

2.3. Modeling requirements and scoping

In order to answer the proposed research questions, several requirements for the modeling of the LEM can be derived. Based on these requirements, scoping decisions with regards to the spatial and temporal model granularity and the model type are made in this section.
To address the main research question as well as research questions 1 and 2, the used simulation model is required to allow analysis on the overall system level of the local energy system. On a more granular level, the participants' energy systems also need to be reflected by the model. This is required to account for the operation of flexible assets like EVs, HPs and the effect of forecast uncertainty (research question 3). Additionally, the model needs to be able to reflect the local grid topology as well as the temporal variability of VRE. To cover all of these aspects within one model, a high interpretability of the model outputs needs to be guaranteed.

2.3.1. Model type

Several mathematical formulations can be used to model and analyze LEMs. Figure 2.13 provides an overview of the most common model formulations used in literature. Each of the modeling formulations has a different modeling focus ranging from the overall system perspective in centralized optimization models to the behavior of single market participants in agent-based simulation models.

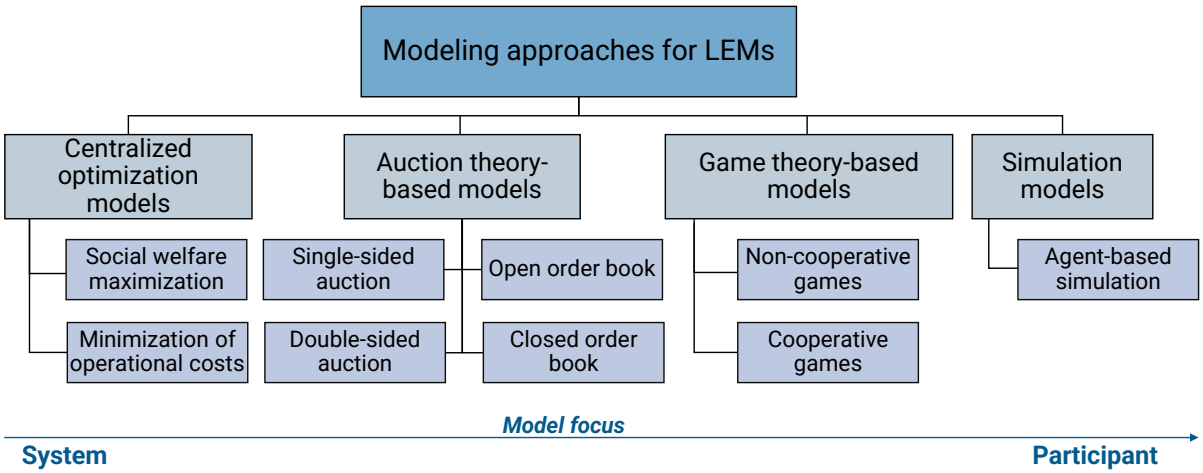

Figure 2.13.: Overview of possible modeling formulations for LEMs. Own illustration based on [115].

Centralized optimization based models take the perspective of the market operator or DSO, which solves an optimization problem, e.g., the maximization of social-welfare or the minimization of operational costs, subject to technical constraints of the local energy system. The maximization of social-welfare, i.e., the maximization of the difference of total consumer utility and producer

costs, is commonly used as an objective function of the overall market, e.g., in [91], [116]–[118]. This approach allows a transparent formulation and interpretation of the optimal operation of the LEM. The formulation of the market as an optimization problem also allows to cover multi-timestep optimization (e.g., to model storage flexibility) and can be extended by additional constraints such as grid constraints. The on-site energy systems of market participants are assumed to be centrally controllable and the participant behavior is not modeled in detail.

Resource allocations within a LEM can also be modeled using auction theory, similar to the existing wholesale market, where auctions are used for day-ahead and intraday market matching (see Section 2.2.3). In contrast to the wholesale market, the sizes of the orders sent to the market (quantity to buy or sell) can be as small as the overall load of a household [91], [118], [119] or even only one appliance within the participants energy system [93]. Several design aspects need to be considered when designing an auction. Single-sided auctions are used if a fixed demand has to be supplied by multiple sellers[11] or vice versa. Double-sided auctions are the more common design for energy markets and are used if both sellers and buyers can submit their price and quantity limits to the auctioneer (market operator). Additionally, the auction can either be executed at a certain point in time or continuously, with sealed orders (closed order book) or with exposure of the order information to the market participants (open order book). Auction theory based models allow to model both the participants energy system and interaction with the market through orders as well as the perspective of the market operator as an auctioneer. However, more complex optimization tasks like the optimal operation of flexible assets (as described in the previous sections) are harder to achieve through auctions.

Game theoretic models are used to model the decision process of multiple rational actors in competitive situations, where the decision taken by one actor may influence the actions of others. Two main types of game theoretic models are used to model the participants in LEMs: non-cooperative and cooperative games [120]. In non-cooperative games, actors are restricted to take decisions without the possibility to communicate with other actors. Typically, this type of model is used to analyze the bidding behavior and market outcome of competing market participants (e.g., in [121], [122]). The state of the Nash equilibrium, i.e., the condition where no actor can benefit by unilaterly deviating from it's own strategy, is commonly used to determine the solution of the model [123]. In cooperative games, actors are allowed to exchange information and form coalitions to improve their overall position by sharing the surplus among the group. For different household actors owning VRE and energy storages, the authors in [124] show that forming coalitions decreases overall costs compared to optimization of the single households. As shown in [125], this concept can also be applied one level above single household participants by creating coalitions between different Microgrids optimizing the interaction and optimum operation of various micogrids. Game theoretic models allow a detailed modeling of market participants and their interaction with each other. However, most game theory based models rely on an iterative, sometimes stochastic process of price determination through algorithms for each type of player (e.g., as described in [121], [126]). This can lead to multiple results or equilibria as solutions of a simulation instance [127], which makes the interpretation of the overall optimization targets, e.g., maximization of costs subject to grid constraints, difficult.

An even stronger focus on the behavior of participants in LEMs is achieved in agent based simulation models. Within the context of smart grids, agent based modeling allows to simulate the individual actions and interactions with other agents and learning of agents [128]. These type of models have

[11] For example a fixed amount of flexibility procured by a TSO supplied by multiple flexibility providers

the advantage of being highly flexible with regards to the modeled agents, e.g., market participants, DSO, market operator, and the complexity of the decision making process of the participants, e.g., by including the continues learning of optimal bidding strategies [129]. On the other side, this increases the level of complexity when describing stochastic processes of agent decisions and interactions and hence leads to low interpretability of the outputs and high computational effort [115].

Both, game theory and agent based simulation models, are unsuitable as they do not provide highly interpretable model results for the overall LEM. For this Thesis, a combination of centralized and auction-based models is chosen to cover the overall system optimization as well as an adequate representation of participants. This approach allows to model the central optimal dispatch of VREs, EVs, HPs owned by multiple market participants through an enhanced market matching. The market matching is adjusted to cover multiple timesteps, grid constraints and flexibility (described in section 3.1). This market matching is formulated as a linear optimization problem LP to ensure a higher scalability for an increasing number of participants compared to non-linear problems or non-convex problems such as mixed integer linear programs MILP.

2.3.2. Spatial model scope and distribution grid assumptions

As illustrated in Section 2.1.1, the most severe grid integration challenges are caused by volatile, locally concentrated generation from VRE as well as increasing demand from EVs and HPs. The majority of VREs are connected to the low and medium voltage level of the distribution grid [25]. A major increase in demand from EVs and HPs will most probably also affect distribution grids [7]. The most severe effect of additional generation and load on voltages and congestion in the grid can be observed in rural, radial distribution grids with high PV concentration and low load [29]. Most problems of over or under voltage appear at long feeder lines in the low voltage grid with high active resistance. Therefore the spatial scope in this thesis is focusing on specific rural distribution grids modeling low/medium voltage substations and feeder lines.
To model a market design without a central coordinator, the energy systems of each market participant need to be modeled separately to evaluate the impact of the participants' actions on the distribution grid. This level of granularity does not allow the modeling of a whole country or region due to computational complexity [130]. Therefore, only specific market set ups at low voltage and medium voltage level are evaluated in this thesis. The exchange with the upstream grid/rest of the power system is assumed to be only limited by the respective connection to the high voltage grid neglecting the direct interaction with other LEMs.
The literature shows that the technical properties of these grids, e.g., rated power of the substation, line length, cable type, number of connection points and households per substation or peak power per connection point vary significantly [29], [131], [132]. Typical substations used in rural areas or villages are dimensioned with a rated apparent power of 250, 400 or 630 kVA. The number of grid connection points per substation ranges between 30-90 [132] resulting in a wide range of power per connection point, e.g., 3.38/4.52 $\frac{\text{kVA}}{\text{HH}}$ (Grids GO and BW in [131]), 7.02 $\frac{\text{kVA}}{\text{HH}}$ (Kerber village grid [29]) and roughly 3-20 $\frac{\text{kVA}}{\text{HH}}$ (based on Fig. 4.8 in[132]). While well dimensioned distribution grids with a high potential rated power per connection point are suited to cope with additional generation from VRE and load from HPs and EVs. Schlömer [132] points out that numerous distribution grids with a rated power per connection point below 3 kVA can be found. In these types of distribution grids, grid-integration challenges become most apparent as the grid infrastructure

might not withstand additional generation or load[12]. Hence, in the simulated scenarios in this Thesis, low rated power per connection point in the range of 3-5 kVA per connection point is assumed to demonstrate the potential effect of LEMs to reduce peak loads and peak feed-in.
Following a recent report of the German federal network regulator (Bundesnetzagentur) among 59 representative DSOs [133], only 3 report to fully and automatically monitor their LV grid automatically keeping track of the status of the grid (e.g., switching states). Therefore it is assumed, that the full grid topology and switching states are not known to the market operator. Only simplified information on the grid, e.g., which participants are connected to which substation or feeder lines are considered.

2.3.3. Temporal model scope

Computation time of energy system models is highly dependent on the number of timesteps considered [134]. With an increasing number of timesteps (higher temporal granularity), both model accuracy and computation time increase. Similar to the spatial scoping, the requirement of modeling VRE influences the decision on the temporal model scope. As the main type of VRE in low voltage grids is PV, the temporal granularity should be able to reflect its variability. Short term variability of PV is induced by cloud movement. The correlation of this variability between two sites decreases significantly with an increasing distance between the sites [135], i.e., the larger the spatial scope of the model the lower the impact of the variability. In order to capture the relevant variability in a typical distribution grid, a temporal resolution of 15 min is a widely accepted compromise [136]. Faster ramp rates and variability induced by fast moving clouds in the domain of minutes or seconds are neglected.

Since an optimal scheduling requires to plan and forecast the electric load, the impact of temporal granularity on the forecasting error needs to be taken into account when deciding on the temporal model scope. Yildiz et al. [137] show that an increase in temporal granularity results in higher forecast errors leading to extremely high forecasting errors for a granularity below 15 min.
An additional factor for setting the temporal granularity to 15 min is the data availability. Yearly timeseries data in high quality are required to model the seasonal variability of demand and generation and are mostly only available at resolutions up to 15 min. Also, the temporal resolution used in most energy economic processes, e.g., for billing (larger customers), is 15 min. The temporal resolution of the models used in this thesis is hence set to 15 min to adequately model VRE variability and forecasts with sufficient data availability.

[12]Especially load with a high simultaneity factor such as the charging of EVs in the evening or generation from PV.

3. Modeling

This chapter provides an overview of the mathematical models used to simulate the LEM. First, the overall market model is developed based on the modeling scope and requirements introduced in Section 2.3. This includes the objective function of the market operator, the definition of market orders and the formulation of constraints representing the inputs of the DSO and the utility. Secondly, a generic formulation of the on-site energy system model of the market participants is presented followed by the description of the main components modeled in this Thesis - VREs, EVs, HPs, and battery systems.

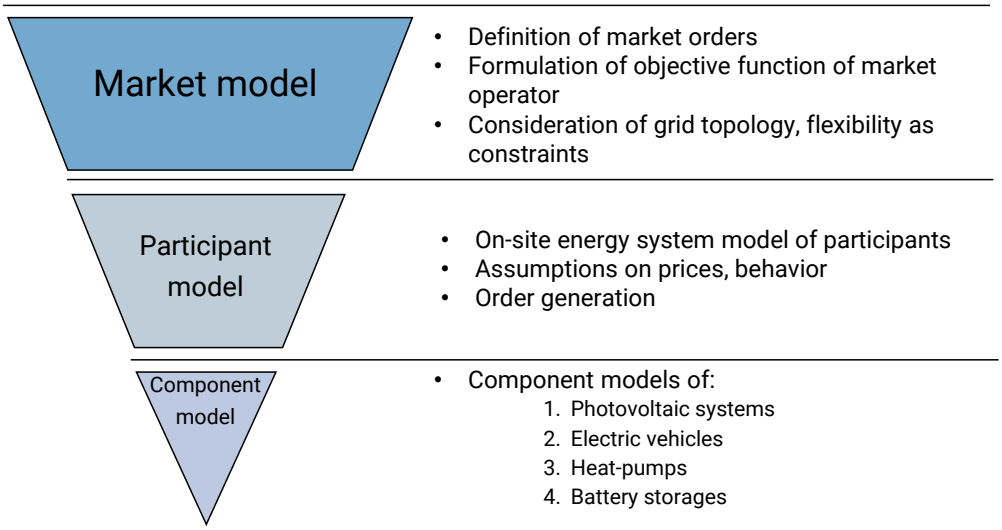

Figure 3.1.: Overview of the modeling chapter.

3.1. Market model

As derived in Section 2.3.1, the core of the market matching is a linear optimization problem implemented as a closed order book. Due to the inherently lower market liquidity of LEMs, a closed order book with one specific market matching time per day is used to concentrate all bids to one market matching. The central concept is that participants send orders to the market which contain the parameters used in the objective function and constraints of the optimization problem (lower and upper bounds, price parameters for the objective function). Participants submit their sealed market orders, which are valid for a certain time period $\mathcal{T}$ (e.g., the next day), before a

predefined market matching time (e.g., 5:00 pm). The orders (Section 3.1.1) contain all relevant parameters for the market operator to perform the market matching (Section 3.1.2). Additional parameters and constraints are supplied by other parties like the DSO to account for distribution grid limits and REPCs (Section 3.1.3).

3.1.1. Order definition

The simplest form of a double-sided auction for one timestep can be achieved through price-quantity value tuples expressing either a buy order (maximum quantity, maximum price) or a sell order (maximum quantity, minimum price). This is sufficient to model non-dispatchable generation and load at the market side. In traditional wholesale energy markets the calculation of the optimal dispatch of the market participants assets through the trading period is handled at the participant side. Including flexible demand or generation at the market side, however, requires the incorporation of multiple timesteps and the respective quantities and prices for sell (Table 3.1) and buy orders (Table 3.2). To also consider the flexibility of storages, which can act as both buyers and sellers in the market, a new order type is introduced (storage order, Table 3.3).

Sell order

A sell order s, from a set of sell orders ($\mathcal{S}$), can be defined for a freely selectable range (t_{start}, t_{end}) within the market horizon $\mathcal{T}$. For each defined timestep, both the maximum power output ($p_{s,t}^{\max}$) and a minimum sell price ($c_{s,t}^{\min}$) are defined. Additionally, a maximum $e_s^{\max}$ and minimum amount of energy $e_s^{\min}$ can be defined[1]. This formulation covers both the definition of flexible and inflexible sell orders.
A flexible sell order s can be defined if less energy is available throughout the time period $\mathcal{T}$ then potentially available,

$$e_s^{\max} \leq \sum_{t=t_{\text{start}}}^{t_{\text{end}}} p_{s,t}^{\max} \Delta t, \quad \forall s \in \mathcal{S}, \tag{3.1}$$

with Δt as the time delta of one market matching interval, e.g., 15 minutes.
For inflexible generation, e.g., PV[2], the maximum available energy is defined as the sum of the potentially available generation,

$$e_s^{\max} = \sum_{t=t_{\text{start}}}^{t_{\text{end}}} p_{s,t}^{\max} \Delta t, \quad \forall s \in \mathcal{S}. \tag{3.2}$$

It should be noted that a minimum power and energy output could also be defined in the sell order. This, however, requires that there is a guaranteed buyer of the offered generation (backup supplier introduced in Section 3.1.4) and that the generation does not cause a violation of grid constraints.

[1] The definition of a minimum energy amount is only possible if a backup supplier which buys local excess generation is defined (compare Section 3.1.4).
[2] With regards to shifting in time, disregarding curtailment.

Table 3.1.: Overview of the definition of a generic sell order.

Parameter	Unit	Description
$c_{s,t}^{\min}$	[ct/kWh]	Minimum sell price for each timestep
$p_{s,t}^{\max}$	[kW]	Maximum power output for each timestep
$e_{s}^{\max}$	[kWh]	Maximum amount of sold energy within timeperiod $\mathcal{T}$

Buy order

A buy order b, from a set of buy orders ($\mathcal{B}$), can be defined analogous to the sell order. The only difference being that the maximum buy price $c_{b,t}^{\max}$ and power input $p_{b,t}^{\max}$ needs to be defined for the respective time range. A flexible buy order is defined if the maximum amount $e_{b}^{\max}$ to be consumed is smaller than the sum of the maximum power input. This flexible demand is, for example, required when defining a buy order for the charging of an EV, i.e., requiring a certain charging energy $e_{b}^{\max}$ to be provided within the interval t_{start}-t_{end},

$$e_{b}^{\max} \leq \sum_{t=t_{\text{start}}}^{t_{\text{end}}} p_{b,t}^{\max} \Delta t, \quad \forall b \in \mathcal{B}. \tag{3.3}$$

For inflexible demand (e.g., lighting) the maximum available energy is defined as the sum of demand over time,

$$e_{b}^{\max} = \sum_{t=t_{\text{start}}}^{t_{\text{end}}} p_{b,t}^{\max} \Delta t, \quad \forall b \in \mathcal{B}. \tag{3.4}$$

Table 3.2.: Overview of the definition of a generic buy order.

Parameter	Unit	Description
$c_{b,t}^{\max}$	[ct/kWh]	Maximum buy price for each timestep
$p_{b,t}^{\max}$	[kW]	Maximum power input for each timestep
$e_{b}^{\max}$	[kWh]	Maximum amount of requested energy within timeperiod $\mathcal{T}$

Storage order

The proposed matching algorithm also considers the flexibility of storages, both for self-consumption optimization (internal, int) and for the overall LEM (external, ext). To calculate the optimal dispatch of the storage, i.e., when to charge and when to discharge, several asset parameters need to be communicated to the market operator via a storage order. Most importantly, the maximum storage capacity $e_{st,t}^{\max}$ needs to be defined. This can either be the full rated capacity of the storage or a part of it, e.g., respecting minimum and maximum State Of Charge (SOC) limits. Additionally, a value for the initial SOC e_{st}^{ini} and final SOC e_{st}^{end} needs to be provided. This allows the storage to be operated within these limits with a maximum charge and discharge power ($p_{st,t}^{\max,\text{ch}}$, $p_{st,t}^{\max,\text{dch}}$). To

account for losses within the operation, charging and discharging efficiencies need to be defined ($\eta_{st}^{\mathrm{ch}}, \eta_{st}^{\mathrm{dch}}$). A limit for the maximum amount of storage cycles[3] can be defined with the parameter $n_{st}^{\max}$. In order to financially compensate the usage of the storage for the LEM a minimum discharge price $c_{st}^{\mathrm{dch,min}}$ is introduced. The storage will hence only be used externally if the price difference between a bought amount of energy at time t_1 and a sold amount at t_2 is higher than $c_{st}^{\mathrm{dch,min}}$ including efficiency losses.

Table 3.3.: Overview of the definition of a generic storage order.

Parameter	Unit	Description
$e_{st,t}^{\max}$	[kWh]	Maximum storage capacity
e_{st}^{ini}	[kWh]	Initial storage capacity
e_{st}^{end}	[kWh]	Final storage capacity
$c_{st}^{\mathrm{dch,min}}$	[ct/kWh]	Minimum discharge price
$p_{st,t}^{\mathrm{max,ch}}$	[kW]	Maximum charging power
$p_{st,t}^{\mathrm{max,dch}}$	[kW]	Maximum discharging power
$\eta_{st}^{\mathrm{ch}}, \eta_{st}^{\mathrm{dch}}$	[-]	Charge and discharge efficiency
$n_{st}^{\max}$	[-]	Maximum number of cycles

3.1.2. Market matching problem

Figure 3.2 shows an overview of the market matching problem.

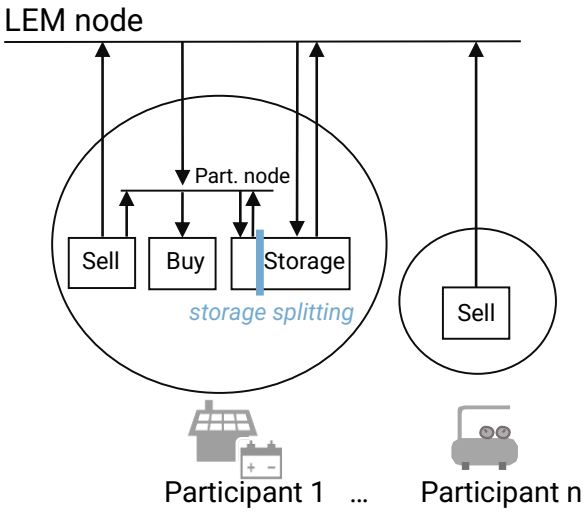

Figure 3.2.: Representation of orders and participant energy system in the market matching

A LEM with a set of $\mathcal{P}$ participants (e.g., prosumers, consumers, producers), a set of buy orders $\mathcal{B}$, a set of sell orders $\mathcal{S}$ and a set of storage orders $\mathcal{ST}$ is considered. The objective function formulated as the maximization of social welfare (SW) with the decision variables $P_{b,t}, P_{s,t}, P_{st,t}^{\mathrm{dch,ext}}$:

[3] One cycle = full charge and discharge.

$$\max(\mathrm{SW}) = \max_{(P_{b,t}, P_{s,t} P_{st,t}^{\mathrm{dch,ext}})} (\sum_{t \in \mathcal{T}} \Delta t \sum_{p \in \mathcal{P}} (\sum_{b \in \mathcal{B}_p} P_{b,t} c_{b,t}^{\max} - \sum_{s \in \mathcal{S}_p} P_{s,t} c_{s,t}^{\min} - \sum_{st \in \mathcal{ST}_p} P_{st,t}^{\mathrm{dch,ext}} c_{st}^{\mathrm{dch,min}})), \tag{3.5}$$

where $P_{b,t}$, $P_{s,t}$, $P_{st,t}^{\mathrm{dch,ext}}$ are continuous variables ($\mathbb{R}_0^+$) defining the matched quantity of each order. With $\mathcal{B}_p$, $\mathcal{S}_p$ and $\mathcal{ST}_p$ as the respective subsets of orders belonging to a participant p. The respective orders are limited by price limits $c_{b,t}^{\max}$, $c_{s,t}^{\min}$ and c_{st}^{dch}. To model possible self-consumption of a prosumer, a participant node is introduced (Figure 3.2). The node balance constraint of each prosumer is defined as:

$$\sum_{s \in \mathcal{S}_p} P_{s,t}^{\mathrm{int}} + \sum_{b \in \mathcal{B}_p} (-P_{b,t}^{\mathrm{int}} + P_{b,t}^{\mathrm{ext}}) + \sum_{st \in \mathcal{ST}_p} (-P_{st,t}^{\mathrm{ch,int}} + P_{st,t}^{\mathrm{dch,int}}) = 0, \quad \forall\, p \in \mathcal{P}, t \in \mathcal{T}, \tag{3.6}$$

where superscripts int and ext indicate the connections of each order to the participant node and LEM node respectively (compare Figure 3.2). Equation 3.6 is required to formulate a differentiation between internally (behind the meter) consumed energy and energy bought from other participants or the grid. As REPCs are usually only applied for externally purchased energy, this formulation allows to financially favor self-consumption over externally purchased energy (later shown in Section 3.1.3). Additionally, a virtual splitting of energy storages into an internal (int) and external (ext) part is introduced. Externally discharged energy can now be associated with a discharge price while the internal usage of the storage is free.

The LEM node balance for an exchange with other participants via the grid is further formulated as:

$$\sum_{s \in \mathcal{S}_p} P_{s,t}^{\mathrm{ext}} - \sum_{b \in \mathcal{B}_p} P_{b,t}^{\mathrm{ext}} + \sum_{st \in \mathcal{ST}_p} (-P_{st,t}^{\mathrm{ch,ext}} + P_{st,t}^{\mathrm{dch,ext}}) = 0. \quad \forall\, p \in \mathcal{P}, t \in \mathcal{T}, \tag{3.7}$$

Additional constraints to account for the power and energy limits of the specific order types are introduced. For sell orders:

$$P_{s,t} = P_{s,t}^{\mathrm{int}} + P_{s,t}^{\mathrm{ext}}, \quad \forall\, t \in \mathcal{T}, s \in \mathcal{S}, \tag{3.8}$$

$$P_{s,t} \leq p_{s,t}^{\max}, \quad \forall\, t \in \mathcal{T}, s \in \mathcal{S}, \tag{3.9}$$

$$\sum_{t=t_{\mathrm{start}}}^{t_{\mathrm{end}}} P_{s,t} \Delta t \leq e_s^{\max}. \quad \forall\, s \in \mathcal{S}. \tag{3.10}$$

For buy orders:

$$P_{b,t} = P_{b,t}^{\mathrm{int}} + P_{b,t}^{\mathrm{ext}}, \quad \forall\, t \in \mathcal{T}, s \in \mathcal{B}, \tag{3.11}$$

$$P_{b,t} \leq p_{b,t}^{\max}, \quad \forall\, t \in \mathcal{T}, b \in \mathcal{B}, \tag{3.12}$$

$$\sum_{t=t_{\text{start}}}^{t_{\text{end}}} P_{b,t} \Delta t \leq e_{b}^{\max}, \quad \forall\, b \in \mathcal{B}. \tag{3.13}$$

For storage orders, a storage constraint is introduced to couple the charging behavior and the SOC of the storage. For the internal ($E_{st,t}^{\text{int}}$) and external ($E_{st,t}^{\text{ext}}$) energy content of the storage respectively,

$$\frac{E_{st,t}^{\text{int}} - E_{st,t-1}^{\text{int}}}{\Delta t} = P_{st,t}^{\text{ch,int}} \eta_{st}^{\text{ch}} - \frac{1}{\eta_{st}^{\text{dch}}} P_{st,t}^{\text{dch,int}}, \quad \forall\, t \in \mathcal{T}, t > t_{\text{start}}, p \in \mathcal{P}, st \in \mathcal{ST}_p, \tag{3.14}$$

$$\frac{E_{st,t}^{\text{ext}} - E_{st,t-1}^{\text{ext}}}{\Delta t} = P_{st,t}^{\text{ch,ext}} \eta_{st}^{\text{ch}} - \frac{1}{\eta_{st}^{\text{dch}}} P_{st,t}^{\text{dch,ext}}, \quad \forall\, t \in \mathcal{T}, t > t_{\text{start}}, p \in \mathcal{P}, st \in \mathcal{ST}_p. \tag{3.15}$$

Limits for the storage variables are defined as:

$$E_{st,t}^{\text{int}} + E_{st,t}^{\text{ext}} \leq e_{st,t}^{\max}, \quad \forall\, t \in \mathcal{T}, p \in \mathcal{P}, st \in \mathcal{ST}_p, \tag{3.16}$$

$$P_{st,t}^{\text{dch,int}} + P_{st,t}^{\text{dch,ext}} \leq p_{st,t}^{\text{max,dch}}, \quad \forall\, t \in \mathcal{T}, p \in \mathcal{P}, st \in \mathcal{ST}_p, \tag{3.17}$$

$$P_{st,t}^{\text{ch,int}} + P_{st,t}^{\text{ch,ext}} \leq p_{st,t}^{\text{max,ch}}, \quad \forall\, t \in \mathcal{T}, p \in \mathcal{P}, st \in \mathcal{ST}_p. \tag{3.18}$$

Initial and final SOC are set according to the storage order as[4] :

$$E_{st,t_{\text{start}}} = e_{st}^{\text{ini}} = E_{st,t_{\text{end}}}. \tag{3.19}$$

The number of storage cycles is constrained, defining one cycle as a full charge and discharge of the system:

$$\frac{\sum_{t \in \mathcal{T}} \Delta t (P_{st,t}^{\text{ch,int}} + P_{st,t}^{\text{dch,int}} + P_{st,t}^{\text{ch,ext}} + P_{st,t}^{\text{dch,ext}})}{2 e_{st,t}^{\max}} \leq n_{st}^{\max}, \quad \forall\, p \in \mathcal{P}, st \in \mathcal{ST}_p. \tag{3.20}$$

The introduced market model until now is a single node model without the consideration of the distribution grid. The market price in this simplified model can be derived from the dual variables of Equation 3.7. The dual variables at the node balance can be interpreted as the marginal price required to influence the node balance by a marginal power.

[4]The SOC at the end of the market interval can not be set arbitrary by the participant. This could lead to possible infeasibilities, i.e., if the final SOC is set greater than the the initial SOC and no sell order is offered by other market participants.

3.1.3. Grid topology and fees

In this section, the market model is extended to account for a simplified grid topology. Thus, three key market features can be represented by the model:

1. Consideration of simplified grid limits during market matching.
2. Representation of localized REPCs along the topology.
3. Regionally resolved price information (nodal prices) if the grid is congested.

The simplified grid topology and its constraints and grid fees are supplied by the DSO. This interface and its input parameters are described in Table 3.4. It consists of a set of $\mathcal{N}$ nodes and $\mathcal{L} \subseteq \mathcal{N} \times \mathcal{N}$ lines connecting the nodes. Additionally, participant parameters and their associated nodes are added to the model. The main idea is to add maximum real power capacity constraints of lines, nodes and participants to the optimization problem. Moreover, each topology element can be assigned with a specific relative energy fee and power fee which are added to the objective function (Equation 3.24).

Table 3.4.: Overview of the grid topology input parameters.

	Symbol	Unit	Description
Line	j, k	[-]	Start and end node of line
	$p^{\max}_{(j,k),t}$	[kW]	Maximum real power capacity for a specific timestep and node j -> k
	$c^{\mathrm{e}}_{(j,k),t}$	[ct/kWh]	Line energy fee
	$c^{\mathrm{p}}_{(j,k)}$	[ct/kW]	Line power fee
	$p^{\min,\mathrm{p}}_{l}$	[kW]	Contracted power above which power fees apply
Node	$p^{\max,\mathrm{in}}_{n,t}$	[kW]	Maximum real power capacity for an import to the node
	$p^{\max,\mathrm{out}}_{n,t}$	[kW]	Maximum real power capacity for an export from the node
	$c^{\mathrm{e,in}}_{n,t}$	[ct/kWh]	Node energy fee
Participant	$p^{\max,\mathrm{in}}_{p,t}$	[kW]	Maximum real power for an import to the participant
	$p^{\max,\mathrm{out}}_{p,t}$	[kW]	Maximum real power for an export from the participant
	$c^{\mathrm{e,in}}_{p,t}$	[ct/kWh]	Participant energy fee in

Figure 3.3 shows an example of a typical radial distribution grid model (a) and the simplified model used in the LEM market matching (b). It consists of two LV/MV substations and a MV/HV substation. An exemplaric participant with PV, a battery storage and a load is connected to the first feeder of the first MV/HV substation.

The LEM model consists of four layers: The participant bus, the low voltage feeder, the substation and the backup grid. The participant bus represents the exchange from the orders of that participant used for self-consumption (behind the meter). The lowest aggregation level in the LEM model is one feeder line of the LV grid. All participants connected to that feeder line may exchange energy only passing one line associated with fees (blue participant fees). An exchange with other feeders at the same substation (orange feeder fee) requires an additional fee (e.g., low voltage grid fees) to be paid. With this approach, stress on a specific feeder line, e.g., a long line with high

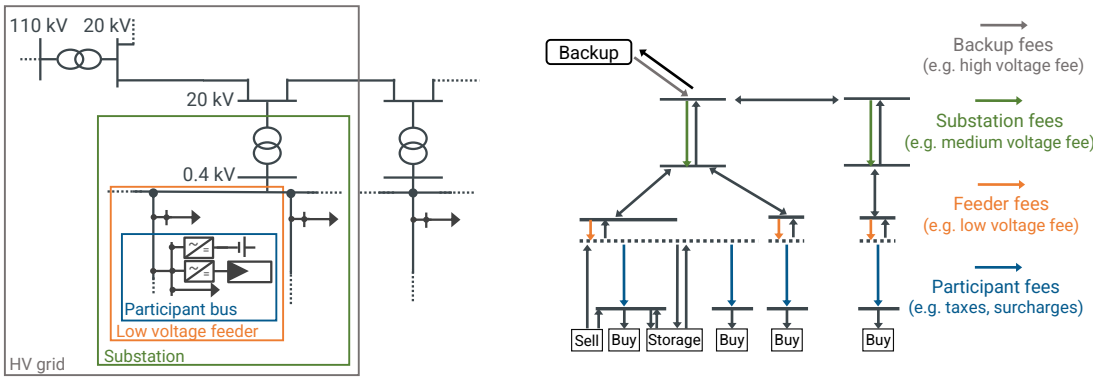

(a) Grid model (b) Simplified LEM model

Figure 3.3.: Representation of a typical radial distribution grid topology (a) and the respective simplified model of the LEM (b). Colors of arrows indicate a possible splitting of REPCs along the grid topology [21].

PV penetration, might be reduced. In this case, flexible demand at the same feeder line would be incentivized to be covered at times of feed in at the same feeder. At the next layer, an exchange between participants connected to different substations is additionally penalized with a substation fee (green). This approach might reduce the overall loading of a substation for the same rational as explained for the feeder. To reduce the overall exchange with the rest of the grid, i.e., all energy not supplied or over-generated locally, a backup fee is introduced at the highest voltage level.

The objective function (Equation 3.24) is extended to cover energy (f^{e}) and power fees (f^{p}) of REPCs:

$$\mathrm{REPCs} = f^{\mathrm{e}} + f^{\mathrm{p}}, \tag{3.21}$$

$$f^{\mathrm{e}} = \sum_{t \in \mathcal{T}} \Delta t \Big(\sum_{(j,k) \in \mathcal{L}} P_{(j,k),t} c^{\mathrm{e}}_{(j,k),t} + \sum_{n \in \mathcal{N}} P^{\mathrm{in}}_{n,t} c^{\mathrm{e,in}}_{n,t} + \sum_{p \in \mathcal{P}} P^{\mathrm{in}}_{p,t} c^{\mathrm{e,in}}_{p,t} \Big), \tag{3.22}$$

where $P_{(j,k),t}$ is the active power flow from node j to node k. Energy fees $c^{\mathrm{e}}_{(j,k),t}$ are considered for the usage of a line. Energy fees $c^{\mathrm{e,in}}_{n,t}$ are paid for an active power flow $P^{\mathrm{in}}_{n,t}$ into a low voltage feeder. Energy fees $c^{\mathrm{e,in}}_{p,t}$ every participant has to pay are added for the consumption $P^{\mathrm{in}}_{p,t}$ of buy orders from the external grid (Equation 3.25). Equation 3.23 introduces the possibility to add a power price $c^{\mathrm{p}}_{(j,k),t}$ to lines:

$$f_p = \sum_{(j,k) \in \mathcal{L}} P^{\mathrm{bil}}_{(j,k)} c^{\mathrm{p}}_{(j,k)}, \tag{3.23}$$

with $P^{\mathrm{bil}}_{(j,k)}$ as a variable defining the billable active power over a line during a market matching interval for which power fees apply. Depending on the day of the market matching interval, power fees might not be applied since they were already paid for a higher peak in an earlier interval during the simulation horizon. Respective constraints are introduces in Equations 3.34, 3.35, 3.36.

The overall objective function is extended to account for both, the maximization of SW and the minimization of REPCs with the decision variables of orders $P_{b,t}, P_{s,t}, P^{\mathrm{dch,ext}}_{st,t}$ and grid elements $P_{(j,k),t}, P^{\mathrm{in}}_{n,t}, P^{\mathrm{in}}_{p,t}, P^{\mathrm{bil}}_{(j,k)}$:

$$\min_{(P_{b,t},P_{s,t},P^{\mathrm{dch,ext}}_{st,t},P_{(j,k),t},P^{\mathrm{in}}_{n,t},P^{\mathrm{in}}_{p,t},P^{\mathrm{bil}}_{(j,k)})} (\mathrm{REPCs} - \mathrm{SW}). \tag{3.24}$$

The following additional constraints and adaptions to previous constraints are made to account for the grid topology. The power balance of the participant bus (3.6) stays untouched, however for simplification the sum of all buy orders covered from outside the participant systems is reduced to:

$$P^{\mathrm{in}}_{p,t} = \sum_{b \in \mathcal{B}_p} P^{\mathrm{ext}}_{b,t}, \quad \forall\, t \in \mathcal{T}, p \in \mathcal{P}, \tag{3.25}$$

and the sum of all sell orders to:

$$P^{\mathrm{out}}_{p,t} = \sum_{s \in \mathcal{S}_p} P^{\mathrm{ext}}_{s,t}, \quad \forall\, t \in \mathcal{T}, p \in \mathcal{P}. \tag{3.26}$$

The internal balance of the feeder node can hence be formulated as:

$$\sum_{p \in \mathcal{P}_n} (P^{\mathrm{in}}_{p,t} - P^{\mathrm{out}}_{p,t}) - \sum_{st \in \mathcal{ST}_n} (P^{\mathrm{dch,ext}}_{st,t} - P^{\mathrm{ch,ext}}_{st,t}) + P^{\mathrm{in}}_{n,t} - P^{\mathrm{out}}_{n,t} = 0, \quad \forall\, n \in \mathcal{N},\ t\ \in \mathcal{T}. \tag{3.27}$$

$P^{\mathrm{dch,ext}}_{st,t}$ is the inflow from the external part of the node to the internal node and $P^{\mathrm{out}}_{n,t}$ is the respective outflow to the external part of the node. The sets P_n, ST_n are subsets of Participants and Storage orders associated with the node n. The transport equation, connecting the external part of the nodes via lines is formulated as:

$$\sum_{k:(k,n) \in \mathcal{L}} P_{l(k,n),t} - \sum_{k:(n,k) \in \mathcal{L}} P_{(n,k),t} + P^{\mathrm{in}}_{n,t} - P^{\mathrm{out}}_{n,t} = 0, \quad \forall\, n \in \mathcal{N}, t \in \mathcal{T}. \tag{3.28}$$

The following inequality constraints are introduced to allow the DSO to define upper bounds for lines, nodes and participants:

$$P_{(j,k),t} \leq p^{\mathrm{max}}_{(j,k),t}, \quad \forall\, (j,k) \in \mathcal{L},\ t \in \mathcal{T}, \tag{3.29}$$

$$P^{\mathrm{in}}_{n,t} \leq p^{\mathrm{max,in}}_{n,t}, \quad \forall\, n \in \mathcal{N},\ t \in \mathcal{T}, \tag{3.30}$$

$$P^{\mathrm{out}}_{n,t} \leq p^{\mathrm{max,out}}_{n,t}, \quad \forall\, n \in \mathcal{N},\ t \in \mathcal{T}, \tag{3.31}$$

$$P^{\mathrm{in}}_{p,t} + \sum_{st \in \mathcal{ST}_p} P^{\mathrm{ch,ext}}_{st,t} \leq p^{\mathrm{max,in}}_{p,t}, \quad \forall\, p \in \mathcal{P},\ t \in \mathcal{T}, \tag{3.32}$$

$$P_{p,t}^{\text{out}} + \sum_{st \in \mathcal{ST}_p} P_{st,t}^{\text{dch,ext}} \leq p_{p,t}^{\text{max,out}}, \quad \forall\, p \in \mathcal{P},\ t \in \mathcal{T}. \tag{3.33}$$

The variables $P_{st,t}^{\text{ch,ext}}$ and $P_{st,t}^{\text{dch,ext}}$ for external charging and discharging of the storages are separated from $P_{p,t}^{\text{in}}$ and $P_{p,t}^{\text{out}}$ as they are associated with different prices (e.g., minimum discharging price) in the objective function.

In current regulatory frameworks, power prices are paid for the maximum consumed power in a time interval Δt within a contractual period of, e.g., a year. To reflect this in the shorter matching time period of the LEM, e.g., one day, a threshold power (e.g., $p_{p,\min}^{n}$, Table 3.4) is introduced. The power price is only paid if the maximum power of the respective grid element exceeds this threshold during the market matching interval. Additional variables for the actual power price $P_{(j,k)}^{\text{bil}}$ are introduced and constrained by equations 3.34, 3.35, 3.36 to reflect the maximum power during the matching interval exceeding the threshold power. Additionally, a power price for feed-in to the grid $c_{p,\text{out}}$ is introduced to penalize feed-in peaks.

The billable peak power variables $P_{(j,k)}^{\text{bil}}$ are constrained with the following inequalities. To simplify, $P_{l,t}^{\text{bil}}$ is used as an equivalent for both line directions.

$$P_l^{\text{T}_{\max}} \geq P_{l,t}, \quad \forall\, t \in \mathcal{T}, l \in \mathcal{L}, \tag{3.34}$$

$$P_l^{\text{T}_{\max}} \geq P_l^{\text{min,p}}, \quad \forall\, l \in \mathcal{L}, \tag{3.35}$$

$$P_l^{\text{bil}} \geq P_l^{\text{T}_{\max}} - P_l^{\text{min,p}}, \quad \forall\, l \in \mathcal{L}. \tag{3.36}$$

Equation 3.34 defines the helper variable $P_l^{\text{T}_{\max}}$ as the maximum power during the matching interval $\mathcal{T}$. With Equations 3.35 and 3.36 the actual billable power P_l^{bil} is defined. If $P_l^{\text{T}_{\max}}$ does not exceed the contractual threshold power $P_l^{\text{min,p}}$, Equation 3.36 introduces a lower bound of P_l^{bil} of 0. Hence no power price will be charged as a deviation from 0 would introduce costs in the objective function (Equation 3.23). If $P_l^{\text{T}_{\max}}$ exceeds the the contractual threshold power P_l^{bil}, power fees are added to the objective function since the RHS of Equation 3.36 would be positive. With this approach a lower limit P_l^{bil} for the power price can be defined which can dynamically be adapted during the simulation. For example if a high power peak already occurred on a day in January, following simulation days are not affected by the power price except a higher peak would occur.

3.1.4. Backup energy supply

The formulation of the market model until now does not guarantee the fulfillment of all buy and sell orders. If there are no or insufficient local sell order available to match a buy order, the buy order will not be fulfilled. If price preferences of counterparts do not match, i.e., if minimum sell prices exceed maximum buy prices, a local matching is also not possible.
A backup energy supplier is introduced to overcome this issue and to provide additional liquidity to the market. The backup supplier is modeled as an additional participant (bu) connected to the LEM (compare Figure 3.3) which offers to buy excess energy and supply missing demand with a sufficiently large amount on the buy ($\sum_{b \in \mathcal{B}} p_{b,t}^{\max} \ll p_{b,t}^{\max,\text{bu}}$) and sell side ($\sum_{s \in \mathcal{S}} p_{s,t}^{\max} \ll p_{s,t}^{\max,\text{bu}}$).

This solves the issue of availability of supply and demand on the LEM. However, a mismatch in price preferences between seller and buyer could still lead to unsupplied energy or curtailment. Unlike market participants at the wholesale market, most participants at LEMs do not have access to other means of buying or selling electricity. Especially with regards to the field test[5] of the LEM (Chapter 6), the concept of exclusiveness is introduced. A sell or buy order can be marked as exclusive by the market participant ($\varepsilon_s = 1$, $\varepsilon_b = 1$). This implies that the full amount of the ordered quantity has to be fulfilled either by other market participants or the backup supplier. The following constraints apply either for exclusive sell orders $S_e = \{s \in \mathcal{S} | \varepsilon_s = 1\}$ or buy orders $\mathcal{B}_e = \{b \in \mathcal{B} | \varepsilon_b = 1\}$. For flexible buy orders ($\sum_{t \in \mathcal{T}} \Delta t P_{b,t}^{\max} > E_b^{\max}$), the overall demanded energy amount is fixed:

$$\sum_{t=t_{\text{start}}}^{t_{\text{end}}} \Delta t (P_{b,t} + P_{b,t}^{\text{bu}}) = e_b^{\max}, \quad \forall\, b \in \mathcal{B}_e. \tag{3.37}$$

For inflexible buy orders ($\sum_{t \in \mathcal{T}} \Delta t p_{b,t}^{\max} \leq e_b^{\max}$), each power demand is fixed to its maximum:

$$P_{b,t} + P_{b,t}^{\text{bu}} = p_{b,t}^{\max}, \quad \forall\, b \in \mathcal{B}_e, t \in \mathcal{T}. \tag{3.38}$$

The same logic applies for the sell side. For flexible generation ($\sum_{t \in \mathcal{T}} \Delta t p_{s,t}^{\max} > E_s^{\max}$),

$$\sum_{t=t_{\text{start}}}^{t_{\text{end}}} \Delta t (P_{s,t} + P_{s,t}^{\text{bu}}) = e_s^{\max}, \quad \forall\, s \in \mathcal{S}_e, \tag{3.39}$$

and inflexible generation ($\sum_{t \in \mathcal{T}} \Delta t p_{s,t}^{\max} \leq e_s^{\max}$),

$$P_{s,t} + P_{s,t}^{\text{bu}} = p_{s,t}^{\max}, \quad \forall\, s \in \mathcal{S}_e, t \in \mathcal{T}. \tag{3.40}$$

With this formulation, inflexible demand and generation will directly be matched with the respective maximum amounts. For flexible order types, the objective function of social welfare maximization will still lead to the cost optimal match within the time horizon T.

It should be noted that if the concept of exclusiveness is applied alongside grid constraints, the optimization problem might be infeasible, for example, if a participant without own generation or storage demands more power than transportable via the connecting node. In this case, too much generation or demand which might lead to a violation of grid constraint violations must be curtailed. To still provide numerical solutions, additional slack variables for the buy and sell constraints can be introduced on the left hand side of equations 3.37-3.40. Additionally, sufficiently high costs for curtailed demand and low costs for curtailed generation have to be introduced in the objective function to avoid that the slack variables are used instead of order variables. In this Thesis, exclusiveness of orders and active power limits of grid components are not applied simultaneously. This approach would require to modify market orders in order to reach feasible solutions for the market matching problem. However, this would circumvent the interpretation of the dual variables of node balances as market prices.

[5] A mismatch of price preferences can be handled in simulations, however price preferences set by real actors (backup supplier and market participants) might lead to unmatched load or generation.

The introduction of power fees also influences the interpretability of node balance dual variables as market prices as they are considered in each daily market matching but are only billed for the highest peaks of the year later. This process is later introduced in Section 4.3.2 (Equation 3.23).

Further features of the market model such as a distinguishability of electricity categories are implemented in the field-test but not evaluated in this thesis. A detailed description can be found in Appendix A.2.

3.2. Participant model

Figure 3.4 shows an overview of a generic energy system model of a participant including the modeled assets. The energy system of LEM participants is modeled as a two-bus system for the commodities electricity and heat. Energy assets (generation, load, storage) can be connected to either of the buses or convert one commodity to another (e.g., HPs). Connections to the grid are modeled separately for the LEM and the Backup supplier as different prices may occur.

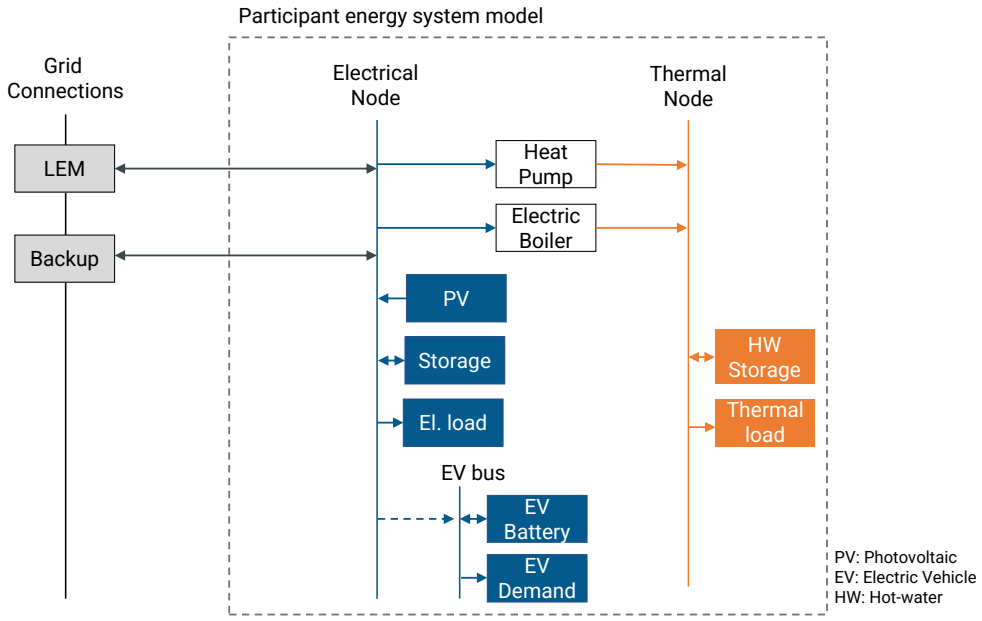

Figure 3.4.: Overview of a generic participant energy system model with all considered energy assets.

The main equations of the participant energy system model are the balance equations of the electrical and thermal buses. For a set of Loads L, Storages ST, Generators G and Converters C the electrical balance equation is defined as:

$$\sum_{l\in\mathcal{L}} P_{l,t}^{\mathrm{el}} + \sum_{st\in\mathcal{ST}} P_{st}^{\mathrm{el,ch}} + \sum_{c\in\mathcal{C}} P_{c}^{\mathrm{el,in}} + \sum_{g\in\mathcal{G}} P_{g}^{\mathrm{el}} + P_{t}^{\mathrm{bu,out}} + P_{t}^{\mathrm{LEM,out}} = \sum_{st\in\mathcal{ST}} P_{st}^{\mathrm{el,dch}} + \sum_{c\in\mathcal{C}} P_{c}^{\mathrm{el,out}} + P_{t}^{\mathrm{bu,in}} + P_{t}^{\mathrm{LEM,in}}, \quad \forall\, t \in \mathcal{T}, \tag{3.41}$$

with $P_{l,t}^{\mathrm{el}}$ as the active power demand of a load, $P_{st}^{\mathrm{el,ch}}$ and $P_{st}^{\mathrm{el,dch}}$ as charging and discharging powers of a storage, $P_{c}^{\mathrm{el,in}}$ as power input to a converter, $P_{c}^{\mathrm{el,out}}$ as power output from a converter and P_{g}^{el} as power output from a generator. $P_{t}^{\mathrm{LEM,in}}$ and $P_{t}^{\mathrm{LEM,out}}$ represent exchange from and to the LEM. $P_{t}^{\mathrm{bu,in}}$ and $P_{t}^{\mathrm{bu,out}}$ represent exchange from and to the backup supplier.

The thermal balance constraint can be defined as:

$$\sum_{l\in\mathcal{L}} P_{l,t}^{\mathrm{th}} + \sum_{st\in\mathcal{ST}} P_{st}^{\mathrm{th,ch}} = \sum_{st\in\mathcal{ST}} P_{st}^{\mathrm{th,dch}} + \sum_{c\in\mathcal{C}} P_{c}^{\mathrm{th,out}}, \quad \forall\, t \in \mathcal{T} \tag{3.42}$$

with $P_{l,t}^{\mathrm{th}}$ as thermal loads, $P_{st}^{\mathrm{th,ch}}$ and $P_{st}^{\mathrm{th,dch}}$ as input and output from a thermal stroage. $P_{c}^{\mathrm{th,out}}$ represents the thermal output of a converter converting electric power to thermal power.

A detailed description of the asset models and respective constraints is provided in Section 3.3.

Asset-based order generation

As described in Section 3.1.2, the optimal operation of the energy system is performed by the market matching algorithm. Hence, no local optimization of the participants energy system is required to participate in the LEM. Participants with a local Energy Management System (EMS) might also participate in the market solving a local optimization problem with, e.g., minimizing operation costs, to then submit the residues as market orders. This requires an accurate forecast of market prices at the LEM as an input to the objective function of the EMS.
The simulations in this Thesis focus on participants without a local EMS which submit orders to the markets mapped to the assets of the participant. For inflexible assets (e.g., baseload of a participant or PV), buy and sell orders are generated with the forecast of the respective time series. Flexible assets like EVs or HPs and their representation as market orders are described in the following section. The participation of a market participant with a local Energy Management System (EMS) is demonstrated in the field test.

Price parameters of the market orders are assumed to reflect the opportunity costs of the asset to the participant. The opportunity costs in this case reflect the value or costs which would have been generated when not participating in the LEM and purchasing or selling at another opportunity. More concretely, e.g., the minimum sell price for a PV asset at the LEM is the price the participant would earn for directly feeding into the grid (fixed feed-in tariff). The detailed derivation of asset prices for the evaluated simulations is described in Section 4.2.2.

3.3. Asset models

For inflexible demand (baseload), inflexible generation (PV) and storage assets the mathematical models describing their behavior are equivalent to the models already introduced in the market model (Section 3.1.2). For the flexible demand of EVs and HPs a detailed model and the generation of market orders is introduced in the following sections.

3.3.1. Electric vehicles

To model flexibility provided by an electric vehicle as a flexible order to the LEM, three main order inputs are required:

- When are the vehicles plugged in/plugged out?
- How much energy needs to be provided during the time the vehicles are plugged in?
- What is the maximum rated charging power of the EV?

To generate the respective time series of plugin state $\mu_{\mathrm{pl}}(t)[0/1]$ synthetic profiles for individual EVs are generated mainly based on empirical data of the mobility behavior in Germany which provides a detailed dataset differentiated by modes of transport, region, trip reason, etc. [138]. Additionally, parameters of the individual EVs and charging facility (battery capacity, charging efficiency, rated power of charger) are taken into account to calculate the consumed energy and the SOC at plugin and plugout events $SOC(\mu_{\mathrm{pl}}(t))$.

The representation of an EV charging station within the energy system of a participant is shown in Figure 3.5.

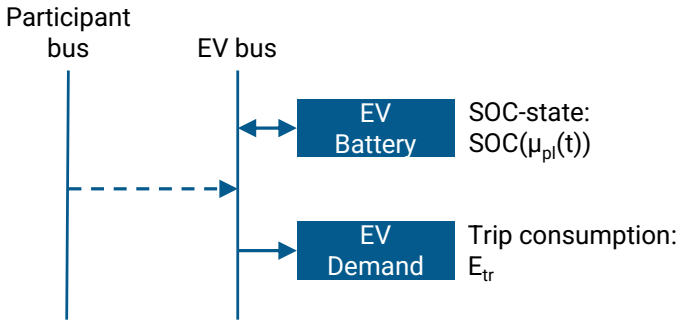

Figure 3.5.: Model of EV within the participant energy system

Figure 3.6 provides an overview of the modeling procedure to generate the required model inputs for one trip. The departure time is chosen on the basis of the day type (weekday/weekend).

Assumptions for the departure time are based on a distribution function derived from empirical data which is upsampled to match the intervals of the market period $\mathcal{T}$ (96 time intervals per day). A comparison of the derived distributions for weekdays and weekend is shown in Figure 3.7. Assumptions for the driven distance, duration and speed (trip parameters) are also derived from [138]. For an individual EV, these parameters and the duration of the average working day are

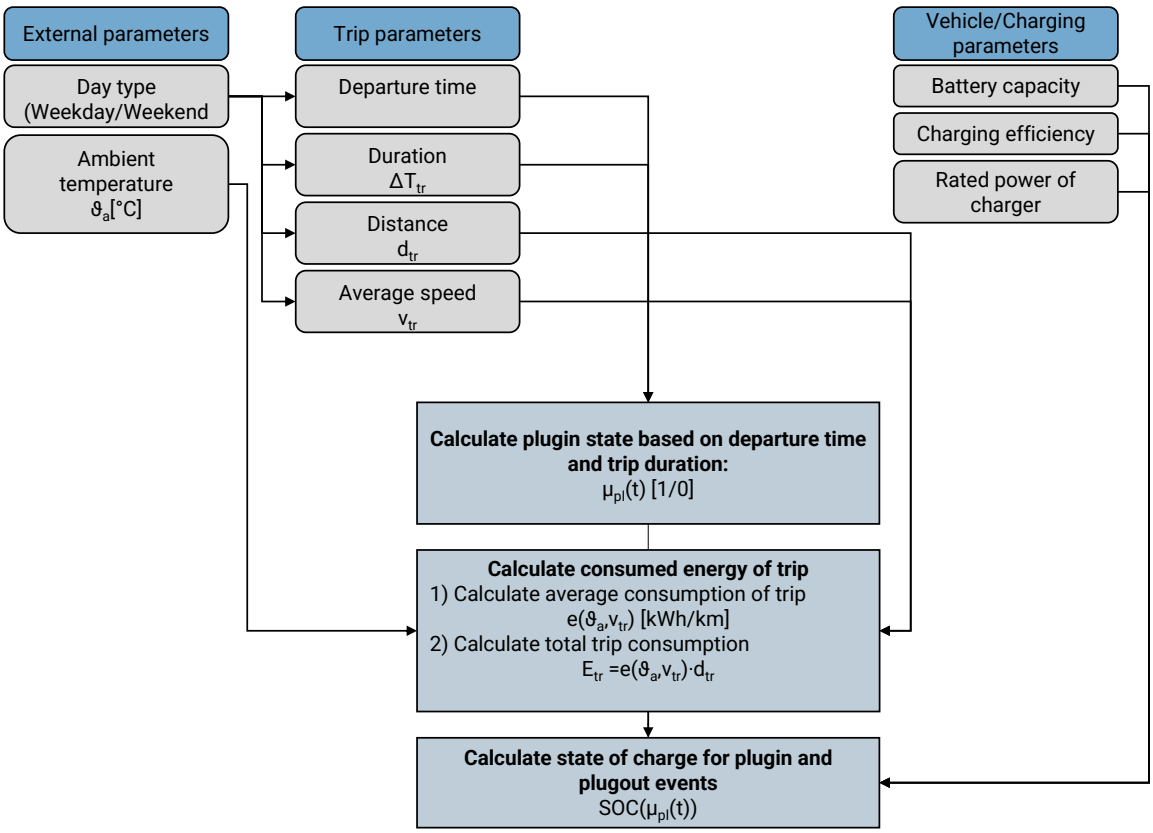

Figure 3.6.: Overview of modeling approach to generate synthetic EV charging curves as an input for the LEM model.

kept constant throughout the generation of trips in one year assuming the participant behavior and work place do not change.

On the basis of the trip parameters, the plugin state of the EV is calculated assuming that the EV is directly plugged in when reaching the charger. Two types of EV charging behaviors are considered. For residential LEM participants, the EV is only charged at home assuming that it has to be fully charged when starting the next trip, i.e., when plugged in after work in the evening the EV is fully charged when departing to work. For commercial LEM participants, e.g., an office building with a charging facility, EVs are charged once they arrive at the work destination (ref. Figure A.3). A combination of both, i.e., an EV charging at home and at work, is not considered here.

The consumed energy of one trip is mainly depending on the average speed driven and the ambient temperature (ref. Figure A.2). This is mainly caused by the additional demand of air conditioning for warm periods and heating for cold periods. Based on the ambient temperature and the average speed of the trip the energy consumption rate [kWh/100 km] is calculated with a piecewise linear interpolation of the data points provided by [139]. Multiplied by the trip distance, the total energy consumption of the trip is calculated (E_{tr}). Self-discharge of the battery is neglected. If the calculated trip is infeasible, e.g., if the calculated trip consumption exceeds the available battery

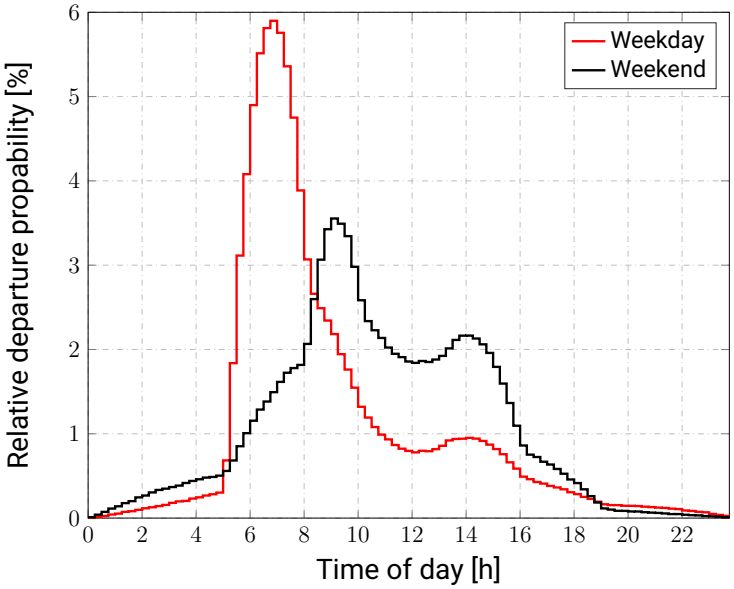

Figure 3.7.: Probability of departure times for trips on weekdays and weekends. Based on empirical data in [138] with selected trip reasons work ("Arbeit, dienstlich / geschäftlich") and education ("Ausbildung") for weekdays - shopping ("Besorgung") and leisure ("Freizeit") for weekends.

capacity, input assumptions (distance, speed) are reduced to feasible levels.

In the last step, the SOC at the arrival at the charger is calculated based on the SOC at the last plug out $SOC(\mu_{pl-1})$ and the total consumption of the trip E_{tr} and the maximum battery capacity $E^{\mathrm{bat,max}}$:

$$SOC(\mu_{\mathrm{pl}}) = SOC(\mu_{\mathrm{pl}-1}) - 100\% \frac{E_{\mathrm{tr}}}{E^{bat,\mathrm{max}}} \tag{3.43}$$

Based on the available plugin time Δt_{pi}, rated power of the charger $P^{\mathrm{r,ch}}$ and charging efficiency η^{ch}, the maximum SOC at departure is calculated as:

$$SOC(\mu_{\mathrm{pl}+1}) = \min(100\%, SOC(\mu_{\mathrm{pl}}) + \frac{P^{\mathrm{r,ch}} \Delta t_{pi}}{\eta^{\mathrm{ch}} E^{\mathrm{bat,max}}}) \tag{3.44}$$

A resulting plugin state and SOC profile is shown for a home-charged example vehicle for one week in Figure 3.8. A regular commuter pattern during workdays and two short trips during the weekend are generated. With the generated data, the participation of the EV as a flexible load at the LEM can now be modeled as an order considering the valid timeperiod (t_{start}, t_{end}) as the plugin time of the vehicle, the maximum power input as the rated charging power $P^{\mathrm{r,ch}}$ and the ordered energy as the difference between the energy amount at plugin and plugout.

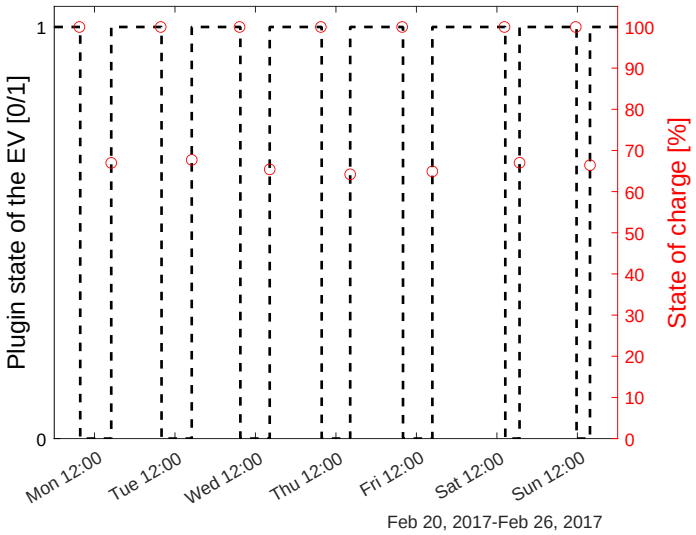

Figure 3.8.: Generated plugin state and SOC for plugin and plugout events for home charging in an example week. Assumptions: Battery capacity = 30 kWh, one way distance to work = 25 km, average speed = 50 km/h, working hours = 8 h.

Order generation

EVs are represented in the market model as flexible demand. The maximum power $p_{b,t}^{\max}$ of a buy order for an EV can be defined with the generated EV driving data defining the maximum power of the order as:

$$p_{b,t}^{\max} = \begin{cases} p^{\mathrm{r,ch}}, & \mu_{\mathrm{pl}}(t) = 1 \\ 0, & \mu_{pl}(t) = 0 \end{cases} \tag{3.45}$$

With $p^{\mathrm{r,ch}}$ as the rated charging power and the required energy as:

$$e_b^{\max} = SOC(\mu_{\mathrm{pl}+1}) - SOC(\mu_{\mathrm{pl}+1}) \tag{3.46}$$

3.3.2. Heat pumps

Heat pumps allow the coupling of the electricity and heat demand at the participants energy system. As the commodity heat is not traded at the investigated LEM in this Thesis, the heat demand has to be translated into a flexible buy order at the LEM. Within the participant model, heat is supplied either by the heat pump or a peak electric boiler. A Hot Water Storage (HWS) tank is assumed which uncouples the generation of heat and the thermal demand (ref. Figure 3.9).

To simplify, the equations presented are limited to a system containing only one asset per asset type (e.g., heat pump, electric boiler, heat storage, and thermal load). The thermal load balance constraint of a participant can be formulated as:

$$P_{hp,t}^{\mathrm{th}} + P_{eb,t}^{\mathrm{th}} + P_{st,t}^{\mathrm{th,dch}} = P_{st,t}^{\mathrm{th,ch}} + P_{l,t}^{\mathrm{th}}, \quad \forall\, t \in \mathcal{T}, \tag{3.47}$$

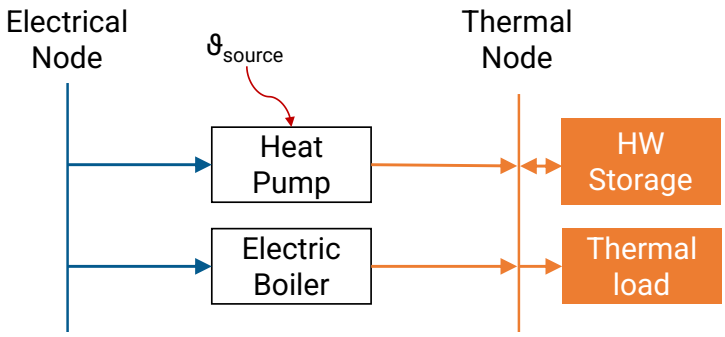

Figure 3.9.: Model of HP, electric boiler and thermal system within the participant energy system.

with $P^{\text{th}}_{hp,t}$ as the thermal power output of the heat pump hp, $P^{\text{th}}_{eb,t}$ the thermal power output of an electric boiler eb, $P^{\text{th,ch/dch}}_{st,t}$ as the charge and discharge power of the HWS and $P^{\text{th}}_{l,t}$ as the thermal load. The coupling of the electricity node and the thermal node through the electric boiler and heat pump are defined as:

$$P^{\text{el}}_{eb,t}\eta_{eb} = P^{\text{th}}_{eb,t}, \quad \forall\, t \in \mathcal{T}, \tag{3.48}$$

with η_{eb} as the efficiency of the electric boiler. And

$$P^{\text{el}}_{hp,t}COP_{hp,t} = P^{\text{th}}_{hp,t}, \quad \forall\, t \in \mathcal{T}, \tag{3.49}$$

with $COP_{hp,t}$ as the Coefficient Of Performance (COP) of the heat pump. The COP, i.e., the ratio of the provided thermal energy per spent electrical energy, is dependent on the source temperature $\vartheta_{\text{source}}$ and the supply temperature $\vartheta_{\text{supply}}$. It can be derived from the Carnot-efficiency and the heat pump efficiency (η_{hp}) following [140] as:

$$COP_{hp,t} = \frac{\vartheta_{\text{supply},t}}{\vartheta_{\text{supply},t} - \vartheta_{\text{source},t}}\eta_{hp}, \quad \forall\, t \in \mathcal{T}, \tag{3.50}$$

assuming a fixed supply temperature $\vartheta_{\text{supply}}$ and a variable source temperature $\vartheta_{\text{source},t}$ (e.g., for air source heat pumps). For the simulative evaluations a constant supply temperature of $55°C/328.15K$ and an η_{hp} of 0.36 is assumed based on [140].

Order generation

A buy order of the heat pump can be interpreted as a flexible buy order at the LEM, as the HWS provides a decoupling of the thermal demand and electrical power consumption to a certain extent. For the simulative evaluation, a sufficiently sized HWS is assumed which can supply the thermal demand for a specific time horizon (T), e.g., a quarter of a day. For the residual demand, it is assumed that the peak electric boiler can cover the demand and peaks which can not be covered by the heat pump or HWS. It is assumed that the total heat demand over the time horizon T (E^{l}_{th}) and the ambient temperature $\vartheta_{\text{source}}$ is known before submitting the order. Relevant parameters for a buy order b are defined as:

$$p_{b,t}^{\max} = P_{hp}^{\mathrm{r,el}}. \tag{3.51}$$

With $P_{hp}^{\mathrm{r,el}}$ as the rated electrical power of the heat pump and the maximum electricity demand as:

$$e_b^{\max} = \frac{\sum_{t \in \mathcal{T}} \Delta t P_{l,t}^{\mathrm{th}}}{\overline{COP_t^{\mathrm{hp}}}}.$$

This formulation might lead to a suboptimal solution of the operation of the participant heat pump as an average $\overline{COP_t^{\mathrm{hp}}}$ over the temporal set $\mathcal{T}$ is assumed. However, the flexibility incorporated in the order might lead to cheaper buy prices at times with a suboptimal COP_t^{hp}. The order generation for heat pumps could be improved, e.g., by specifying different maximum buy prices for a varying COP_t^{hp}. However, within the scope of this Thesis, it is assumed that the maximum buy price of the order is constant over time.

4. Method

4.1. Overview

The methodological part of this work is divided into three parts: Scenario generation, simulation, and result evaluation (Figure 4.10).

The scenario generation (Section 4.2) aims at providing a set of consistent distribution grid topologies along with modeled assets and price assumptions. To model the effect of an increasing number of DERs, four scenario years (2020, 2025, 2030, 2035) are considered. Further, a multi-year analysis allows to model more detailed assumptions on the distribution of order prices, e.g., for PV assets considering future feed-in tariffs and assets which run out feed-in tariff. Another main focus is put on the effect of a LEM on a variation of typical LV distribution grids (rural, semiurban, urban). Hence, a variation of typical load, generation and asset distribution characteristics can be analyzed. To evaluate seasonal and daily effects yearly time series of VRE electrical and thermal loads are considered. A plausibility check is applied to ensure the consistency of the generated scenario assumptions. Additionally, a method to synthetically generate erroneous load forecasts is developed and applied.

The simulation of the generated scenarios (Section 4.3), includes two modes of operation logic of the energy system. The Business As Usual (BAU) mode represents the benchmark case and assumes an individual rule-based operation of the participants' energy systems. The LEM mode represents an operation of the energy system with a market operator, market participants and a variation of fee scenarios (flat-, variable-, feeder- and power-fees). Considering the permutations of all parameter variations, i.e., grid types, scenario years, fee scenarios and modes of operation, results in 60 yearly simulation scenarios.

The result evaluation (Section 4.4) focuses on generating a set of interpretable/normalized KPIs on the basis of market, participant and grid results to answer the research questions.

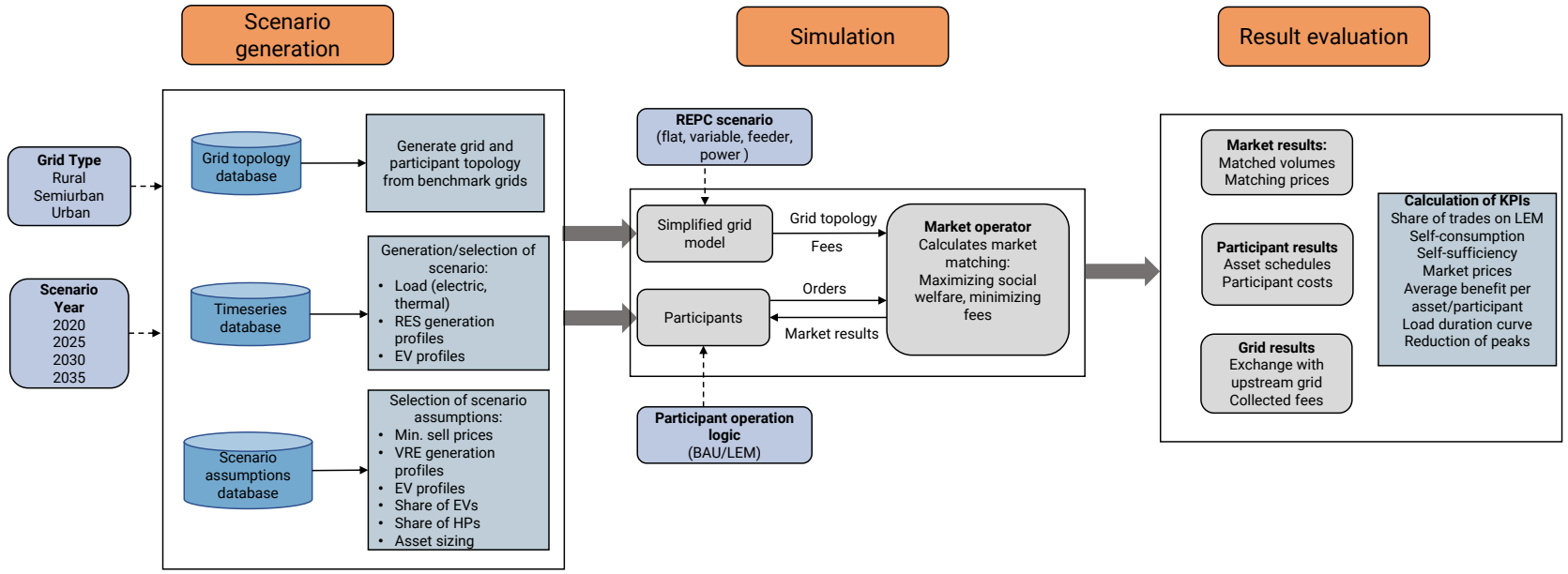

* VRE: Variable Renewable Energy, EV: Electric Vehicle, HP: Heat Pump, BAU: Business as Usual, LEM: Local Energy Market, REPC: Regulated Electricity Price Component

Figure 4.1.: Overview of the methodological framework and steps for the simulative evaluation.

4.2. Scenario generation

4.2.1. Benchmark grids

To provide comparability of the results, benchmark grids derived from typical LV distribution grids from the Simbench dataset [141] are used. This dataset also provides expansion scenarios of assets (PV, HP, EV and battery storages) for a baseline year 2016 and expansion scenarios for 2024 and 2034. The expansion scenarios are mainly based on the German grid development plan of 2019 [33]. These assumptions are taken as a baseline for the generated scenarios, however, are adapted to the latest grid development plan [142] and the equidistant scenario years 2020, 2025, 2030, 2035.

Three different distribution grid types (rural, semiurban, urban) are evaluated to cover the full bandwidth of different shares of residential and commercial participants as well as load or generation dominated regions. From the Simbench dataset grids with a similar amount of grid connection points are chosen (rural: LV2.101, semiurban: LV5.201, urban: LV6.201). A full list of the technical parameters of the grids can be found in [140].

The number of EVs for the scenario years are adapted to the updated grid development plan taking into account the mean of the described scenarios for the scenario years of 2020 and 2035 and linearly interpolating for others. The relative share of EVs per household is calculated by accounting for the specific cars per participants for the respective regions. Figure 4.2 shows the adapted cars per household assuming a steady number of private cars (42.5 Million in 2020 [143]) and 1.1, 1.2 and 1.3 cars per household for urban, suburban and rural regions respectively from the German mobility statistics database [144].

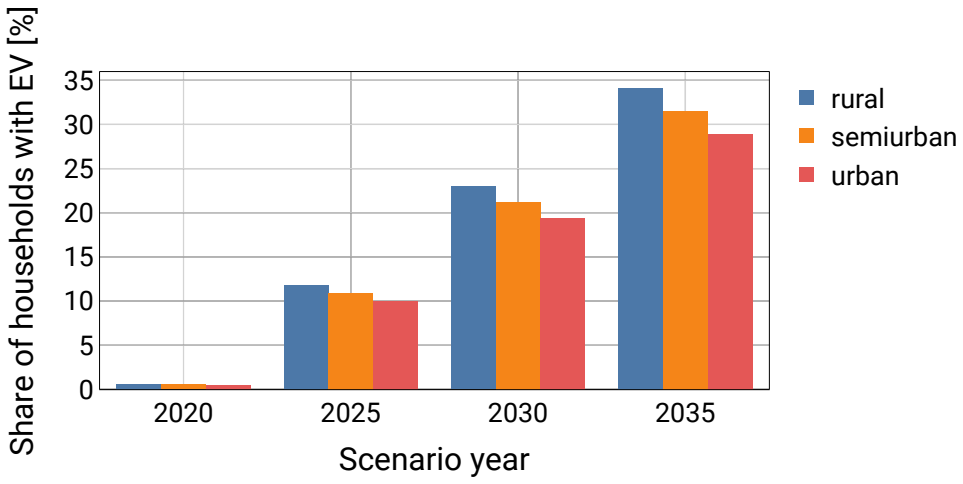

Figure 4.2.: Scenario assumptions for the development of electric vehicles per household based on [142], [143] and [144].

Besides the shares of EVs, scenario assumptions for HPs are also adapted to new projections from the grid development plan and based on the assumption of a stable number of heating systems (20.2 Million [145]) for the scenario years. The resulting share of heatpumps per heating system are 5 %, 6.6 %, 13.2 %, 24.8 % for the scenario years 2020, 2025, 2030 and 2035. Since further parameters like the installed PV capacity or battery storage capacity do not significantly change

between the grid development plan used in Simbench and the plan used in this Thesis, Simbench scenario assumptions are used and linearly inter- and extrapolated to fit to the scenario years in this Thesis.

Timeseries for electric vehicles are developed using the algorithm described in Section 3.3.1. Since the Simbench dataset only provides timeseries for the electric demand of the heat pumps, the thermal load required to generate flexible demand orders (Section 3.1.1) is derived as described in Equations 3.49, 3.50. Weather data based timeseries (PV-profile, ambient temperature) in the Simbench benchmark grids are based on data from northern Germany (Hannover, Lübeck).

The resulting asset parameters and assumptions for the benchmark grids and the scenario year 2035 are shown in Table 4.1, data for all other scenarios can be found in the Appendix A.3.

Table 4.1.: Simulation scenario parameters and assumptions for the scenario year 2035.

Parameter	Type/Unit	Rural	Semiurban	Urban
Grid connection points	Count [-]	96	110	58
Residential loads	Count [-]	92	92	102
Commercial loads	Count [-]	7	12	9
Photovoltaic systems	Rated power [kW]	326.7	432.4	222.1
	Count [-]	19	30	19
Heat pumps	Rated power [kW]	138.1	100.9	63.4
	Count [-]	24	27	14
	share	24.2	26.0	12.6
Electric vehicles	Rated power [kW]	241.0	262.8	166.2
	Count [-]	33	35	17
Battery	Rated power [kW]	93.0	247.7	50.8
	Count [-]	8	15	7
	Capacity [kWh]	186.3	495.5	101.7
Electric load	Energy [MWh]	257.9	470.3	530.9
Thermal load	Energy [MWh]	159.5	166.9	102.0
Electric load EV	Energy [MWh]	111.2	90.6	62.0

Plausibility check

To check the plausibility of the scenario assumptions, the overall electric, thermal and mobility (EVs) demand of the final scenarios are compared to average values found in the literature.
The overall demand for EVs for the rural grid in the year 2035 for instance is 111.2 MWh. Broken down to the 33 EVs in this scenario case and considering a charging efficiency of 90 % an average of 3032 kWh is consumed per EV and year. Assuming an average mileage of 21.58 $\frac{\mathrm{kWh}}{100\mathrm{km}}$ [146][1], this results in a total driving distance of 14 053 $\frac{\mathrm{km}}{\mathrm{a}}$. This distance is slightly above the average driving distance of 13 323 $\frac{\mathrm{km}}{\mathrm{a}}$ reported by the German Federal Motor Transport Authority for private vehicles in 2020 [147], which is plausible for in a rural environment compared to the national average and well within the same order of magnitude.

[1] Average mileage of 49 investigated EV models in a test under real conditions.

The yearly electricity demand for the same scenario is 257.9 MWh. Divided by the total number of participants/loads this yields an average annual demand of 2605 kWh, which is close to the average yearly demand of 2782 kWh reported in [148].
The yearly thermal energy demand of the whole LEM (159.5 MWh) is distributed to households with a HP resulting in a thermal consumption of 6625 $\frac{\mathrm{kWh}}{\mathrm{a}}$ per household with a HP. Considering a specific heat demand of typically well insulated buildings equipped with heat pumps of 67 $\frac{\mathrm{kWh}}{\mathrm{m^2 a}}$ [149] and an area of 100m^2 for a 3 person household [150] this leads to a similar value for the thermal demand of 6700 $\frac{\mathrm{kWh}}{\mathrm{a}}$.
Besides this rough plausibility check, a thorough plausibility analysis on the asset parameters of the benchmark grids is performed in [140].

4.2.2. Order prices

Price assumptions for orders at the LEM are based on the opportunity costs of the involved assets. Minimum sell prices for PV are for example based on the expectable revenue for selling one kWh at the guaranteed feed-in tariff. Maximum buy prices are based on the next cheapest option, i.e., the price directly buying from an energy retailer or utility. In this section the method to generate the relevant prices for the simulation scenarios is described.

Photovoltaic

Opportunity costs for PV systems are derived from the historic and projected feed-in tariffs in Germany, which are valid for 20 years, and the current as well as projected installations. For the currently installed systems the database "Anlagenstammdaten" of the four German TSOs is used which provides technical (e.g., the installed rated power) and non-technical (e.g., the installation date) data on renewable energy power plants in Germany. In this thesis the latest dataset including data until 2021 is used [151]. The dataset is filtered for the relevant power plants, i.e., PV plants which are still in operation resulting in around 2.02 Million assets.

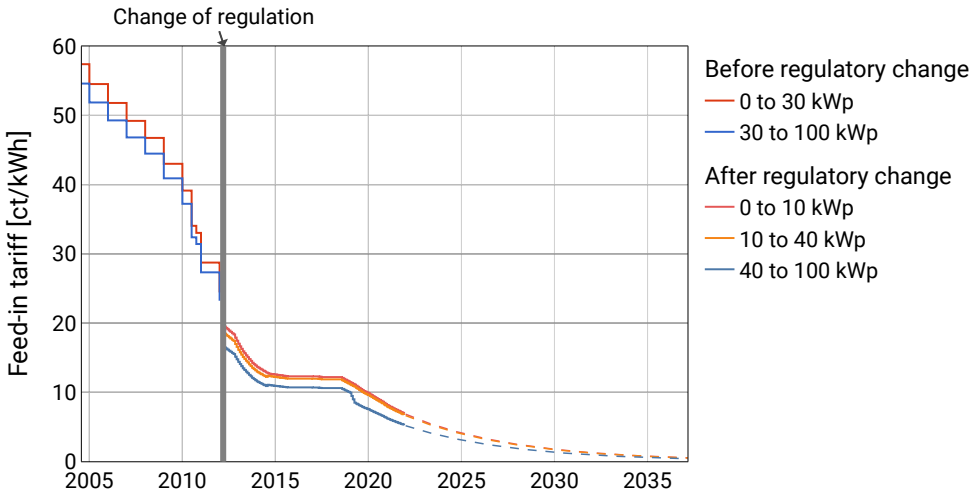

Figure 4.3.: Historic and projected guaranteed feed-in tariffs for PV power plants with a rated capacity between 0 and 100 kWp in Germany based on [152], [153].

To map the installed asset base with the respective feed-in tariff, each asset is assigned with its feed-in tariff based on the installation date and the size of the assets. The historic and projected feed-in tariffs are shown in Figure 4.3. Within the last 15 years, the feed-in tariffs reduced drastically from a level of around 55 ct/kWh in 2005 to below 10 ct/kWh in 2020. For the future development of the tariffs, a monthly degression of 1.4 % is assumed based on the regulatory framework [153]. After an adaption of the regulatory framework in 2012, the structure of the feed-in tariff changed to a more granular assessment of the PV size and a decrease of the guaranteed feed-in times to a monthly adaption.

To obtain relevant price distributions for the modeled scenario years, each PV asset is assigned with its feed-in tariff based on the date of construction. For PV assets which operate longer than 20 years in the considered scenario, the feed-in tariff of the scenario year is applied to the asset, assuming a technical lifetime of 30 years [154] and the market value of the sold energy based on direct marketing and feed-in premium [155]. The increase of PV capacity until the last scenario year (2035) is based on the latest grid development plan [142].

In Figure 4.4, the resulting average feed-in tariffs and share of assets without a feed-in tariff are shown. With a steeply increasing share of PV assets without feed-in tariff within 2025 and 2035 and an increasing feed-in tariff of new assets, the average feed-in tariffs drop from the baseline 30.9 ct/kWh (in 2020) to 21.4 ct/kWh in 2025, 10.3 ct/kWh in 2030 to 3.2 ct/kWh in 2035.

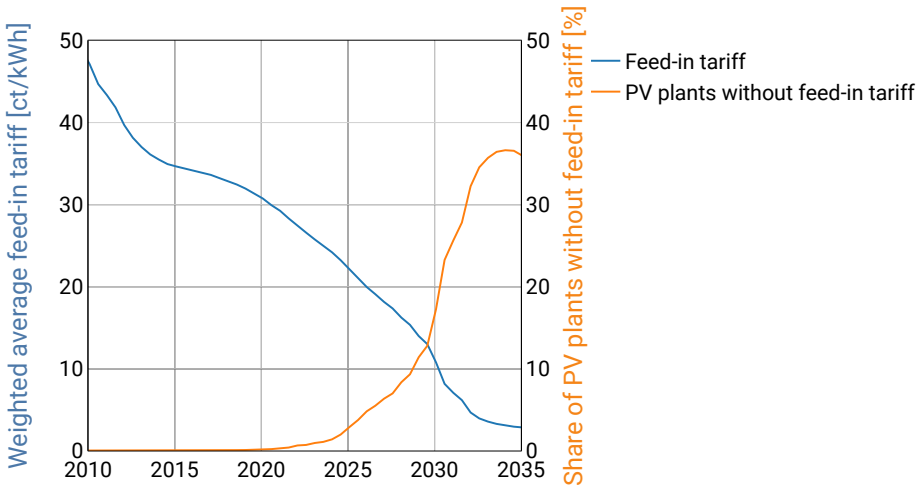

Figure 4.4.: Development of weighted average feed-in tariffs and the share of PV plants without feed-in tariff for in Germany. Based on [151]–[153].

To model individual assets for different benchmark grids, each modeled asset is assigned with a minimum sell price based on the yearly distributions shown in Figure 4.5. For each asset in the modeled grid, a feed-in tariff is randomly drawn from the yearly distribution until the average of the year is reached with a stopping criterion of a 0.1 % difference. This approach allows to model the prices of individual assets while retaining a consistent average price allowing an improved generalization of the simulation results. It should be noted that depending on the geographical area these price assumptions might differ as certain areas with early adopters of PV assets will

reach lower prices earlier as the number of assets without feed-in tariffs are higher in the respective scenario years.

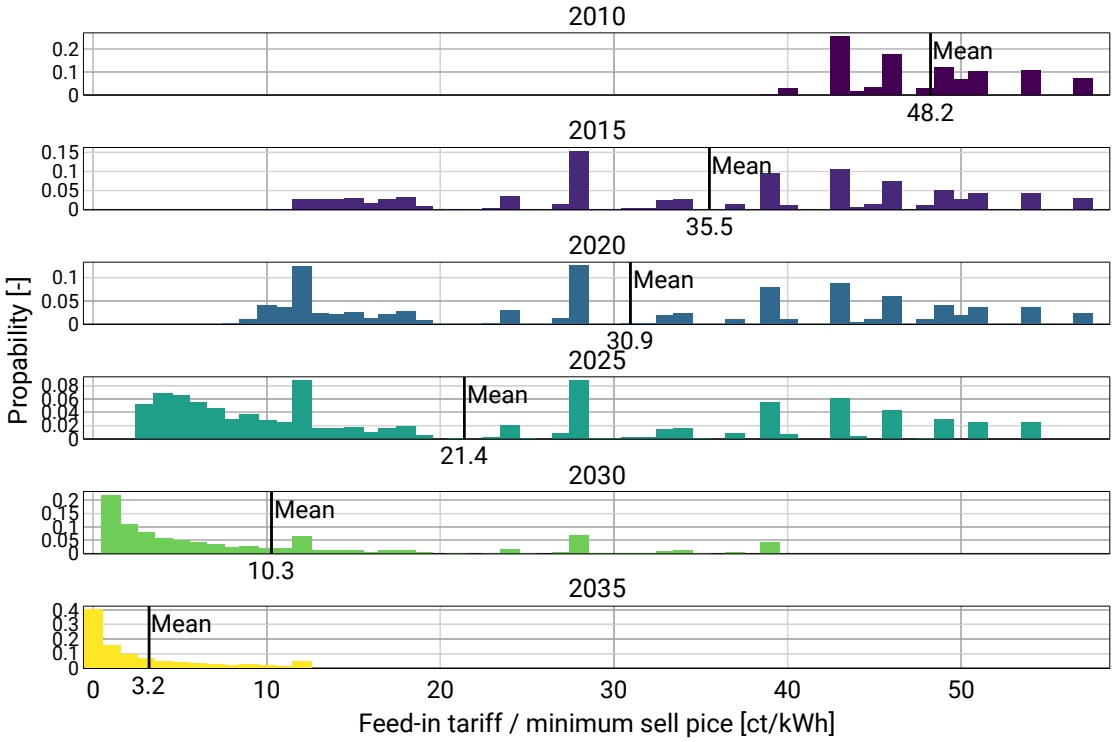

Figure 4.5.: Histograms of feed-in tariffs or minimum sell price assumptions for 2010, 2015 and the modeled scenarios (2020, 2025, 2030, 2035). Bin size: 1 ct/kWh.

Battery storages

As described in the order definition (Section 3.1.1), storage orders are submitted with a minimum discharge price. Each sold kWh from a battery storage system needs to be previously bought from the market. The minimum sell price hence, represents the arbitrage opportunity costs of the battery operator benefiting from buying at lower prices (e.g., at high PV feed-in) and selling at higher prices. It is assumed that the arbitrage opportunity at the wholesale market can be used as an approximation for the expectable revenue of a battery storage owner. Figure 4.6 visualizes the daily maximum arbitrage as the difference of the daily maximum and minimum prices at the day-ahead spot market.

The minimum storage sell price ($c_{st}^{\mathrm{dch,min}}$) is required as an input parameter to storage orders in the LEM. It is approximated as the average of typically daily price spreads at the day-ahead wholesale market, as:

$$c_{st}^{\mathrm{dch,min}} = \frac{\sum_{d=1}^{D} max\left\{\lambda_{d,t1},...,\lambda_{d,t24}\right\} - min\left\{\lambda_{d,t1},...,\lambda_{d,t24}\right\}}{D}, \tag{4.1}$$

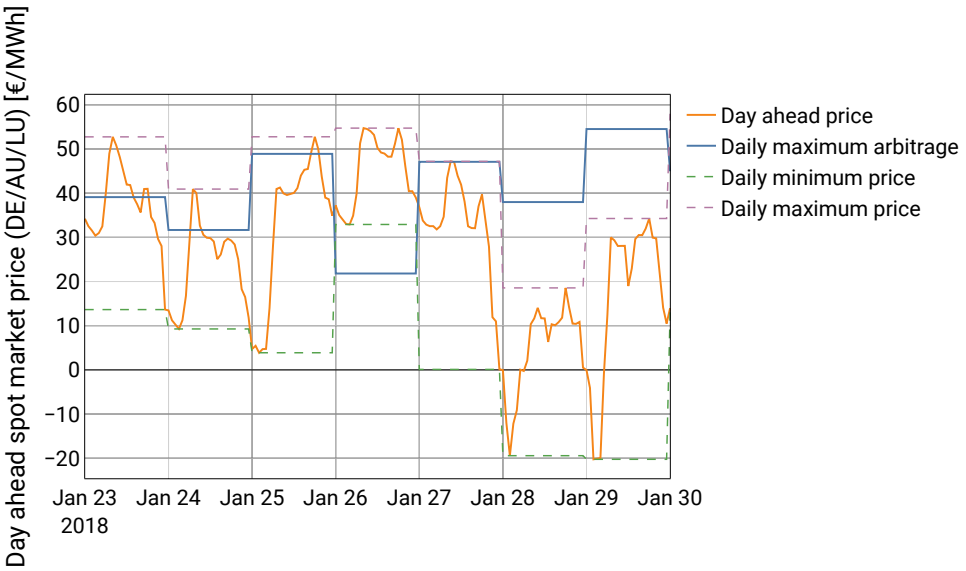

Figure 4.6.: Exemplaric day ahead spot market price and arbitrage opportunities for a week in January 2018. Data source: [156].

with D as the number of evaluated days and $\lambda_{d,t}$ as the day-ahead market price for day d at hour t.

For the evaluation period of the years 2016 ... 2019 an average daily arbitrage of 28.7 €/MWh or 2.87 ct/kWh is calculated, which is assumed as the minimum discharge price in the simulations. The full price curves over the years are shown in Figure A.5. It should be noted that this is an optimistic assumption, as the operator of the battery might only achieve the maximum arbitrage if a perfect foresight of the prices and an optimal trading strategy is assumed. The degradation of the battery and its associated costs are not taken into account in this assumption. Depending on the battery type and battery usage degradation, costs might be higher than the calculated opportunity costs. In this case the maximum of opportunity costs and degradation costs should be considered as the minimum discharge price.

4.3. Simulation

4.3.1. Business as usual scenario

In the Business As Usual (BAU) scenario, the operation of assets at the participant site are not optimized in the simulation. The operation of flexible assets (EVs, HPs, battery storages) are based on rules described in this section. While EVs and HPs are operated individually, the operation of a combination of battery, PV and loads is coordinated.

Operation of PV and battery storage

The operation of a prosumers energy system with a PV installation, a battery storage system and electric loads is modeled with a simple rule based strategy (Algorithm 1). For each simulation timestep t the residual load of the system P_t^{res} is calculated as the difference of all electric loads and the PV feed-in. If the residual load is negative, i.e., if more generation than consumption is present, the algorithm tries to charge the battery system with the residual load if the maximum charge power is not exceeded and the state of charge of the battery is not exceeded. If otherwise the residual load is positive, the battery storage is discharged with the residual load if the maximum discharge power is not exceeded or the battery storage is not empty. The strategy aims at maximizing the self-consumption of generated PV energy and is commonly applied for small roof mounted PV systems and battery storage systems in the residential domain [157], [158]. Figure 4.7 illustrates the resulting battery storage dispatch. At the start of the day, the storage is used to serve the residential demand. Once, the PV generation exceeds the residential demand, the storage is charged with excess PV electricity. If the maximum SOC is reached, the excess PV electricity is fed into the grid. While obtaining a high degree of self-consumption, this approach results in a full feed in of the PV output during the midday.

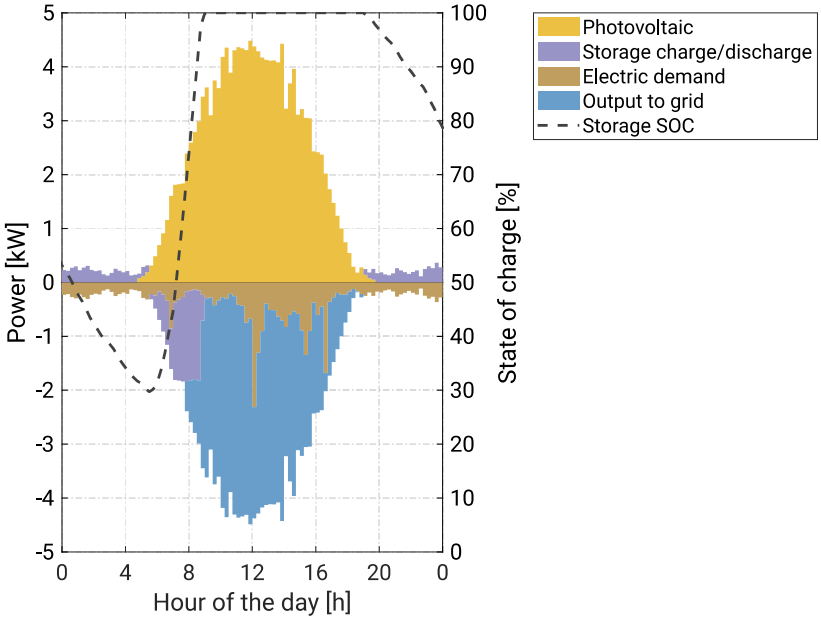

Figure 4.7.: Simulated daily operation of residential system with PV and storage for the BAU case. PV rated power = 6 kW_p, storage capacity = 5 kWh.

Algorithm 1 Determination of rule based storage dispatch for a timestep t, a battery storage st, a PV plant PV and an electric load l

Variables

P_t^{res}: Residual load
$SOC_{st,t}$: Storage state of charge
$P_{st,t}^{\text{ch}}$: Charging power
$P_{st,t}^{\text{dch}}$: Discharging power

Parameters

$P_{\text{PV},t}$: PV power output
$P_{l,t}$: Electric load
$SOC_{st}^{\max}$: Maximum storage state of charge
$SOC_{st}^{\min}$: Minimum storage state of charge
$P_{st}^{\text{ch,max}}$: Maximum charging power
$P_{st}^{\text{dch,max}}$: Maximum discharging power
η_{st}^{ch}: Charging efficiency
η_{st}^{dch}: Discharging efficiency

$P_t^{\text{res}} = P_{l,t} - P_{PV,t}$
if $P_t^{\text{res}} < 0$ **then**
  $P_{st,t}^{\text{ch}} = min(P_{st}^{\text{ch,max}}, |P_t^{\text{res}}|, \frac{SOC_{st}^{\max} - SOC_{st,t-1}}{\Delta t \cdot \eta_{st}^{\text{ch}}})$
  $P_{st,\text{dch},t} = 0$
else if $P_t^{\text{res}} > 0$ **then**
  $P_{st,t}^{\text{dch}} = min(P_{st}^{\text{dch,max}}, P_t^{\text{res}}, \frac{(SOC_{st,t-1} - SOC_{st}^{\min}) \cdot \eta_{st}^{\text{dch}}}{\Delta t})$
  $P_{st,\text{ch},t} = 0$
else
  $P_{st,t}^{\text{ch}} = 0$
  $P_{st,t}^{\text{dch}} = 0$
end if
$SOC_{st,t} = SOC_{st,t-1} + (P_{st,t}^{\text{ch}} \cdot \eta_{st}^{\text{ch}} - \frac{P_{st}^{\text{dch,max}}}{\eta_{st}^{\text{dch}}}) \cdot \Delta t$

Electric vehicles

The BAU operation of EVs assumes that the charging process begins right after the vehicle is plugged in (t_{start}). The charging process then operates for n timesteps until the final State Of Charge (SOC) $SOC_{\text{t}_{\text{end}}}$ is reached. To calculate the number of timesteps required the following equation is applied for one charging process:

$$n = \frac{(SOC_{t_{\text{end}}} - SOC_{t_{\text{start}}}) E_{ev}^{max}}{P_{ev}^{\text{max,ch}} \eta_{ev}^{\text{ch}} \Delta t}, \tag{4.2}$$

with $P_{ev}^{\text{max,ch}}$ as the maximum nominal charging power of the electric vehicle, η_{ev}^{ch} as the charging efficiency, Δt as the simulation timestep size and E_{ev}^{max} as the storage capacity of the electric vehicle. Since this equation might yield non-integer values for n, all timesteps where full charging

is applied are the floor values ($\lfloor n \rfloor$), the remaining charging power for the last until the full SOC is reached can then be calculated as:

$$P_{t_{\text{end}}} = (n - \lfloor n \rfloor) P_{ev}^{\max,\text{ch}}. \tag{4.3}$$

Heat pumps

The operation of heat pumps is based on the operation strategy proposed in the Simbench dataset [140]. It is based on the assumption that the heating and hot water demand is supplied by the heat storage systems. The SOC of the storages is kept at a minimum of 50 % and once this threshold is undercut the storage is filled again by the heat pump or electric boiler depending on the operation mode ([140] Section 3.5.2). Additionally, off-times for the heat pumps are defined for peak demand times: 07:45 - 09:30, 11:30 - 12:30 and 16:45-19:00.

4.3.2. Local energy market

This section describes the procedure for a yearly simulation of one simulation scenario, i.e., for one scenario year, distribution grid topology and REPC scenario. The full method is shown in Figure 4.9. In a first step, the market operator and the grid model is initialized. The simplified grid topology is derived from the Simbench grid model as described in Section 3.1.3. Depending on the REPC scenario, the revelant parts of the grid topology are subsequently assigned with energy and or power fees.

REPC scenarios

The analyzed variation of REPC scenarios is shown in Figure 4.8.

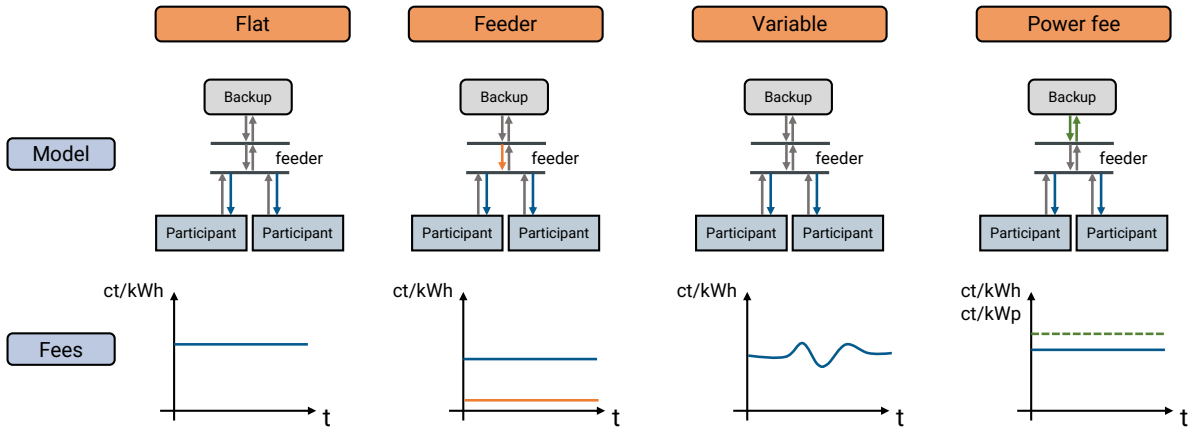

Figure 4.8.: Overview of the simulation scenarios varying the grid tariff design.

Starting on the left, the *Flat* scenario reflects the current state of the regulatory framework. A time independent (flat) energy fee is paid for every consumed kWh by the participant. These constant REPCs are set to 24.17 $\frac{\text{ct}}{\text{kWh}}$ for the baseline year 2020 (compare Section 2.1.2).

The scenario *Feeder* assumes a reduction of the flat participant fee and adds the difference of the reduction to the feeder node. This scenario is based on the approach of locational grid fees (Section 2.1.3) and incentivizes trades between participants at the same feeder. The assumed reduction in this scenario are based on current regulations in Germany [66] with of the participant fee of $2.44\frac{\text{ct}}{\text{kWh}}$ and an introduction of a node fee with the same amount.
A time variable tariff structure is assumed in the *Variable* scenario. Parts of the fee paid by a consumer is adjusted by a factor influenced by the wholesale market day-ahead price. This scenario incentivizes the operation of flexible demand at times of low wholesale market prices. The participant fee $c_{p,t}$ per timestep t is calculated as:

$$c_{p,t}^{\text{e,in}} = c_{p,\text{base}} + c_{p,\text{variable}} \frac{\lambda_{\text{WM},t}}{\overline{\lambda_{\text{WM},T}}}, t \in \mathcal{T}, p \in \mathcal{P} \tag{4.4}$$

where $c_{p,\text{base}}$ is a constant base fee at $24.17\frac{\text{ct}}{\text{kWh}}$, $c_{p,\text{variable}}$ the variable part of the fee at $2.44\frac{\text{ct}}{\text{kWh}}$ adjusted by the ratio of the wholesale market price of the timestep ($\lambda_{\text{WM},t}$) and the mean price $\overline{\lambda_{\text{WM},T}}$ of the simulation horizon T.

The scenario *Power fee* combines a flat participant fee with a power fee for the exchange of the community with the backup provider (for consumption and generation). With this approach a direct influence on the daily peaks of the overall LEM can be achieved, since the usage of flexibility will be incentivized to avoid generation and demand peaks. A relative power price of 3.7 $\frac{\text{e}}{\text{kW}}$ is assumed based on [159]. During the simulation procedure, the maximum peak and feed-in power is passed on to the next day, i.e., a peak once reached is not to be paid again when undercut. Additionally, a mechanism is introduced rewarding the usage of flexible assets to avoid peaks. It is performed after market matching for a whole billing period. The overall paid power fees (C_{power}) are distributed and weighted to the cost contribution c_p of each participant. The set $\mathcal{D}$ of timesteps with the highest daily demand peak ($P_d^{\text{max,in}}$) of the overall LEM are taken into account and the total power fee costs C_{power} are split amongst the contributing participants:

$$c_p = C_{\text{power}} \frac{\sum_{b \in \mathcal{B}_p} \sum_{d \in \mathcal{D}} P_{b,d}}{\sum_{d \in \mathcal{D}} P_d^{\text{max,in}}}, p \in \mathcal{P} \tag{4.5}$$

with $P_{b,d}$ as the contracted power of a buy b order at timestep d. For now, the calculation is limited to demand peaks ($P_{\text{max,in},d}$) to stay closer to current regulations on peak power pricing.

Simulation loop

After the initialization of market operator and grid model, the simulation is performed consecutively for each day within the simulation horizon of one year. Each participant model is generated from the asset assumptions and time series described in the previous section. For each asset of a participant the respective order (sell-, buy-, storage-order) is generated for one day (96 timesteps) according to the model and method described in Sections 3.3 and 3.1.1.
Once all orders are collected for the day, the market matching problem (Section 3.1.2) is triggered and solved. The market results are saved and fixed to the participants assets, e.g., the resulting SOC of an EV at the end of the day. Once the last day is reached, the simulation terminates and all

relevant asset, participant and market results are saved. The software environment/framework for the implementation of this method is later described in Section 4.3.5.

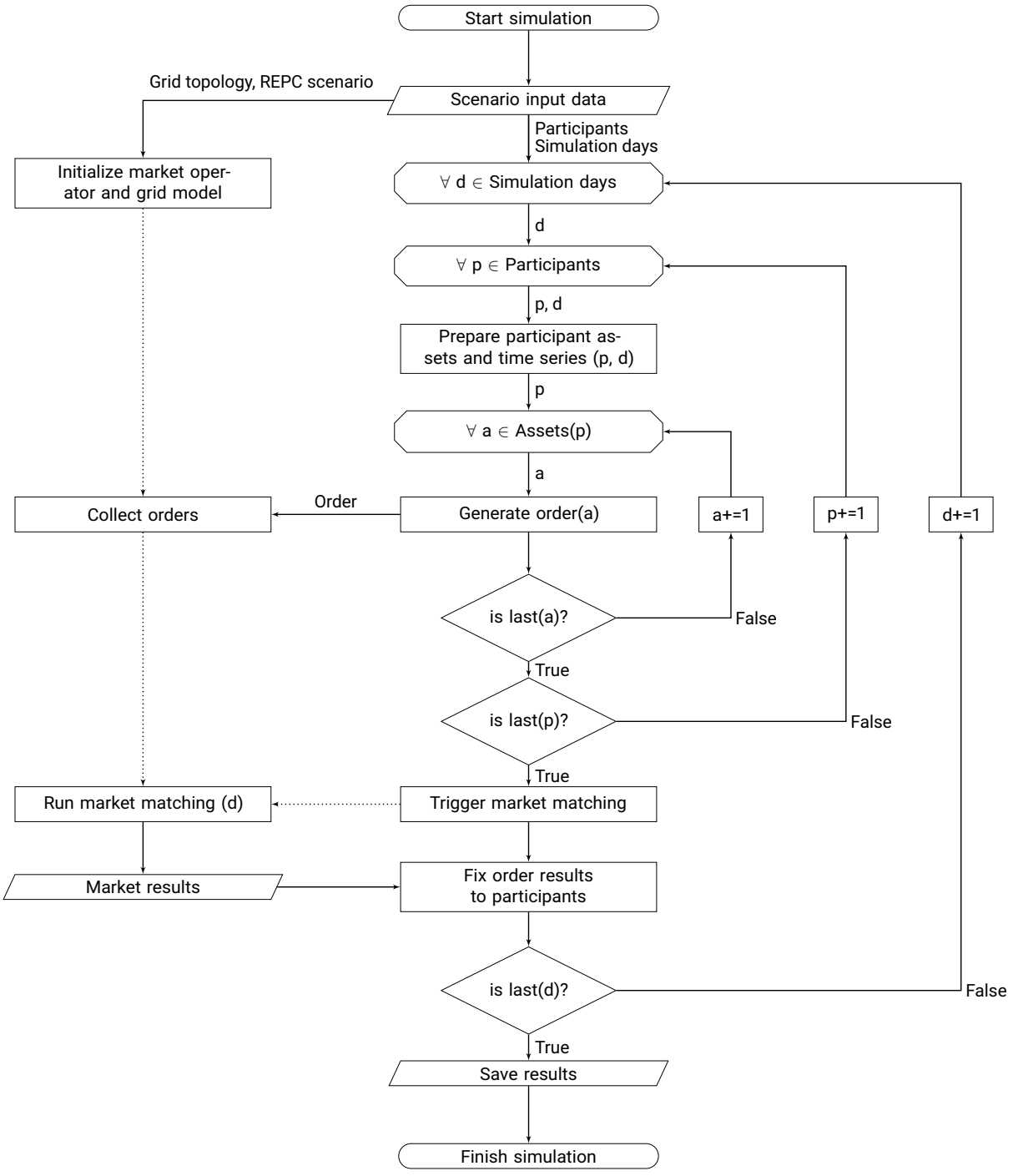

Figure 4.9.: Simplified overview of the simulation method for one LEM simulation case.

4.3.3. Generation of synthetic forecast errors

The following methodological framework is developed to evaluate the impact of load forecast errors on the benefit of individual market participants. The full description, evaluation and classification in the literature can be found in Schreck et al. [22]. Figure 4.10 provides a schematic overview of the method. The central aim is to modify an input load profile in such a way that a predefined forecast error value E_s is achieved within the generated synthetic forecast profile $\hat{P}_t$. Instead of arbitrarily shifting the load profiles values, e.g., by adding a random noise, the method aims to produce similar statistical properties as produced by typical forecasting methods in the literature.

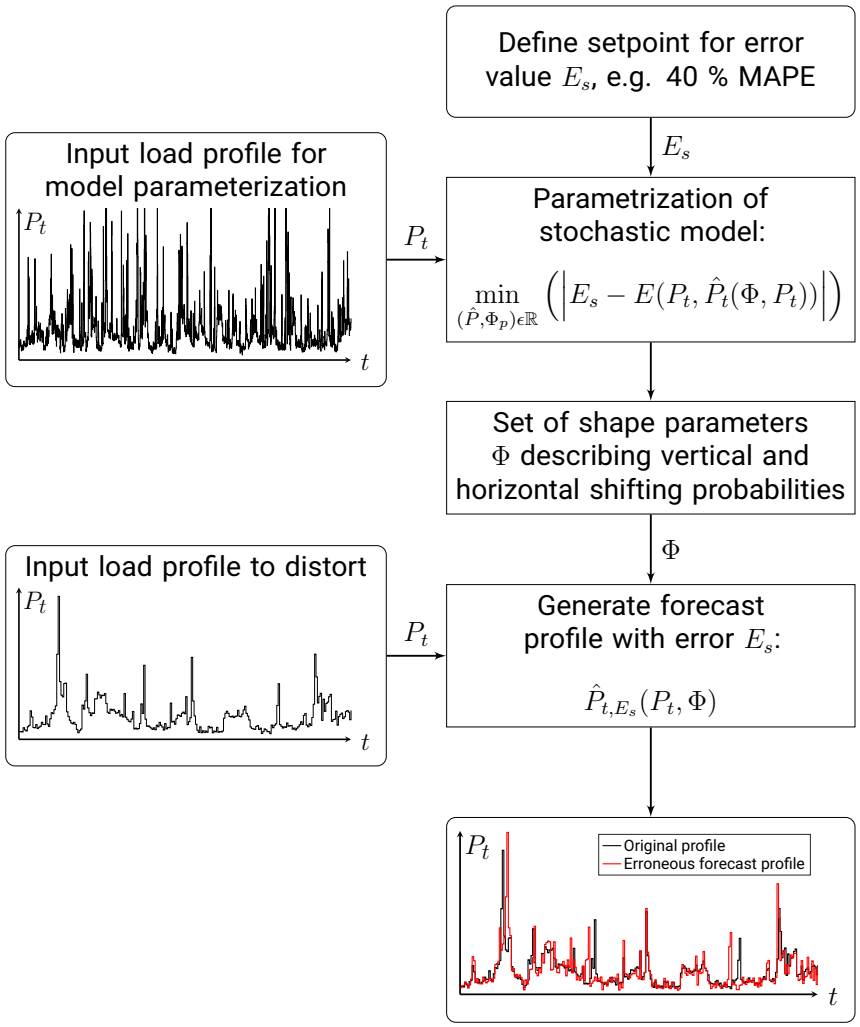

Figure 4.10.: Schematic overview of the method to generate realistic electric load forecast profiles with a previously defined error set point from [22].

The to be adapted load profile P_t is shifted and parameterized by solving the following nonlinear optimization problem. The objective function minimizes the difference between the to be achieved error value E_s and the error of the generated profile:

$$\min_{(\hat{P}_t,\Phi)\epsilon\mathbb{R}} \left(\left| E_s - E(P_t, \hat{P}_t(\Phi, P_t)) \right| \right). \tag{4.6}$$

The error function $E(P_t, \hat{P}_t(\Phi, P_t))$ can be arbitrarily chosen, e.g., Mean Absolute Percentage Error (MAPE), Normalized Root Mean Square Error (NRMSE). Φ represents a set of shape-variables ($\alpha, \beta, \gamma, \sigma_h$) which are relevant in the following constraints. The constraints are used to shift the load profile in such a way that typical error distributions found in the literature are reproduced. Stephen et al. [110] demonstrate that various forecasting models show distinguishable strengths and weaknesses predicting the load profile depending on the type of day and time of day. They also show that times of low consumption and low variability, e.g., during the night, are mostly associated with low forecasting errors throughout different forecasting methods. On the contrary, consumption peaks are notably more difficult to predict as also demonstrated by Shi et al. [160]. This context is the baseline for the definition of the following vertical shift of the profile which is modeled as a random walk process. To keep the structure of demand patterns of appliances (e.g., demand of an oven over multiple timesteps) in the distorted profile, an additional logic of a horizontal shift is later defined.

Vertical-shift

The vertical-shift is defined as:

$$\hat{P}_t = P_t + \delta_t, \tag{4.7}$$

with

$$\delta_t \sim \mathcal{N}(\mu_t, \sigma_t^2), \tag{4.8}$$

$$\mu_t = \alpha(\hat{P}_{t-1} - P_{t-1}), \tag{4.9}$$

$$\sigma_t = \gamma\omega_t(P_t) + \beta(P^{\max} - P^{\min}). \tag{4.10}$$

For each timestep t of the original value P_t is distorted with δ_t which is drawn from a normal distribution (Equation 4.8). The mean and standard deviation of the normal distribution depend on the respective timestep and are adjusted according to Equations 4.9 and 4.10. Through the consideration of the vertical shift of the previous timestep (Equation 4.9) the mean is damped and a strong base oscillation is prevented. The shape variable α gives the option to increase or decrease the relative vertical shifting throughout all timesteps. The standard deviation σ_t is defined by two influences. On the one hand, a weight $\omega_t(P_t)$ is applied based on Equations 4.11 and 4.12. The weight is designed to reduce the standard deviation for values close to the minimum and maximum loads of the profile ($P^{\min}$, $P^{\max}$) as shown in Figure 4.11. This approach avoids, that the resulting profile will show values significantly lower that the minimum baseload or maximum peak. The quadratic formulation of $\omega_t^{\min}$ is applied to ensure that values of P_t that are closer $P^{\min}$ are non-proportionally assigned with a lower standard deviation.

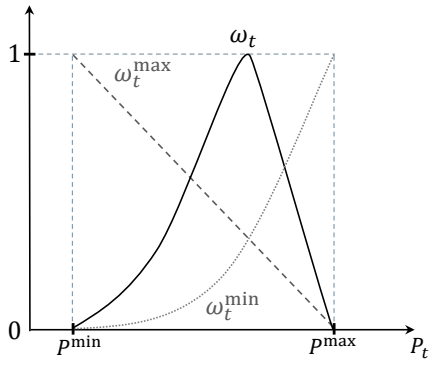

Figure 4.11.: Schematic illustration of weights for the vertical shifting of the demand. Figure from [22].

4.11).

$$\omega_t = 1 - \left|\omega_t^{\max} - \omega_t^{\min}\right|, \tag{4.11}$$

$$\omega_t^{\max} = \frac{P^{\max} - P_t}{P^{\max} - P^{\min}}. \tag{4.12}$$

$$\omega_t^{\min} = \frac{P_t^2 - 2P_t P^{\max} + P^{\max 2}}{(P^{\max} - P^{\min})^2}. \tag{4.13}$$

On the other hand, a second shape-parameter β is introduced which is able to increase the overall standard deviation of the profile for higher error values. This is achieved by the multiplication of β with the spread of the overall profile. Hence, higher values of delta will lead to an overall higher vertical distortion of the profile.

Horizontal-shift

The horizontal-shift is introduced to shift an aggregation of coherent timesteps at once. In a first step relevant consumption patterns are defined with the following Equations:

$$\Delta P_{\mathrm{t_{start}}} > \theta_h \overline{\Delta P_t}, > 0, \tag{4.14}$$

$$\frac{\sum_{t=1}^{T_h} P_t - P^{\min}}{P^{\min}} > \nu_h(\overline{P_t} - P^{\min}), \tag{4.15}$$

$$\Delta P_{\mathrm{t_{end}}} < \theta_h \overline{\Delta P_t}, < 0. \tag{4.16}$$

A coherent block for a horizontal shift is defined if a sufficiently large ramp in the consumption $P_{t_{\mathrm{start}}}$ (Equation 4.14), is enclosed by a sufficiently large negative ramp in the consumption $P_{t_{\mathrm{end}}}$

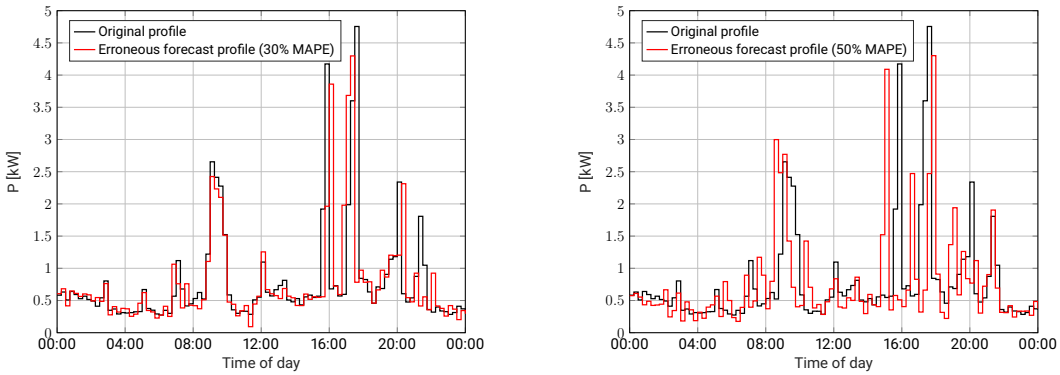

(a) Shape parameters: $\alpha = 0.022$, $\beta = 0.003$, $\gamma = 0.636$, $\sigma_h = 1.100$

(b) Shape parameters: $\alpha = 0.100$, $\beta = 0.006$, $\gamma = 1.763$, $\sigma_h = 2.200$

Figure 4.12.: Exemplaric results for the application of the method for an example day of a household load profile for (a) 30 % MAPE and (b) 50 % MAPE. Figure from [22].

(Equation 4.16). Additionally, the average load within t_{start} and t_{end} (T_h) needs to be sufficiently large compared to the overall mean of the profile and the minimum load to avoid shifthing blocks close to the baseload. With θ_h and ν_h, the sensitivity for the detection of coherent blocks can be adjusted, i.e. a higher value of θ_h or ν_h will lead to less detection of start and end timesteps of peaks as the threshold for a peak detection is increased.

Once the coherent blocks are identified, the shifting of these blocks in time are achieved by moving them in time by a time Δt_p drawn from the zero-mean normal distribution:

$$\Delta t_p \sim \mathcal{N}(0,\, \sigma_h^2). \tag{4.17}$$

Depending on the size of the error that is being reproduced, the standard deviation σ_h of this horizontal shift can be adapted . Two examples of distorted load profiles and the respective shape parameters are shown in Figure 4.12. The original profile in Figure (a) is distorted with a forecast error of 30 % (MAPE) and Figure (b) with a forecast error of 50 % (MAPE). Both, the vertical and horizontal shifting can be visually detected. While the morning peak load (8:00-10:00) is not shifted horizontally in Figure (a), it is slightly shifted to the left in Figure (b). The vertical shifts are also more distinctive in Figure (b) than in Figure (a).

4.3.4. Scalability analysis

A scalability analysis is performed to evaluate the solving time of the developed market matching problem for a variation of model parameters. As a main parameter the effect of an increasing number of market participants is analyzed. Additionally, the impacts of the number of considered nodes, the share of flexibility orders (storage-orders), and the number of market timesteps are considered. Table 4.2 provides an overview of the parameter variations. The scalability analysis is performed for all reasonable permutations of the parameter variations listed in the table, i.e., a combination of one participant and 1000 nodes is not considered.

Table 4.2.: Overview of parameters and parameter variations of the scalability analysis

Parameter	Parameter Variation
Number of participants [-]	1, 10, 100, 1000, 10000
Share of participants with a battery storage [%]	0, 50, 100
Number of nodes [-]	1, 10, 100, 1000
Number of timesteps [-]	24, 96

For each set of parameters, a synthetic LEM with reasonable parameters for orders, participants and grid topology is generated. In the default case, each participant is modeled with one base load (buy-order) and one generation (sell-order). For a variation of the share of battery storages, participants are additionally equipped with a battery storage (storage-order). Input parameters of the orders are randomly chosen from uniform distributions within similar ranges as in the scenario simulations. Generated participants are subsequently assigned to a node. Each node is connected to the previous node and additionally to 3 random nodes.

The scalability analysis is performed on a windows machine with an Intel Core i7-7820HQ CPU, 16 GB of RAM using the solver Gurobi (9.1.12) [161]. Each permutation of the parameters is run 5 times to reduce the influence of other processes running on the machine. The focus of the evaluation is put on the overall solver time. The model generation time is not considered in detail as it highly relies on the used programming language (interpreted or compiled) and the implementation of the API to the solver.

4.3.5. Simulation framework

The simulation framework is implemented as an object-oriented software package in Python. This section gives a broad overview of the used libraries, frameworks and solvers. The framework contains the previously introduced models/classes for the market operator, grid operator, participants and assets as well as the simulation logic defined in Section 4.3. The linear optimization problem of the market matching is formulated using the mathematical programming language AMPL [162]. The integration of the optimization problem into the python framework is achieved using AutoLP [163] which provides an autogenerated formulation of the optimization problem with direct access to the solver. The solver SCIP [164] is used to solve the generated optimization problem accessed by the solver API pyscipopt [165] from python. For the scalability analysis, Gurobi [161] is used as a solver.

The nonlinear optimization problem to generate erroneous forecasting profiles (Section 4.3.3) is formulated in MATLAB using the fmincon solver [166].

For testing and productive implementation of the market matching in the field test (Section 6), a .NET Framework solution written in C# is build around the core market matching functionality which is also implemented using AMPL, AutoLP and SCIP.

4.4. Evaluation metrics

The evaluation metrics are chosen to enable comparability among the the scenarios. Hence, where applicable, relative evaluation metrics are used normalized. The metrics are chosen to evaluate the simulation results from the overall market level perspective, from the perspective of a participant and the perspective of the grid operator.

4.4.1. Market

Share of generation sold on LEM

The share of generation sold on the LEM (SL) is evaluated as a first metric to analyze the impact of decreasing minimum sell prices throughout the scenario years. It is defined as the ratio of the electric power of all sell orders $\mathcal{S}$ of all participants $\mathcal{P}$ contracted at LEM ($P_{s,t}$) to the overall contracted electric power of all sell orders including sale to the Backup $P_{s,t}^{bu}$:

$$\mathrm{SL} = \frac{\sum_{s\in\mathcal{S}}\sum_{t\in\mathcal{T}} P_{s,t}}{\sum_{s\in\mathcal{S}}\sum_{t\in\mathcal{T}}(P_{s,t}+P_{s,t}^{bu})}. \tag{4.18}$$

Average market prices

Weighted average sell prices and buy prices (including REPCs) are used to evaluate the economic incentivation especially regarding the price difference between the different grid types (load, feed-in dominated) and REPC scenarios. They are evaluated on different time scales, e.g., 15 min averages or averages over the whole year to allow an assessment of short-term flexibility and a general yearly evaluation. The weighted average sell price is defined as:

$$\lambda_s = \frac{\sum_{s\in\mathcal{S}}\sum_{t\in\mathcal{T}}(P_{s,t}\lambda_{s,t})}{\sum_{s\in\mathcal{S}}\sum_{t\in T} P_{s,t}}, \tag{4.19}$$

and can be evaluated for contracted sells either to the LEM, the backup or both. Since the developed market model considers REPCs already in the matching sell and buy prices can differ. The weighted average buy price can be formulated accordingly:

$$\lambda_b = \frac{\sum_{b\in\mathcal{B}}\sum_{t\in\mathcal{T}}(P_{b,t}\lambda_{b,t})}{\sum_{b\in\mathcal{B}}\sum_{t\in\mathcal{T}} P_{b,t}}, \tag{4.20}$$

The weighted average buy prices implicitly also contains the prices of bought energy from storages.

Self-consumption

The overall self-consumption SC of participants at the LEM enables an evaluation of the usage of flexibility options when compared to the BAU scenario. A high share of self-consumption indicates that locally generated energy is either directly used or stored to later be discharged. It is defined as the share of the total local generation directly consumed by participants at the LEM. An equivalent definition, i.e., the share of generation not sold to the backup can be formulated as

$$\mathrm{SC} = 1 - \frac{\sum_{s \in \mathcal{S}} \sum_{t \in T} P_{s,t}^{\mathrm{bu}}}{\sum_{s \in \mathcal{S}} \sum_{t \in T} (P_{s,t} + P_{s,t}^{\mathrm{bu}})}. \tag{4.21}$$

Self-sufficiency

The self-sufficiency ratio SSR, also referred to as autarky rate, indicates to which degree the demand of participants at the LEM can be covered by local resources, i.e., local sell orders or local storage orders and can similarly to the self-consumption be defined as:

$$\mathrm{SSR} = 1 - \frac{\sum_{b \in \mathcal{B}} \sum_{t \in T} P_{b,t}^{\mathrm{bu}}}{\sum_{b \in \mathcal{B}} \sum_{t \in T} (P_{b,t} + P_{b,t}^{\mathrm{bu}})}. \tag{4.22}$$

4.4.2. Participants

To evaluate the incentivation of participants at the LEM their relative benefit of participation is calculated. Since the structure of participants and their assets can be diverse, e.g., participant with load, prosumer with load and generation, prosumer with battery storage, etc., an asset-based evaluation of benefits is performed. This additionally allows the evaluation of the benefit of specific assets, e.g., EV charging at home or EV charging at work.

The average benefit can be derived by subtracting the achieved revenues or costs from the opportunity costs of the scenario without a LEM. The weighted average cost benefit CB can hence be defined as:

$$\mathrm{CB} = \lambda_b^{bu} - \frac{\sum_{b \in \mathcal{B}} \sum_{t \in T} (P_{b,t} \lambda_{b,t})}{\sum_{b \in \mathcal{B}} \sum_{t \in T} P_{b,t}}, \tag{4.23}$$

where $\mathcal{B}$ can either be a set of all buy orders or buy orders of specific asset type with λ_b^{bu} as the reference price for buying from the backup supplier. Vice versa, the average revenue benefit RB can be calculated as:

$$\mathrm{RB} = \frac{\sum_{s \in \mathcal{S}} \sum_{t \in T} (P_{s,t} \lambda_{s,t})}{\sum_{s \in \mathcal{S}} \sum_{t \in T} P_{s,t}} - \lambda_s^{\mathrm{bu}}, \tag{4.24}$$

with λ_s^{bu} as the reference price for selling to the backup supplier.The benefits are calculated on an asset type basis to make a more general assessment per asset type rather then per participant type. A

direct evaluation on participant level (e.g., participant w/ PV, participant w/ PV and HP, participant w/ EV and Battery, etc.) would weaken the generalizability of the results as a whole permutation of participant types would leave few groups with only a small sample size in some scenarios (e.g., only one participant w/ PV, Battery, HP and EV). This asset based formulation additionally allows a subsequent bottom up calculation of typical yearly benefits of specific participant types with greater generalizability.

Load forecast error

The Mean Absolute Percentage Error (MAPE) is used to evaluate load forecasting errors. Although this metric has shortcomings with regards to the impact of small or close to zero actual values [167] it is a widely used metric [22] and allows for a comparison of errors within the literature. For a forecasted load ($\hat{y}$) and the actual load (y) the MAPE is defined as:

$$\text{MAPE}[\%] = 100\% \frac{\sum_{t=1}^{T} \left| \frac{\hat{y}_t - y_t}{y_t} \right|}{T}, \tag{4.25}$$

considering T timesteps.

To include the effect of load forecast uncertainty in the calculation of the participant benefit (relevant for Section 4.3.3), Equation 4.23 needs to be adapted by the penalty cost $\lambda_t^{b,pc}$ for not satisfying the contracts due to forecast errors. Simplified for a single participant p the Participant Benefit (PB) is formulated:

$$PB = \sum_{b \in \mathcal{B}} \sum_{t \in \mathcal{T}} \Delta t (\lambda_{b,\text{bu}} P_{b,t} - \lambda_{b,t}^{\text{LEM}} P_{b,t}^{\text{LEM}} - \lambda_{b,t}^{\text{pc}} (P_{b,t} - P_{b,t}^{\text{LEM}})), \tag{4.26}$$

with $P_{b,t}$ as the actual measurement at the PCC of the participant and $P_{b,t}^{\text{LEM}}$ as the contracted power at the LEM. Depending on whether the demand was under- or over-forecasted, the penalty price $\lambda_{b,t}^{\text{pc}}$ is calculated as:

$$\lambda_{b,t}^{\text{pc}} = \begin{cases} \lambda_b^{bu} + \lambda^{fee}, & P_t > P_t^{b,\text{LEM}} \quad (4.27) \\ -\lambda^{fee}, & P_t < P_t^{b,\text{LEM}} \quad (4.28) \end{cases}$$

where λ^{fee} are constant additional energy fees added to to the backup utility price λ_b^{bu} for under-forecasting (first condition). For over-forecasting no additional backup energy needs to be bought, therefore only λ^{fee} applies for the second condition.

4.4.3. Grid

Peak assessment

To evaluate the impact of the LEM on the local distribution grid, the power peaks in the exchange with the backup supplier, i.e., the load of the transformer, are analyzed. The observed peaks of all LEM scenarios are compared to the BAU scenario both, for demand peaks and feed-in peaks. To avoid overestimation of single peak events, N daily peaks within the yearly simulation are analyzed. The relative deviation is calculated as:

$$PD = \frac{1}{N} \sum_{n \in N} \max_{n} \left(\frac{P_n^{\mathrm{BAU}} - P_n^{\mathrm{LEM}}}{P_n^{\mathrm{BAU}}} \right), \tag{4.29}$$

with P_n^{BAU} and P_n^{LEM} as the daily maximum peaks at the transformer connection the LEM to the superior grid level. The absolute deviation can be calculated by removing the denominator P_n^{BAU}.

To evaluate the frequency of the maximum utilizations which occurred during the field test operation, a utilization factor UF is introduced. The utilization factor describes the ratio of actual utilization and utilization limit and is calculated for a feeder node n and a timestep t as:

$$\mathrm{UF}_{n,t}[\%] = 100 \begin{cases} \frac{P_{n,t}^{\mathrm{in}}}{P_{n,t}^{\mathrm{max,in}}}, & P_{n,t}^{\mathrm{in}} \geq 0, \\ \frac{P_{n,t}^{\mathrm{out}}}{P_{n,t}^{\mathrm{max,out}}}, & P_{n,t}^{\mathrm{out}} > 0, \end{cases}$$

Collected regulated electricity price components

An introduction of reduced REPCs as described in Section 4.3.2, might lead to a reduction of the collected grid fees, taxes and levies. For each simulation scenario with the same scenario year and grid type the collected REPCs might hence differ for a variation of grid tariffs. The relative share of the collected REPCs (α_s) compared to the BAU scenario is calculated for a scenario z as:

$$\alpha_z = 1 - \frac{\mathrm{REPCs}_z}{\mathrm{REPCs}_{\mathrm{BAU}}}, \tag{4.30}$$

with $\mathrm{REPCs}_{\mathrm{BAU}}$ as the collected REPCs in the baseline scenario defined as:

$$\mathrm{REPCs}_{\mathrm{BAU}} = \sum_{t \in \mathcal{T}} \sum_{p \in \mathcal{P}} \Delta t c_e P_{t,p}^{\mathrm{bu,in}} \tag{4.31}$$

with $P_{t,p}^{\mathrm{bu,in}}$ as the power drawn from the grid by one participant p and the constant energy fees c_e (ct/kWh). Collected REPCs in the LEM scenario REPCs_z can be directly calculated as a part of the objective function of the market matching problem (Equation 3.21).

5. Simulative evaluation

The simulative evaluation consists of four major assessments. Section 5.1 and 5.2 deal with the 60 yearly simulation scenarios with variations of scenario year, grid type and REPC scenarios described in Section 4.2 and their implications on market and participant economics as well as the impact on the grid. Section 5.3 focuses on the economic impact of load forecast uncertainty. Finally, Section 5.4 presents the results of the scalability analysis for the proposed market matching algorithm.

5.1. Effects of grid type and scenario year: Comparison to BAU

The results presented in this section are focused on the comparison between the BAU scenario and the *Flat* LEM scenario as defined in Section 4.3.2. Hence, there is no adaption of the fee structure in the LEM scenario compared to the BAU scenario, i.e., full REPCs are paid by each participant.

5.1.1. Overview of main scenario KPIs

Figure 5.1 shows the development of the self-consumption ratio of the considered distribution grids for the BAU and LEM scenario.

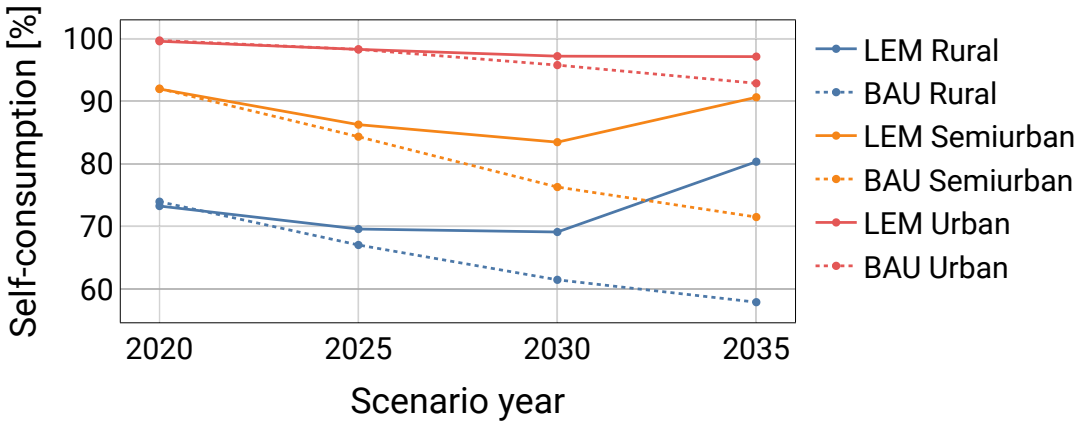

Figure 5.1.: Development of self-consumption in the BAU and LEM scenarios over the scenario years and a variation of grid types. LEM REPCs scenario: *Flat*.

The self-consumption is almost equal for the BAU and LEM scenario in the base scenario year 2020 for all grid types. In the base year, the Urban scenario reaches a self-consumption of almost 100 %, while the Semiurban and Rural scenarios reach 92 % and 73 % respectively. Throughout the scenario years 2025, 2030 and 2035 the self-consumption in the BAU scenarios consistently decreases. Compared to the LEM scenarios, the self-consumption first decreases with lower rate until the year 2030, to then increase for the scenario year 2035. While overall the introduction of a LEM increases self-consumption, there are considerable difference between the studied distribution grids. The relative increase of self-consumption compared to the BAU scenario is substantially lower for the Urban grid (4.3 percentage points), than for the Semiurban grid (19.1 percentage points) and Rural grid (22.5 percentage points) in 2035.

A similar effect is reflected in the self-sufficiency ratio (Figure 5.2). The leverage of the LEM to increase the self-sufficiency is lower for the Urban grid (1.1 percentage points), than for the Semiurban grid (7.2 percentage points) and Rural grid (9.4 percentage points) in 2035.

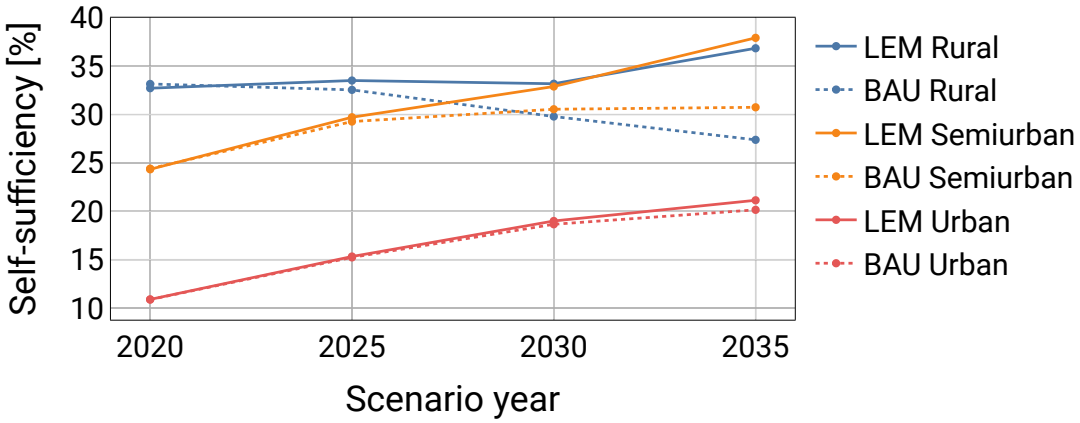

Figure 5.2.: Development of self-sufficiency in the BAU and LEM scenarios over the scenario years and a variation of grid types. LEM REPCs scenario: *Flat*.

The overall reachable self-sufficiency in the final scenario year is 21.1 % for the Urban, 37.9 % for the Semiurban and 36.9 % for the Rural grid. The difference between the BAU and LEM scenarios increases over the scenario years and is less distinct for the Urban than for the Semiurban and Rural grids.

The described effects are caused by two main influences. Firstly, the relative increase of the impact of the introduction of a LEM on the KPIs over time can be attributed to the overall share of generation which is sold at the LEM (Figure 5.3). Due to the high minimum sell-prices in the first scenario years (compare Section 4.2.2), almost no buy and sell orders are matched in scenario year 2020. As the maximum buy prices and the REPCs prices stay constant during the scenario years, an increasing share of the local generation is matched at the LEM starting from scenario year 2025. With this increasingly cheaper local generation (Figure 5.4), it becomes profitable for storage assets to increase the self-consumption not only of individual participants, but for the overall market. Secondly, the significantly lower impact on the Urban grid can be allocated to the lower ratio of generation capacity to overall demand in this scenario (Rural: 0.9 $\frac{\mathrm{kW_p}}{\mathrm{kW_{el}}}$, Semiurban:

0.75 $\frac{\mathrm{kW_p}}{\mathrm{kW_{el}}}$, Urban: 0.37 $\frac{\mathrm{kW_p}}{\mathrm{kW_{el}}}$). While the feed-in from additional PV installations can be utilized for flexibility in the Semiurban and Rural cases, it is mostly directly consumed in the Urban case leading to the highest self-consumption rates.

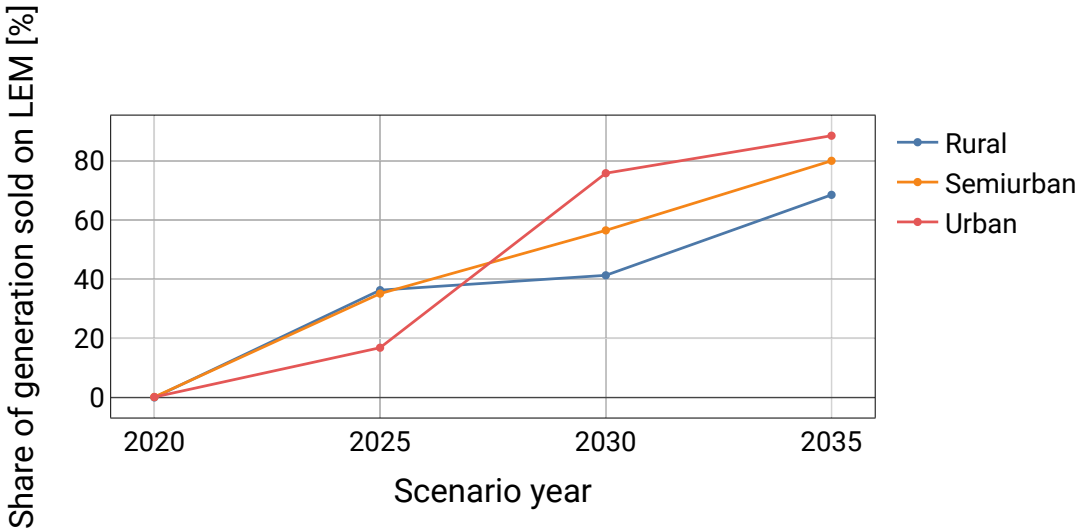

Figure 5.3.: Share of generation sold via the LEM over the scenario years for a variation of grid types. LEM REPCs scenario: *Flat*.

Figure 5.4 shows the average sell prices for the LEM scenario starting from the scenario year 2025. Generally, the prices decrease over time due to the decreasing feed-in remuneration and minimum sell-prices. In the load dominated scenario (Urban) the weighted average sell prices are consistently higher than in the other cases, since the sell orders are mostly the price setting units, as the demand is higher than the overall supply. The price development for the different grid types and economic evaluation of specific assets is analyzed further in the following section.

5.1.2. Economic evaluation

Figure 5.5 provides a more detailed assessment of the development of market prices over the year for the different grid types. The gross weighted average buy prices (including REPCs) are plotted over the day of the year (x-axis) and the time of the day (y-axis). Various effects of the LEM can be explored within the two time dimensions, i.e., seasonal effects on the x- and daily effects on the y-axis.
The seasonal effect of reduced PV generation and increased demand in the winter months is reflected in higher prices in these months. In these months, the market price is set by the buy orders and their maximum price (31.37 ct/kWh). During spring and summer months, the prices are reduced during the main hours of PV feed-in when the supply is greater than the demand. This effect is explicitly visible for the Rural and Semiurban scenarios, whereas the Urban scenario is still dominated by demand in summer times with a few exception dates, mostly weekends.

Regarding the daily price evolution (Figure 5.5) various observations can be made. First, prices during daytime are dominated by the availability of excess PV generation. The higher the availability the lower the prices. During nighttime in the winter periods, there are no trades at the LEM, hence,

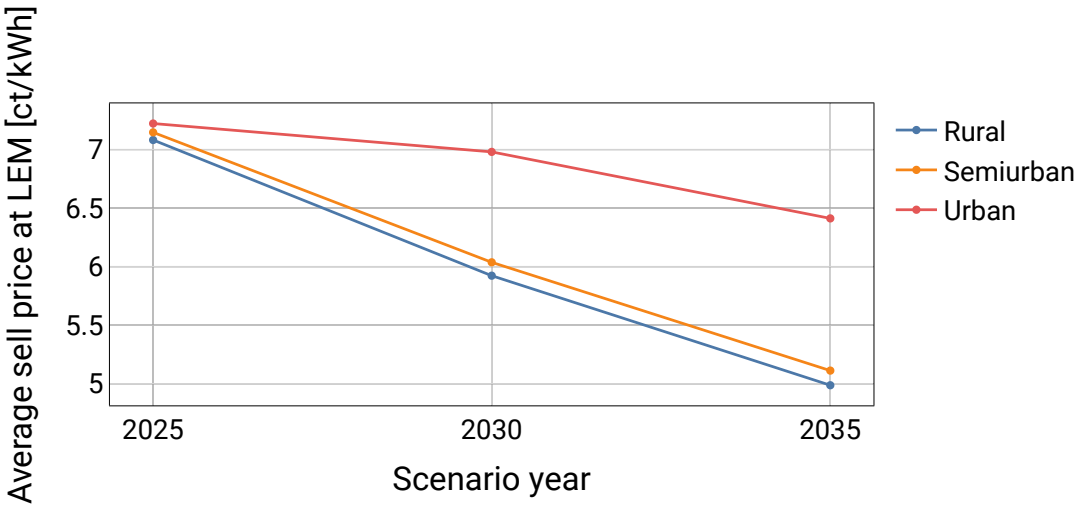

Figure 5.4.: Weighted average sell price over the scenario years for a variation of grid types. LEM REPCs scenario: *Flat*.

no prices. During nighttime (summer period), the prices reach the maximum buy price. This price is dominated by storage orders, which are the only source of supply during night times. Due to the lack of excess PV which can be stored and later discharged, only few days with trades at night are observed in the Urban grid scenario. In the Rural and Semiurban grid scenarios, nighttime trades occur more frequently. In the early morning (06:00-7:30) and evening hours (16:30:18:00), prices reach the upper end (maximum buy price) during summer time in the Rural and Semiurban scenarios indicating an efficient price signal for hours where the PV supply is limited.

Figure 5.6 shows the impact of the temporal and grid type specific price developments on the average benefit per asset type. As described in Section 4.4 the average benefit is calculated as the difference of costs and revenues to the BAU scenario. The asset-specific benefits, i.e., cost reduction for buy orders, increased revenue for sell-orders, additional revenue for storage orders, are shown for the different grid types and the scenario year 2035.
There is an observable difference between the grid types, but also comparing the asset types. As expected by the previous results on the market prices, the highest benefits for generation assets (PV) are achieved in the Urban scenario (4.4 $\frac{\text{ct}}{\text{kWh}}$), followed by the Semiurban (2.5 $\frac{\text{ct}}{\text{kWh}}$) and the Rural scenario (2.0 $\frac{\text{ct}}{\text{kWh}}$). However, the demand side shows only small benefits (0-0.2 $\frac{\text{ct}}{\text{kWh}}$) in the Urban grid scenario. This can be contributed to the only few days where the price drops below the maximum buy price (compare Figure 5.5 (c)).
For the other grid scenarios a significant difference in the benefit per asset type on the demand side is visible ranging from 0.2-1.6 $\frac{\text{ct}}{\text{kWh}}$. The highest benefit is achieved for EVs charging at work in the Rural scenario. In this case only a few work charging stations benefit from the low market prices during the midday. Also in the Semiurban case the biggest profiteer are EVs charging at work with a benefit of 1 $\frac{\text{ct}}{\text{kWh}}$. Interestingly, for other flexible demand assets (EVs charging at home and HPs) a benefit below the benefit of inflexible baseloads is achieved. This effect can mainly be accounted for the lack of supply during the heating periods for HPs and the increased demand and low supply for typical charging patterns for EVs charging at home.
The additional benefits achieved by storage orders range from 3.5 to 4.3 $\frac{\text{ct}}{\text{kWh}}$. In all cases this

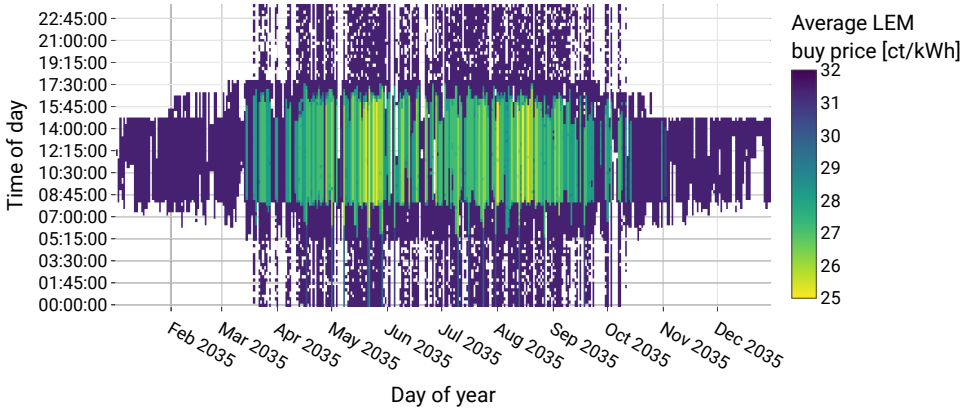

(a) Rural

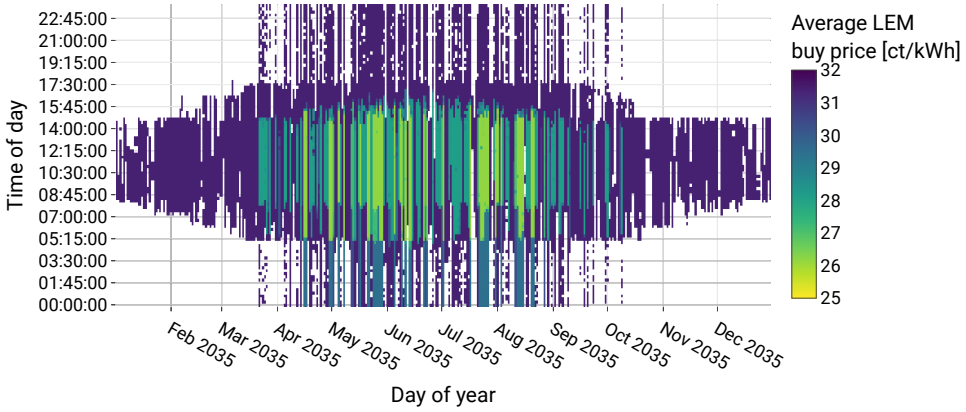

(b) Semiurban

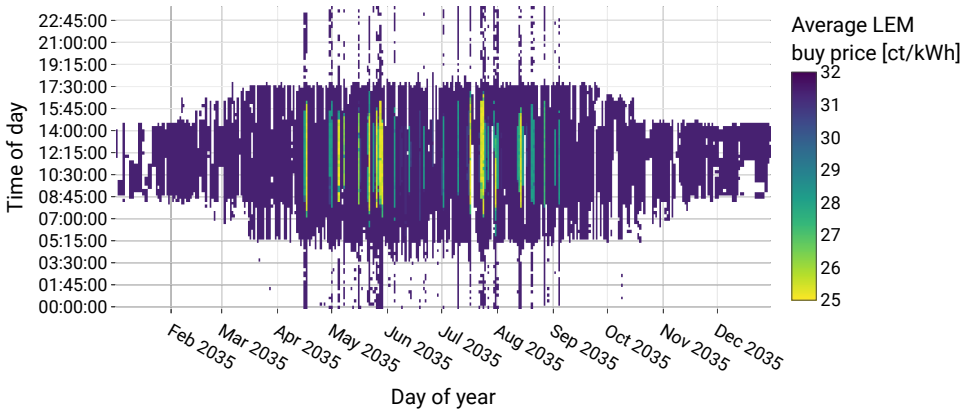

(c) Urban

Figure 5.5.: Heatmaps of the weighted average buy price at the LEM (*Flat* scenario) over one simulation year (2035) for the grid scenarios Rural (a), Semiurban (b) and Urban (c).

is above the minimum price (2.87 $\frac{\text{ct}}{\text{kWh}}$) for the external usage of a storage defined above. The relative benefit is the lowest for the Semiurban grid. In this case, the most storage capacity is available among the scenarios.

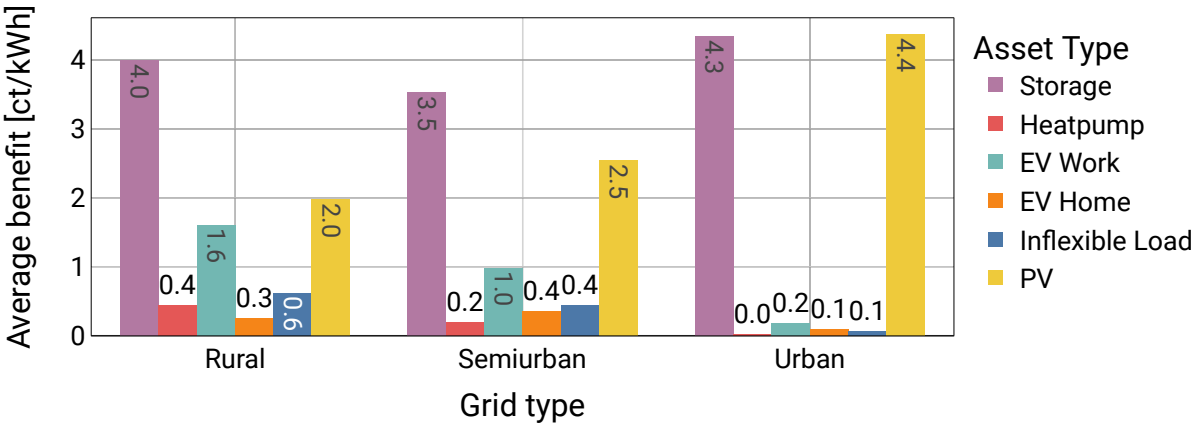

Figure 5.6.: Average benefit of various asset types for the simulation year 2035. The benefit represents an increased revenue for Storage and PV systems and a cost reduction for demand assets compared to the BAU scenario.

5.1.3. Exchange with upstream grid

Besides the described impact on participant benefits, the introduction of a LEM additionally influences the overall exchange with the upstream grid, i.e., the power flow at the LV/MV substation. Figure 5.7 shows exemplary two heatmaps of the power exchange at the LV/MV substation for the rural grid in the scenario year 2035. Positive values (green-yellow) indicate an import from the MV grid, negative values (blue-black) indicate an export through excess generation.

The BAU scenario (a) shows typical morning and evening load peaks and feed-in peaks during midday. The evening peaks are the highest, amplified by the charging strategy of EVs, i.e., they are directly charged to a full SOC after plug-in. In this Rural scenario the dominance of EVs charged at home further increases this effect. The overall highest load peaks can be observed in winter, and the highest feed-in peaks in summer. Furthermore, a clear workday- weekend pattern can be observed analyzing the load peaks at the evening time, which are drastically higher for workdays than for weekends.
Similar seasonal patterns can be observed in the LEM case (b). However, the occurrence of multi-timestep load peaks is not as distinct as in the BAU case. The overall load and feed-in peaks are below the BAU case. The highest load peaks do not occur in the same range of the evening peaks in the BAU scenario, but are rather distributed over the nighttime.
Figure 5.8 provides the numeric evaluation of the peak values. It shows the average reduction/increase of the 5 % highest daily load/feed-in peaks compared to the BAU scenario.

The potential reduction of load and feed-in peaks consistently increases over the scenario years. Starting from the base year (2020) almost no deviation from the BAU or even a small increase of

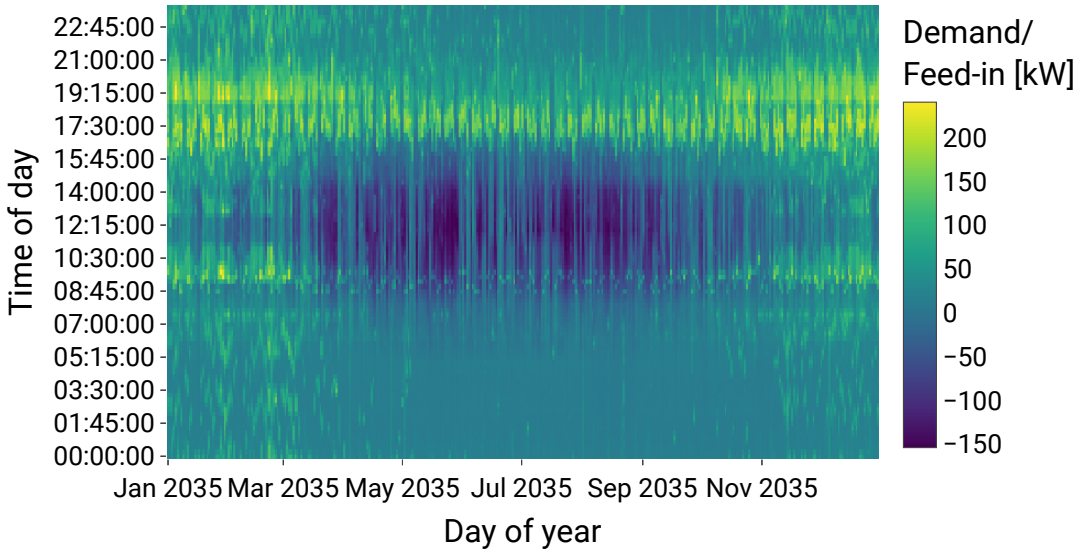

(a) Business as usual

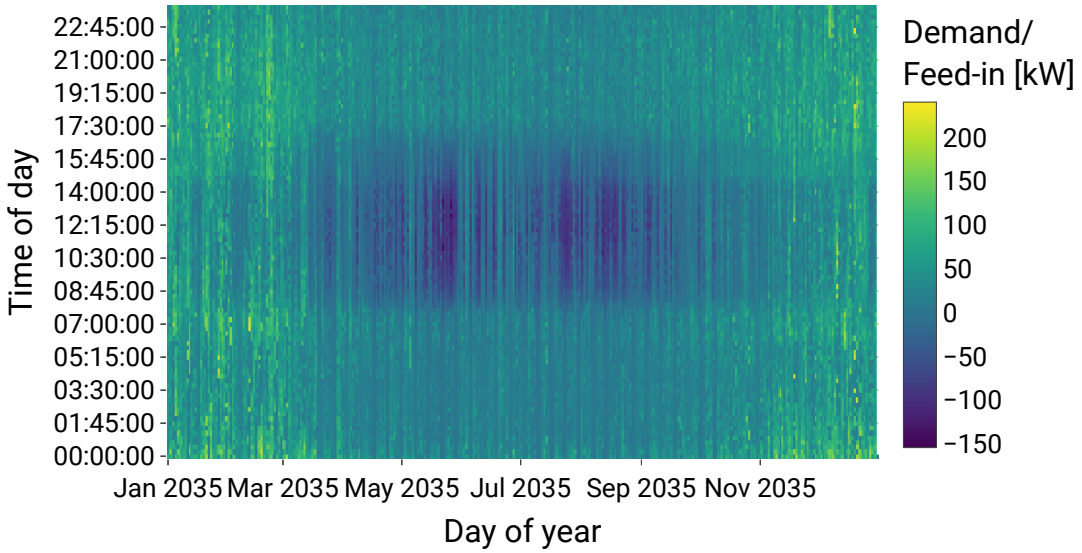

(b) Local energy market

Figure 5.7.: Heatmaps of the exchanged power with the backup (load of the LV/MV transformer) for one simulation year (2035) for the Rural grid and for the Business As Usual (BAU) (a) and Local Energy Market (LEM) (b) scenario. Positive values indicate import from backup supplier, negative values indicate export.

peaks can be observed. This is due to the low share of trades on the LEM in this timeframe. Still, the optimal operation of the energy systems (exchange with backup) is calculated by the LEM for

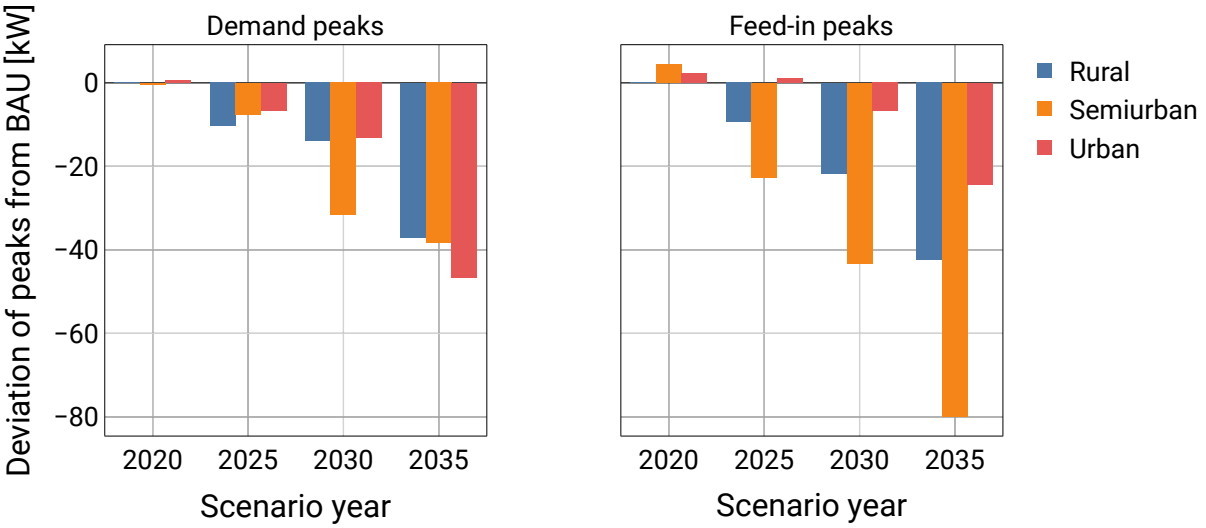

Figure 5.8.: Relative change of absolute daily load- (a) and feed-in- (b) peaks between the scenarios Business As Usual (BAU) and Local Energy Market (LEM) for a variation of scenario years and grid types. The relative change is calculated as the average of the 5 % highest daily peaks.

the individual participants. However, in the *Flat* scenario there is no incentive for a reduction of peaks and hence the small deviation occurs. For the final scenario year, a peak reduction of 37-47 kW is achieved which is equivalent to a reduction of 15-20 % compared to the BAU peaks. The highest reduction is achieved for the Urban grid followed by the Semiurban and Rural grid.
The reduction of feed-in peaks shows a similar increasing trend over the scenario years, however, the difference between the grid scenarios is more apparent. The highest peak reduction is achieved in the Semiurban grid (80 kW, 42 %), followed by the Rural (42 kW, 28 %) and the urban (24 kW, 37 %). Due to the high ratio of installed storage capacity to installed generation capacity in the Semiurban case (compare Section 4.2.1), the majority of excess generation can be charged by the storages during midday, thus, reducing feed-in peaks. The lower reduction in feed-in peaks for the Urban scenario, is consistent with the previous observations as most generation is directly consumed leading to a high share of self-consumption.

Summing up the impacts of introducing a LEM with a flat tariff scheme compared to the BAU operation:

- Clear potential to increase self-consumption and self-sufficiency throughout the scenario years.
- Low impact in the scenario years 2020, 2025 as an economic participation for most generation assets is not yet given.
- Potential to reduce demand and feed-in peaks: Highest demand reduction achieved in the Urban case. Highest feed-in reduction in the Semiurban case.

- Higher economic benefit for sellers in the Urban case. Higher benefit for buyers in the Semiurban and Rural case. Storage orders reach higher benefit compared to the set minimum price in all scenarios.
- No clear economic incentive for specific flexible load assets (EVs at home, HPs) for the provided flexibility. In all cases the reached benefit is below the benefit of baseloads.

The following section will expand the found results with regards to a variation of the applied tariff structure (REPCs scenario) focusing on the impact on the operation of assets, the effects on the grid and the economic incentivation of flexibility.

5.2. Effects of regulated electricity price components

This section deals with the analysis of effects introduced by an adaption of the Regulated Electricity Price Components (REPC)s as described in Section 4.3.2. The analysis focuses on the scenario year with the highest amount of flexibilities (2035).

5.2.1. Operational differences

To obtain a first impression on the operational differences between the scenarios, Figure 5.9 and 5.10 show the operation of the LEM under different REPC regimes for example days (Summer, Winter). In Figure 5.9 the market matching results are shown separated by the order categories (sell, buy, storage). The result includes the market results for trades between market participants on the LEM as well as the matched orders with the Backup supplier (lower opacity). Several observations can be made for all scenarios: An external usage of storage orders (non self-consumption operation of storage) is only visible at Summer days. Excess PV generation (sell orders) is used to charge storages during midday and discharge them during the night. Additionally, the overall higher demand and lower generation in the Winter case leads to a lower self-sufficiency in the Winter case where all residual load has to be covered by the backup supplier.

Besides the mentioned operational similarities, severe differences in the resulting residual load curve are obtained for the different scenarios. Especially in the winter day, significant differences in the operation can be shown for the residual demand peaks. While the operation between scenario *Flat* and *Feeder* does not show a significant difference in demand peaks (both at around 150 kW), the scenario *Variable* shows a peak of around 250 kW while the scenario *Power fees* shows an almost constant backup residue of around 70 kW. Since the time variable fees in the *Variable* scenario (c) provide incentives for the consumption at certain timesteps (correlated to the wholesale market prices), peaks at these timesteps are generated. The *Power fees* scenario however tries to limit the demand to a peak above which additional power fees need to be paid. The feed-in peaks are similar for scenarios *Flat*, *Feeder* and *Variable* at around 150 kW at around 12:00. In the *Power fees* scenario the feed-in power fees again result in a flattening of the feed-in peak at around 100 kW.

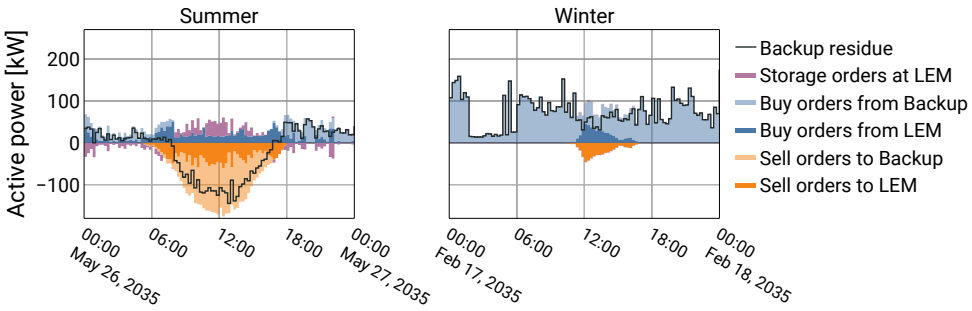

(a) Flat fees

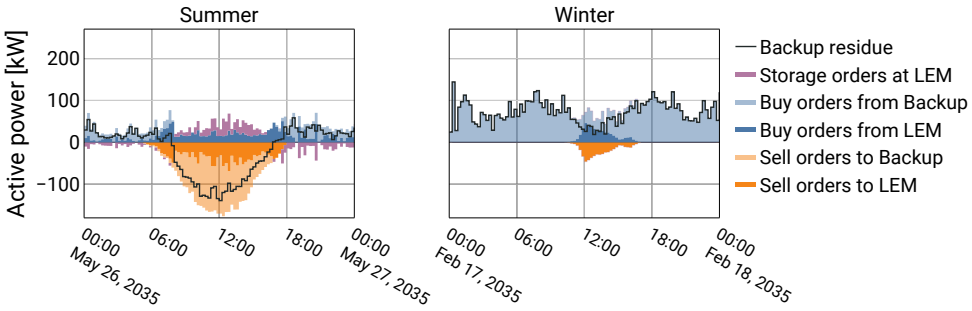

(b) Reduced feeder fees

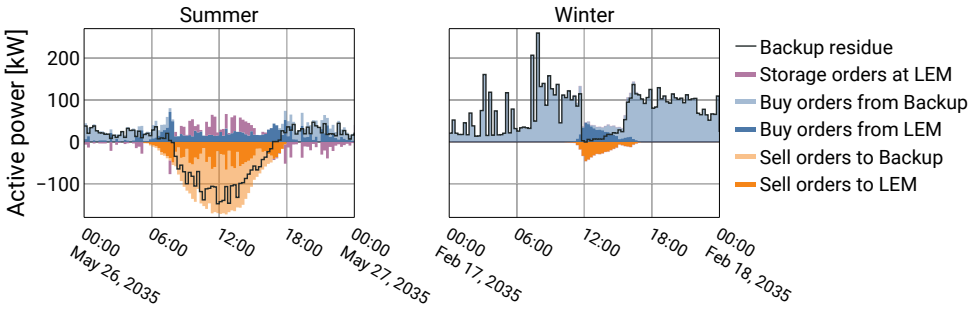

(c) Time variable

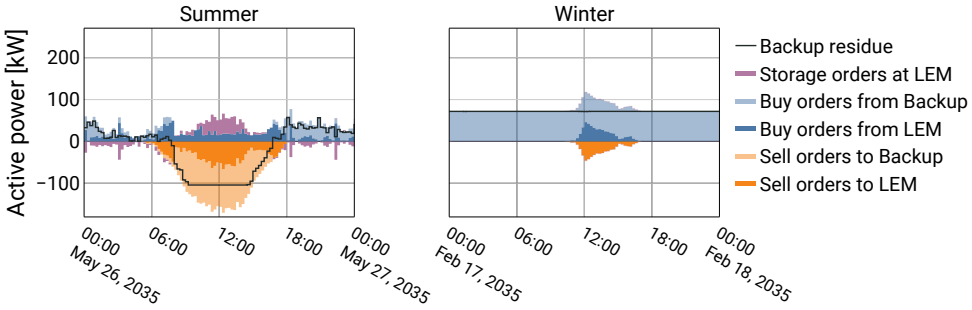

(d) Power fees

Figure 5.9.: Exemplary market matching results for a variation of REPC scenarios. Grid: rural, scenario year: 2035.

A more detailed analysis is provided in Figure 5.10 which shows the underlying asset specific operation. The observed load peaks at the winter day in the *Variable* scenario are clearly caused by the flexible consumption of HPs and EV. In Figure 5.10 (a) and (b) these flexible assets are more evenly distributed while the *Power fees* scenario (c) results in a perfect alignment of the flexible loads with the inflexible baseload. A major share of the operation of HPs is shifted to the midday where the backup residue is reduced due to PV feed-in. At the summer day the operation of assets does not differ significantly during nighttime. However, during midday the charging of storages and EVs at work are well aligned with the highest PV feed-in hence reducing the feed-in peaks.

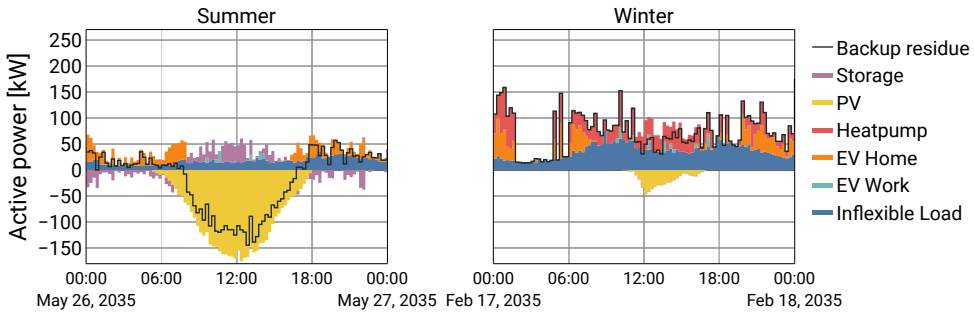

(a) Flat fees

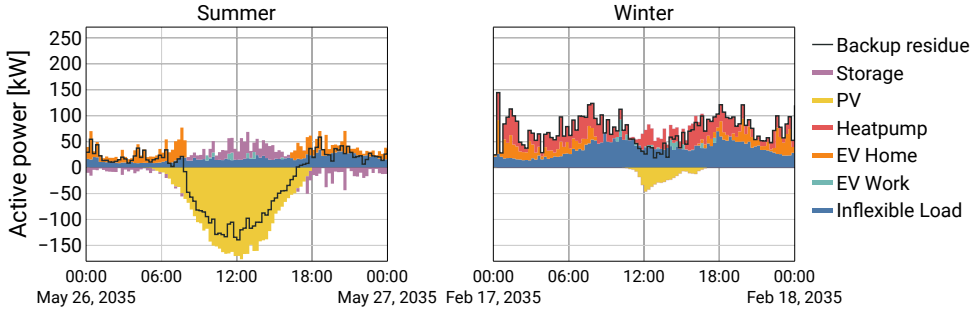

(b) Reduced feeder fees

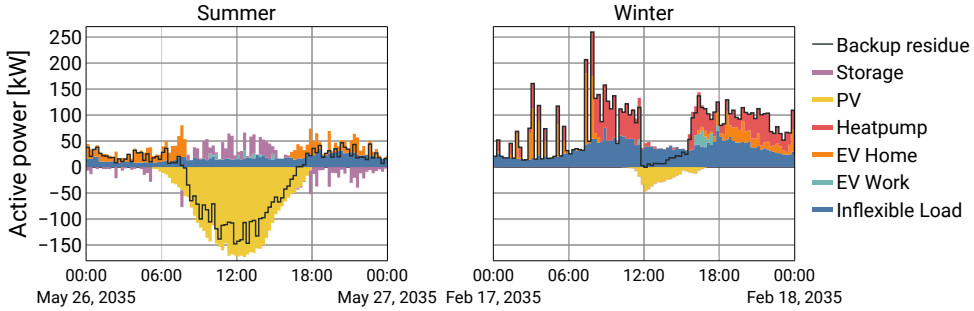

(c) Time variable

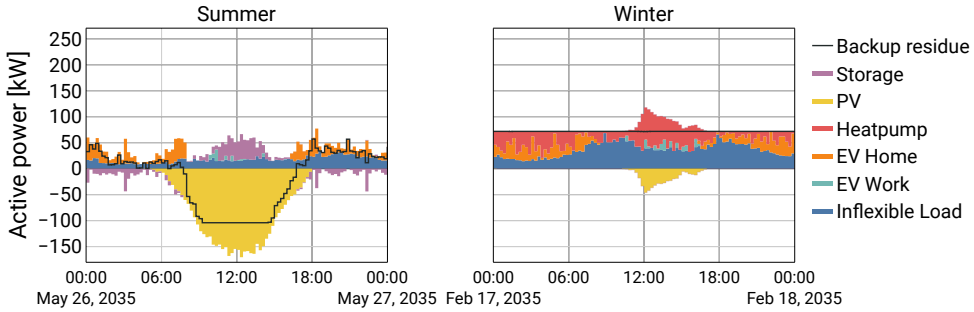

(d) Power fees

Figure 5.10.: Exemplary asset specific market results results for a variation of REPC scenarios. Grid: rural, scenario year: 2035.

5.2.2. Impact on the distribution grid

This section deals with the translation of the described exemplary operational differences on the full simulation horizon.

Figure 5.11 shows the load duration curve of the residual loads for the scenario year 2035 and the rural grid for a variation of REPC scenarios. Positive values on the y-Axis indicate an import from the MV grid, negative values indicate an export. At a first glance at Subfigure (a), the REPC scenarios seem to almost overlap. Within a residue range of 0-50 kW the curves are even almost similar to the BAU scenario.

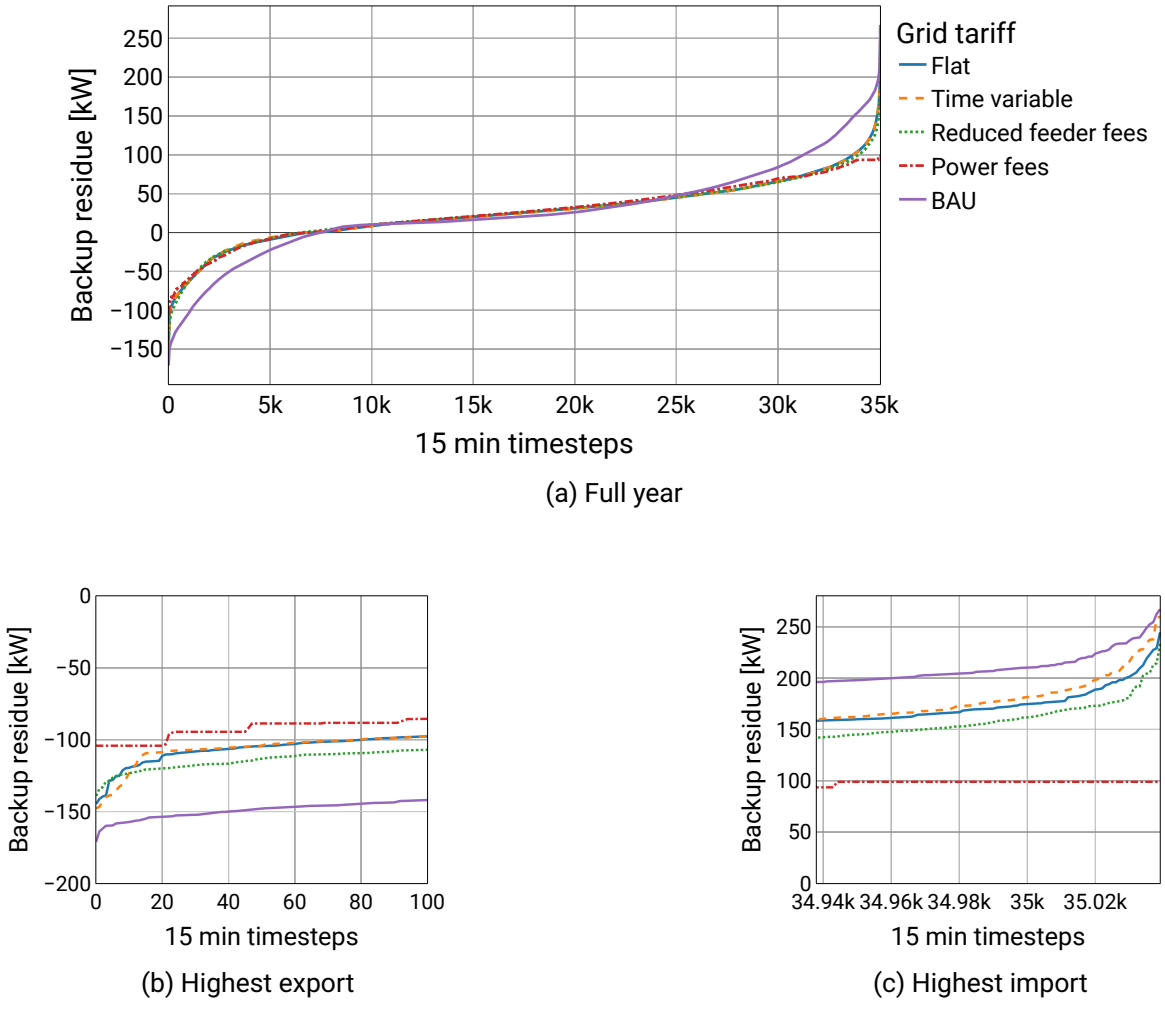

Figure 5.11.: Load duration curves of the REPC scenario variation. Positive residues represent import from the MV grid. Negative values represent feed-in. Figure (a) shows the full load duration curve of all 30,540 15-min timesteps of the simulation. Figure (b) shows the 100 timesteps with the highest feed-in and Figure (c) the 100 timesteps with the highest import. Grid type: Rural, Scenario year: 2035.

A closer inspection of the highest 100 feed-in peaks (Subfigure (b)) and the highest 100 demand peaks (Subfigure (c)) reveal significant differences. In both cases, the scenario *Power fees* shows the lowest peak values which are almost flat for the highest 100 timesteps. Compared to the BAU scenario the highest absolute peaks are observed for the scenarios *Time variable*, which shows even higher peaks than the *Flat* scenario, followed by *Reduced feeder fees* and the *Flat* scenario. This observation confirms the findings from the example days. However, additionally compared to the BAU a substantial reduction of the highest peak values can only be achieved in the *Power fees* scenario.

Figure 5.12 shows a more comprehensive analysis on the feed-in and demand peaks. It includes a parameter variation of the scenario years and grid types and shows the average difference of the highest 5 % peaks compared to the BAU scenario.

The first analysis on the peaks in the rural scenario (load duration curve) can be confirmed for other scenarios. The biggest leverage of peak reduction can be achieved within the *Power fee* scenario. Depending on the grid type, the difference of the *Power fee* scenario to the other scenarios can be more severe (e.g., demand peak reduction for the rural grid) or less pronounced (e.g., demand peak reduction for the urban grid).

With an increase of available demand flexibility and storages throughout the scenario years, the potential peak reduction consistently increases for the *Power fee* scenario. For other scenarios however, the relative reduction might even decrease over the scenario years, e.g., demand peaks for the *Time variable* scenario between the scenario years 2030 and 2035 in the rural case. This might be caused by the uncoordinated usage of flexibility which does not cover the increase of loads and generation in these scenarios.

Overall, a demand peak reduction of 30-60 % depending on the distribution grid can be achieved with the *Power fee* scenario. The highest reduction is achieved in the rural distribution grid with its high share of EVs charging at home. Compared to the BAU the charging (especially during plugin times in the evening) can be distributed over the night hence reducing the overall load peak. This effect is further illustrated in Figure 5.13. It shows the average contribution to the demand peaks by asset type over a variation of scenarios. It shows that the contribution of flexible loads (EVs and HPs) can be drastically reduced to only 29 % in the *Power fees* scenario, while flexible loads account for more than 80 % of the load peaks in other scenarios. In the semiurban and urban case, the peak reduction is at 32 % and 30 % respectively. The other REPC scenarios which are solely based on energy fees (ct/kWh) show a significantly lower reduction between 8 % (*Time variable*, 2035, rural grid) and 22 % (*Feeder fees*, 2035, rural grid).

The discrepancy between the *Power fees* and the energy fee based scenarios is not as severe for the feed-in peaks. For the scenario year 2035 the *Power fees* scenario reaches a reduction of 46-64 %, while the energy fee scenarios reach a reduction between 21 and 49 %. There is no clear trend for the best performance within the REPC scenarios with energy fees. For the semiurban and urban scenario a relative increase of feed-in can be observed for all REPC scenarios, but *Power fee*, for the scenario year 2020. As shown in Section 5.1.3, the absolute difference is only a few kW in these cases. This effect is caused by the operation of the storages, which in the BAU case might lead to a reduction at peak feed-in hours. However, in scenarios without a power fee, charging of the storages is not specifically incentivized at peak hours and might be adversely distributed alongside the generation peak of PV.

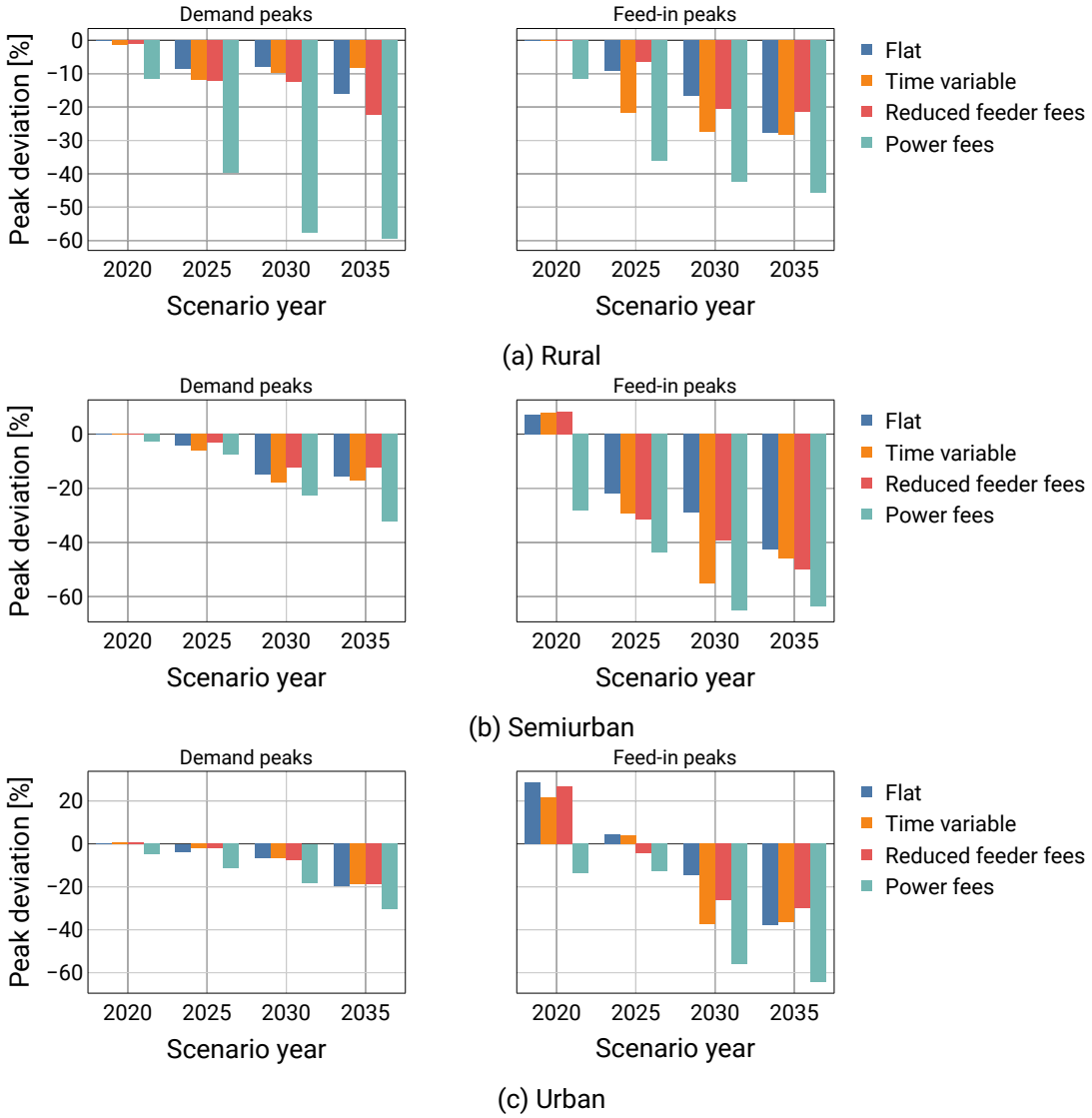

Figure 5.12.: Relative change of daily load- (left) and feed-in- (right) peaks between the scenarios Business As Usual (BAU) and Local Energy Market (LEM) for a variation of scenario years (x-axis) and REPC scenarios. Different grid types are represented by Subplots. The relative change is calculated as the average of the 5 % highest daily peaks.

The development of peak reductions over the scenario years for the variation of scenarios behaves similar to the results above. Detailed boxplots of the absolute daily maximum peaks and heatmaps can be found in the Appendix (Figure A.6 and A.7).

5.2.3. Analysis of economic impacts

As shown in the previous Section (Figure 5.6), the *Flat* scenario introduces asset specific benefits for a variation of grid types which do not specifically value the operation of flexible assets. In some cases inflexible baseloads achieve a higher benefit than flexibilities such as EVs or HPs. Figure

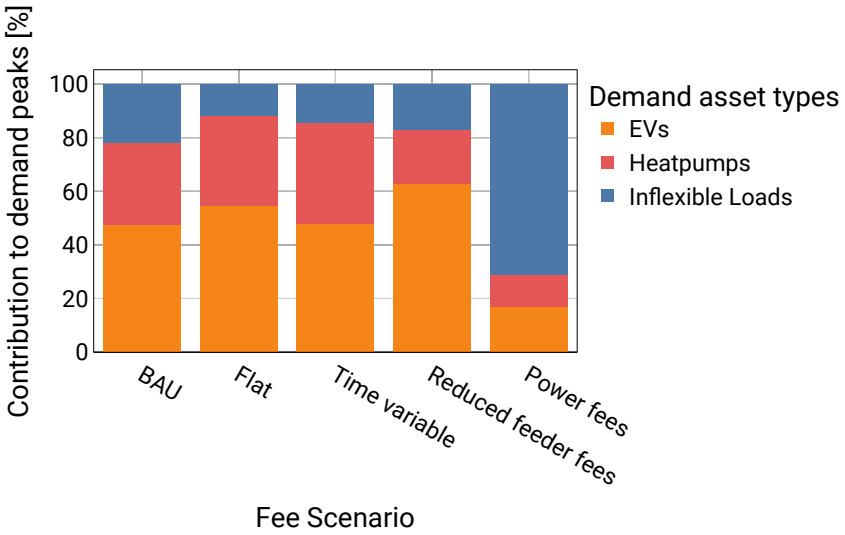

Figure 5.13.: Relative contributions to the highest 5 % demand peaks per asset type. Scenario year: 2035, Grid type: Rural

5.14 shows the same assessment for a variation of REPC scenarios for the semiurban scenario. Compared to the *Flat* scenario, the other energy fee scenarios (Time variable, Feeder fees) show a higher benefit throughout all asset categories (0.1-0.3 ct/kWh) for demand assets, 1.6-2.3 ct/kWh for PV and 0.8-1.8 ct/kWh for storage orders. This can be explained through the further reduction of the energy fees in both scenarios. However, a similar observation can be made for these more advanced scenarios: in both cases flexible loads like HPs and EVs charging at home show a lower benefit than the inflexible baseload . EVs charging at work benefit from the overall low sell prices during the midday (PV excess) and show a constantly higher benefit than the inflexible load.

Through the introduction of the power fee distribution based on the contribution of the buy order to the overall peak load (Section 4.3.2), the *power fee* scenario shows a clear incentivation for the usage of flexibilities to avoid peak loads. In all cases the average benefit for flexible loads is higher (1.4-2.8 ct/kWh) than the benefit for the inflexible load (0.3 ct/kWh).

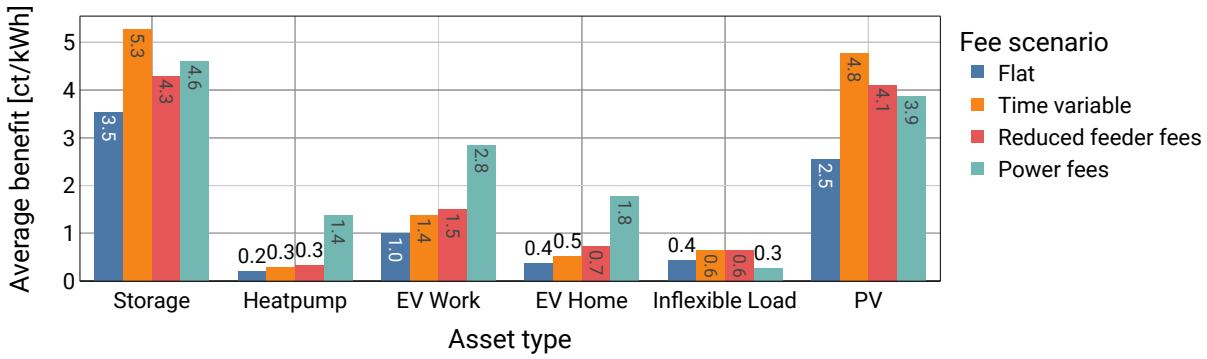

Figure 5.14.: Average asset benefit of assets types for a variation of fee scearios. Scenario year: 2035, Grid type: Semiurban.

The presented results show that an introduction of a LEM can benefit both the grid and participants. However, as introduced earlier, this comes with a reducing the Regulated Electricity Price Components (REPC) components in the more advanced scenarios. REPC collected by the DSO and other tax collecting entities will hence be reduced compared to the BAU scenario and the scenario without a reduction (*Flat* scenario). Figure 5.15 shows the impact of the introduction of a LEM on the overall collected REPCs by the DSO and other legal entities (state taxes etc.). Since there is no adaption of energy fees in the Flat scenario, the same amount of REPCs are collected in this case. Over all, for other scenarios a reduction of around 5 % in collected fees can be observed. The introduction of time variable fees might lead to a slightly (around 1 %) higher reduction in collected fees than the other scenarios.

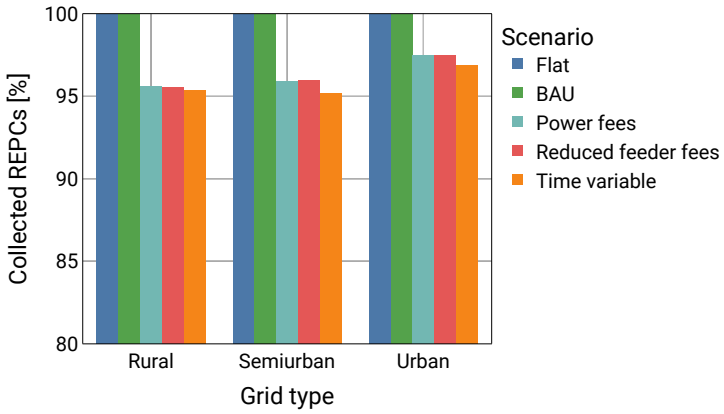

Figure 5.15.: Collected Regulated Electricity Price Components (REPC) for the different grid types and scenarios. Scenario year: 2035

5.3. Impacts of load forecast uncertainty

Main results regarding the impact of forecast uncertainty are presented in this section. For a more detailed analysis please refer to [22].
The economic impacts of a variation of forecasts errors are evaluated using the method proposed in Section 4.3.3 to generate erroneous synthetic load profiles. The method is applied to typical household profiles for Germany [168]. A variation of the Mean Absolute Percentage Error (MAPE) is applied with a MAPE ranging from 10 to 100 % in steps of 10 %. An example of the resulting error distribution for one example household load profile is shown in Figure 5.16. Clearly, a distinguishable pattern between times of low inflexible load (e.g., during the night) consumption with a tighter error bandwidth and times of peak consumption (e.g., evening times) is generated.

The generated profiles are applied to an application case (Figure 5.17), which is based on a single node LEM with 72 household participants. Representative household load profiles for Germany [168] are utilized to cover a wide range of yearly consumptions and load patterns. A total of 195.5 kWp of PV installations are distributed among 24 households, of which 12 additionally own a battery storage (total capacity 68 kWh). The sizing of PV and battery storages is based on typical installations in Germany [169]. An additional small scale CHP (25 kW_{el}) supplies the market

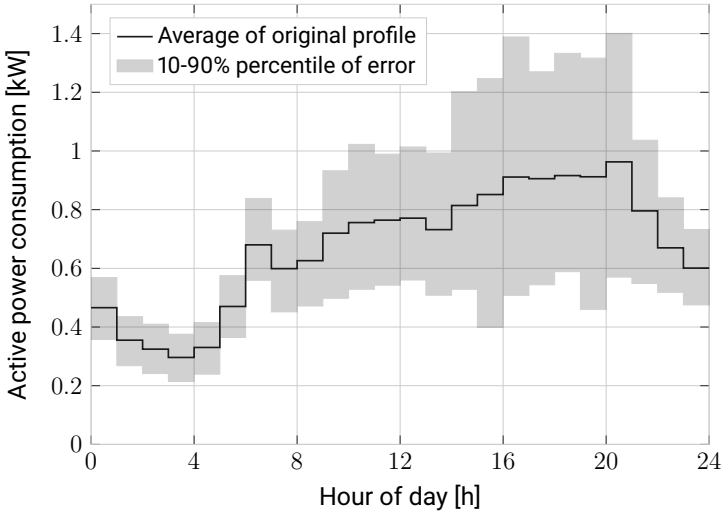

Figure 5.16.: Average yearly consumption profile and the 10-90 % percentile of generated forecast errors of an exemplary household and a MAPE of 30 %.

during times of low PV feed-in. After the simulation of the application case, the Participant Benefit (PB) is calculated (Equation 4.26) including penalty payments for over- or under-consumed energy. A variation of penalty prices (0/2/4 ct/kWh) is analyzed. The considered REPC are set to 10 ct/kWh.

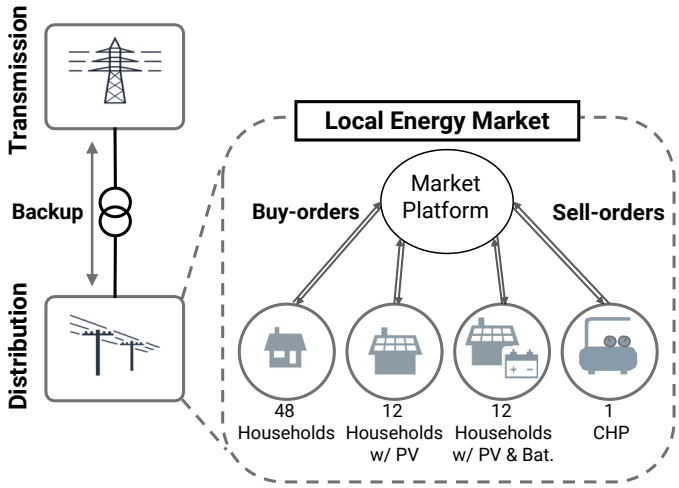

Figure 5.17.: Application case of the forecast uncertainty evaluation.

Figure 5.18 shows the PB for a variation of forecast errors (x-axis) and penalty prices for two households. A household solely with electric consumption (blue lines) and one household with a 6.5 kWp PV and a 5 kWh storage-installation (orange lines). The plot shows that for the household without flexible assets, the PB declines with increasing forecast errors reaching negative values between a forecast error of around 30-40 % depending on the penalty price. The household with PV and storage also sees a declining PB for a forecast error until 40 %, then stabilizes with positive benefits. Hence, in this case forecast errors can be compensated through the battery storage.

In Figure 5.19, 20 household participants without generation and flexible assets are evaluated. With a yearly consumption range of 1400-7500 kWh the households reflect a variety of potential participants. The tight 95 % confidence interval suggest that the participant benefit in this case is not significantly related to the underlying consumption profile. In this set-up a day-ahead forecast error below 30 % is required in order to achieve a positive PB.

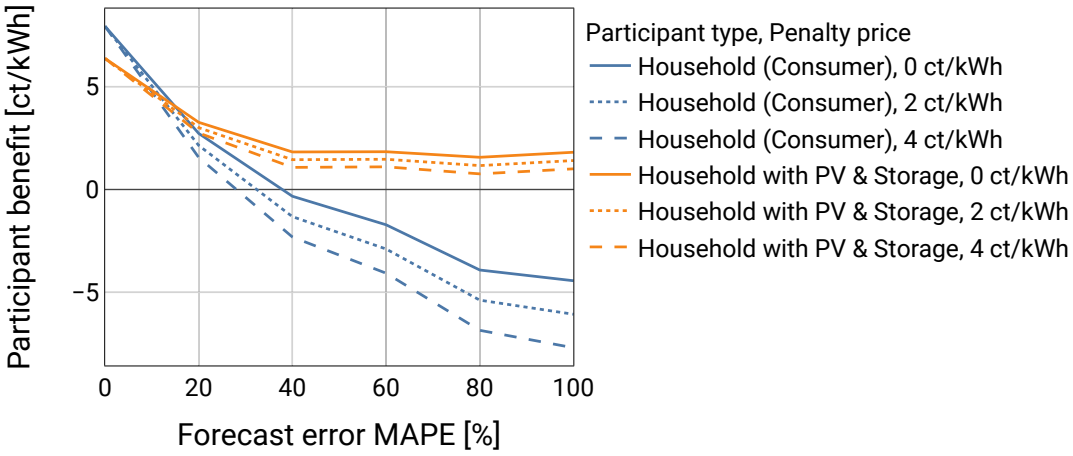

Figure 5.18.: Participant benefit of two households for a variation of forecast error and penalty prices.

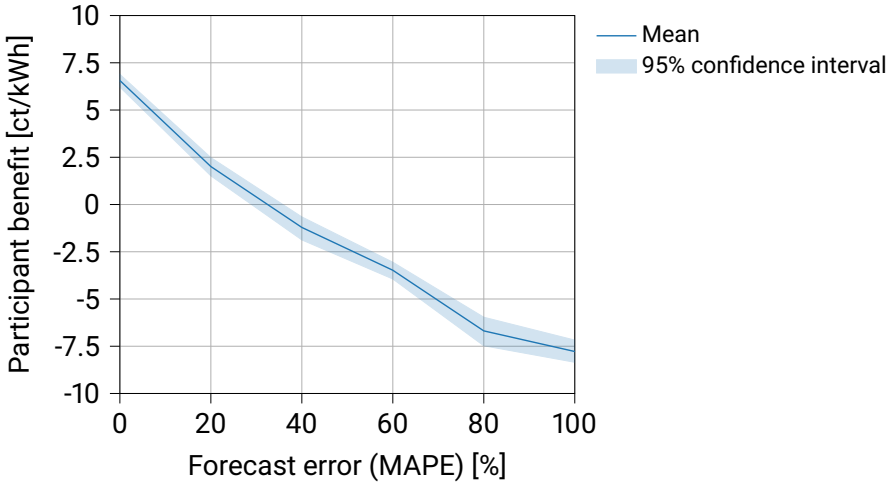

Figure 5.19.: Participant benefit of 20 household participants (consumers) over increasing forecast errors. Penalty price: 2 ct/kWh.

5.4. Scalability analysis

Figure 5.20 shows the required solver time over an increasing amount of participants for a variation of the shares of participants with battery storages. For all variation cases, a linear growth on the log-log axis can be observed. The slope of the curves on the log-log axis can be interpreted as the power s of the underlying relationship between the variables y (solver-time) and x number of participants[1]. The slope of the linear fitted curves for the three cases (0 %/50 %/100 %) are 0.96, 1.12 and 1.11 revealing that the problem scales below linear without the consideration of storages and non-linear with the consideration of storages. While the market matching for one day with 96 15min timesteps requires 92s for 10 000 participants, a significant increase of computation time can be observed for a share of storages of 50 %/100 % with 451s and 796s respectively. Since the machine ran out of memory for the most extreme case (10 000 participants with one storage each) the value is extrapolated. On average, a doubling of the number of storages (from 50 % to 100 %) increases the solver time by the factor of 2.45.

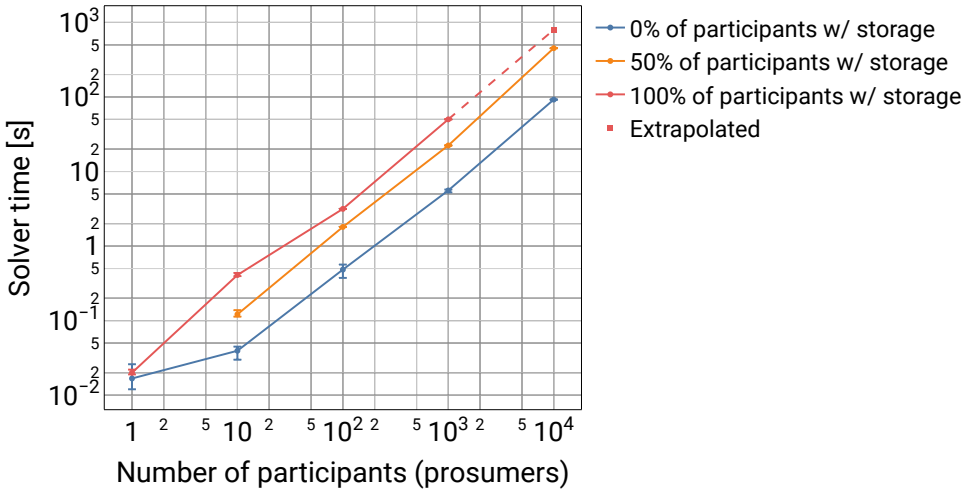

Figure 5.20.: Elapsed solver time over an increasing number of market participants and a variation of the share of participants with a battery storage systems. Constant parameter settings: Number of timesteps: 96, number of nodes: 1, problem formulation: LP.

Figure 5.21 depicts the impact of the number of timesteps taken into acount in the market matching. For a whole day either 24-hourly timesteps or 96 15-min timesteps are considered. For the most extreme case (10,000 participants) the solver time reaches 451 s and 80 s for 96 and 24 timesteps respectively. Both curves run almost parallel with an average factor of 5.19 between 96 and 24 timesteps. Hence, doubling the number of timesteps might lead to an increase of solver time by the factor of 2.6.

The impact of an increasing number of nodes is shown in Figure 5.22. In this case, no storages are considered. For the most extreme case (1000 nodes and 10 000 participants) the solver time reaches 81s. To take more datapoints into account the increase factor for 10 and 100 nodes is evaluated. A

[1]The power function $y = ax^s$.

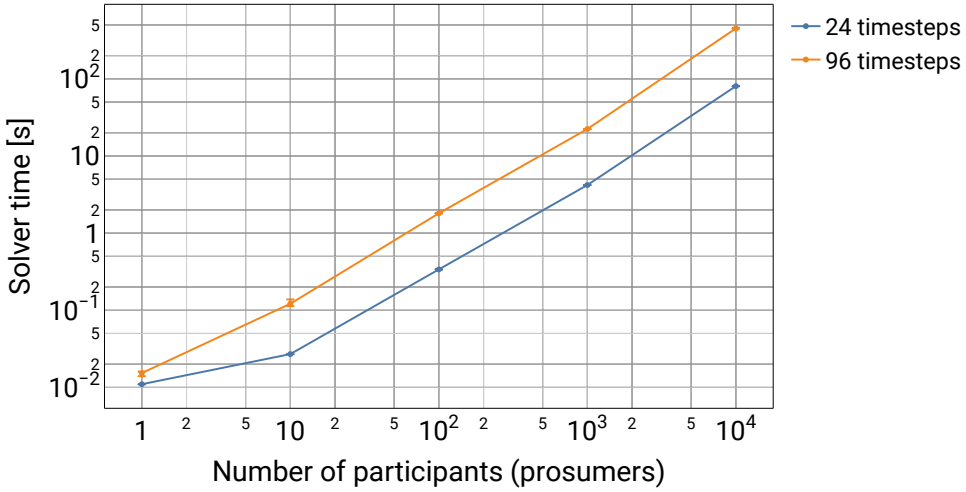

Figure 5.21.: Elapsed solver time over an increasing number of market participants and a variation of the number of timesteps. Constant parameter settings: Share of participants with battery storage: 50 %, number of nodes: 1, problem formulation: LP.

tenfold increase of the number of nodes hereby leads to an increase in computational time with a factor of 2.3. Hence, doubling the number of nodes leads to an increase of computational time of 0.46 (46%).

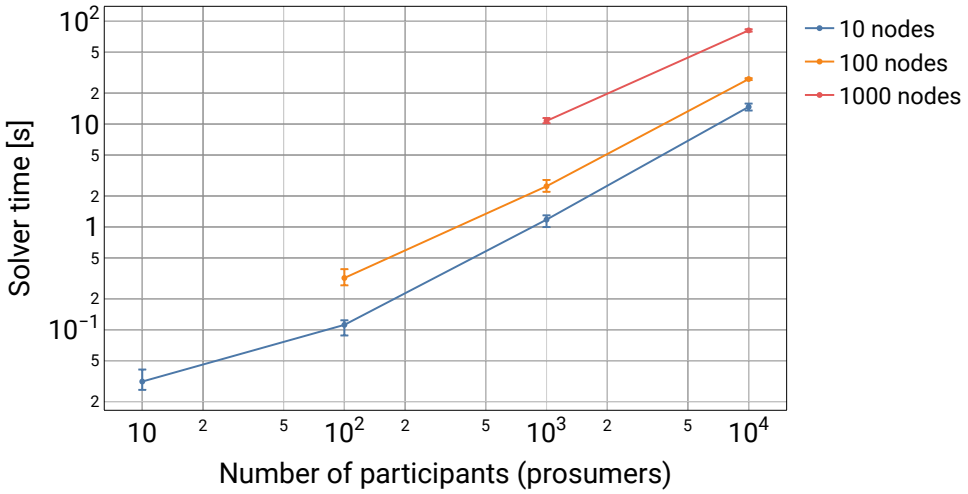

Figure 5.22.: Elapsed solver time over an increasing number of market participants and a variation of the number of nodes. Constant parameter settings: Number of timesteps: 24, share of participants with battery storage: 0, problem formulation: LP.

5.5. Discussion

This section discusses the presented simulative evaluations with respect to the desired market features introduced in Section 2.2.2. The found results are put into context of similar studies in the literature. Limitations and potential future research directions are evaluated.

Regarding the desired market features of optimal dispatch and the consideration of flexibility of DER, the results indicate that the proposed market model can significantly increase relevant KPIs (Section 5.1). Compared to the benchmark operation (Business as Usual), an increase of self-consumption and self-sufficiency of the local energy system is achieved through the optimal usage of flexible assets like EVs, HPs and battery storages. The potential increase ranges from 1.1 to 22.5 percentage points for a scenario year 2035. A similar study on LEMs by Cramer et al. [170] shows an even higher increase for the same scenario year (10-74 percentage points). This study, however, takes into account all market participants below a HV/MV substation and includes large-scale DER such as wind power and CHP. Compared to this Thesis, only including PV at the LV level, the potential of increasing self-consumption and self-sufficiency is naturally higher due to the additional generation during the night (wind power) and dispatchable generation which match a higher share of the local demand.

The results indicate that the optimal scheduling of flexibilities through the LEM can reduce consumption and feed-in peaks in the considered grid. Significant differences in the reduction potential are observed depending on the REPC incentivation scheme. The highest reduction is achieved when power fees are applied in addition to energy fees (30-60 % demand peak reduction, 46-64 % feed-in peak reduction). Lower reductions are achieved in the energy fee based scenarios (8-22 %). These findings coincide with findings in [170] which show an average reduction of 39 % for a simulation case with power fees and 17 % for a simulation case without power fees. The results presented in Section 5.2, show that a tariff scheme based on wholesale market prices (*Variable* scenario) induces higher demand peaks than other REPC scenarios. Gemassmer et al. [171] draw similar conclusions showing that a purely market-oriented charging strategy for EVs leads to increasing peak loads compared to a balanced charging strategy.
It should be noted that the reduction of feed-in and demand peaks from the upstream grid should be considered as a theoretical maximum. For the main sources of demand side flexibility, i.e., EVs and HPs, the actual achievable flexibility potential might be lower in reality. For EVs the potential demand shifts in the charging process highly depend on the actual arrival times of the EV, the charging duration and the energy demand. All of these parameters are associated with a forecast uncertainty which is not considered in the day-ahead simulation and will in reality lead to a reduction of the achievable flexibility utilization. For HPs, the estimated ability to shift the demand in time significantly depends on the sizing of the thermal storage as for example demonstrated in [172]. In the evaluated demonstration cases, a sufficiently sized thermal storage is assumed to allow a shifting of the heat-demand.
An additional factor that needs to be considered is that the presented simulations assume that all private and commercial grid users are participating at the LEM. Thus, potential peak reduction will be lower in absolute numbers and might be lower in relative numbers for smaller shares of participants depending on the composition of the participants.

The market feature of participants' financial incentivation is well covered in the found results. The implemented market design shows that market prices reflect scarcity or excess on a temporal dimension but also depending on the assets of participants and the considered grid type. Higher

benefits are achieved for generation assets in the urban case with higher demand. In generation dominated grids (rural/semiurban) demand assets show higher benefits. In scenarios with energy fees, no clear financial incentivation for flexible loads (EVs and HPs) is given compared to uncontrollable loads which might influence the willingness of participants to provide the flexibility to the system. Including a distributional mechanism to value the reduction of peak loads (power fee scenario) flexible assets achieve higher benefits compared to inflexible loads and might hence be incentivized to offer their flexibility. The proposed mechanism, however, might be complex to implement in reality as it would require to track the achieved reductions on participant level.
It should be noted, that the results for the economic evaluation are highly dependent on the development of future energy market prices and regulatory adaptions. The height of the actual REPC-adaption and future remuneration schemes for VRE will determine the actual benefit of participants. The results presented do not aim to answer the question if the incentivation is high enough but rather show that the developed market model is able to efficiently and specifically introduce price signals for DER deployment.
The analysis of the consideration of demand forecast uncertainties on individual participant level shows that forecast errors drastically reduce the benefits due to penalty payments. Other studies, e.g., [173], [174], show that this effect, although not as severe, is additionally increased when considering the uncertainty in generation forecast of PVs. Hence, future research should address this issue. Following measures are conceivable to reduce the described effect: An introduction of an intraday market with smaller lead times (e.g., 15 min) might reduce the impact due to an increasing forecast accuracy. Another approach is to introduce an aggregation of participants, e.g., at feeder level to reduce the stochasticity of individual demand patterns. This approach is demonstrated in [174] showing that an aggregation of a small number of aggregated households (14-23) drastically reduces forecast errors and increases the average benefit of participants.

The scalability analysis shows that the main influence on the computation time of the proposed market matching is introduced by the number of timesteps considered (factor of 2.6 when doubling the number of timesteps), followed by the number of storages considered (factor of 2.5 when doubling the number of storages) and the number of nodes (factor 0.45). The solver time stays below 900s even for a case with 10 000 participants each equipped with a load, generation and a storage. The demonstrated scalability analysis is limited to one single optimization problem combining the full set of participants, orders and grid topology. Further speed-up of the computational time might be achieved by applying temporal or spatial disaggregation techniques as, e.g., described in [175] or [134].

6. Field test

6.1. Field test description

The data of the following results were produced within the field test demonstration of the research project *pebbles*[1] between the 1st of April 2021 and 15th of October 2021. The project was set up in the village of Wildpoldsried in southern Germany and demonstrates the implementation of a LEM with real residential and commercial participants in a rural setting.
Besides the real participants, additional virtual participants were added to the market to increase liquidity. Additionally, a load bank, a large electrical storage, a diesel generator and a back-to-back DC connection were available at the Energy Campus Wildpoldsried (ECW)to physically emulate further participants. A total of 9 real participants, 50 virtual participants and 4 emulated participants were part of the field test (Table 6.1). The distribution grid considered in the field test consisted of a total of 8 secondary substations (LV/MV) distributed across Wildpoldsried and neighboring villages/cities.

The market model and matching algorithms described in Section 3.1 were applied in the field test as a day-ahead market. The following description of the project and result analysis are limited to aspects within the scope of this Thesis and the developed market matching software (from here on referred to as local market platform). For further details on the project please refer to [24], [176]–[178]. For a detailed analysis on the regulatory framework for P2P energy platforms in Germany please refer to [179].

Figure 6.1 shows a simplified sequence diagram of one market cycle and the relevant actors, actions and data exchanges. One market cycle can be separated into three phases:

Before market closing

The market closing time in the field test is set to 17:00 for the matching of the next day. Before the market closing time, the actors need to submit the relevant data required for the matching. The data is submitted to a central data hub (Transaction platform) which can be queried by the local market platform to retrieve the relevant data for the matching.
The trading agent of each participant needs to generate the market orders with the respective parameters (compare Section 3.1.1). This requires user data of the residential participant, e.g., price preferences, asset configurations, as well as a forecast of the inflexible load and generation of the participant. The user data (e.g., price preferences) is supplied by a mobile app and can be adapted by the participants. The forecasts are calculated on the basis of weather forecasts and

[1]Pebbles was funded by the German Federal Ministry of Economic Affairs and Energy within the funding program, 'Smart Service Welt II' (Grant ID.: 01MD18003D).

historic measurements of the respective assets.
The DSO provides the grid topology as well as grid limits and grid fees in the data structure described in Section 3.1.3. For the field test, an iterative power flow simulation is performed by the DSO to calculate active power limits of the LV feeder lines (Figure 6.2). This simulation is performed on a daily basis taking into account producers and consumers which do not participate at the LEM to find active power limits which do not violate voltage band limits.
The backup supplier provides information on the backup prices, i.e., prices for unmatched demand and generation, and information on REPCs such as fees, taxes and levies. The detailed distribution of REPCs along the grid topology is explained in the following section.

After market closing

After the market is closed (17:00), market orders, grid input and the input of the backup supplier are queried by the local market platform. All orders submitted after closing are not considered for the matching of the following day. With the queried data, the local market platform builds the optimization model including the grid topology, grid limitations, REPCs and the orders of the participants. The market matching is performed by solving the optimization problems described in Section 3.1.2. The market results and grid utilization results are then transferred to the transaction platform. All relevant actors can then query the results of the matching from the transaction platform. The trading agents for example retrieve the matched quantities and prices to calculate the schedule for the next day.

Delivery

During the delivery periods (96 15-min intervals of the following day) the local automation devices of controllable assets (e.g., storages, flexible demand, flexible generation) receive setpoints by the trading agent to comply with the results produced by the market (contracts). During delivery, the power consumption and generation of all assets are measured to later calculate the deviation between the traded (forecasted) values and the actual measurement. This is especially relevant for uncontrollable generation and demand such as PV and the baseload as later demonstrated in Section 6.3.5.

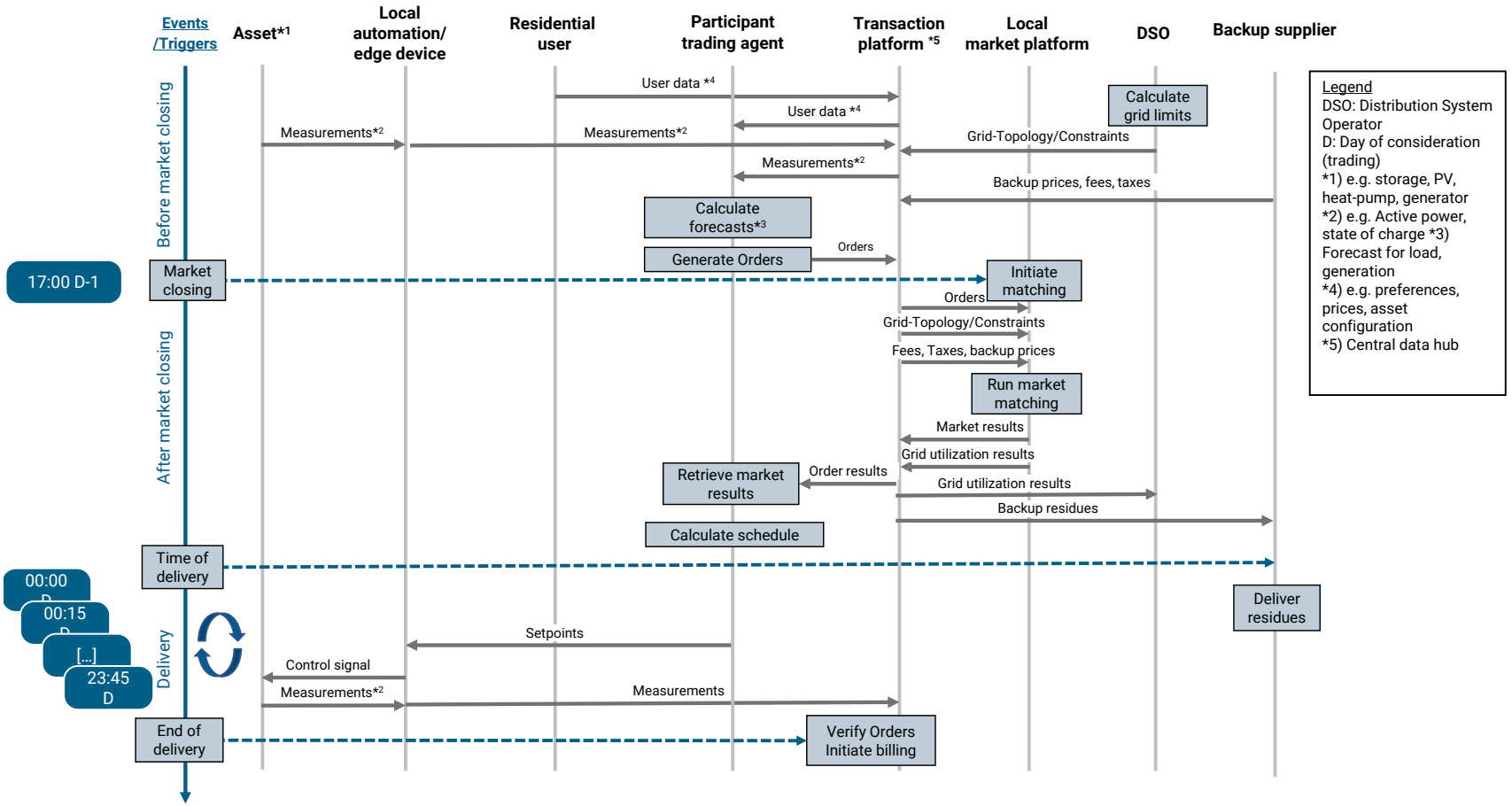

Figure 6.1.: Sequence diagram of one market cycle within the field test.

6.2. Setup and scenarios

During the field test several scenarios adaptions were made to analyze the impact of the market participant set up and the structure of REPC on the LEM. The baseline scenario reflects the year 2020 and an increase of distributed generation and demand was projected for the year 2030. To achieve this projection of parameters in the field test, the asset parameters of the virtual participants were adapted accordingly (Table 6.1). The real participants and emulated participants at the energy campus do not change parameters between the scenarios. The asset parameters of the virtual participants for 2030 show a strong increase in PV capacity as well as controllable demand (EVs and HPs). For the overall system (scenario 2030) a rated PV capacity of 115.5 kWp, an electric storage capacity of 198 kWh, controllable generation of 395 kW (biodiesel and biogas generators) and a controllable demand of 99 kW is installed. The participants are composed of 53 household participant, 6 commercial participants. The emulated participants at the energy campus represent one residential participant and one commercial participant. Additional generation capacity is provided by the Virtual Power Plant (VPP) of the local utility. The VPP acts as participant at the LEM selling electricity at a remote substation of the grid. The minimum sell prices of the VPP are based on forecasts of spot market prices. It should be noted that especially due to the high rated power of controllable generation, the considered system is oversized with regards to the available generation.

Table 6.1.: Set up of market participants of the field test for the baseline (2020) and expansion (2030) scenarios.

		Scenario 2020	Scenario 2030
Virtual participants	Number of households [-]	45	45
	Number of commercial participants [-]	5	5
	Electrical storage rated power [kW]	3	8
	Electrical storage capacity [kWh]	5	5
	Rated PV capacity [kWp]	6	55
	Controllable demand [kW]	14	99
Real participants	Number of households [-]	8	8
	Number of commercial participants [-]	1	1
	Rated PV capacity [kWp]	50.6	50.6
	Controllable generation [kW]	240	240
Energy campus	Emulated participants [-]	4	4
	Electrical storage rated power [kW]	170	170
	Electrical storage capacity [kWh]	193	193
	Rated PV capacity [kWp]	9.9	9.9
	Controllable generation [kW]	155	155

Additionally to the scenario adaption of asset parameters, the structure and quantity of REPC is varied between two scenarios (Table 6.2, Figure 6.2). The *regular fees* scenario is based on the status quo of the regulation, i.e., the main proportion of the overall fees (full grid fees, levies, surcharges) is applied directly to each consumed kWh of a market participant. The electricity tax is assumed as a variable portion which only needs to be paid when electricity is bought from a participant at another substation. In a more progressive scenario (*reduced fees*) the grid fees of 9 ct/kWh are equally split across the LV-, MV- and HV-level. An energy trade within the same substation is hence only charged with LV grid fees, levies and surcharges. Surcharges are additionally reduced by the EEG-surcharge (6.5 ct/kWh). Table 6.3 shows the schedule of the experiment with the respective

expansion and REPC scenarios. The *regular fees* scenario will be referred to as unattractive scenario and the *reduced fees* scenario will be referred to as attractive scenario in the following result section.

Table 6.2.: Distribution of Regulated Electricity Price Components (REPC)s for the two fee structure scenarios

	Scenario Regular fees	Scenario Reduced fees
High voltage grid fees [ct/kWh]	0	3
Electricity tax [ct/kWh]	2.05	2.05
MV grid fees [ct/kWh]	0	3
Levies, surcharges [ct/kWh]	9.416	2.916
LV grid fees [ct/kWh]	9	3

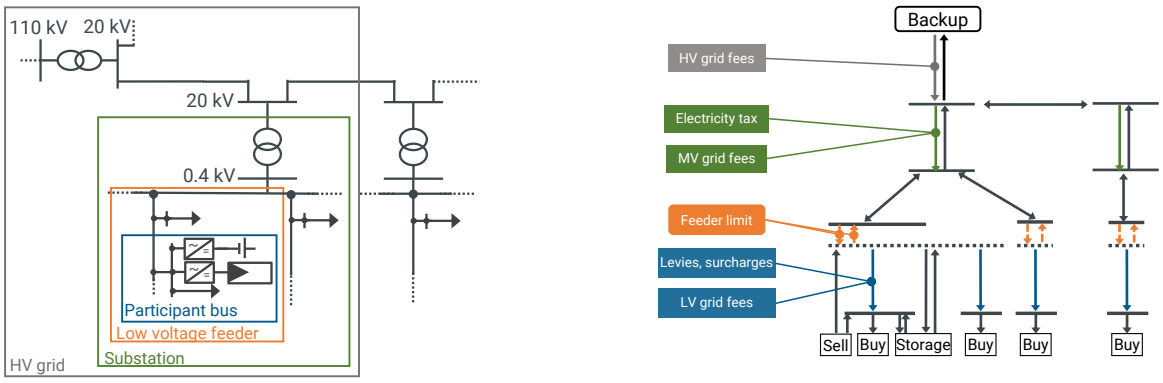

(a) Grid model

(b) LEM Model

Figure 6.2.: Representation of a typical radial distribution grid topology (a) and the applied fee structure and grid limitations in the field test (b).

6.3. Results

6.3.1. Overview

For a first overview, Figure 6.3 shows the daily share of local and non-local generation in the electrical energy consumption of the LEM participants. A clear fluctuation in local generation can be seen across the scenarios. The average degree of self-sufficiency varies from 16% in the 2020 *regular fees* scenario to 97.7% in the 2030 *reduced fees* scenario (see Table 6.4).

Figure 6.4 shows the same plot partitioned into generation types. The Figure provides a first indication of the cause of the strong differences in the degree of self-sufficiency. It can be observed that especially the share of biodiesel and biogas plants decreases strongly and is partly almost zero in the *regular fees* scenarios. Furthermore, the generation share of the VPP is significantly higher in the attractive scenarios (20.9% - 45.5%) than in unattractive scenarios (4.7% - 5.2%). Generation from

Table 6.3.: Overview of time periods of the field test scenarios years and fee structures

Scenario number	Year	Fee structure	Scenario start date	Scenario end date
1	2020	Reduced fees	01.04.2021	30.04.2021
2	2020	Regular fees	01.05.2021	31.05.2021
3	2030	Reduced fees	01.06.2021	30.06.2021
4	2030	Regular fees	01.07.2021	31.07.21
5	2030	Reduced fees	01.08.21	20.09.21
6	2030	Regular fees	21.09.21	15.10.21

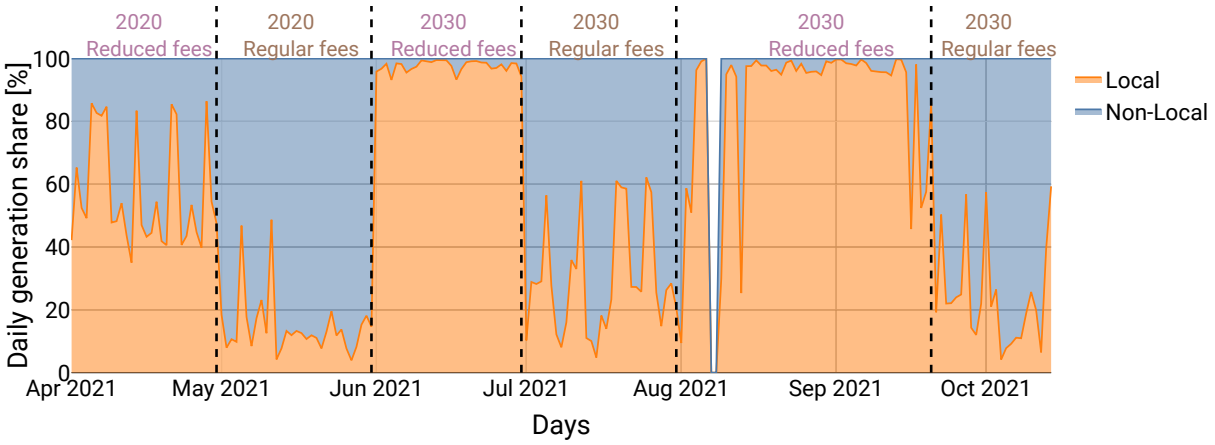

Figure 6.3.: Calculated relative daily generation share of local and nonlocal generation during the field test. Data gap in August due to planned downtime of the system.

PV also varies between scenarios (10.7% - 27.1%), but this variation is not as pronounced compared to the other generators. The strong variations between attractive and unattractive scenarios with respect to VPP and biodiesel/biogas can be explained by the difference in the structure of REPCs. In the case of biodiesel/biogas for example the average minimum sell price (15 ct/kWh) plus all REPCs (20.5 ct/kWh in the *regular fees* scenario) exceed the maximum purchase price preference of most participants (31 ct/kWh). Generation with lower minimum prices, e.g., from PV plants, is matched more frequently at the LEM almost regardless of the scenario. The overall share of PV generation increases from scenario 2020 to scenario 2030 as the installed PV capacity of virtual participants is increased almost tenfold while the overall demand only increases slightly (Table 6.1).

Another remarkable observation is that the share of generation supplied by the VPP drastically decreases between scenario 3 (45.4%) and 5 (20.9%) although the scenario settings are the same (2030 *reduced fees*). This reduction can be attributed to the increase of day-ahead wholesale market prices from an average of 74 €/MWh in scenario 3 to an average of 106 €/MWh in scenario 5 during that time (Appendix Figure A.8). The VPP which forwards these prices to the sell orders gets hence matched less at the LEM as the prices exceed the maximum buy price of market participants.

Table 6.4.: Scenario assumptions for base case, medium and high expansion cases

Scenario Scenario Name Share of Generation	1 2020 Reduced	2 2020 Regular	3 2030 Reduced	4 2030 Regular	5 2030 Reduced	6 2030 Regular
Backup supplier [%]	40.4	84.0	2.3	69.9	7.7	75.1
Biodiesel/Biogas [%]	17.5	0.0	22.9	-	45.5	2.9
PV [%]	16.7	10.7	27.1	20.6	24.3	16.1
Storage discharge [%]	1.2	0.6	2.2	0.9	1.5	0.6
Virtual power plant [%]	24.2	4.7	45.4	8.6	20.9	5.2
Self-sufficiency [%]	59.6	16.0	97.7	30.1	92.3	24.9
Average buy prices [ct/kWh]	26.6	29.3	25.3	28.8	26.3	29.1
Average sell prices [ct/kWh]	13.8	9.0	11.6	8.3	13.9	9.6

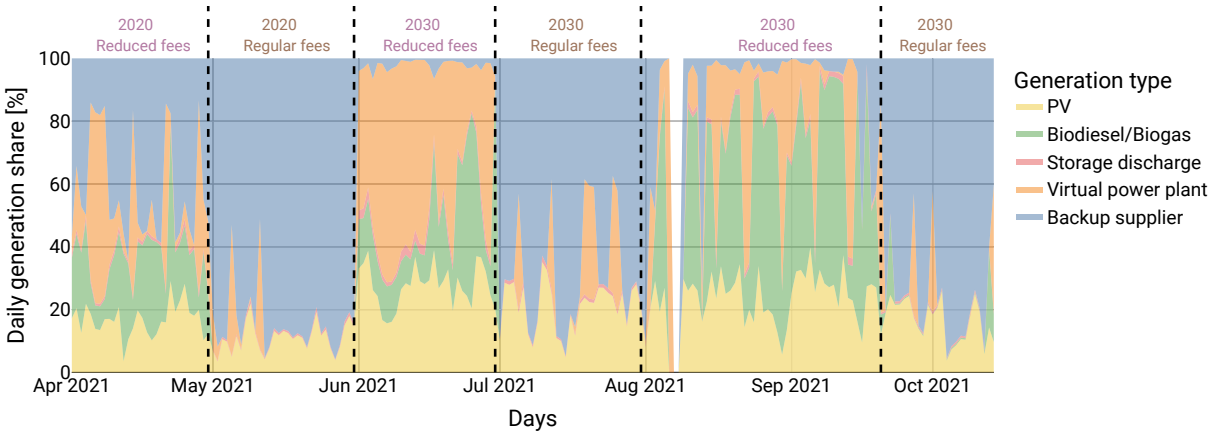

Figure 6.4.: Calculated relative daily generation share of generation different generation types during the field test. Data gap in August due to planned downtime of the system.

6.3.2. Flexibility

One goal of the LEM is to make optimal use of the available local flexibility. In the following, this is illustrated by the example of flexible generation from biodiesel/biogas and storage flexibility. Figure 6.5 shows the share of the different types of generation for three days in the attractive scenario 2020. Flexible generation from biodiesel/biogas is matched by the LEM only when there is little supply from PV plants and the VPP at the LEM. This is the case, for example, in the morning and evening hours. Furthermore, in the sales bids of the biodiesel/biogas plants, a total energy quantity, a maximum nominal power as well as a time range (02:00 - 22:00) were specified (compare Chapter 3.1.1). For the night hours between 22:00 and 02:00, the only source available locally are the storages which discharge during this time frame.

In contrast to the dispatch scenario the *reduced fees* scenario, Figure 6.6 shows three days from a *regular fees* scenario. It can be seen, that no biodiesel/biogas generator is utilized in this case. The storages are discharged at night, but to a much smaller degree than in the *reduced fees* scenario. This is due to the fact that the storage facilities in the *regular fees* scenario are only used to meet the individual participants' own demand and are not made available to other participants as flexibility. This is uneconomical in the *regular fees* scenario due to the higher REPCs.

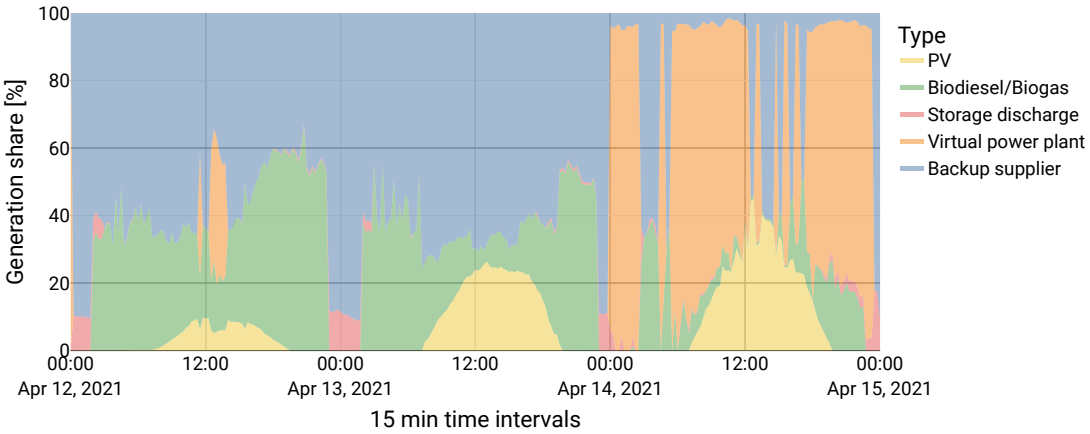

Figure 6.5.: Three example days (12.04.2021 - 15.04.2021) of the generation share within 15 min trading periods in the scenario 2020 *reduced fees*.

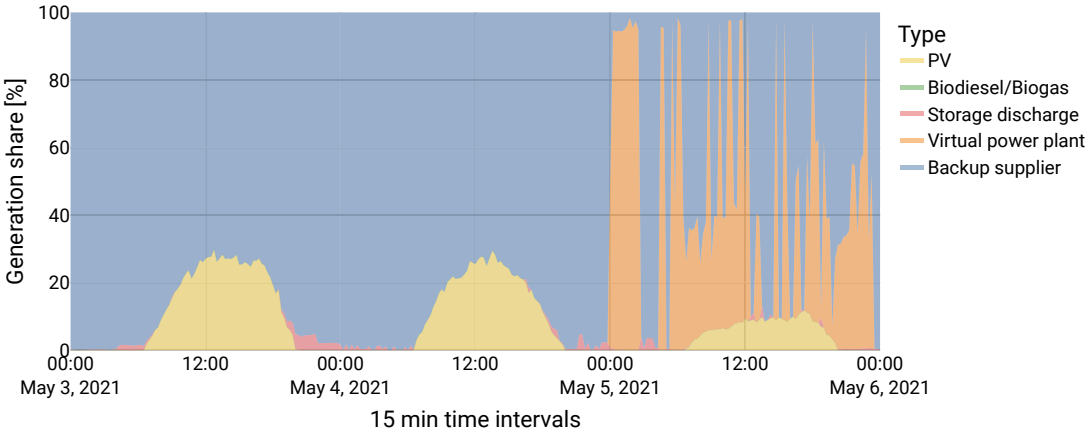

Figure 6.6.: Three example days (03.05.2021 - 06.05.2021) of the generation share within 15 min trading periods in the scenario 2020 *regular fees*.

A detailed dispatch schedule of all storages over the entire field test period is shown in Figure 6.7. As expected, the storage units are mainly charged over the midday period when low-cost PV electricity is available. The storages are then discharged in the evening hours or at night. In the *reduced fees* scenarios, there is additional charging power in the midday hours and discharging power in the evening hours. This is particularly pronounced in the 2030 scenarios with increased PV capacity. In addition, especially in the first scenario (2020 *reduced fees*), individual quarter hours with high charging capacities can be seen. The patterns described in the *reduced fees* scenarios can be explained by the use of the community storage at the energy campus. The main discharge periods are in the night hours starting from 22:00. As explained above, this is the time period where no flexible generation from biogas/biodiesel generators is available.
The storages are mainly used for self-consumption in the *regular fees* scenarios because the additional revenue that must be generated by buying and selling a kWh cannot be generated (higher REPCs, see above). In the *reduced fees* scenarios, however, favorable prices at the midday

peak of the PV feed-in or low prices of the VPP are used to charge the storage and then profitably sell it again in the evening when there is an under supply. This effect will be examined in more detail in the following chapter with a detailed analysis of the market prices.

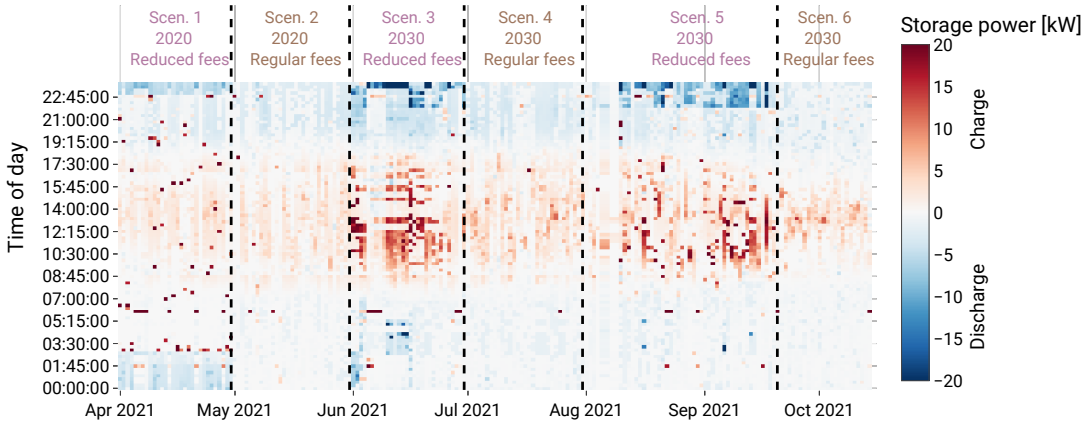

Figure 6.7.: Calculated heatmap of the storage usage throughout the field test.

6.3.3. Market prices

Figure 6.8 shows the volume-weighted sell prices at the LEM over the days (X-axis) and time of day (Y-axis) of all six scenarios. The prices range from about 6 ct/kWh to about 20 ct/kWh and differ strongly between the individual scenarios. Both the composition of the participants (2020 vs. 2030) and the design of REPCs have a strong influence on the pricing. For white fields (missing values), no local trading occurred. In the *reduced fees* scenarios, generation from biodiesel/biogas dominates the price in the evening or at night (15 ct/kWh). As already described in the previous section, the storage facilities feed in during the night hours (22:00 - 02:00) and are the only "producers" that determine the price here. With a typical maximum purchase price of about 31 ct/kWh (gross), storages can get paid more then 20 ct/kWh (net) for their electricity. In the most favorable case (trading at the same transformer station), the electricity tax, medium and high voltage grid fees as well as the EEG levy are omitted, which leads to a reduced REPCs of 5.9 ct/kWh. For several days in the reduced fees scenarios, the prices also drop to 6-8 ct/kWh during evening and night hours. In these days, the price is predominantly influenced by the VPP. This influence decreases comparing scenario 3 and 5 due to the increased wholesale market prices (compare Figure A.8 in the Appendix).
In the *regular fees* scenario 2030, the prices are mainly influenced by the generation of PV electricity. In case of a strong surplus at midday, the price drops down to 6 ct/kWh hour. In the *regular fees* scenario 2020, significantly less PV power is installed than in the *reduced fees* scenario 2020. In both scenarios, the load at midday is dominated by commercial participants who have increased consumption at midday. Thus, in the attractive scenario 2020, the price at midday is determined by the PV installations, but since there is mostly shortfall in the market, the price is determined by the buyers and leads to increased revenues on the generation side (about 18 ct/kWh).

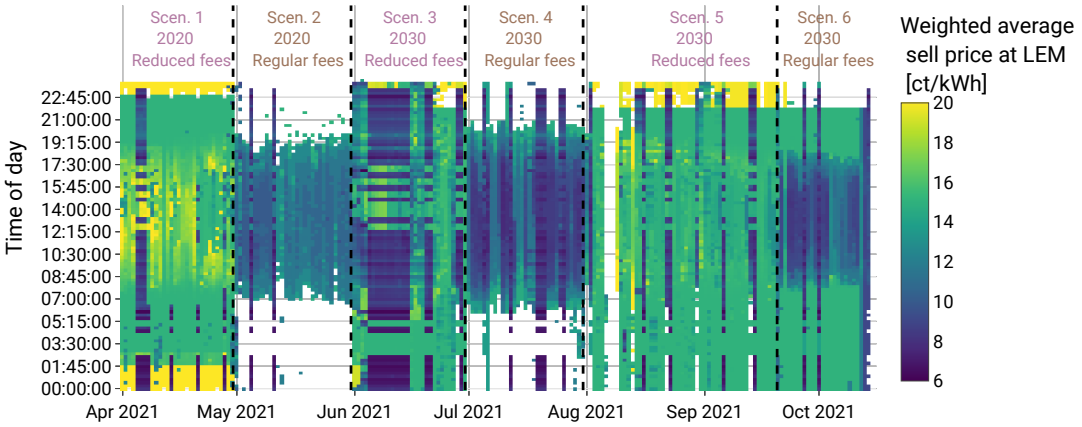

Figure 6.8.: Calculated heatmap of weighted average buy prices at the LEM within the demonstrator period.

The consideration of the grid topology and topology dependent REPCs in the market matching optimization lead to nodal prices as a result of the market matching. Figure 6.9 shows the average buy prices for the 2030 scenarios plotted over the share of generation which is supplied directly to demand at the same substation. Especially in the *reduced fees* scenario a strong reduction of the average buy price can be observed for increasing generation shares at the same substation. At the most expensive substation with no generation the weighted average price is 26.5 ct/kWh, whereas the cheapest price is 21.2 ct/kWh at a substation with 52.3 % generation. The same effect can be observed for the *regular fees* scenario. However the influence of the generation share is not as prominent, as the reduction of fees is only 2.05 ct/kWh (electricity tax) in this scenario.

6.3.4. Grid utilization

As described in Section 6.1, the DSO is able to influence the market matching by sending daily power limits. During the field test, the low voltage feeder lines where limited both for imports to the feeder as well as exports from the feeder. The feeder node IDs are anonymized (mapped with random numbers) in the following evaluations. Figure 6.10 shows an example of a feeder with 4 market participants including PV generation. The import and export limits are represented with the dotted lines. The residual load at the feeder is the result of the market matching and represents the trades at the LEM [2]. The example days demonstrate that the export limit follows the inverse of a typical PV generation profile. With this, the DSO is able to limit the local trades during the peak feed-in times around 13:00 at midday. At several 15 minute intervals, e.g., on the 9th of April, the residual load reaches the limit of the feeder export. The demand limit however is not reached in this example.

[2]Trades with the backup utility are not shown here as they are not limited by the market. These trades could result in a violation of the constraints. However, curtailment of load and generation through the market which, would solve this issue, was not considered during the field test.

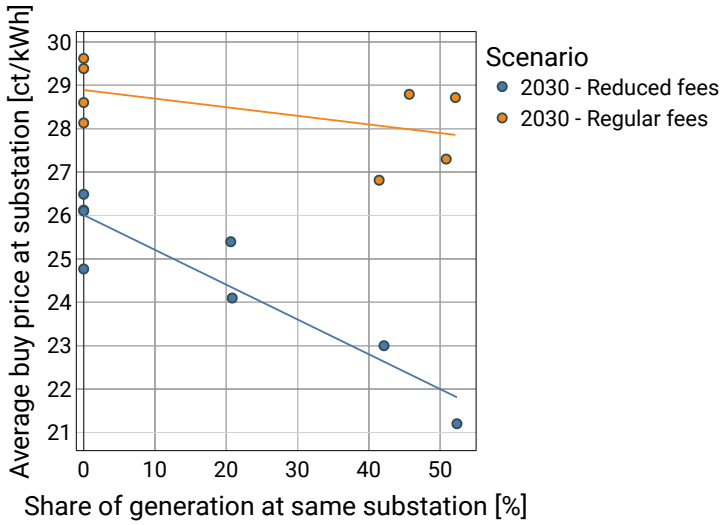

Figure 6.9.: Calculated weighted average buy prices at 8 substations in the field test over the share of generation at the same substation (self-sufficiency). Each scatter represents one substation.

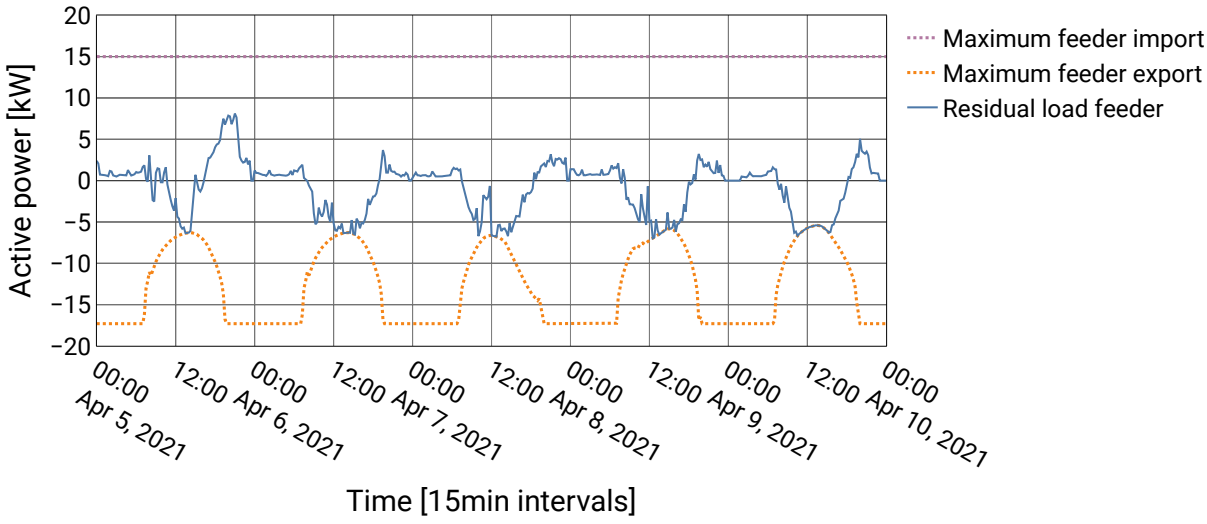

Figure 6.10.: Example of low voltage feeder limits and residual load of feeder #N4 between 05.04.2021 and 10.04.2021. The residual load represents the result of all buy, sell and storage orders traded locally at the feeder. Feeder limits are inputs from the DSO.

For all quarter-hourly time steps of the demonstrator, the distribution of the utilization of the individual low-voltage lines is shown in Figure 6.11. While a large part of the feeders show a low average utilization, some feeders show a significant amount of 15 minute intervals with full utilization. High utilization rates are registered in particular on the feed-in side. A full (100 %)

utilization can be interpreted as an avoidance of a voltage violation, as this is the limit is set by the DSO exactly at a rate where no voltage violations are expected.

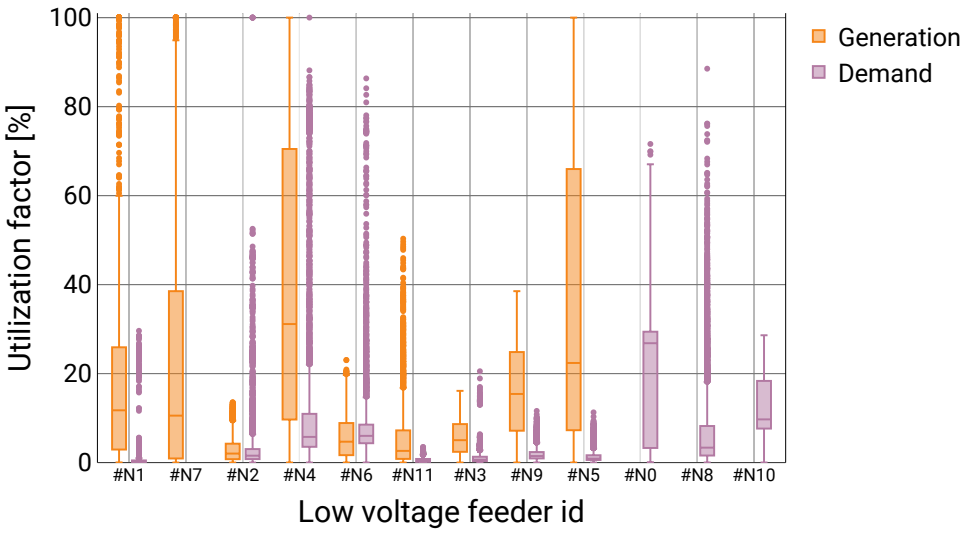

Figure 6.11.: Boxplots of the calculated utilization factor at low voltage feeders for all 15 minute intervals during the field test.

In Figure 6.12 the sum of these violations is plotted for the affected low voltage feeders. A total of six low voltage feeders are affected by critical utilization. A total of 1499 trading intervals were limited by the input of the DSO. 99.5 % of all avoided violations can be attributed to limiting the generation at low voltage feeders. Only 0.5 % are due to demand limitations.

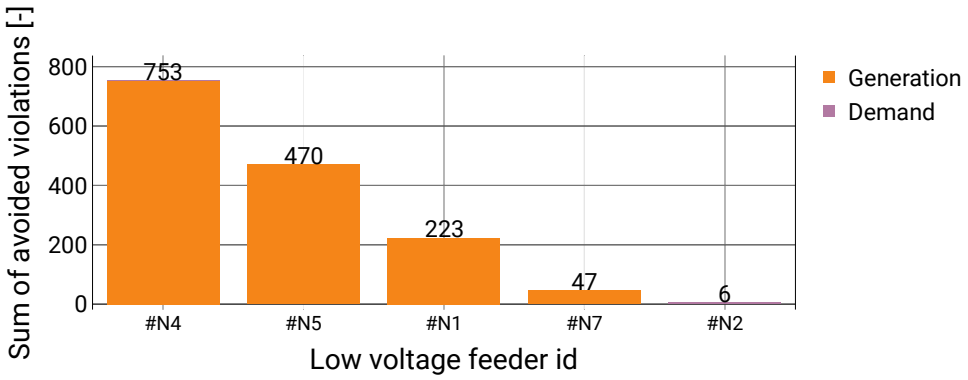

Figure 6.12.: Sum of all 15 minute time intervals where a voltage violation is avoided (feeder is fully utilized) during the field test period.

6.3.5. Forecast uncertainty

As demonstrated in the simulative results (Section 5.3), day-ahead load forecasting for individual participants is challenging and leads to high errors between forecasted/traded demand and the actual measurement. Figure 6.13 shows the Mean Absolute Percentage Error (MAPE) of the demand forecasts for all real participants divided into three categories (Commercial, Household and Household with EV). The forecast errors range between 29 % and 330 %, which is in line with typical forecast errors found in the literature (Figure 2.12). The household with EV stands out as the magnitude of the error is considerably higher than the ones of households and commercial participant. Examples of each category are shown in the following figures.

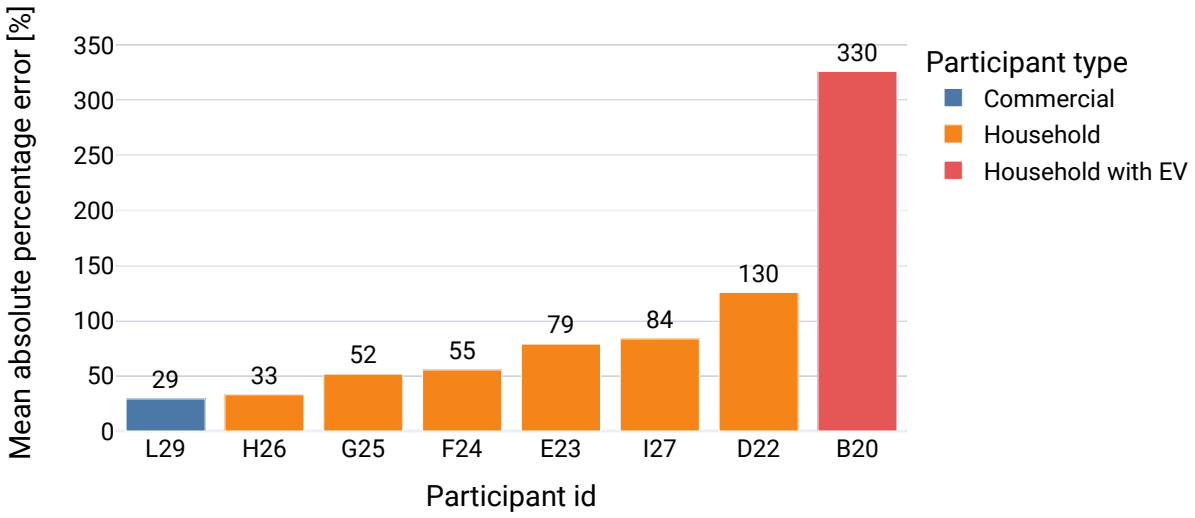

Figure 6.13.: Day-ahead load forecast error of different real participants during the first 4 scenarios of the demonstrator (01.04.2021-30.07.2021)

Figure 6.14 shows exemplaric days of the forecasted and measured demand of participant B20. High measured loads between 9 ... 12 kW during midday of the first days (20.04.21 and 21.04.21) indicate the charging of the EV. The forecasting algorithm anticipates this behavior and forecasts a similiar pattern for the next day (22.04.21). However, no clear charging pattern can be observed for the coming days. This leads to a large positive bias of the forecast and large errors during this period.

The stochastic charging behavior however is not limited to the example days as shown in the heatmap in Figure 6.15. Although there is an observable tendency of charging periods during the middle of the day, this pattern is not regular and hence hard to forecast (MAPE of 330 %).

A contrary household example with a MAPE of only 33 % is shown in the heatmap Figure 6.16. A clear pattern of increased load during the morning hours around 6:00 and midday around 12:00 is observable. However, in the example Figure 6.17, the magnitude of the profile is forecasted accurately however the exact match of the 15 min intervals is still inaccurate. A vertical and horizontal shift comparably to the results of the simulation chapter (section 5.3) can be observed.

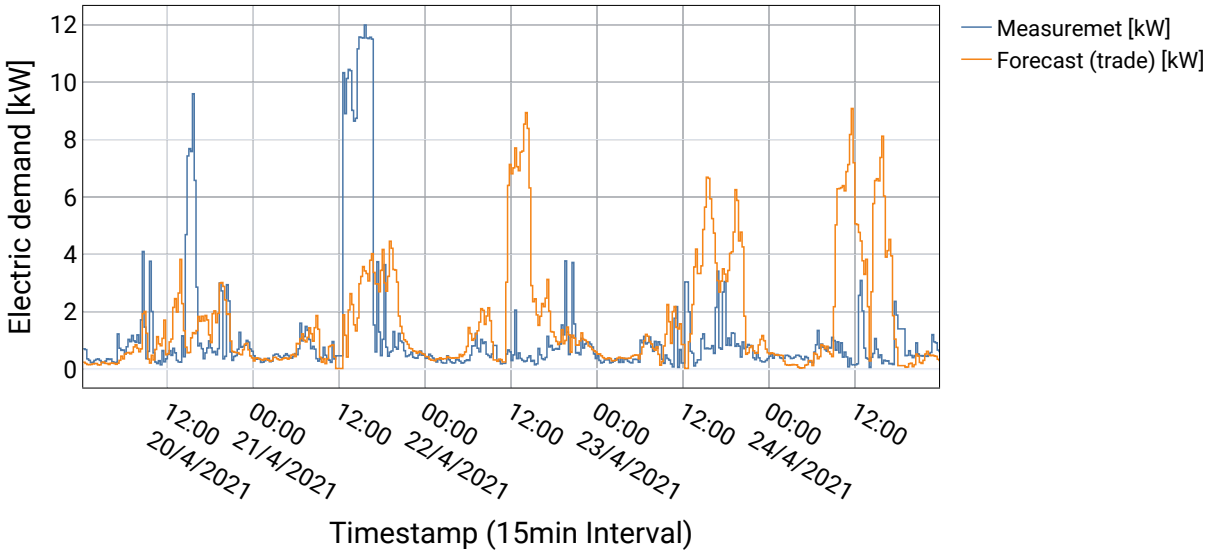

Figure 6.14.: Example days of the measured and forecasted demand of participant B20 (participant with EV).

As an example of a load profile with clear and repetitive demand patterns, heatmap and example days of participant L29 (commercial) are illustrated in Figure 6.18 and 6.19. The heatmap profiles shows regularly weekly pattern with increased demand during 6:00 and 20:00 at 5 days of the week and 6:00 to 17:00 at 1 day of the week. Figure 6.18 shows that this pattern is reproduced well by the forecasting algorithm leading to an overall MAPE of 29 %.

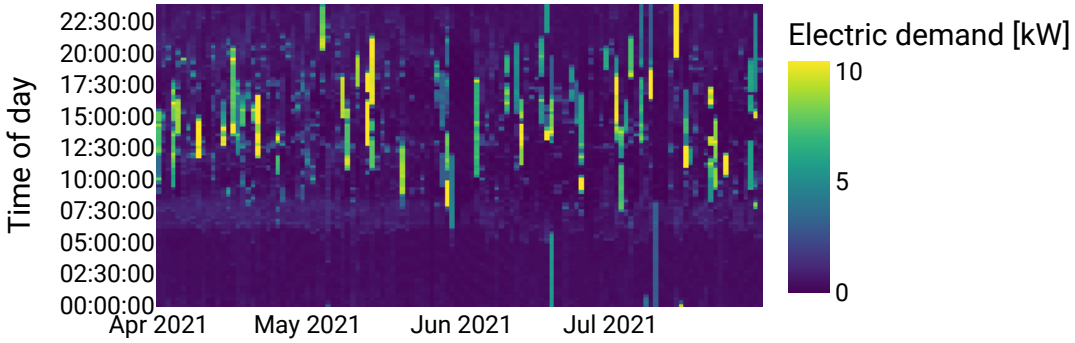

Figure 6.15.: Measured heatmap of the electric demand of participant B20 during the first 4 scenarios.

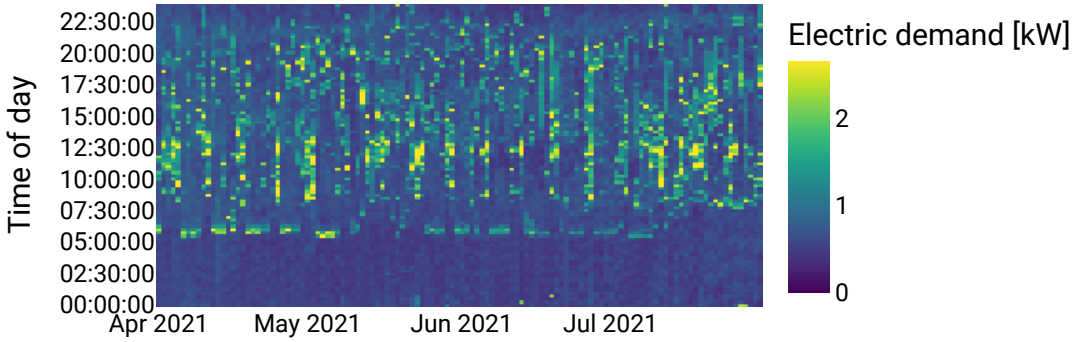

Figure 6.16.: Measured heatmap of the electric demand of participant H26 during the first 4 scenarios.

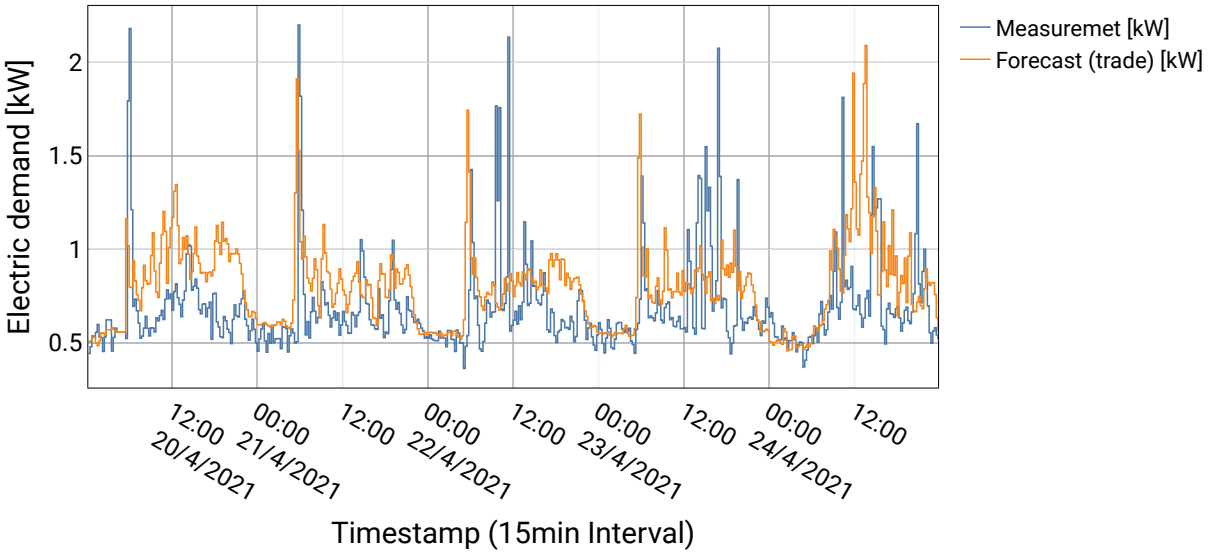

Figure 6.17.: Example days of the measured and forecasted demand of participant H26.

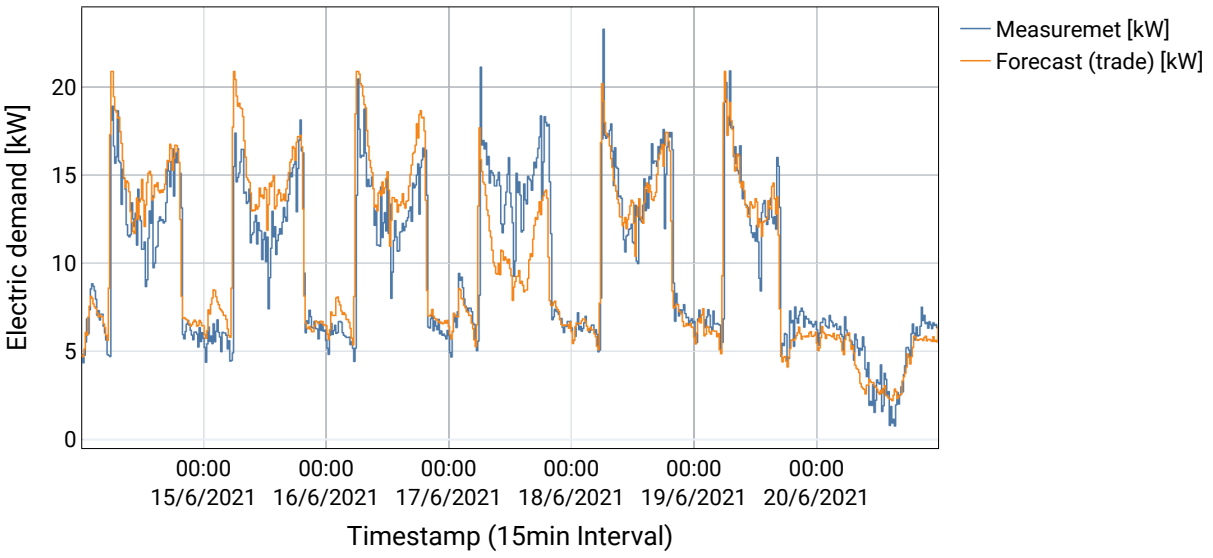

Figure 6.18.: Example days of the measured and forecasted demand of participant L29 (commercial).

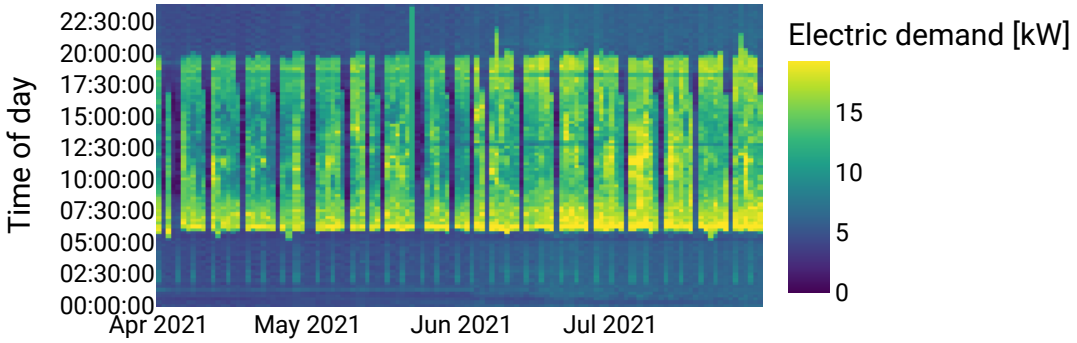

Figure 6.19.: Measured heatmap of the electric demand of participant L29 during the first 4 scenarios.

6.4. Discussion

The field-test application demonstrates that the market model developed in this thesis is implementable in the real-world. The results show similar findings compared to the simulative evaluation and even extends them. This section reflects the field-test results and puts them into context to the findings of the simulative evaluation and discusses limitations.

The introduction of reduced REPCs in the field-test result in an increased self-sufficiency compared to the regular fee structure. Although a benchmark case without a LEM is not analyzed in the field-test, these findings indicate that the additional usage of flexible generation and storages through the LEM drastically increases self-sufficiency. The absolute values of self-sufficiency in the regular fee scenario for the scenario year (25 ... 30 %) are in the same order of magnitude compared to the simulation of the rural grid and the scenario year 2035 (37 %). The absolute self-sufficiency in the scenarios with reduced fees (92 ... 98 %) is drastically higher compared to any scenario in the simulation results. This is mainly due to relatively large dimensioning of dispatchable generation in the field test (biodiesel/biogas) which is able to supply almost all load.

The results additionally show that the desired incentivation of flexibility is achieved. Sellers with higher marginal costs (e.g., Biogas) are only operated if cheaper sources such as PV are not available. The schedule patterns of battery storages show that the batteries are not only used for self-consumption, but are shared amongst participants increasing local self-consumption.

Regarding the price formation at the LEM, two additional observations can be made compared to the simulative study.
In the field-test, prices are not only determined by the scarcity or excess of local PV generation and their minimum prices but also through the local VPP which provides price signals from the wholesale market. It is demonstrated that this coupling works, since with the drastic increase of day-ahead spot prices in the last quarter of the field-test period the share of generation from the VPP decreased.
Through the consideration of multiple LV/MV another observation can be made. The results show an almost linear relationship between increasing self-sufficiency at a substation and decreasing buy prices at the same substation. Reduced fees at substation level might directly incentivize investments of generation capacity at substations with a low share of self-sufficiency and additional demand vice versa (compare Figure 6.9).

The additional interface with the DSO, which can provide upper limits of active power at certain feeders shows that the developed market model limits the traded amount on the LEM to the lower or upper bound of the DSO. This might not necessarily avoid all overloadings/overvoltages in the grid due to forecast uncertainty, but might however give DSOs a hint on specifically stressed grid equipment and critical buses.

The analysis on load forecasting errors of the participants in the field-tests confirms the findings from typical day-ahead forecast errors in the literature for single households (MAPE of 33 ... 130 %, compare Figure 2.12). An additional observation is that the issue of forecasting errors might even further with the uptake of EVs charging at households (MAPE of 330 %). These findings make the topic of handling of uncertainties even more important for future research.

An overall remark has to be made on the generalization of the found results. Since the field-test was performed with only 9 real participants in one specific distribution, the findings on absolute

numbers are not generalizable to other grid types or regulatory frameworks. Future research should address larger use cases or even a commercial long-term experiment.

7. Conclusion and outlook

7.1. Conclusions

This Thesis dealt with the main research question of how Local Energy Markets (LEMs) can be designed to incentivize regional flexibility options and contribute to the grid integration of Variable Renewable Energies (VREs), Electric Vehicles (EVs) and Heat Pumps (HPs). To answer this question a novel market model for LEMs was developed and evaluated through extensive simulations and applied in a field-test. The following sub-questions were formulated after the analysis of the problem and are answered and reflected with regards to the findings in this Thesis in this Section:

1. How can an optimized scheduling of DERs be achieved through a LEM without a central coordinator while providing real world applicability?

To address this question a novel market model formulated as a linear optimization problem was developed in this Thesis. Relevant parameters for an optimal dispatch of DER, e.g., maximum energy and power limits of flexible loads or storage parameters are abstracted as buy-, sell- and storage orders. These orders are generated at participant level thus abstracting the interface to the market operator without revealing specific asset parameters. A simulative framework was developed to analyze the proposed market model. Yearly simulation experiments for generic German rural, semiurban and urban distribution grids were conducted for scenario years 2020, 2025, 2030 and 2035. The simulation results show that the implementation of a LEM increases self-consumption, self-sufficiency and financial benefits of market participants compared to a benchmark case without the introduction of a LEM. The described findings increase throughout the scenario years with the highest impact starting with scenario year 2030.
The implementation of the market model in a field-test in Southern Germany demonstrated the real world applicability of the approach. The field-test revealed similar findings as the simulation and additionally highlights the importance of load forecast uncertainty in LEMs (addressed in Question 3.). The performed scalability analysis showed that the computation time of the LP formulation is highly dependent on the number of considered timesteps, the number of storage orders considered and the number of nodes in the grid model. For a case with 10,000 market participants, each equipped with a load- generation- and storage-asset, the solver time stayed below one time interval (15 min) of the market matching problem.

2. What effect does a dynamization of Regulated Electricity Price Components (REPCs) have on local energy trading? How can REPCs be utilized to steer local energy trading in a grid-friendly manner?

Several potential regulatory schemes of REPCs were analyzed in the simulative evaluation of

this Thesis. An energy fee based flat tariff scheme, i.e., every consumed kWh is attached with a constant REPC, an energy fee based scheme with a reduction of fees for trades at the same feeder, an energy fee based scheme with a time variable component based on spot market prices and a scheme with additional power fees were compared. The results indicate that significant differences of peak loads and peak feed-in occur for the different REPC schemes. While power fees can drastically reduce peaks, a time variable schema might induce higher peak loads compared to solely energy fee based schemas. Policy makers should hence take careful consideration when designing the regulatory framework of LEMs to steer the system operation to a grid-friendly manner.

3. Does the LEM produce price signals which financially incentivize the participation of prosumers? How does forecast uncertainty affect the benefit of participation of prosumers?

The simulative evaluation showed that the market model is able to generate temporal, spatial and asset-specific prices signals. Depending on the grid type and its load-generation ratio, participants with generation assets show higher benefits in the urban, load dominated grids whereas consumers show a higher benefit in generation and flexibility dominated grids (rural and semiurban). An asset-specific analysis of participation benefits reveals that demand assets (EVs, HPs, inflexible loads) show similar average benefits if flexibility to reduce peaks is not additionally incentivized. EVs charging at work benefit from excess PV and low prices during midday, while HPs and EVs charging at home compete for storage discharging capacity during nighttime.
The analysis of the impact of load forecast uncertainty shows that introducing penalty payments for over- or under-consumptions reduces achievable participant benefits drastically and might make a participation uneconomical. An analysis of the forecast errors of participants in the field-test confirmed the ranges of day-ahead forecast errors found in the literature (30 ... 130 % MAPE) and revealed that additional uncertainties introduced by EV charging (330 % MAPE for a single EV) might further significantly increase forecast errors.

7.2. Outlook

Several limitations of the study were identified, which should be addressed in future research.

As demonstrated in the simulative experiments and the field-tests, forecast uncertainty might be a major concern for the implementation of LEMs. This Thesis did not include an analysis of potential measures to reduce the impact of forecast uncertainty such as an intraday market or the aggregation of participants, which could be an interesting future research direction. As shown in [174], optimal aggregation of participant load profiles can significantly reduce forecasting errors and the resulting negative effects.

Macroecomic aspects, e.g., considering the impact of an implementation of a trans-regional energy system with multiple LEMs or the impact of LEMs on the wholesale energy market were not studied in this Thesis. First research in this direction by Schmitt et al. [180] show promising results using a framework to model a pan-European energy system including LEMs. Additional aspects to investigate might be the exploitation of market power by participants at the LEM and measures to avoid market manipulation. Further aspects that requires detailed attention are distributional effects introduced with the adaption of LEMs. Depending on the market design and changes to the regulatory framework, regions or individual customers might benefit to the costs of other regions

or customers [181]. Future research should focus on market designs which prevent or reduce distributional effects.

The technical scope of the model could be extended by, e.g., considering additional sources of VRE such as wind power. The usage of EVs as grid storages (Vehicle-to-Grid) might be another source of flexibility to reduce load and feed-in peaks. Additionally, results of the operation of the energy system through the LEM could be postprocessed in a power flow simulation for a detailed assessment of impacts on the distribution grid. First results [182] indicate that the proposed market matching algorithm is capable of not only reducing power peaks but also mitigating voltage violations at critical busses in the distribution grid. In a further step, power flow equations could be integrated into the market matching problem as for example demonstrated by Guerrero et al. [183].

Regarding the financial incentivation of participation at a LEM, future work should focus on determining the minimal benefit required to make a participation economically viable. This analysis should focus on the costs for hardware like edge devices or smart meters, engineering, commissioning and the operation of the market infrastructure which are not analyzed in this Thesis.

In the introduction of this Thesis research by Schweppe et al. [12], [13] was cited who proposed direct engagement of end-customers in the energy market already in the 1980s. However, almost 40 years later the direct participation of end-customers in the energy market is still not achieved. This Thesis demonstrated that such engagement can technically be realized through LEMs including substantial benefits not only for participants but also for the grid integration of renewables and flexible loads. Regulatory boundaries seem to be major hurdle to overcome for a widespread implementation of end-customer engagement in energy markets. Nevertheless, similar concepts like renewable energy communities, which are closer to regulatory implementation or are already regulated, e.g., in Austria, seem to be a promising future research field with analogous effects to LEMs as for example demonstrated by Sudhoff et al. [184].

Bibliography

[1] International Renewable Energy Agency (IRENA), “Renewable capacity statistics 2021”, International Renewable Energy Agency (IRENA), Tech. Rep., 2021.

[2] International Renewable Energy Agency (IRENA), “Renewable Power Generation Costs in 2019”, International Renewable Energy Agency (IRENA), Tech. Rep., 2020.

[3] Bundesverband der Energie- und Wasserwirtschaft e.V. (BDEW), “Stromerzeugung aus Erneuerbaren Energien: Entwicklung des Anlagenparks”, BDEW, Tech. Rep., 2020.

[4] "*Erneuerbare-Energien-Gesetz vom 21. Juli 2014 (BGBl. I S. 1066), das zuletzt durch Artikel 6 des Gesetzes vom 8. August 2020 (BGBl. I S. 1818) geändert worden ist*, 2017.

[5] Deutsche Energie-Agentur GmbH (dena), “dena-Verteilnetzstudie: Ausbau- und Innovationsbedarf der Stromverteilnetze in Deutschland bis 2030.”, Tech. Rep., 2012.

[6] Bundesministerium fuer Umwelt Naturschutz und nukleare Sicherheit (BMU), “Klimaschutzprogramm 2030 der Bundesregierung zur Umsetzung des Klimaschutzplans 2050 Inhaltsverzeichnis”, Tech. Rep., 2019, pp. 1–173. [Online]. Available: https://www.bundesregierung.de/resource/blob/975226/1679914/e01d6bd855f09bf05cf7498e06d0a3ff/2019-10-09-klima-massnahmen-data.pdf?download=1.

[7] Agora Verkehrswende, Agora Energiewende, and Regulatory Assistance Project (RAP), “Verteilnetzausbau für die Energiewende - Elektromobilität im Fokus”, Tech. Rep., 2019.

[8] Bundesnetzagentur (BNetzA), “Bericht Quartalsbericht Netz- und Systemsicherheit - Gesamtes Jahr 2019”, Tech. Rep., 2019. [Online]. Available: https://www.bundesnetzagentur.de/SharedDocs/Mediathek/Berichte/2020/QuartalszahlenGesamtjahr2019.pdf.

[9] Bundesverband der Energie- und Wasserwirtschaft e.V. (BDEW), “BDEW-Strompreisanalyse Januar 2020 - Haushalt und Industrie”, 2020.

[10] Bundesnetzagentur, *Marktstammdatenregister*, 2019. [Online]. Available: https://www.marktstammdatenregister.de/MaStR (visited on 09/09/2019).

[11] MaxNoe, *plz_plot (GitHub Repository)*, 2017. [Online]. Available: https://github.com/MaxNoe (visited on 09/09/2019).

[12] F. Schweppe, M. Caramanis, R. Tabors, and R. Bohn, *Spot pricing of electricity*. Springer US, 1988. DOI: 10.1007/978-1-4613-1683-1.

[13] F. C. Schweppe, R. D. Tabors, and J. L. Kirtley, “Homeostatic control for electric power usage: A new scheme for putting the customer in the control loop would exploit microprocessors to deliver energy more efficiently”, *IEEE Spectrum*, vol. 19, no. 7, pp. 44–48, 1982, ISSN: 0018-9235. DOI: 10.1109/mspec.1982.6366943.

[14] C. Bose, C. Hoffmann, C. Kern, and M. Metzger, "New principles of operating electrical distribution networks with a high degree of decentralized generation", *20th International Conference and Exhibition on Electricity Distribution (CIRED 2009)*, pp. 1 –4, Jul. 2009. DOI: 10.1049/cp.2009.1019.

[15] Y. Parag and B. K. Sovacool, "Electricity market design for the prosumer era", *Nature Energy*, vol. 1, no. 4, p. 16 032, 2016, ISSN: 2058-7546. DOI: 10.1038/nenergy.2016.32. [Online]. Available: http://www.nature.com/articles/nenergy201632.

[16] P. Pinson, T. Baroche, F. Moret, T. Sousa, E. Sorin, and S. You, "The Emergence of Consumer-centric Electricity Markets", *Distribution & Utilization*, vol. 34, no. 12, pp. 27–31, 2017. [Online]. Available: http://pierrepinson.com/docs/pinsonetal17consumercentric.pdf.

[17] F. Lezama, J. Soares, P. Hernandez-Leal, M. Kaisers, T. Pinto, and Z. M. Almeida do Vale, "Local Energy Markets: Paving the Path Towards Fully Transactive Energy Systems", *IEEE Transactions on Power Systems*, vol. 8950, no. c, pp. 1–8, 2018, ISSN: 08858950. DOI: 10.1109/TPWRS.2018.2833959.

[18] F. Tounquet and C. Alaton, *Benchmarking smart metering deployment in EU*. 2019, ISBN: 9789276172956. DOI: 10.2833/492070. [Online]. Available: https://eur-lex.europa.eu/legal-content/EN/TXT/?qid=1403084595595{\&}uri=COM:2014:356:FIN.

[19] European Comission - Directorate-General for Energy, *Clean energy for all Europeans*. Publications Office, 2019, ISBN: 978-92-79-99835-5. DOI: doi/10.2833/9937.

[20] S. Schreck, S. Thiem, A. Amthor, M. Metzger, and S. Niessen, "Activating current and future flexibility potential in the distribution grid through local energy markets", in *CIRED 2020 Berlin Workshop (CIRED 2020)*, 2020, pp. 606–609. DOI: 10.1049/oap-cired.2021.0133.

[21] S. Schreck, S. Thiem, A. Amthor, M. Metzger, and S. Niessen, "Analyzing potential schemes for regulated electricity price components in local energy markets", in *2020 17th International Conference on the European Energy Market (EEM)*, IEEE, 2020, pp. 1–6, ISBN: 9781728169194. DOI: 10.1109/EEM49802.2020.9221959.

[22] S. Schreck, I. Prieur De La Comble, S. Thiem, and S. Niessen, "A Methodological Framework to support Load Forecast Error Assessment in Local Energy Markets", *IEEE Transactions on Smart Grid*, vol. 11, no. 4, pp. 3212–3220, 2020, ISSN: 19493061. DOI: 10.1109/TSG.2020.2971339.

[23] S. Schreck, R. Sudhoff, S. Thiem, and S. Niessen, "On the Importance of Grid Tariff Designs in Local Energy Markets", *Energies*, vol. 15, no. 17, 2022, ISSN: 1996-1073. DOI: 10.3390/en15176209. [Online]. Available: https://www.mdpi.com/1996-1073/15/17/6209.

[24] Pebbles-Consortium, *Pebbles project*, https://pebbles-projekt.de/en/. [Accessed: 2018-10-13]. [Online]. Available: https://pebbles-projekt.de/en/.[Accessed:2018-10-13].

[25] J. Büchner, J. Katzfey, O. Flörcken, A. Moser, H. Schuster, S. Dierkes, T. van Leeuwen, L. Verheggen, M. Uslar, and M. van Amelsvoort, "Moderne Verteilernetze für Deutschland (Verteilernetzstudie)", *Abschlussbericht Forschungsprojekt Nr. 44/12*, no. 44, p. 209, 2014.

[26] G. Bundesnetzagentur für Elektrizität and P. u. E. Telekommunikation, "Monitoringbericht 2019: Monitoringbericht § 63 Abs. 3 i. V. m. § 35 EnWG und§48Abs.3i.V.m.§53Abs.3GWB", 2020. [Online]. Available: https://www.bundesnetzagentur.de/SharedDocs/Mediathek/Berichte/2019/MonitoringberichtEnergie2019.pdf.

[27] BDEW, "Redispatch in Deutschland - Auswertung der Transparenzdaten April 2013 bis einschließlich März 2020", Tech. Rep. April 2013, 2020.

[28] "Voltage characteristics of electricity supplied by public distribution networks; German version EN 50160:2010", DIN, Tech. Rep. DOI: https://dx.doi.org/10.31030/1737409.

[29] G. Kerber, "Aufnahmefähigkeit von Niederspannungsverteilnetzen für die Einspeisung aus Photovoltaikkleinanlagen", Ph.D. dissertation, Technische Universität München, 2011.

[30] A. Probst, "Auswirkungen von Elektromobilität auf Energieversorungsnetze analysiert auf Basis probabilistischer Netzplanung", Ph.D. dissertation, Universität Stuttgart, 2014.

[31] M. Nour, J. P. Chaves-Ávila, G. Magdy, and Á. Sánchez-Miralles, "Review of positive and negative impacts of electric vehicles charging on electric power systems", *Energies*, vol. 13, no. 18, 2020, ISSN: 19961073. DOI: 10.3390/en13184675.

[32] H.-J. Barth, "Energie- und Klimaschutz-Bericht der Gemeinde Wildpoldsried", *European Energy Award Program*, 2018.

[33] Bundesnetzagentur, "Bedarfsermittlung 2019-2030 - Bestätigung Netzentwicklungsplan Strom", Tech. Rep., 2019. [Online]. Available: https://www.netzentwicklungsplan.de/sites/default/files/paragraphs-files/NEP2019-2030Bestaetigung.pdf.

[34] *EPEX SPOT*. [Online]. Available: https://www.epexspot.com/en (visited on 11/02/2020).

[35] European Commission and Directorate-General for Energy and A. Moser, N. Bracht, and A. Maaz, "Simulating electricity market bidding and price caps in the european power markets : S18 report", Tech. Rep., 2019. DOI: doi/10.2833/252345.

[36] S. Schulte, F. Arnold, and D. Schlund, *EWI Merit-Order Tool 2019*, 2019. [Online]. Available: https://www.ewi.uni-koeln.de/de/news/ewi-merit-order-tool-2019/ (visited on 10/29/2020).

[37] European Network of Transmission System Operators for Electricity (ENTSO-E), *ENTSO-E Transparency Platform*. [Online]. Available: https://transparency.entsoe.eu/ (visited on 10/29/2020).

[38] A. Knaut and S. Paulus, "Hourly price elasticity pattern of electricity demand in the German day-ahead market", *EWI Working Paper, No. 16/07„ Institute of Energy Economics at the University of Cologne (EWI)*, 2016.

[39] L. Hirth, "The market value of variable renewables. The effect of solar wind power variability on their relative price", *Energy Economics*, vol. 38, no. 2013, pp. 218–236, 2013, ISSN: 01409883. DOI: 10.1016/j.eneco.2013.02.004. [Online]. Available: http://dx.doi.org/10.1016/j.eneco.2013.02.004.

[40] J. C. Ketterer, "The impact of wind power generation on the electricity price in Germany", *Energy Economics*, vol. 44, pp. 270–280, 2014, ISSN: 01409883. DOI: 10.1016/j.eneco.2014.04.003. [Online]. Available: http://dx.doi.org/10.1016/j.eneco.2014.04.003.

[41] E. Hillberg, A. A. Zegers, B. Herndler, S. Wong, J. Pompee, J.-Y. Bourmaud, S. Lehnhoff, G. Migliavacca, K. Uhlen, I. Oleinikova, H. Pihl, M. Norström, M. Persson, J. Rossi, and G. Beccuti, *Flexibility needs in the future power system*. 2019. DOI: 10.13140/RG.2.2.22580.71047.

[42] M. Caramanis, R. Bohn, and F. Schweppe, "Optimal Spot Pricing: Practice and Theory", *IEEE Transactions on Power Apparatus and Systems*, vol. 75, no. 9, pp. 3234–3245, 1982.

[43] F. Hein, F. Peter, and P. Graichen, "The German Power Market: State of Affairs in 2019", AGORA Energiewende, Tech. Rep., 2020.

[44] Agora Energiewende, “Neue Preismodelle für Energie. Grundlagen einer Reform der Entgelte, Steuern, Abgaben und Umlagen auf Strom und fossile Energieträger. Hintergrund.”, Agora Energiewende, Berlin, Tech. Rep., 2017.

[45] A. Liebe, S. Schmitt, and M. Wissner, “Quantitative Auswirkungen variabler Stromtarife auf die Stromkosten von Haushalten”, WIK Wissenschaftliches Institut für Infrastruktur und Kommunikationsdienste GmbH, Tech. Rep. November, 2015. [Online]. Available: https://www.vzbv.de/sites/default/files/downloads/Auswirkungen-variabler-Stromtarife-auf-Stromkosten-Haushalte-WIK-vzbv-November-2015.pdf.

[46] BDEW Bundesverband der Energie- und Wasserwirtschaft e.V., “Smart Grid Traffic Light Concept”, BDEW, Tech. Rep. [Online]. Available: https://www.bdew.de/media/documents/Stn20150310Smart-Grids-Traffic-Light-Conceptenglish.pdf.

[47] International Renewable Energy Agency (IRENA), “Time-of-Use Tariffs innovation landscape brief”, International Renewable Energy Agency, Abu Dhabi, Tech. Rep., 2019, pp. 1–18.

[48] J. Freier, M. Arnold, and J. Hesselbach, “Introduction of an approach to develop dynamic electricity prices for residential customers”, in *2019 16th International Conference on the European Energy Market (EEM)*, Ljubljana, Slovenia, 2019, pp. 1–6, ISBN: 9781728112572. DOI: 10.1109/eem.2019.8916431.

[49] J. Andruszkiewicz, J. Lorenc, and A. Weychan, “Demand price elasticity of residential electricity consumers with zonal tariff settlement based on their load profiles”, *Energies*, vol. 12, no. 22, pp. 1–22, 2019, ISSN: 19961073. DOI: 10.3390/en12224317.

[50] L. Conway and D. Prentice, “How much do households respond to electricity prices? evidence from australia and abroad”, *Economic Papers: A journal of applied economics and policy*, vol. 39, no. 3, pp. 290–311, 2020. DOI: https://doi.org/10.1111/1759-3441.12284. eprint: https://onlinelibrary.wiley.com/doi/pdf/10.1111/1759-3441.12284. [Online]. Available: https://onlinelibrary.wiley.com/doi/abs/10.1111/1759-3441.12284.

[51] A. Johannes, “Rechtsfragen zu Zugang und Nutzung von Stromverteilnetzen im Kontext der Energie und Verkehrswende”, in *Kommunales Infrastruktur-Management*, 2019.

[52] *Gesetz für den Ausbau erneuerbarer Energien (Erneuerbare-Energien-Gesetz - EEG 2017) § 9 Technische Vorgaben*. [Online]. Available: https://www.gesetze-im-internet.de/eeg2014l.

[53] Stromnetz Berlin GmbH, “Informationsblatt für die Leistungsbegrenzung auf 70% bei PV-Erzeugungsanlagen < 30 kWp”, Stromnetz Berlin GmbH, Tech. Rep. November, 2017.

[54] Kreditanstalt für Wiederaufbau (KfW, “Merkblatt KfW-Programm Erneuerbare Energien”, KfW, Tech. Rep., 2018, pp. 1–8.

[55] J. Weniger, J. Bergner, T. Tjaden, and V. Quaschning, “Effekte der 50 % Einspeisebegrenzung des KfW-Förderprogramms für Photovoltaik-Speichersysteme”, Hochschule für Technik und Wirtschaft Berlin, Tech. Rep., 2016. [Online]. Available: http://pvspeicher.htw-berlin.de.

[56] L. Hirth, I. Schlecht, C. Maurer, and B. Tersteegen, “Zusammenspiel von Markt und Netz im Stromsystem: Eine Systematisierung und Bewertung von Ausgestaltungen des Strommarkts”, BMWi, Tech. Rep. November, 2018.

[57] C. Maurer, C. Zimmer, and L. Hirth, “Nodale und zonale Strompreissysteme im Vergleich - Bericht für das Bundesministerium für Wirtschaft und Energie”, Tech. Rep., 2018, pp. 1–34.

[58] D. Hladik, C. Fraunholz, and R. Kunze, “Zwei Preiszonen für Deutschland. Eine modellbasierte Analyse der langfristigen Auswirkungen”, *12. Fachtagung Optimierung in der Energiewirtschaft: Würzburg, November 2017*, pp. 145–157, 2017. [Online]. Available: https://publikationen.bibliothek.kit.edu/1000076451.

[59] C. Brandstätt, G. Brunekreeft, and N. Friedrichsen, “Locational signals to reduce network investments in smart distribution grids: What works and what not?”, *Utilities Policy*, vol. 19, no. 4, pp. 244–254, 2011, ISSN: 09571787. DOI: 10.1016/j.jup.2011.07.001. [Online]. Available: http://dx.doi.org/10.1016/j.jup.2011.07.001.

[60] M. Ambrosius, J. Egerer, V. Grimm, and A. H. van der Weijde, “Risk aversion in multilevel electricity market models with different congestion pricing regimes”, *Energy Economics*, vol. 105, p. 105 701, 2022, ISSN: 0140-9883. DOI: https://doi.org/10.1016/j.eneco.2021.105701. [Online]. Available: https://www.sciencedirect.com/science/article/pii/S0140988321005521.

[61] K. Trepper, M. Bucksteeg, and C. Weber, “Market splitting in Germany - New evidence from a three-stage numerical model of Europe”, *Energy Policy*, vol. 87, no. 2015, pp. 199–215, 2015, ISSN: 03014215. DOI: 10.1016/j.enpol.2015.08.016. [Online]. Available: http://dx.doi.org/10.1016/j.enpol.2015.08.016.

[62] M. Vogel, D. Bauknecht, and E.V., Öko-Institut, “Flexibilität für das Netz Flexibilität für das Netz Vergleich und Bewertung von Koordinationsmechanismen für den netzdienlichen Einsatz von Flexibilität”, Öko-Institut, Freiburg, Tech. Rep., 2020.

[63] S. Niessen, S. Paulus, D. Strunski, and P. Vassilopoulos, “Taking markets to all levels: Valuing flexibility to achieve market-based sector integration”, EPEX SPOT SE, SIEMENS CT, Tech. Rep., 2019. [Online]. Available: https://www.epexspot.com/en/news/taking-markets-all-levels-valuing-flexibility-achieve-market-based-sector-integration.

[64] M. Neukirch, “Protests against german electricity grid extension as a new social movement? a journey into the areas of conflict”, *Energy, Sustainability and Society*, vol. 6, no. 1, 2016, ISSN: 2192-0567. DOI: 10.1186/s13705-016-0069-9. [Online]. Available: https://doi.org/10.1186/s13705-016-0069-9.

[65] M. Neukirch, “Die Dynamik des Konflikts um den Stromtrassenbau: Stabilität, Wandel oder Stagnation?”, *SOI Discussion Paper*, vol. No. 2017-0, no. Universität Stuttgart, Institut für Sozialwissenschaften, Abteilung für Organisations- und Innovationssoziologie, Stuttgart, 2017.

[66] *Stromsteuer-Durchführungsverordnung vom 31. Mai 2000 (BGBl. I S. 794), die zuletzt durch Artikel 3 der Verordnung vom 14. August 2020 (BGBl. I S. 1960) geändert worden ist*.

[67] L. Gruber, S. Wogrin, and C. Tischler, “How to energiegemeinschaft”, Graz, Tech. Rep., 2022, Beitrag in einem Konferenzband, pp. 288–289. DOI: 10.3217/978-3-85125-915-5. [Online]. Available: https://doi.org/10.3217/978-3-85125-915-5.

[68] K. P. Kairies, D. Magnor, and D. U. Sauer, “Scientific measuring and evaluation program for photovoltaic battery systems(WMEP PV-speicher)”, *Energy Procedia*, vol. 73, pp. 200–207, 2015, ISSN: 18766102. DOI: 10.1016/j.egypro.2015.07.672. [Online]. Available: http://dx.doi.org/10.1016/j.egypro.2015.07.672.

[69] J. Hoppmann, J. Volland, T. S. Schmidt, and V. H. Hoffmann, "The economic viability of battery storage for residential solar photovoltaic systems - A review and a simulation model", *Renewable and Sustainable Energy Reviews*, vol. 39, pp. 1101–1118, 2014, ISSN: 13640321. DOI: 10.1016/j.rser.2014.07.068. [Online]. Available: http://dx.doi.org/10.1016/j.rser.2014.07.068.

[70] M. Klein, A. Ziade, and L. de Vries, "Aligning prosumers with the electricity wholesale market – the impact of time-varying price signals and fixed network charges on solar self-consumption", *Energy Policy*, vol. 134, p. 110 901, 2019, ISSN: 0301-4215. DOI: https://doi.org/10.1016/j.enpol.2019.110901. [Online]. Available: https://www.sciencedirect.com/science/article/pii/S0301421519304793.

[71] M. Resch, J. Bühler, B. Schachler, and A. Sumper, "Techno-economic assessment of flexibility options versus grid expansion in distribution grids", *IEEE Transactions on Power Systems*, vol. 36, no. 5, pp. 3830–3839, 2021. DOI: 10.1109/TPWRS.2021.3055457.

[72] M. Khorasany, Y. Mishra, and G. Ledwich, "Market framework for local energy trading: a review of potential designs and market clearing approaches", *IET Generation, Transmission & Distribution*, vol. 12, no. 22, pp. 5899–5908, 2018, ISSN: 1751-8687. DOI: 10.1049/iet-gtd.2018.5309.

[73] J. Lee and Y. Cho, "Estimation of the usage fee for peer-to-peer electricity trading platform : The case of South Korea", *Energy Policy*, vol. 136, no. October 2019, p. 111 050, 2020, ISSN: 0301-4215. DOI: 10.1016/j.enpol.2019.111050. [Online]. Available: https://doi.org/10.1016/j.enpol.2019.111050.

[74] E. Mengelkamp, P. Staudt, J. Gärttner, C. Weinhardt, and J. Huber, "Quantifying factors for participation in local electricity markets", pp. 1–5, 2018. DOI: 10.1109/EEM.2018.8469969.

[75] M. J. Fell, A. Schneiders, and D. Shipworth, "Consumer Demand for Blockchain-Enabled Peer-to-Peer Electricity Trading in the United Kingdom: An Online Survey Experiment", *Energies*, vol. 12, no. 20, p. 3913, 2019. DOI: 10.3390/en12203913.

[76] A. Immonen, J. Kiljander, and M. Aro, "Consumer viewpoint on a new kind of energy market", *Electric Power Systems Research*, vol. 180, no. April 2019, p. 106 153, 2020, ISSN: 03787796. DOI: 10.1016/j.epsr.2019.106153. [Online]. Available: https://doi.org/10.1016/j.epsr.2019.106153.

[77] J. Kazempour, "Lecture 3: Desirable properties of market-clearing mechanisms", in *Advanced Optimization and Game Theory for Energy Systems*, 2020.

[78] Y. Zhou, J. Wu, C. Long, and W. Ming, "State-of-the-Art Analysis and Perspectives for Peer-to-Peer Energy Trading", *Engineering*, vol. 6, no. 7, pp. 739–753, 2020, ISSN: 20958099. DOI: 10.1016/j.eng.2020.06.002. [Online]. Available: https://doi.org/10.1016/j.eng.2020.06.002.

[79] E. Mengelkamp, J. Gärttner, K. Rock, S. Kessler, L. Orsini, and C. Weinhardt, "Designing microgrid energy markets: A case study: The Brooklyn Microgrid", *Applied Energy*, vol. 210, pp. 870–880, 2018, ISSN: 0306-2619. DOI: 10.1016/J.APENERGY.2017.06.054. [Online]. Available: https://www.sciencedirect.com/science/article/pii/S030626191730805X.

[80] KIT, *LAMP Landau Microgrid Project*, https://im.iism.kit.edu/english/2881.php [Accessed: 2021-02-06]. [Online]. Available: https://im.iism.kit.edu/english/2881.php (visited on 02/06/2021).

[81] Andreas Zeiselmair, A. Bogensperger, S. Köppl, T. Estermann, D. Wohlschlager, and T. Müller, "ALTDORFER FLEXMARKT (ALF) KONZEPTBESCHREIBUNG, ZIELSETZUNG, FUNKTIONSWEISE UND PROZESSE DES ALTDORFER FLEXMARKTS", Forschungsstelle für Energiewirtschaft e.V., München, Tech. Rep., 2018, pp. 12–14.

[82] Power Ledger, *PowerNet - Trading of rooftop solar energy*, 2020. [Online]. Available: https://www.powerledger.io/client/american-powernet/ (visited on 01/09/2021).

[83] *Piclo. Building a smarter energy future*. [Online]. Available: https://piclo.energy/about{\#}whitepaper (visited on 01/09/2021).

[84] *P2P SmartTest*, 2020. [Online]. Available: https://www.p2psmartest-h2020.eu/ (visited on 01/09/2020).

[85] *Google scholar*. [Online]. Available: https://scholar.google.com/ (visited on 01/09/2021).

[86] S. Thiem, S. Niessen, J. Klaus, M. Metzger, and S. Schreck, "Netzdienlicher Peer-to-Peer Energiehandel durch Erschließung von Flexibilitätspotenzialen durch einen lokalen Energiemarkt", in *Energierevolution getrieben durch Blockchain*, Begleitforschung Smart Service Welt II Institut für Innovation und Technik (iit) in der VDI/VDE Innovation + Technik GmbH, 2020, ch. Netzdienli.

[87] W. Tushar, T. K. Saha, C. Yuen, D. Smith, and H. V. Poor, "Peer-to-Peer Trading in Electricity Networks: An Overview", *IEEE Transactions on Smart Grid*, vol. 3053, no. c, pp. 1–15, 2020. DOI: 10.1109/TSG.2020.2969657. arXiv: 2001.06882. [Online]. Available: http://arxiv.org/abs/2001.06882.

[88] E. Sorin, L. Bobo, and P. Pinson, "Consensus-Based Approach to Peer-to-Peer Electricity Markets with Product Differentiation", *IEEE Transactions on Power Systems*, vol. 34, no. 2, pp. 994–1004, 2019, ISSN: 08858950. DOI: 10.1109/TPWRS.2018.2872880. arXiv: 1804.03521.

[89] F. Luo, Z. Y. Dong, G. Liang, J. Murata, and Z. Xu, "A Distributed Electricity Trading System in Active Distribution Networks Based on Multi-Agent Coalition and Blockchain", *IEEE Transactions on Power Systems*, vol. 34, no. 5, pp. 4097–4108, 2019, ISSN: 15580679. DOI: 10.1109/TPWRS.2018.2876612.

[90] T. Morstyn and M. McCulloch, "Multi-Class Energy Management for Peer-to-Peer Energy Trading Driven by Prosumer Preferences", *IEEE Transactions on Power Systems*, no. May, 2018, ISSN: 08858950. DOI: 10.1109/TPWRS.2018.2834472.

[91] J. Lian, H. Ren, Y. Sun, and D. Hammerstrom, "Performance Evaluation for Transactive Energy Systems using Double-auction Market", *IEEE Transactions on Power Systems*, vol. 34, no. 5, pp. 4128–4138, 2018, ISSN: 0885-8950. DOI: 10.1109/TPWRS.2018.2875919. [Online]. Available: https://ieeexplore.ieee.org/document/8515229/.

[92] W. Tushar, C. Yuen, T. K. Saha, T. Morstyn, A. C. Chapman, M. J. E. Alam, S. Hanif, and H. V. Poor, "Peer-to-peer energy systems for connected communities: A review of recent advances and emerging challenges", *Applied Energy*, vol. 282, no. PA, p. 116 131, 2021, ISSN: 03062619. DOI: 10.1016/j.apenergy.2020.116131. [Online]. Available: https://doi.org/10.1016/j.apenergy.2020.116131.

[93] W. El-Baz, P. Tzscheutschler, and U. Wagner, "Integration of energy markets in microgrids: A double-sided auction with device-oriented bidding strategies", *Applied Energy*, vol. 241, no. January, pp. 625–639, 2019, ISSN: 03062619. DOI: 10.1016/j.apenergy.2019.02.049. [Online]. Available: https://doi.org/10.1016/j.apenergy.2019.02.049.

[94] N. Liu, X. Yu, C. Wang, C. Li, L. Ma, and J. Lei, "Energy-Sharing Model with Price-Based Demand Response for Microgrids of Peer-to-Peer Prosumers", *IEEE Transactions on Power Systems*, vol. 32, no. 5, pp. 3569–3583, 2017, ISSN: 08858950. DOI: 10.1109/TPWRS.2017.2649558.

[95] A. H. Fathima and K. Palanisamy, "Optimization in microgrids with hybrid energy systems - A review", *Renewable and Sustainable Energy Reviews*, vol. 45, pp. 431–446, 2015, ISSN: 18790690. DOI: 10.1016/j.rser.2015.01.059. [Online]. Available: http://dx.doi.org/10.1016/j.rser.2015.01.059.

[96] W. Liu, C. Liu, Y. Lin, K. Bai, and L. Ma, "Interval Multi-Objective Optimal Scheduling for Redundant Residential Microgrid With VESS", *IEEE Access*, vol. 7, pp. 87 849–87 865, 2019. DOI: 10.1109/access.2019.2923612.

[97] E. Kellerer and F. Steinke, "Scalable Economic Dispatch for Smart Distribution Networks", *IEEE Transactions on Power Systems*, vol. 30, no. 4, pp. 1739–1746, 2015, ISSN: 08858950. DOI: 10.1109/TPWRS.2014.2358375.

[98] S. Prabhakar Karthikeyan, I. Jacob Raglend, and D. Kothari, "A review on market power in deregulated electricity market", *International Journal of Electrical Power and Energy Systems*, vol. 48, pp. 139–147, 2013, ISSN: 0142-0615. DOI: https://doi.org/10.1016/j.ijepes.2012.11.024. [Online]. Available: https://www.sciencedirect.com/science/article/pii/S0142061512006771.

[99] S. Chakraborty, T. Baarslag, and M. Kaisers, "Automated peer-to-peer negotiation for energy contract settlements in residential cooperatives", *Applied Energy*, vol. 259, no. November, p. 114 173, 2020, ISSN: 03062619. DOI: 10.1016/j.apenergy.2019.114173. [Online]. Available: https://doi.org/10.1016/j.apenergy.2019.114173.

[100] J. Guerrero, A. C. Chapman, and G. Verbic, "Decentralized P2P Energy Trading under Network Constraints in a Low-Voltage Network", *IEEE Transactions on Smart Grid*, vol. 10, no. 5, pp. 5163–5173, 2018, ISSN: 19493053. DOI: 10.1109/TSG.2018.2878445.

[101] R. Ghorani, M. Fotuhi-Firuzabad, and M. Moeini-Aghtaie, "Optimal Bidding Strategy of Transactive Agents in Local Energy Markets", *IEEE Transactions on Smart Grid*, vol. 10, no. 5, pp. 5152–5162, 2018, ISSN: 19493061. DOI: 10.1109/TSG.2018.2878024. [Online]. Available: https://ieeexplore.ieee.org/document/8509123/.

[102] F Moret, T Baroche, E Sorin, and P Pinson, "Negotiation Algorithms for Peer-to-Peer Electricity Markets: Computational Properties", *2018 Power Systems Computation Conference (PSCC)*, pp. 1–7, 2018.

[103] E. Bullich-Massagué, M. Aragüés-Peñalba, P. Olivella-Rosell, P. Lloret-Gallego, J. A. Vidal-Clos, and A. Sumper, "Architecture definition and operation testing of local electricity markets. the EMPOWER project", *Proceedings - 2017 International Conference on Modern Power Systems, MPS 2017*, 2017. DOI: 10.1109/MPS.2017.7974447.

[104] P. Olivella-Rosell, E. Bullich-Massagué, M. Aragüés-Peñalba, A. Sumper, S. Ø. Ottesen, J. A. Vidal-Clos, and R. Villafáfila-Robles, "Optimization problem for meeting distribution system operator requests in local flexibility markets with distributed energy resources", *Applied Energy*, vol. 210, no. May 2017, pp. 881–895, 2018, ISSN: 03062619. DOI: 10.1016/j.apenergy.2017.08.136.

[105] LO3, *Brooklyn Microgrid*, https://www.brooklyn.energy/. [Accessed: 2018-10-11], 2018. [Online]. Available: https://www.brooklyn.energy/.[Accessed:2018-10-11] (visited on 10/11/2018).

[106] L. Ableitner, A. Meeuw, S. Schopfer, V. Tiefenbeck, F. Wortmann, and A. Wörner, "Quartierstrom – Implementation of a real world prosumer centric local energy market in Walenstadt, Switzerland", 2019. arXiv: 1905.07242. [Online]. Available: http://arxiv.org/abs/1905.07242.

[107] B. Richter, E. Mengelkamp, and C. Weinhardt, "Vote for your energy: A market mechanism for local energy markets based on the consumers' preferences", *International Conference on the European Energy Market, EEM*, vol. 2019-Septe, pp. 1–6, 2019, ISSN: 21654093. DOI: 10.1109/EEM.2019.8916544.

[108] R. Ghorani, M. Fotuhi-Firuzabad, and M. Moeini-Aghtaie, "Main Challenges of Implementing Penalty Mechanisms in Transactive Electricity Markets", *IEEE Transactions on Power Systems*, vol. 34, no. 5, pp. 3954–3956, 2019, ISSN: 15580679. DOI: 10.1109/TPWRS.2019.2908587.

[109] K. Worthmann, C. M. Kellett, L. Grüne, and S. R. Weller, "Distributed control of residential energy systems using a market maker", *IFAC Proceedings Volumes (IFAC-PapersOnline)*, vol. 19, pp. 11 641–11 646, 2014, ISSN: 14746670. DOI: 10.3182/20140824-6-za-1003.01785.

[110] B. Stephen, X. Tang, P. R. Harvey, S. Galloway, and K. I. Jennett, "Incorporating practice theory in sub-profile models for short term aggregated residential load forecasting", *IEEE Transactions on Smart Grid*, vol. 8, no. 4, pp. 1591–1598, 2017, ISSN: 19493053. DOI: 10.1109/TSG.2015.2493205.

[111] A. Veit, C. Goebel, R. Tidke, C. Doblander, and H. A. Jacobsen, "Household electricity demand forecasting - Benchmarking state-of-the-art methods", in *e-Energy 2014 - Proceedings of the 5th ACM International Conference on Future Energy Systems*, 2014, pp. 233–234, ISBN: 9781450328197. DOI: 10.1145/2602044.2602082. arXiv: 1404.0200.

[112] F. Rodrigues, C. Cardeira, and J. M. Calado, "The daily and hourly energy consumption and load forecasting using artificial neural network method: A case study using a set of 93 households in Portugal", in *Energy Procedia*, vol. 62, Elsevier B.V., 2014, pp. 220–229. DOI: 10.1016/j.egypro.2014.12.383. [Online]. Available: http://dx.doi.org/10.1016/j.egypro.2014.12.383.

[113] Y. Iwafune, Y. Yagita, T. Ikegami, and K. Ogimoto, "Short-term forecasting of residential building load for distributed energy management", in *ENERGYCON 2014 - IEEE International Energy Conference*, IEEE, 2014, pp. 1197–1204, ISBN: 9781479924493. DOI: 10.1109/ENERGYCON.2014.6850575.

[114] S. Humeau, T. K. Wijaya, M. Vasirani, and K. Aberer, "Electricity load forecasting for residential customers: Exploiting aggregation and correlation between households", in *2013 Sustainable Internet and ICT for Sustainability, SustainIT 2013*, IEEE, 2013, pp. 1–6, ISBN: 9783901882562. DOI: 10.1109/SustainIT.2013.6685208.

[115] X. Jin, Q. Wu, and H. Jia, "Local flexibility markets: Literature review on concepts, models and clearing methods", *Applied Energy*, vol. 261, no. January, p. 114 387, 2020, ISSN: 03062619. DOI: 10.1016/j.apenergy.2019.114387. [Online]. Available: https://doi.org/10.1016/j.apenergy.2019.114387.

[116] E. Sorin, L. Bobo, and P. Pinson, "Consensus-based approach to peer-to-peer electricity markets with product differentiation", vol. X, no. X, pp. 1–10, 2018. arXiv: 1804.03521. [Online]. Available: http://arxiv.org/abs/1804.03521.

[117] J. Guerrero, A. C. Chapman, and G. Verbič, "Local energy markets in LV networks: Community based and decentralized P2P approaches", *2019 IEEE Milan PowerTech, PowerTech 2019*, pp. 1–6, 2019. DOI: 10.1109/PTC.2019.8810588.

[118] B. P. Majumder, M. N. Faqiry, S. Das, and A. Pahwa, "An efficient iterative double auction for energy trading in microgrids", *IEEE Symposium on Computational Intelligence Applications in Smart Grid, CIASG*, vol. 2015-Janua, no. January, 2015, ISSN: 23267690. DOI: 10.1109/CIASG.2014.7011556.

[119] W. Tushar, B. Chai, C. Yuen, S. Huang, D. B. Smith, H. V. Poor, and Z. Yang, "Energy Storage Sharing in Smart Grid: A Modified Auction-Based Approach", *IEEE Transactions on Smart Grid*, vol. 7, no. 3, pp. 1462–1475, 2016, ISSN: 19493053. DOI: 10.1109/TSG.2015.2512267. arXiv: 1512.07700.

[120] W. Tushar, C. Yuen, H. Mohsenian-Rad, T. Saha, H. V. Poor, and K. L. Wood, "Transforming energy networks via peer-to-peer energy trading: The potential of game-theoretic approaches", *IEEE Signal Processing Magazine*, vol. 35, no. 4, pp. 90–111, 2018, ISSN: 10535888. DOI: 10.1109/MSP.2018.2818327. arXiv: 1804.00962.

[121] A. Paudel, K. Chaudhari, C. Long, and H. B. Gooi, "Peer-to-peer energy trading in a prosumer-based community microgrid: A game-theoretic model", *IEEE Transactions on Industrial Electronics*, vol. 66, no. 8, pp. 6087–6097, 2019, ISSN: 02780046. DOI: 10.1109/TIE.2018.2874578.

[122] C. Zhang, J. Wu, Y. Zhou, M. Cheng, and C. Long, "Peer-to-Peer energy trading in a Microgrid", *Applied Energy*, vol. 220, no. February, pp. 1–12, 2018, ISSN: 03062619. DOI: 10.1016/j.apenergy.2018.03.010. [Online]. Available: https://doi.org/10.1016/j.apenergy.2018.03.010.

[123] I. Atzeni, L. G. Ordóñez, G. Scutari, D. P. Palomar, and J. R. Fonollosa, "Noncooperative and cooperative optimization of distributed energy generation and storage in the demand-side of the smart grid", *IEEE Transactions on Signal Processing*, vol. 61, no. 10, pp. 2454–2472, 2013, ISSN: 1053587X. DOI: 10.1109/TSP.2013.2248002.

[124] A. Chis and V. Koivunen, "Coalitional game-based cost optimization of energy portfolio in smart grid communities", *IEEE Transactions on Smart Grid*, vol. 10, no. 2, pp. 1960–1970, 2019, ISSN: 19493053. DOI: 10.1109/TSG.2017.2784902. arXiv: 1705.04118.

[125] W. Saad, Z. Han, H. V. Poor, and T. Başar, "Game-theoretic methods for the smart grid: An overview of microgrid systems, demand-side management, and smart grid communications", *IEEE Signal Processing Magazine*, vol. 29, no. 5, pp. 86–105, 2012, ISSN: 10535888. DOI: 10.1109/MSP.2012.2186410.

[126] G. Tsaousoglou, P. Pinson, and N. G. Paterakis, "Transactive Energy for Flexible Prosumers Using Algorithmic Game Theory", *IEEE Transactions on Sustainable Energy*, vol. 3029, no. 754462, pp. 1–1, 2021, ISSN: 1949-3029. DOI: 10.1109/tste.2021.3055764.

[127] G. Li, J. Shi, and X. Qu, "Modeling methods for GenCo bidding strategy optimization in the liberalized electricity spot market-A state-of-the-art review", *Energy*, vol. 36, no. 8, pp. 4686–4700, 2011, ISSN: 03605442. DOI: 10.1016/j.energy.2011.06.015. [Online]. Available: http://dx.doi.org/10.1016/j.energy.2011.06.015.

[128] P. Ringler, D. Keles, and W. Fichtner, "Agent-based modelling and simulation of smart electricity grids and markets - A literature review", *Renewable and Sustainable Energy Reviews*, vol. 57, pp. 205–215, 2016, ISSN: 18790690. DOI: 10.1016/j.rser.2015.12.169. [Online]. Available: http://dx.doi.org/10.1016/j.rser.2015.12.169.

[129] J. G. Kim and B. Lee, "Automatic P2P energy trading model based on reinforcement learning using long short-term delayed reward", *Energies*, vol. 13, no. 20, 2020, ISSN: 19961073. DOI: 10.3390/en13205359.

[130] C. Schmitt, K. Samaan, H. Schwaeppe, and A. Moser, "Bottom-up Modeling of Local Energy Markets within a Pan-European Wholesale Electricity Market Model", pp. 631–636, 2020. DOI: 10.1109/ENERGYCon48941.2020.9236612.

[131] L. Liu, "Einfluss der privaten Elektrofahrzeuge auf Mittel- und Niederspannungsnetze", Ph.D. dissertation, Technische Universität Darmstadt, 2018, p. 181.

[132] G. Schlömer, "Planung von optimierten Niederspannungsnetzen", Ph.D. dissertation, Gottfried Wilhelm Leibniz Universität Hannover, 2017. [Online]. Available: https://edocs.tib.eu/files/e01dh17/1007490438.pdf.

[133] Bundesnetzagentur, "Bericht zum Zustand und Ausbau der Verteilernetze 2020. Berichte der Verteilernetzbetreiber gem. § 14 Abs. 1a und 1b", Bundesnetzagentur, Bonn, Tech. Rep., 2020, pp. 1–44.

[134] K. K. Cao, K. Von Krbek, M. Wetzel, F. Cebulla, and S. Schreck, "Classification and evaluation of concepts for improving the performance of applied energy system optimization models", *Energies*, vol. 12, no. 24, 2019, ISSN: 19961073. DOI: 10.3390/en12244656.

[135] A. D. Mills and R. H. Wiser, "Implications of geographic diversity for short-term variability and predictability of solar power", *IEEE Power and Energy Society General Meeting*, pp. 1–10, 2011, ISSN: 19449925. DOI: 10.1109/PES.2011.6039888.

[136] R. Perez, S. Kivalov, J. Schlemmer, K. Hemker, and T. E. Hoff, "Short-term irradiance variability: Preliminary estimation of station pair correlation as a function of distance", *Solar Energy*, vol. 86, no. 8, pp. 2170–2176, 2012, ISSN: 0038092X. DOI: 10.1016/j.solener.2012.02.027. [Online]. Available: http://dx.doi.org/10.1016/j.solener.2012.02.027.

[137] B. Yildiz, J. I. Bilbao, J. Dore, and A. B. Sproul, "Short-term forecasting of individual household electricity loads with investigating impact of data resolution and forecast horizon", *Renewable Energy and Environmental Sustainability*, vol. 3, p. 3, 2018. DOI: 10.1051/rees/2018003.

[138] BMVI, *Mobilität in Tabellen, dataset*. [Online]. Available: https://www.mobilitaet-in-tabellen.de/mit/ (visited on 03/04/2020).

[139] A. Schmidt, "Flottenbetrieb von elektrischen und autonomen Serviceagenten im städtischen Personennahverkehr", Dissertation, Karlsruher Institut für Technologie, 2017, ISBN: 978-3-7315-0633-1. DOI: 10.5445/ksp/1000065890. [Online]. Available: https://publikationen.bibliothek.kit.edu/1000065890.

[140] S. Meinecke, D. Sarajlić, S. R. Drauz, A. Klettke, L.-P. Lauven, C. Rehtanz, A. Moser, and M. Braun, "SimBench - Dokumentation Dokumentationsversion DE-1.0.1", Universität Kassel, Fraunhofer IEEE, RWTH Aachen and Technische Universität Dortmund, Tech. Rep., 2021.

[141] S. Meinecke, D. Sarajlić, S. R. Drauz, A. Klettke, L. P. Lauven, C. Rehtanz, A. Moser, and M. Braun, "SimBench-A benchmark dataset of electric power systems to compare innovative solutions based on power flow analysis", *Energies*, vol. 13, no. 12, 2020, ISSN: 19961073. DOI: 10.3390/en13123290.

[142] Bundesnetzagentur, "Genehmigung des Szenariorahmens 2021-2035", Bundesnetzagentur, Bonn, Tech. Rep., 2020.

[143] Kraftfahrt-Bundesamt, "Der Fahrzeugbestand im Überblick am 1. Januar 2020 gegenüber dem 1. Januar 2019", Kraftfahrt-Bundesamt, Tech. Rep., 2020, p. 2833. [Online]. Available: https://www.kba.de/DE/Statistik/Fahrzeuge/Bestand/Jahresbilanz/.

[144] C. Nobis and T. Kuhnimhof, "Mobilität in Deutschland MiD Ergebnisbericht. Studie von infas, DLR, IVT und infas 360 im Auftrag des Bundesministers für Verkehr und digitale Infrastruktur (FE-Nr. 70.904/15)", p. 135, 2018. [Online]. Available: http://www.mobilitaet-in-deutschland.de/.

[145] Fraunhofer IWES/IBP, "Wärmewende 2030. Schlüsseltechnologien zur Erreichung der mittel- und langfristigen Klimaschutzziele im Gebäudesektor. Studie im Auftrag von Agora Energiewende", no. 107/01, 2017.

[146] ADAC, *Elektroautos im Test: So hoch ist der Stromverbrauch*. [Online]. Available: https://www.adac.de/rund-ums-fahrzeug/tests/elektromobilitaet/stromverbrauch-elektroautos-adac-test/ (visited on 05/11/2022).

[147] Kraftfahrt-Bundesamt (KBA), "Verkehr in Kilometern - Inländerfahrleistung. Entwicklungen der Fahrleistungen nach Fahrzeugarten seit 2015", pp. 1–9, 2020. [Online]. Available: https://www.kba.de/DE/Statistik/Kraftverkehr/VerkehrKilometer/vkinlaenderfahrleistung/vkinlaenderfahrleistunginhalt.html?nn=2351604.

[148] BDEW, *Durchschnittlicher Haushaltsstromverbrauch*. [Online]. Available: https://www.bdew.de/service/daten-und-grafiken/durchschnittlicher-haushaltsstromverbrauch/ (visited on 05/11/2022).

[149] U. Bigalke, A. Armbruster, F. Lukas, O. Krieger, C. Schuch, and J. Kunde, "Statistiken und Analysen zur Energieeffizienz im Gebäudebestand", *dena-Gebäudereport Kompakt 2016*, pp. 1–48, 2016. [Online]. Available: https://www.powerfuels.org/fileadmin/dena/Dokumente/Pdf/9254Gebaeudereportdenakompakt2018.pdf.

[150] Umweltbundesamt, *Umweltbundesamt - Wohnfläche*. [Online]. Available: https://www.umweltbundesamt.de/daten/private-haushalte-konsum/wohnen/wohnflaeche-zahl-der-wohnungen-gestiegen (visited on 05/11/2022).

[151] 50Hertz, Amprion, TenneT, and TransnetBW, *EEG-Anlagenstammdaten*. [Online]. Available: https://www.netztransparenz.de/EEG/Anlagenstammdaten (visited on 03/04/2022).

[152] Bundesnetzagentur, *Archivierte EEG-Vergütungssätze und Datenmeldungen*. [Online]. Available: https://www.bundesnetzagentur.de/DE/Fachthemen/ElektrizitaetundGas/ErneuerbareEnergien/ZahlenDatenInformationen/EEGRegisterdaten/ArchivDatenMeldgn/artikel.html (visited on 05/09/2022).

[153] Bundesminiterium der Justiz, *Gesetz für den Ausbau erneuerbarer Energien (Erneuerbare-Energien-Gesetz - EEG 2021) § 49 Absenkung der anzulegenden Werte für Strom aus solarer Strahlungsenergie*.

[154] Wirth Harry and Fraunhofer ISE, *Aktuelle Fakten zur Photovoltaik in Deutschland*, 2021. [Online]. Available: https://www.ise.fraunhofer.de/de/veroeffentlichungen/veroeffentlichungen-pdf-dateien/studien-und-konzeptpapiere/aktuelle-fakten-zur-photovoltaik-in-deutschland.pdf (visited on 11/30/2021).

[155] A. Held, J. Winkler, M. Ragwitz, H. Jachmann, T. Kelm, J. Metzger, L. Bangert, C. Maurer, B. Tersteegen, M. Kahles, S. Tiedemann, and F. Wiegand, "Zukünftige Finanzierung von PV-Anlagen unter 750 kW - Bedarf, Anforderungen, Kosten, Szenarien und Förderung", Bundesministeriums für Wirtschaft und Energie, Tech. Rep., 2019.

[156] Bundesnetzagentur, *SMARD*, https://www.smard.de//en/. [Accessed: 2021-12-13], 2021.

[157] T. Lühn and J. Geldermann, "Operating Strategies for Battery Storage Systems in Low-Voltage Grids to Limit the Feed-In Power of Solar Power Systems Using Fuzzy Control", *Operating Strategies for Battery Storage Systems in Low-Voltage Grids to Limit the Feed-In Power of Solar Power Systems Using Fuzzy Control*, vol. 41, no. 3, pp. 169–186, 2017, ISSN: 0343-5377. DOI: 10.1007/s12398-017-0198-7.

[158] V. Bertsch, J. Geldermann, and T. Lühn, "What drives the profitability of household PV investments, self-consumption and self-sufficiency?", *Applied Energy*, vol. 204, pp. 1–15, 2017, ISSN: 03062619. DOI: 10.1016/j.apenergy.2017.06.055. [Online]. Available: http://dx.doi.org/10.1016/j.apenergy.2017.06.055.

[159] Bundesnetzagentur and Bundeskartellamt, "Monitoringbericht 2021 Monitoringbericht gemäß § 63 Abs. 3 i.V.m. § 35 EnWG und § 48 Abs. 3 i.V.m. § 53 Abs. 3 GWB Stand: 15. März 2022", Bonn, Tech. Rep., 2021, pp. 281+284. [Online]. Available: https://de.statista.com/statistik/daten/studie/154902/umfrage/strompreise-fuer-industrie-und-gewerbe-seit-2006/.

[160] H. Shi, M. Xu, and R. Li, "Deep Learning for Household Load Forecasting-A Novel Pooling Deep RNN", *IEEE Transactions on Smart Grid*, vol. 9, no. 5, pp. 5271–5280, 2018, ISSN: 19493053. DOI: 10.1109/TSG.2017.2686012.

[161] L. Gurobi Optimization, *Gurobi Optimizer Reference Manual*, 2022. [Online]. Available: https://www.gurobi.com.

[162] R. Fourer, D. M. Gay, and B. W. Kernighan, "AMPL: A Mathematical Programing Language", *Algorithms and Model Formulations in Mathematical Programming*, pp. 150–151, 1989. DOI: 10.1007/978-3-642-83724-1_12.

[163] C. Moll, "Applications at Siemens tackled by the optimization team at SIEMENS Corporate Technology", in *CO@Work, Zuse Institute Berlin*, 2020.

[164] K. Bestuzheva, M. Besançon, W.-K. Chen, A. Chmiela, T. Donkiewicz, J. van Doornmalen, L. Eifler, O. Gaul, G. Gamrath, A. Gleixner, L. Gottwald, C. Graczyk, K. Halbig, A. Hoen, C. Hojny, R. van der Hulst, T. Koch, M. Lübbecke, S. J. Maher, F. Matter, E. Mühmer, B. Müller, M. E. Pfetsch, D. Rehfeldt, S. Schlein, F. Schlösser, F. Serrano, Y. Shinano, B. Sofranac, M. Turner, S. Vigerske, F. Wegscheider, P. Wellner, D. Weninger, and J. Witzig, "The SCIP Optimization Suite 8.0", no. 773897, pp. 1–40, 2021. arXiv: 2112.08872. [Online]. Available: http://arxiv.org/abs/2112.08872.

[165] S. Maher, M. Miltenberger, J. P. Pedroso, D. Rehfeldt, R. Schwarz, and F. Serrano, "PySCIPOpt: Mathematical programming in python with the SCIP optimization suite", *Lecture Notes in Computer Science (including subseries Lecture Notes in Artificial Intelligence and Lecture Notes in Bioinformatics)*, vol. 9725, pp. 301–307, 2016, ISSN: 16113349. DOI: 10.1007/978-3-319-42432-3_37.

[166] *MATLAB Optimization Toolbox*, 2019. [Online]. Available: http://www.mathworks.com/products/optimization/.

[167] S. Kim and H. Kim, "A new metric of absolute percentage error for intermittent demand forecasts", *International Journal of Forecasting*, vol. 32, no. 3, pp. 669–679, 2016, ISSN: 01692070. DOI: 10.1016/j.ijforecast.2015.12.003. [Online]. Available: http://dx.doi.org/10.1016/j.ijforecast.2015.12.003.

[168] T. Tjaden, J. Bergner, J. Weniger, and V. Quaschning, "Representative electrical load profiles of residential buildings in Germany with a temporal resolution of one second", *Dataset, HTW Berlin - University of Applied Sciences Research*, no. November, pp. 1–7, 2015. DOI: 10.13140/RG.2.1.3713.1606.

[169] J. Figgener, D. Haberschusz, K.-P. Kairies, O. Wessels, B. Tepe, and D.-U. Sauer, "Wissenschaftliches Mess- und Evaluierungsprogramm Solarstromspeicher 2.0 - Jahresbericht 2018", RWTH Aachen, Tech. Rep. [Online]. Available: http://www.speichermonitoring.de.

[170] W. Cramer, K. Schumann, M. Andres, C. Vertgewall, A. Monti, S. Schreck, M. Metzger, S. Jessenberger, J. Klaus, C. Brunner, F. Heringer, A. Alvarado, A. Armstorfer, and N. Beg, "A simulative framework for a multi-regional assessment of local energy markets - A case of large-scale electric vehicle deployment in Germany", *Applied Energy*, vol. 299, no. June, p. 117 249, 2021, ISSN: 03062619. DOI: 10.1016/j.apenergy.2021.117249. [Online]. Available: https://doi.org/10.1016/j.apenergy.2021.117249.

[171] J. Gemassmer, C. Daam, and R. Reibsch, "Challenges in grid integration of electric vehicles in urban and rural areas", *World Electric Vehicle Journal*, vol. 12, no. 4, pp. 1–11, 2021, ISSN: 20326653. DOI: 10.3390/wevj12040206.

[172] F. D'Ettorre, M. De Rosa, P. Conti, D. Testi, and D. Finn, "Mapping the energy flexibility potential of single buildings equipped with optimally-controlled heat pump, gas boilers and thermal storage", *Sustainable Cities and Society*, vol. 50, no. June, p. 101 689, 2019, ISSN: 22106707. DOI: 10.1016/j.scs.2019.101689. [Online]. Available: https://doi.org/10.1016/j.scs.2019.101689.

[173] P. Angaphiwatchawal and S. Chaitusaney, "Centralized Optimal Operations of Local Energy Trading Market in Distribution System", *IEEE Access*, vol. PP, no. April, p. 1, 2022. DOI: 10.1109/ACCESS.2022.3164705.

[174] H. Houmy, *Uncertainty in Local Energy Markets - Development and Evaluation of Methods to Handle Forecast Uncertainties in Local Energy Markets (Master's Thesis)*. Technical University of Munich, 2020.

[175] L. Kotzur, L. Nolting, M. Hoffmann, T. Groß, A. Smolenko, J. Priesmann, H. Büsing, R. Beer, F. Kullmann, B. Singh, A. Praktiknjo, D. Stolten, and M. Robinius, "A modeler's guide to handle complexity in energy systems optimization", *Advances in Applied Energy*, vol. 4, no. August, p. 100 063, 2021, ISSN: 26667924. DOI: 10.1016/j.adapen.2021.100063. arXiv: 2009.07216. [Online]. Available: https://doi.org/10.1016/j.adapen.2021.100063.

[176] Pebbles-Konsortium and Stiftung Umweltenergierecht, “Ein Plattform-Konzept für eine kostenoptimierte Energiewende mit Hilfe lokaler Energiemärkte”, Tech. Rep., 2021.

[177] M. Vasconcelos, W. Cramer, C. Schmitt, A. Amthor, S. Jessenberger, C. Ziegler, A. Armstorfer, and F. Heringer, “The PEBBLES project - enabling blockchain based transactive energy trading of energy flexibility within a regional market”, *CIRED 2019*, no. June, pp. 3–6, 2019, ISSN: 2032-9644. [Online]. Available: https://www.cired-repository.org/handle/20.500.12455/363.

[178] S. Gebhardt, C. Brunner, T. Vogler, J. Klaus, A. Lüllwitz, F. Heringer, M. Metzger, A. Amthor, A. Hammer, S. Schreck, L. Wagner, N. Zupan, J. Bamberger, and K. S. HKE – Andreas Armstorfer, Prof. Dr. Helmuth Biechl FIT – Julius Zocher, Yücel Uzun, Clemens Eyhoff, “Abschlussbericht zum Verbundvorhaben pebbles Peer-to-Peer-Energiehandel auf Basis von Blockchains”, AÜW, egrid, Allgäu Netz, Siemens AG, HKE, Fraunhofer FIT, Tech. Rep., 2022, pp. 1–50.

[179] D. Fietze, A. Papke, M. Wimmer, O. Antoni, and J. Hilpert, “Der Rechtsrahmen für regionale Peer to Peer Energieplattformen”, *Würzburger Studien zum Umweltenergierecht*, vol. 16, 2020.

[180] C. Schmitt, K. Schumann, K. Kollenda, and A. Blank, “How will Local Energy Markets influence the pan-European Day-ahead Market and Transmission Systems ? A Case Study for Local Markets in France and Germany How will Local Energy Markets influence the pan-European Day-ahead Market and Transmission Systems ?”, 2022. DOI: 10.36227/techrxiv.19785331.v1.

[181] A. Lüth, J. Weibezahn, and J. M. Zepter, “On Distributional Effects in Local Electricity Market Designs—Evidence from a German Case Study”, *Energies*, vol. 13, no. 8, p. 1993, 2020, ISSN: 19961073. DOI: 10.3390/en13081993.

[182] I. Kalysh, *Local Energy Markets : Impacts on Distribution Grids and Mitigation Strategies for Grid Violations (Master’s Thesis)*. Hochschule Offenburg, 2021.

[183] J. Guerrero, A. C. Chapman, and G. Verbic, “Decentralized P2P Energy Trading under Network Constraints in a Low-Voltage Network”, *IEEE Transactions on Smart Grid*, vol. 10, no. 5, pp. 5163 –5173, 2018, ISSN: 19493053. DOI: 10.1109/TSG.2018.2878445. arXiv: arXiv:1809.06976v1.

[184] R. Sudhoff, S. Schreck, S. Thiem, and S. Niessen, “Operating Renewable Energy Communities to Reduce Power Peaks in the Distribution Grid: An Analysis on Grid-Friendliness, Different Shares of Participants, and Economic Benefits”, *Energies*, vol. 15, no. 15, 2022, ISSN: 1996-1073. DOI: 10.3390/en15155468. [Online]. Available: https://www.mdpi.com/1996-1073/15/15/5468.

[185] S. Just, “The German market for system reserve capacity and balancing energy”, *EWL Working Paper,*, no. No. 06/15 University of Duisburg-Essen, Chair for Management Science and Energy Economics, Essen, 2015.

[186] D. Meadows, P. Vis, and P. Zapfel, “The EU Emissions Trading System”, Tech. Rep., 2012, pp. 66–94. DOI: 10.4324/9789276082569-4.

A. Appendix

A.1. Appendix to background and analysis chapter

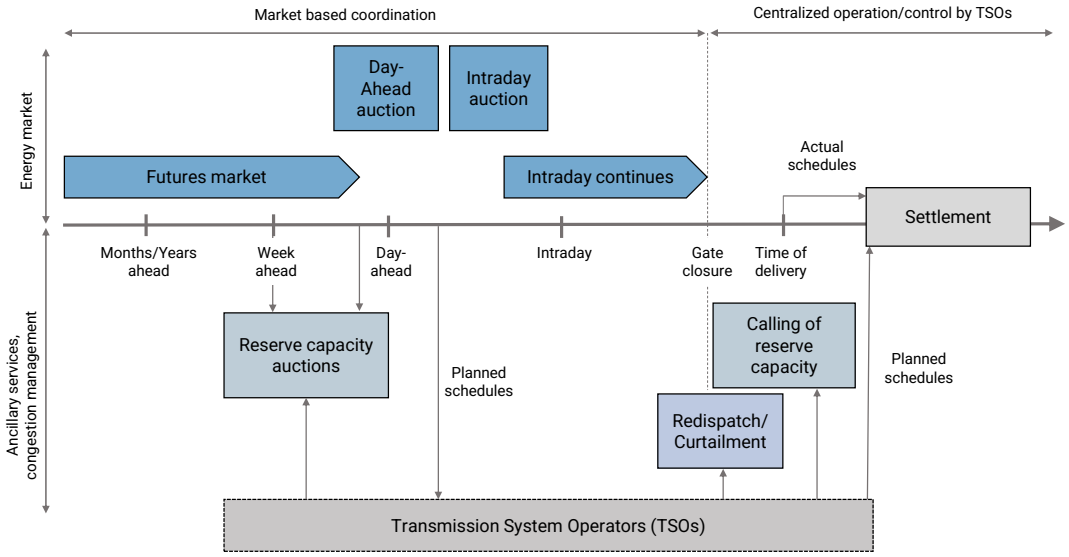

Figure A.1.: Temporal sequence of energy and ancillary service markets in Germany. Own illustration based on [185].

A.2. Appendix to modeling chapter

Electricity categories

Electricity categories are introduced to further incentivize participation at the LEM. Buyers can specify additional markups for preferred electricity categories from a set of available categories C (Figure A.4). The maximum buy price $c^b_{max,t}$ specified in the buy order is extended to $c^b_{max,t,c}$ to define an absolute price for each available category (if applicable). Sellers mark their sell order with one of the categories[1]. The whole optimization model is extended by the dimension of categories. Node balance equations, for example (Equation 3.27, 3.28) are extended to cover the balance not

[1] In a real world application this requires a calibration and certification of the respective measurement device to perform billing.

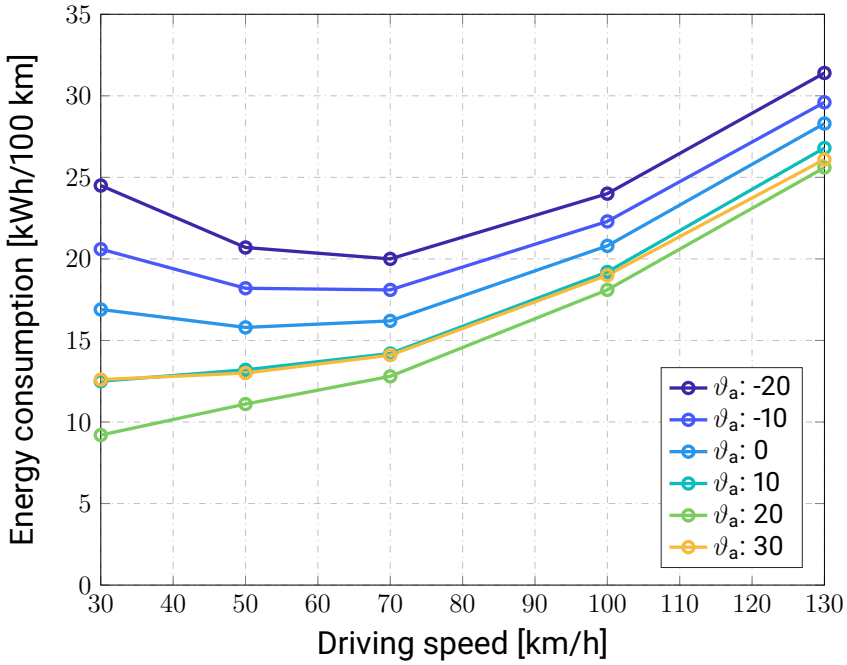

Figure A.2.: Piecewise linear interpolation of EV consumption dependency of ambient temperature (θ_a) and driving speed for an average vehicle based on [139].

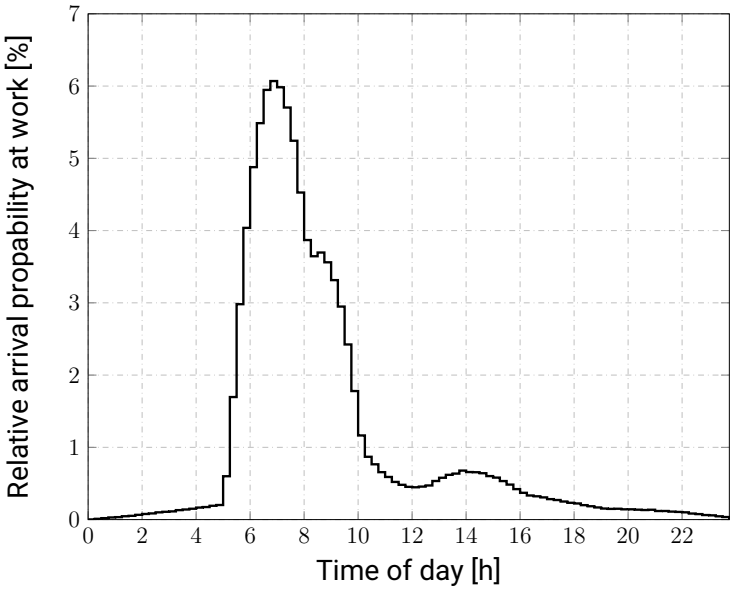

Figure A.3.: Probability of arriving at work based on empirical data in [138].

only in time but also category wise.
The new formulation can be pictured as multiple grid layers for each category. To introduce permeability between these layers, available categories are organized in a hierarchical manner (Figure A.4). Categories with the highest quality (Wind, Bio, Solar, Hydro) can be sold as their own category, green, local or non-local. The category green, e.g., chosen by a participant which

wants to consume arbitrary renewable energy, can only supply green, local or non local customers. A seller of local energy (e.g., a CHP power plant) can only sell on the local layer or to the backup supplier (non-local).

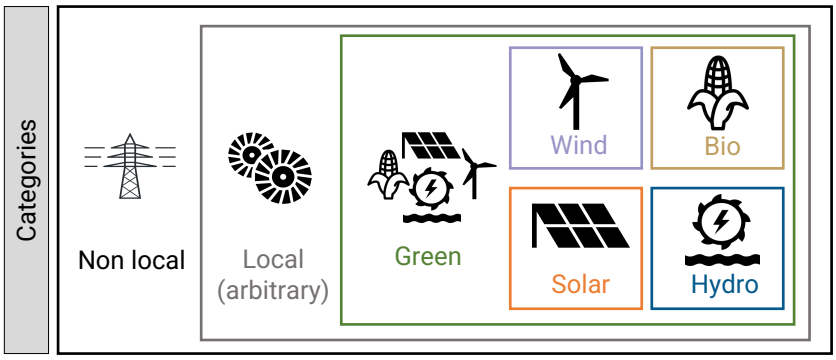

Figure A.4.: Overview of tradable electricity product categories on the LEM

While the physical layer of the grid is not directly affected by this, it might incentivize further investment in generation units supplying the most demanded category. The currently implemented scheme for trading renewable energy certificates in the European Union [186] does not account for the exact time the renewable energy is generated and consumed. The described model allows to make the category wise generation traceable on the basis of the time interval of the model, e.g., on a 15 min basis.

A.3. Appendix to method chapter

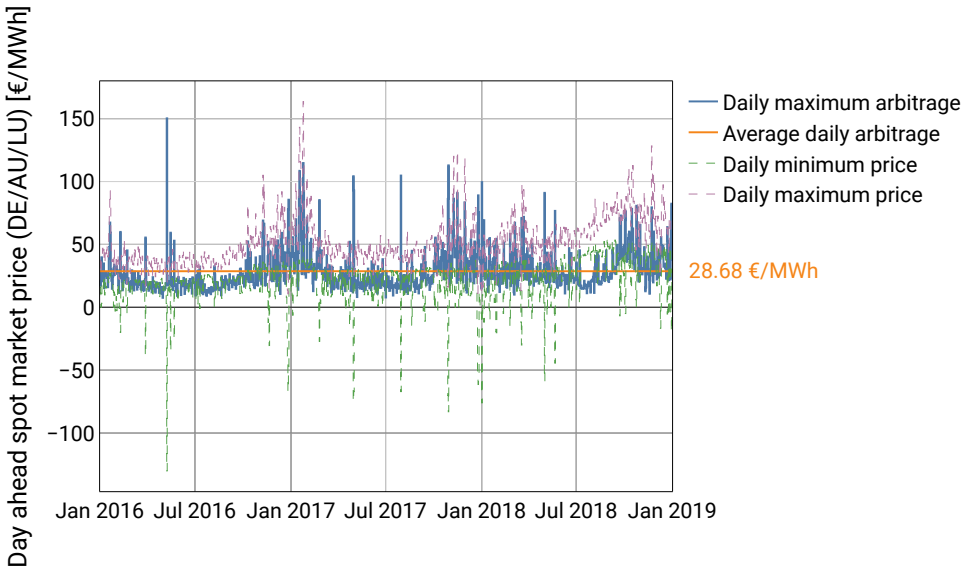

Figure A.5.: Day ahead spot market price and arbitrage opportunities for the time frame 2016-2018

Table A.1.: Simulation scenario parameters and assumptions for the scenario year 2020.

Parameter	Type/Unit	Rural	Semiurban	Urban
Grid connection points	Count [-]	96	110	58
Residential loads	Count [-]	92	92	102
Commercial loads	Count [-]	7	12	9
Photovoltaic systems	Rated power [kW]	185.7	202.7	93.8
	Count [-]	19	30	19
Heat pumps	Rated power [kW]	16.8	19.8	13.8
	Count [-]	5	5	3
	share	5.1	4.8	2.7
Electric vehicles	Rated power [kW]	22.0	29.2	0
	Count [-]	1	1	0
Battery	Rated power [kW]	20.7	55.0	11.3
	Count [-]	8	15	7
	Capacity [kWh]	41.4	110.1	22.6
Electric load	Energy [MWh]	257.9	470.3	530.9
Thermal load	Energy [MWh]	19.1	31.2	27.7
Electric load EV	Energy [MWh]	4.6	3.3	0.0

Table A.2.: Simulation scenario parameters and assumptions for the scenario year 2025.

Parameter	Type/Unit	Rural	Semiurban	Urban
Grid connection points	Count [-]	96	110	58
Residential loads	Count [-]	92	92	102
Commercial loads	Count [-]	7	12	9
Photovoltaic systems	Rated power [kW]	236.0	284.8	139.6
	Count [-]	19	30	19
Heat pumps	Rated power [kW]	38.6	26.7	15.8
	Count [-]	6	7	4
	share	6.1	6.7	3.6
Electric vehicles	Rated power [kW]	80.4	91.3	82.3
	Count [-]	11	12	6
Battery	Rated power [kW]	46.5	123.9	25.4
	Count [-]	8	15	7
	Capacity [kWh]	93.2	247.8	50.8
Electric load	Energy [MWh]	257.9	470.3	530.9
Thermal load	Energy [MWh]	37.8	42.0	33.7
Electric load EV	Energy [MWh]	40.1	30.7	20.8

Table A.3.: Simulation scenario parameters and assumptions for the scenario year 2030.

Parameter	Type/Unit	Rural	Semiurban	Urban
Grid connection points	Count [-]	96	110	58
Residential loads	Count [-]	92	92	102
Commercial loads	Count [-]	7	12	9
Photovoltaic systems	Rated power [kW]	286.4	366.8	185.4
	Count [-]	19	30	19
Heat pumps	Rated power [kW]	102.0	63.2	41.6
	Count [-]	13	15	8
	share	13.1	14.4	7.2
Electric vehicles	Rated power [kW]	157.1	175.2	122.4
	Count [-]	22	23	11
Battery	Rated power [kW]	72.3	192.7	39.5
	Count [-]	8	15	7
	Capacity [kWh]	144.9	385.4	79.1
Electric load	Energy [MWh]	257.9	470.3	530.9
Thermal load	Energy [MWh]	101.8	98.7	64.3
Electric load EV	Energy [MWh]	75.2	62.7	36.7

A.4. Appendix to results chapter

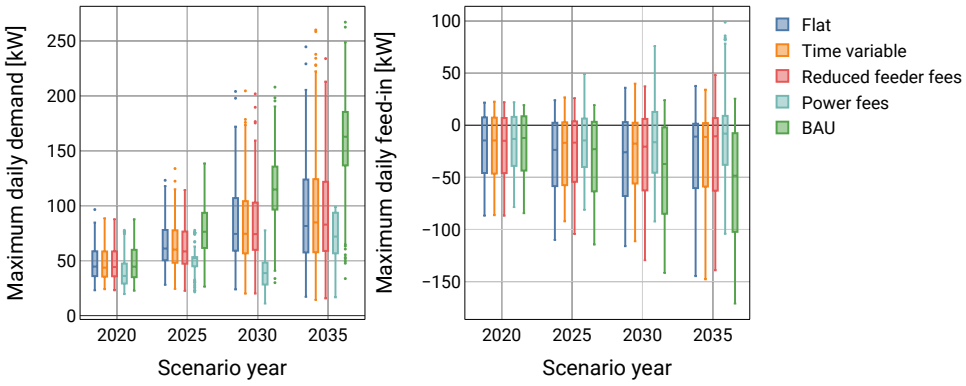

(a) Rural

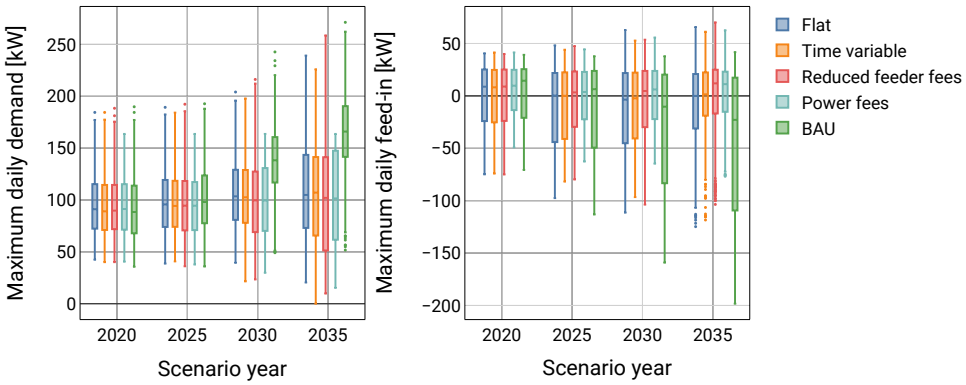

(b) Semiurban

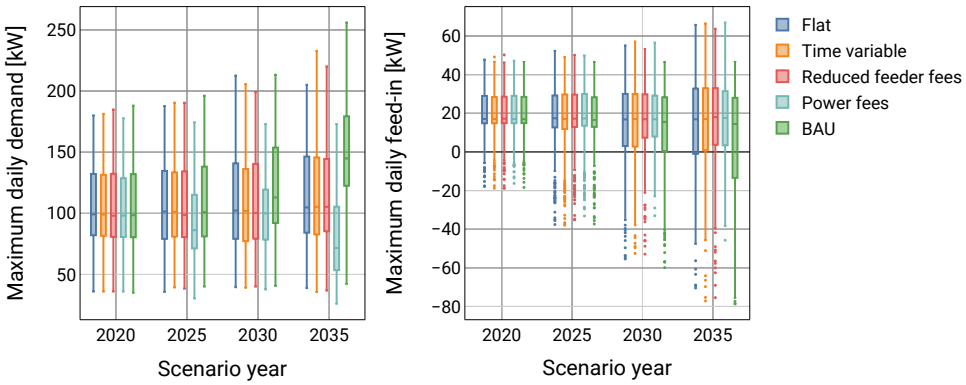

(c) Urban

Figure A.6.: Boxplots of the daily maximum and minimum exchange with the backup utility for a variation of scenario years and REPC scenarios.

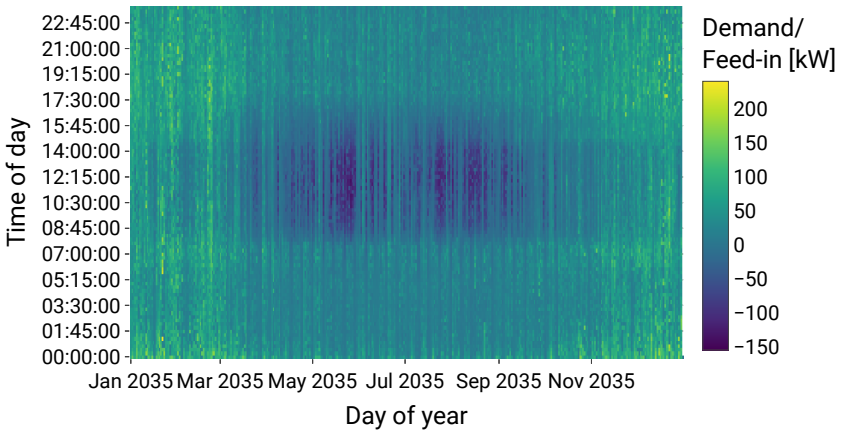

(a) Feeder fees

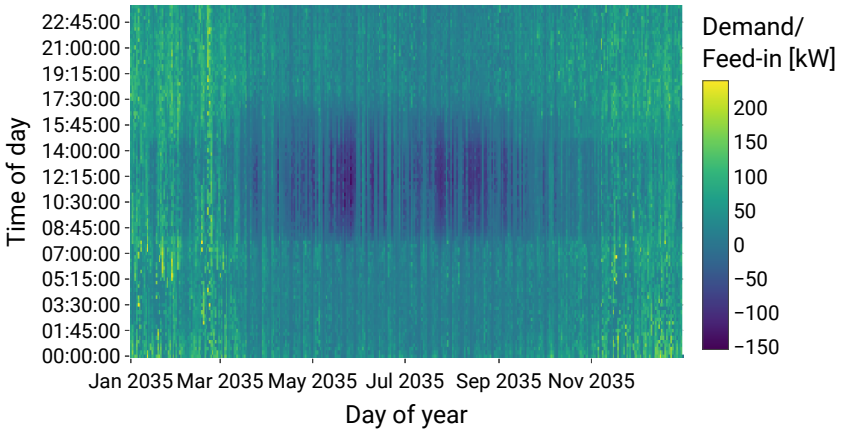

(b) Variable fees

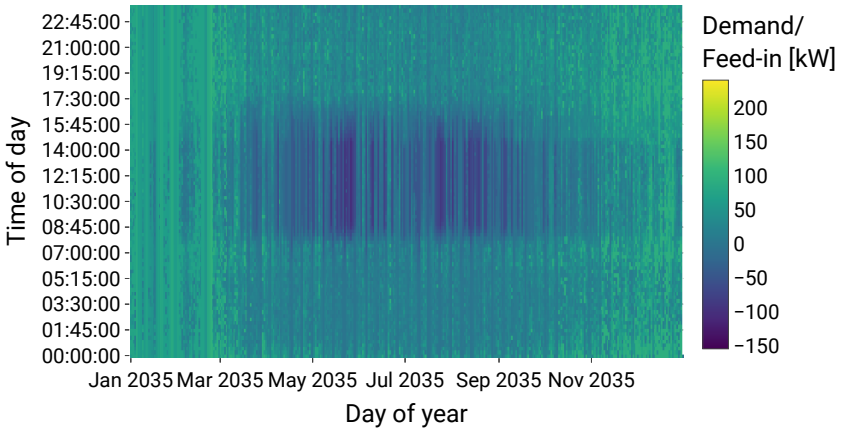

(c) Power fees

Figure A.7.: Heatmaps for a variation of REPC scenarios. Grid type: Rural, Scenario year: 2035.

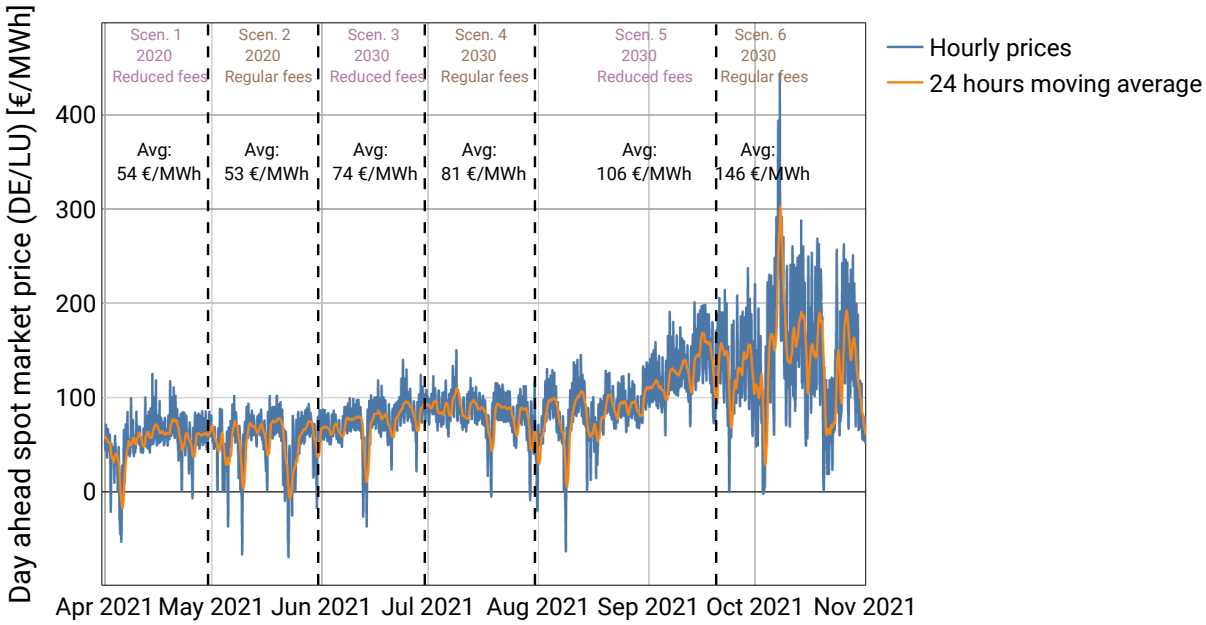

Figure A.8.: Day ahead spot market prices for the zone Germany/Luxembourg at EPEX Spot during the field test. Source: [156].